Inaugural dissertation

for

obtaining the doctoral degree

of the

Combined Faculty of Mathematics, Engineering and Natural Sciences

of the

Ruprecht - Karls - University

Heidelberg

Presented by

M.Sc. Tobias Dag Strobel

born in: Pfullendorf

Oral examination: 16 December 2024

Evaluating the Role of STAT3 for the Phenotype of HPV-Positive Cervical Cancer Cells

Referees: Prof. Dr. Britta Brügger

Prof. Dr. Felix Hoppe-Seyler

Table of Contents

Summary

Oncogenic HPV types cause up to 5% of all human cancers worldwide, including cervical cancer. In order to improve cervical cancer treatment options, novel therapeutic strategies are urgently required. As a prevailing concept in the field, the signal transducer and activator of transcription 3 (STAT3) protein is considered to be a highly promising therapeutic target in HPV-positive cancer cells, since it was reported that STAT3 is essential for the proliferation of cervical cancer cells and, furthermore, undergoes mutually stimulatory interactions with the HPV E6/E7 oncogenes. One strategy to block STAT3 could be the application of the iron chelator Ciclopirox (CPX) which induces the destabilization of STAT3 and inhibits the proliferation of HPV-positive cancer cells.

This thesis aimed to explore the role of STAT3 for the malignant phenotype of cervical cancer cells in detail, focusing on its role for cell proliferation, its reported crosstalk with the HPV oncogenes and its significance for the anti-proliferative effects of CPX. By applying a broad spectrum of experimental methods to modulate STAT3 activity or expression, several unexpected findings were obtained. A number of widely used small molecule STAT3 inhibitors inhibited the proliferation not only of parental cervical cancer cells, but also of corresponding STAT3 knockout derivatives, indicating that they act through off-target effects. In contrast, thoroughly controlled depletion of STAT3 by RNA interference or by CRISPR/Cas9 genome editing did not considerably affect cell proliferation, strongly arguing against an essential role of STAT3 for the growth of cervical cancer cells. In line, transcriptome analyses revealed that STAT3 silencing did not affect expression of its putative pro-proliferative target genes in these cells. Further, despite increased STAT3 activation levels in response to therapeutic drugs, such as PI3K or MEK inhibitors, this did not provide therapeutic resistance to cervical cancer cells. In addition, whereas first insights into the mechanism of CPX-induced STAT3 degradation were obtained, STAT3 was found to be dispensable for the anti-proliferative effects of CPX in cervical cancer cells. Finally, and of particular importance for the field of HPV-induced carcinogenesis, no evidence for an appreciable crosstalk between STAT3 and the viral E6/E7 oncogenes was obtained in either direction, by employing multiple experimental strategies.

Collectively, these findings strongly question the prevailing concept that STAT3 is essential for cervical cancer cell proliferation as well as for efficient HPV E6/E7 oncogene expression. Besides providing unexpected novel insights into the significance of STAT3 for the malignant phenotype of cervical cancer cells, these results are also informative to reshape the discussion on STAT3 serving as a highly promising therapeutic target in HPV-positive cancers.

Zusammenfassung

Onkogene HPV-Typen verursachen weltweit bis zu 5 % aller menschlichen Krebserkrankungen, darunter auch das Zervixkarzinom. Um die Behandlungsmöglichkeiten für das Zervixkarzinom zu verbessern, werden dringend neue Therapiestrategien benötigt. In diesem Kontext wird das „Signal Transducer and Activator of Transcription 3“ (STAT3)-Protein derzeit als vielversprechende therapeutische Zielstruktur angesehen, da es nach Literaturlage für die Proliferation von Zervixkarzinomzellen essenziell ist und außerdem wechselseitig stimulierende Interaktionen mit den HPV E6/E7 Onkogenen eingeht. Eine Strategie zur Inhibierung von STAT3 könnte eine Anwendung des Eisenchelators Ciclopirox (CPX) sein, welches eine Destabilisierung von STAT3 induziert und die Proliferation von HPV-positiven Krebszellen hemmt.

Ziel dieser Arbeit war es, die Rolle von STAT3 für den malignen Phänotyp von Zervixkarzinomzellen im Detail zu untersuchen, wobei die Schwerpunkte auf der Rolle von STAT3 für die Zellproliferation, der postulierten Wechselwirkung von STAT3 mit den HPV-Onkogenen sowie der Bedeutung von STAT3 für die antiproliferative Wirkung von CPX lagen. Unter Einsatz eines breiten Spektrums experimenteller Methoden zur Modulation der Aktivität oder Expression von STAT3 wurden mehrere unerwartete Befunden erhalten. Multiple, experimentell häufig verwendete niedermolekulare STAT3-Inhibitoren hemmten nicht nur die Proliferation parentaler Zervixkarzinomzellen, sondern auch davon abgeleiteter STAT3-Knockout Zellen, was darauf hindeutet, dass sie durch unspezifische („Off-Target“)-Effekte wirken. Im Gegensatz dazu hatten sorgfältig kontrollierte genetische Ansätze zur Hemmung der STAT3-Expression durch RNA-Interferenz oder durch CRISPR/Cas9 Genom-Editierung keine nennenswerten Auswirkungen auf die Zellproliferation. Dies spricht stark gegen eine wesentliche Rolle von STAT3 für das Wachstum von Zervixkarzinomzellen. Transkriptomanalysen ergaben zudem, dass eine Inhibierung von STAT3 die Expression vieler seiner mutmaßlichen, pro-proliferativen Zielgene in diesen Zellen nicht beeinträchtigte. Auch führte eine gesteigerte STAT3-Aktivierung als Reaktion auf die Anwendung von niedermolekularen PI3K- oder MEK-Inhibitoren nicht zu einer erhöhten therapeutischen Resistenz von Zervixkarzinomzellen. Des Weiteren wurden erste Einblicke in den Mechanismus der durch CPX induzierten STAT3-Destabilisierung gewonnen, die jedoch nicht notwendig für die antiproliferative Wirkung von CPX in Zervixkarzinomzellen ist. Außerdem, und von besonderer Bedeutung für die HPV-induzierte Karzinogenese, wurden unter Anwendung verschiedener experimenteller Strategien keine Hinweise auf eine nennenswerte wechselseitige Beeinflussung von STAT3 und den viralen E6/E7-Onkogenen erhalten.

Insgesamt stellen diese Befunde das vorherrschende Modell im Arbeitsfeld stark in Frage, nach dem STAT3 für die Proliferation von Zervixkarzinomzellen sowie für eine effiziente HPV-Onkogenexpression essenziell ist. Die Ergebnisse liefern damit nicht nur unerwartete neue Erkenntnisse über die Bedeutung von STAT3 für den malignen Phänotyp von Zervixkarzinomzellen, sondern sollten auch Auswirkungen auf das derzeit favorisierte Konzept haben, nach dem STAT3 als vielversprechende therapeutische Zielstruktur in HPV-positiven Tumorformen in Frage kommt.

Acknowledgements

First and foremost, I thank Prof. Dr. Felix Hoppe-Seyler for giving me the opportunity to pursue my dissertation in his group's laboratory. I am grateful for his constant guidance, all the insightful feedback, and for fostering an environment that encouraged my scientific curiosity. I enjoyed our lively political discussions which added an amusing dimension to my journey. I am equally grateful to Prof. Dr. Karin Hoppe-Seyler for her invaluable input, her experimental advice, and for creating a welcoming atmosphere in the lab and, importantly, also during coffee breaks.

I further wish to thank Prof. Dr. Britta Brügger for being chair of my defense committee and for the helpful advice during my TAC meetings. Additionally, I want to thank Prof. Dr. Peter Angel and Prof. Dr. Tim Waterboer for their participation as members of my defense committee as well was Prof. Dr. Frank Rösl for his role in my TAC meetings, offering valuable feedback that helped shape my research project.

Importantly, I want to extend my gratitude to Claudia Lohrey, Angela Holzer, and Julia Bulkescher for their exceptional technical support and advice in the lab. During the more stressful times, their expertise was instrumental, and I deeply appreciated their willingness to lend a helping hand when needed. A special thank you also goes to Maria Weber, whom I had the pleasure of supervising during her master's thesis, for the entertaining yet productive collaboration in the lab.

I also wish to express my deep appreciation for my fellow doctoral and master's students Milica Velimirović, Alicia Avenhaus, Nora Heber, Anja Herrmann, Kristin Frensemeier, Dongyun Yang, Julia Mändl and Katharina Siebenkäs. You were key for the supportive, collaborative, and friendly environment that made working in the lab such a positive experience. I will gladly remember not only our stimulating discussions and the laughter we shared in the lab – but especially also the moments we spent outside, which were a highlight of my PhD life. My sincere appreciation also goes to Thomas Holz for his reliable IT support, being always available at a moment's notice.

Lastly, above all, I extend my deepest gratitude to Selina. Your unwavering support, patience, and understanding, despite the physical distance between us, meant more to me than I can express. Many thanks also to my friends and family, in particular my parents, for their constant support throughout my studies and the warm welcomes I received during countless weekend visits. Without all of you, this journey would have been far more difficult, and I am truly grateful for your presence in my life.

Publications & Presentations

Publications

Heber N, Kuhn BJ, **Strobel TD**, Lohrey C, Krijgsveld J, Hoppe-Seyler K, Hoppe-Seyler F. The impact of cycling hypoxia on the phenotype of HPV-positive cervical cancer cells. *J Med Virol*. 2023; 95(12):e29280

Strobel TD, Weber M, Heber N, Holzer A, Hoppe-Seyler K, Hoppe-Seyler F. Revisiting the role of endogenous STAT3 in HPV-positive cervical cancer cells. *J Med Virol*. 2023; 95(11):e29230

Yang D, **Strobel TD**, Bulkescher J, Tessmer C, Hofmann I, Hoppe-Seyler F, Hoppe-Seyler K. FAM57A (Family with Sequence Similarity 57 Member A) Is a Cell-Density-Regulated Protein and Promotes the Proliferation and Migration of Cervical Cancer Cells. *Cells*. 2022; 11(20):3309

Hoppe-Seyler K, Herrmann AL, Däschle A, Kuhn BJ, **Strobel TD**, Lohrey C, Bulkescher J, Krijgsveld J, Hoppe-Seyler F. Effects of Metformin on the virus/host cell crosstalk in human papillomavirus-positive cancer cells. *Int J Cancer*. 2021; 149(5):1137

Patent application

Hoppe-Seyler F, Hoppe-Seyler K, **Strobel T**, Herrmann A. Treatment of STAT3 related diseases by iron chelators, International Publication Number WO2021078937A1. 2021.

Presentations

Strobel TD, Hoppe-Seyler K, Hoppe-Seyler F. Revisiting the role of STAT3 in cervical cancer. Helmholtz International Graduate School for Cancer Research 2023 PhD Retreat. 17.-19.07.2023. Löwenstein, Germany. Poster Presentation.

Strobel TD, Hoppe-Seyler K, Hoppe-Seyler F. Revisiting the role of STAT3 in cervical cancer. i3 Immunology, Infection and Inflammation @ DKFZ Seminar Series. 15.12.2022. Heidelberg, Germany. Oral Presentation.

Strobel T, Hoppe-Seyler K, Hoppe-Seyler F. STAT3 modulates the DNA damage response in cervical cancer cells. Helmholtz International Graduate School for Cancer Research 2022 PhD Poster Presentation. 18.11.2022. Heidelberg, Germany. Poster Presentation.

Strobel T, Hoppe-Seyler K, Hoppe-Seyler F. STAT3 modulates the DNA damage response in cervical cancer cells. 15th International PhD Student Cancer Conference. 08.-10.06.2022. Heidelberg, Germany. Poster Presentation.

CHAPTER 1

Introduction

1. Introduction

1.1 Human papillomaviruses

Human papillomaviruses (HPVs) are non-enveloped viruses and possess a circular, double-stranded DNA genome[1]. Collectively, more than 400 individual types of HPVs were discovered up to now[1]. HPVs are strictly constrained to infect human keratinocytes of the skin and mucosa, causing mostly benign warts, however certain types of the *Alphapapillomavirus* genus are classified as high-risk HPVs according to the International Agency for Research on Cancer[2]. These high-risk HPVs are causative agents of a range of invasive cancers in the anogenital and head and neck region[2]. Due to their importance, the following chapters relate to high-risk HPVs, in particular HPV16 and HPV18.

1.1.1 The biology of HPVs

The genome of HPVs is organized into early (E) and late (L) regions as well as the long control region (LCR) which harbors essential binding sites for transcription factors and other proteins facilitating replication of the viral genome as well as transcription of viral genes. Generally, transcription of the HPV16 or HPV18 E6/E7 oncogenes is controlled by the early P_{97}[3] or P_{105}[4] promoters, respectively, which are located at the 3' end of the LCR and induce the generation of polycistronic transcripts coding for E6 and E7. Besides these, several other promoters exist to regulate the complex expression patters of viral genes[5], which are tightly coupled to the viral life cycle. The E region in total contains six open reading frames (ORFs) coding for E1, E2, E4, E5, E6 and E7 which enable progression through the viral life cycle. Specifically, E1 encodes the only HPV protein with enzymatic function – a viral DNA helicase, which is recruited by E2 to the LCR to initiate viral genome replication in conjunction with cellular DNA polymerases and replication factors[6, 7]. In addition to its role in replication of the viral genome, E2 functions as a crucial regulatory factor of viral gene transcription, for example by repressing transcription of E6/E7 in oncogenic HPV types[7]. The E4 protein is an important factor to support viral genome amplification, virion assembly as well as viral shedding[8]. The E5 protein mediates evasion from elimination by the immune system as well as promotion of cell proliferation[9] and can thus be classified as an oncoprotein. However, *in vitro*, expression of the HPV E5 protein displays only weak to modest transforming activity[9, 10] and the gene is often deleted in advanced cancers[11]. E5 is therefore presumed to only play a role in early stages of transformation. The HPV E6 and E7 proteins are major direct and indirect promoters of cell proliferation, immune evasion, immortalization and cell survival and are the main drivers responsible for the transforming potential of HPVs[12], as described in more detail below in

section 1.1.2. Finally, the L regions are only transcribed in late stages of the viral life cycle and encode the major (L1[13]) and minor (L2[14]) viral capsid proteins.

The HPV life cycle starts with infection of keratinocytes located at the basal membrane by attaching to heparin sulfate proteoglycans[15]. Importantly, only actively proliferating cells in the basal layer can be successfully infected by HPVs, presumably because entering of viral DNA into the nucleus of infected cells requires active progression through mitosis[16], which is not the case for upper layers of the epithelium. Importantly, progression of viral gene expression during the viral life cycle is coupled to the differentiation state of infected cells with high amounts of virion release in the uppermost layer of the epithelium only[17]. Thus, early proteins are expressed predominantly, but not exclusively, in the basal cell layer while expression of the late capsid proteins is confined to the more differentiated upper epithelial layers[17].

1.1.2 HPV infection and cancer

Overall, cancer incidence is continuously rising[18] and around 13% of all cancers are estimated to be linked to infectious agents[18, 19]. In total, approximately 4% of all cancers or 31% of virus-induced cancers are dependent on HPV infection[19]. Of those, cervical cancer is responsible for the majority of cases, being the 4th most common[18] cancer in women resulting in close to 660,000 new cases and 350,000 deaths per year worldwide, especially in less developed countries[18]. Notably, while not all cases of other infection-linked cancers such as gastric cancer[18] can be attributed to infectious agents, virtually all cases of cervical cancer are caused by HPV infections[19, 20], in particular by HPV16 and HPV18, which together cause around 70% of all cases[21]. Notably however, although HPV infection is required to induce cervical cancer, only the lesions of a small minority of women infected with high-risk HPV types will eventually progress to cervical cancer, since the immune system eliminates approximately 90% of cervical HPV infections early during the disease[22]. However, persistent HPV infections can eventually progress to precancerous cervical intraepithelial neoplasia (CIN), categorized from stage 1 to 3 by increasing degrees of dysplasia, followed by invasive cancer[23, 24]. Besides cervical cancer, HPV infection is also the causative agent of a subset of cancers in the head and neck region, especially the oropharynx, as well as other cancers in the anogenital region[18], such as vulvar, penile and anal cancers.

The most important oncogenic properties of high-risk HPVs are strongly linked to the transforming activities of the HPV E6/E7 oncoproteins. E6 and E7 both interact with a multitude of essential host factors to drive carcinogenesis, the most important of which are described in the following. Specifically, E7 induces uncontrolled cellular proliferation by targeting pocket proteins such as the retinoblastoma protein[25, 26], pRb, for degradation through a cullin-2 ubiquitin-ligase complex[27]. Due to the impairment of pRb, the G1/S checkpoint is abrogated

and entry into the cell cycle is enforced, mediated through release of E2F transcription factors from pRb and subsequent induction of transcription of pro-proliferative factors[28]. Inactivation of pRb by E7 further also leads to induction of transcription of $p16^{INK4A}$, which inhibits phosphorylation of pRb, and thus inactivation, by cyclin dependent kinases (CDKs)[29, 30]. Importantly, in this context, $p16^{INK4A}$ is unable to halt cell-cycle progression in E7 expressing cells[31] since pRb is already inactivated by E7[25-27]. The high levels of $p16^{INK4A}$ expression are however exploited as a biomarker for diagnosis of CINs[32]. Further, the loss of pocket protein functionality in E7 expressing cells leads to disruption of the DREAM complex (dimerization partner, Rb-like, E2F and MuvB complex) which is critically involved in controlling cell cycle progression[33]. Additionally, E7 inhibits the function of cyclin-dependent kinase inhibitors such as $p21^{Cip1/Waf1}$ and $p27^{Kip1}$, which are important negative regulators of proliferation[34]. Importantly, even though E7 exerts these transforming activities on its own, sole expression of E7 can also lead to increased expression of the pro-apoptotic tumor suppressor p53 via an increase in $p14^{ARF}$ in response to unchecked cellular proliferation induced by the actions of E7 on pRb[35, 36].

However, in HPV-positive tumor cells, E7 is always co-expressed with E6 to cooperatively drive transformation. E6 interacts with the ubiquitin-protein ligase E3A (UBE3A, also known as E6-associated protein, E6AP) and subsequently the p53 tumor suppressor, forming a trimeric complex which leads to the proteolytic degradation of p53[37, 38]. Thereby, E6 prevents p53-induced, bax-dependent apoptosis[39] in response to the E7-induced deregulation of cell proliferation and enables evasion from p53-dependent tumor-suppressive activities. Besides p53, E6 is able to facilitate degradation of bak[40] and interfere with the activity of tumor necrosis factor receptor 1[41] to block their pro-apoptotic actions. Importantly, E6 proteins of high-risk HPVs also harbor a PDZ (post synaptic density protein, drosophila disc large tumor suppressor, and zonula occludens-1 protein)-binding motif allowing the targeted degradation of critical cellular PDZ-domain containing proteins[42], including several tumor suppressor proteins. Additionally, expression of high-risk E6 leads to transcriptional activation of telomerase reverse transcriptase (TERT)[43] and the activation of several pro-survival and pro-proliferative pathways[44] such as the protein kinase B/AKT, mechanistic target of rapamycin complex 1 (mTORC1), notch or wingless and int-1 (wnt) pathways.

Besides these pro-proliferative and anti-apoptotic functions of E6 and E7, both further contribute to the development of invasive cancer by promoting immune evasion, for example by affecting interferon regulatory factors and signal transducer and activator of transcription 1 (STAT1) signaling to interfere with the interferon response[45, 46] as well as by affecting the function or expression of interleukin 1β (IL-1β)[47], the cytosolic DNA sensor STING[45] and toll-like receptors[45, 48]. Additionally, through the actions of E6 and E7, genome instability and

chromosomal alterations are promoted which can contribute to the acquirement of mutations that further drive cancer development[49-52]. Notably, E6 and E7 were further also reported to affect cellular metabolism[53, 54], intracellular and exosomal miRNA composition[55] as well as cell invasion[56], promoting carcinogenesis.

During the course of cancer development, parts of the HPV genome, typically harboring the LCR and the E6/E7 oncogenes, are frequently integrated into the host genome[57, 58]. Importantly, the ability to express E2, which can repress expression of the E6 and E7 oncogenes, is commonly lost in this process[59], for example via disruption of the E2 gene during the integration event. Alternatively, in cases where functional E2 is expressed in cancer cells, it is often observed that E2 binding sites in the LCR are epigenetically silenced via DNA methylation[60, 61]. As a result, E6 and E7 are expressed at high levels and drive transformation to malignant cancer, as specified above. HPV-induced cancer cells are considered oncogene addicted[11], since abrogation of E6 and E7 expression and function by RNA interference (RNAi)[62] or ectopic expression of E2 leads to rapid induction of cellular senescence[63 64, 65]. Underlining the addiction to both E6 and E7 proteins to sustain both cell growth and survival, sole abrogation of E6 expression or functions leads to efficient induction of apoptosis[66, 67].

1.1.3 Therapy of cervical cancers

Since preventive measures and prophylactic vaccines are available protecting from most common high risk HPV types, HPV-induced malignancies are principally to a large part preventable[68-70]. However, due to the worldwide low vaccination rates and the long course of the disease, taking many years from infection to malignancy, cervical cancer will remain an unresolved medical problem for decades to come[68, 69]. In addition, although initially the treatment options as outlined below are effective, treatment of advanced cervical cancers is often non-curative and recurrence is often observed[71]. HPV-linked transformation processes are therefore still intensely investigated, also with the aim develop novel and more effective therapeutic strategies.

In early-stage cervical cancers surgical removal of the lesion is the preferred therapeutic option while in more advanced or metastatic stages radical hysterectomy is combined with adjuvant radiotherapy or simultaneous chemo-radiotherapy[71]. Additionally, these therapy regimens may be combined with targeted treatments. In specific, current treatment standards include platinum-based chemotherapeutics such as cisplatin – sometimes substituted by or combined with paclitaxel, topotecan or gemcitabine[72]. Targeted treatment strategies for advanced cervical cancer stages include application of the vascular endothelial growth factor (VEGF)-targeting antibody bevacizumab[73] to block angiogenesis or immunotherapeutic approaches using the programmed cell death protein 1 (PD-1)-targeting antibody pembrolizumab[74].

Since the malignant phenotype of HPV-positive cancer cells critically depends on constitutive expression of E6 and E7, approaches to exploit this addiction for therapeutic purposes are intensely studied[12, 75]. Extensive research was conducted on the identification of inhibitors for E6 and/or E7, for example via inhibitory peptide aptamers[67], small molecules[76] or RNA interference (RNAi)[77]. More indirect approaches previously and currently investigated are the application of proteasome inhibitors[78] and immunotherapeutic strategies, for example targeting major histocompatibility complex 1 (MHC1)-presented E6/E7 peptides via therapeutic vaccines or autologous T-cell therapies[79, 80]. Although promising preclinical results were obtained, none of these approaches was thus far approved for clinical use, warranting further research on urgently needed therapeutic options[12]. One possibility are targeted therapies for example against the growth-promoting phosphatidylinositol 3-kinase (PI3K) or mitogen-activated protein kinase (MAPK) pathways since these are often mutated and/or hyperactive in cervical cancer[81-83]. Another such novel strategy is the targeting of abnormal cancer cell metabolism, which is highly altered in HPV-positive cancer cells[53, 54]. Promisingly, drugs like Metformin[84], 2-Deoxy-D-glucose (2-DG)[85] and the iron chelator Ciclopirox (CPX)[86, 87] were previously found to repress E6/E7 and block proliferation. However, even though these drugs are – in the case of Metformin and CPX – already in clinical use for non-malignant indications[88, 89], further research is warranted on their mechanisms in HPV-positive cancer cells before clinical assessment of their suitability for cancer treatment can be initiated.

1.2 Iron metabolism

In terms of aforementioned metabolic drugs, iron chelators such as CPX are especially promising, as these – in comparison to Metformin or 2-DG – strongly induce both apoptosis and senescence, besides blocking the E6/E7 oncogene expression in treated cervical cancer cells[84, 86, 87]. Generally, the target of CPX, iron ions, are essential, evolutionarily conserved co-factors in a multitude of physiological processes, especially in metabolism[90, 91].

1.2.1 Physiological functions of iron

Iron in the form of ferrous (Fe^{2+}) or ferric (Fe^{3+}) cations is an essential factor in cells and therefore its homeostasis is tightly controlled. Systemically, iron is transported in the serum bound to transferrin while release into the blood by iron storing cells in the liver is tightly regulated by hepcidin levels[92, 93]. Intracellularly, after iron ions are taken up via the transferrin receptor 1[94], iron is released into the labile pool[95] and subsequently stored in ferritin complexes which contain around 20% of total iron in humans[93, 96]. A large fraction of the remaining 80% of iron are incorporated into the heme group in hemoglobin[93].

Expression of many iron-responsive proteins is regulated post-transcriptionally by the iron regulatory protein-iron responsive element (IRP-IRE) system[97]. IRPs are iron-responsive proteins which bind to IREs, cis-regulatory hairpin structures in the 3’ or 5’ untranslated regions of responsive mRNAs, when levels of the labile iron pool are low[97]. IRPs can thereby induce or repress translation depending on the location of the IRE element in responsive mRNAs.

Generally, iron ions are incorporated in heme groups, Fe-S clusters or in the form of individual ions, usually in the enzymatically active center of enzymes[91]. One of the most important functions of iron lies in oxygen transport by hemoglobin and oxidative phosphorylation (OXPHOS). Both hemoglobin as well as complex I, II, III, IV and cytochrome C (cyt. C) in the respiratory chain incorporate heme groups or Fe-S clusters and are strictly dependent on iron[98, 99]. Furthermore, iron ions possess important roles for the function of ribonucleotide reductase M2[100], certain DNA polymerases[101] and helicases[102], dioxygenases acting as histone demethylases[103] and the cyclin-dependent kinase 1[104, 105]. Further, iron is indirectly involved in function or expression, respectively, of the eukaryotic translation initiation factor 5A[106, 107] and cyclin D1[108].

1.2.2 Iron and cancer

Because many of the aforementioned factors are critical in maintaining efficient proliferation, DNA homeostasis and repair, ATP generation as well as mRNA translation, iron-dependent proteins and processes are often abnormally regulated or expressed in cancer cells[109]. In line with this, high dietary iron intake is associated with increased cancer risk[110], potentially due to

the critical function of iron in pro-tumorigenic processes, as specified above, as well as increased levels of reactive oxygen species arising from high levels of iron availability through the Fenton reaction[111].

Generally, to fuel their high metabolic demands resulting from continuous proliferation, cancer cells often upregulate key factors in iron metabolism. For example, through upregulation of IRP2[112] and transferrin receptor 1[113] cancer cells increase iron uptake. Furthermore, increased levels of intracellular as well as serum levels of ferritin have been found to play a crucial role in tumorigenesis[112, 114]. In line with this, women with increased expression of ferritin were found to be less likely to eliminate existing HPV16 infections, exposing these women to a greater risk for progression to cervical cancer[115]. Thus, due to the increased demand of cancer cells – including cervical cancer cells – for iron, the therapeutic application of iron metabolism-targeting compounds is under discussion to possibly serve as a promising anticancer strategy[116, 117].

1.2.3 Iron chelators for cervical cancer therapy

One such strategy is the application of iron chelators such as CPX[118]. Notably, as indicated above, iron chelation by CPX, which is already in clinical use for the treatment of mycoses[89], was previously found by our laboratory to induce profound anti-tumorigenic effects in cervical cancer cells, including repression of both proliferation and E6/E7 oncogene expression[86, 87].

Interestingly, by investigating the underlying mechanism of CPX in more detail with mass spectrometry-based proteome analyses, the transcription factor signal transducer and activator of transcription 3 (STAT3) was found to be a prominent target of CPX[119]. Specifically, we uncovered that the stability of the STAT3 protein is strongly reduced by CPX treatment in an iron-dependent manner, which could be reversed using the proteasome inhibitor MG132[119]. Importantly, this destabilization led to strongly reduced total STAT3 and STAT3 Y705 phosphorylation levels[119]. Furthermore, the downregulation of STAT3 by CPX was observed to be independent of the HPV-type in the cancer cells[119]. As described in detail below, STAT3 is reported as a crucial oncogenic driver in many cancers, including cervical cancer, and is therefore currently considered a highly interesting therapeutic target for cancer treatment. Collectively, these considerations raised the possibility that the pronounced destabilization of STAT3 by CPX could underlie the strong anti-tumorigenic effects of CPX in cervical cancer cells.

1.3 Signal transducer and activator of transcription 3 (STAT3)

Signal transducers and activators of transcription (STATs) encompass a family of nine latent cytosolic transcription factors, including major splice variants, undergoing dimerization and nuclear translocation upon activation[120]. In general, STATs are composed of six domains of which the coiled-coil domain and the src-homology 2 (SH2) domain are particularly important for dimerization and activation while the DNA binding and the transactivation domain are in addition critical for their function as transcription factors[121]. Of all STATs, STAT3 is one of the most thoroughly investigated members and is associated with a range of diseases, including cancer[121, 122]. Importantly, STAT3 is also considered to be indispensable for development since knockout (KO) of STAT3 was found to be embryonic lethal in mice[123]. For STAT3 as well as STAT1 two major splice variants exist[122]. Importantly, in contrast to the well-characterized *alpha* variants, the *beta* variants lack a functional transactivation domain[120]. In the following, my thesis focuses on canonical signaling, i.e. STAT3 function as a transcription factor upon phosphorylation of the most widely studied STAT3 *alpha* variant as described below in more detail. If not indicated otherwise, 'STAT3' therefore refers to the *alpha* variant, as is common in the literature and 'STAT3 signaling' or 'STAT3 activity' refers to canonical STAT3 *alpha* variant signaling.

1.3.1 Canonical STAT3 signaling

Originally, STAT3 was discovered as an important transcription factor mediating the effects of IL-6 signaling as it occurs during the innate immune response, hence its alternative name acute phase response factor (APRF)[124-126]. Thus, cytokine dependent STAT3 signaling is usually termed canonical STAT3 signaling. Briefly, cytokines such as the IL-6 family cytokines[127] IL-6, oncostatin M (OSM) or leukemia inhibitory factor (LIF) as well as IL-10 bind to their respective receptors followed by cross-phosphorylation and subsequent receptor phosphorylation by receptor-associated janus kinases (JAKs) such as JAK2[120]. This triggers binding of STAT3 to the phosphorylated cytosolic part of the cytokine receptor via its SH2 domain[120]. JAKs then phosphorylate receptor bound STAT3 molecules at Y705[120, 126]. Levels of STAT3 Y705 phosphorylation are therefore usually determined to assess activation levels of canonical STAT3 signaling. Phosphorylated STAT3 molecules then dissociate from the receptor and form homo- or heterodimers, for example with STAT1[128], and subsequently translocate to the nucleus to induce transcription of target genes harboring binding sites (Figure 1) like gamma-activated sequences (GAS) in their promoters[129-131]. Besides cytokine signaling, STAT3 responds also to epidermal[132, 133], vascular endothelial[134] or insulin-like growth factor[135] signaling as well as to activity of non-receptor-associated tyrosine kinases such as src-family

kinases[136-138]. All of these also lead to STAT3 Y705 phosphorylation, subsequent dimerization and translocation of STAT3 to the nucleus.

Figure 1: STAT3 binding motif according to the JASPAR 2024 database[139]. *Matrix ID: MA0144.3*

After translocation into the nucleus in the context of canonical signaling, STAT3 can induce transcription of a plethora of genes involved in the immune response and homeostasis, cell proliferation, survival, migration, stem cell renewal and embryonic development [121, 140]. The exact factors determining which particular gene is under control of STAT3 activity in distinct cellular contexts is not yet fully understood for every target gene, however many different factors have been discovered which can regulate and fine-tune the transcriptional signature induced by STAT3 activity, as detailed below.

1.3.2 Regulation of STAT3 signaling

Overall, mutations of STAT3 in cancer are rare and only few have been reported to play a frequent role for certain hematologic cancers as well as non-malignant diseases[141-144]. Instead, canonical STAT3 signaling in both health and disease is mainly regulated via modulation of cytokine or growth factor concentrations as well as expression or activity of intracellular factors[120].

Interestingly, STAT3 signaling was described to induce activation of a positive feedback loop involving increased transcription of the *STAT3* and *IL-6* genes itself to drive a second wave of IL-6 induced gene expression in response to the initial stimulation[145]. To counteract cytokine signaling through STAT3, one of the most important negative regulators is SOCS3, belonging to the suppressor of cytokine signaling (SOCS) family[146]. SOCS3 directly inhibits activation of JAKs[147] and destabilizes the cytokine receptor complex through ubiquitination[148]. Importantly, *SOCS3* itself is another well-known target of canonical STAT3 signaling and thereby acts as a negative feedback regulator[149-151]. Furthermore, the protein inhibitor of activated STAT3 (PIAS3) plays an important role in attenuating canonical STAT3 signaling by inhibition of STAT3 DNA binding[146, 152] while protein tyrosine phosphatases (PTPs) such as PTP receptor

type D (PTPRD) directly dephosphorylate STAT3 at position Y705, thereby reducing canonical STAT3 signaling in an early phase[146]. Additionally, the STAT3 *beta* splice variant was previously considered to act as a dominant negative factor to canonical STAT3 *alpha* signaling[153]. Recently however, multiple studies indicate that STAT3 *beta* is not simply a dominant negative variant but has to be rather considered as a distinct factor inducing a unique transcriptional signature[154, 155].

Besides these negative regulators of canonical STAT3 activity, multiple factors were identified which regulate total amounts of STAT3 protein and consequently affect all postulated functions of STAT3, including non-canonical signaling (please refer to 1.3.3). Importantly, alterations in the activity or expression of many of these factors were found to be linked to the high STAT3 activities in various cancers[156-162]: For example, ubiquitin-specific peptidase 28 (USP28) was found to increase STAT3 stability through deubiquitination[157] while melanoma-associated antigen C2 (MAGEC2) was described to inhibit polyubiquitination of STAT3[158]. On the other hand, PDZ and LIM domain protein 2 (PDLIM2)[163] and the E3 ubiquitin ligases constitutive photomorphogenic protein 1 (COP1)[160], tumor necrosis factor receptor associated factor 6 (TRAF6)[161] and F-box and WD repeat domain containing 7 (FBW7)[162] induce polyubiquitination and subsequent proteasomal degradation of STAT3. Additionally, besides proteasomal degradation, the calcium-dependent protease calpain[164] as well as caspases[165] were found to cleave STAT3 and thereby interfere with STAT3 functions.

Another layer of regulation of STAT3 signaling is conferred by post-translational modification of STAT3[166]. Besides the Y705 phosphorylation site, STAT3 is also phosphorylated at S727, for example by members of the MAPK pathway[167-169] or mTOR[170]. Phosphorylation at S727 is important for some non-canonical functions of STAT3, e.g. in the mitochondria[171], while also being reported to be required for maximal transcriptional activity in the context of canonical signaling[168, 170, 172]. Additionally, the presence of S727 phosphorylation was described as an important negative modulator of Y705 phosphorylation[167, 173], reportedly by negatively affecting the half-life of Y705 phosphorylation[173]. Apart from phosphorylation, a range of further post-translational modifications such as acetylation[174, 175], methylation[176] and oxidation, for example by peroxiredoxin 2[177], were identified. Interestingly, post-translational modifications can modulate both the spectrum of STAT3 target genes as well as the intensity of STAT3 signaling[166] and additionally, whether STAT3 influences transcription in an activating or repressing manner, the latter of which is considered to be non-canonical[178, 179].

Additionally, the initial stimulus, i.e. which cytokine or growth factor initially induced activation of the signaling cascade, is a major determinant of the biological consequences[180]. Overall, almost 40 cytokine receptors are known to signal through a combination of four distinct JAKs

and seven (nine including *beta* variants) STAT family members[180]. For example, both the pro-inflammatory cytokine IL-6 as well as the anti-inflammatory cytokine IL-10 induce canonical STAT3 signaling[181, 182]. In this specific example it was reported that different sensitivities with respect to negative feedback loops[181] as well as the differences in temporal duration[182] of STAT3 signaling induced by IL-6 compared to IL-10 are major determinants of the differential biological outcomes between induction of signaling through both cytokines. Furthermore, in response to different cytokines, the presence and activity of other signaling pathways and transcription factors such as nuclear factor κB (NfκB)[145, 183, 184], activator protein 1 (AP-1)[185-187] or other STATs[128, 185] can contribute to shaping the cellular response. Interplay of these factors with STAT3 signaling can be mediated through direct physical interaction with Y705-phosphorylated[183, 188] or unphosphorylated[145, 184] STAT3, indirect mutual influence of their transcriptional activities[185] or simply by regulating the same cellular processes and genes independently of each other[189]. Thus, STAT3 regulation and activities are part of a central, intricate signaling network and must be interpreted in the context of partially parallel and interconnected pathways.

Consequently, many different factors can influence the strength of STAT3 signaling, the spectrum of affected target genes and the functional consequences of STAT3 activation, making it difficult to predict the exact role of STAT3 in distinct cellular settings. A further level of complexity is added by the fact that STAT3 can exert functions, which are independent of canonical signaling.

1.3.3 Non-canonical STAT3 functions

In general, functions of STAT3 which are not related to its role as a transcription factor in response to Y705 phosphorylation are considered to be non-canonical[190]. One of the most prominent non-canonical STAT3 functions is related to its translocation to mitochondria[171] which was reported to require phosphorylation at S727[169, 191]. In mitochondria, STAT3 is involved in regulating OXPHOS via increasing throughput of the electron transport chain (ETC) complexes I, II and V[191-193]. However, the exact mechanism underlying this regulation remains yet to be elucidated. A direct interaction between STAT3 and ETC complexes is rather unlikely since ETC complexes greatly outnumber the available mitochondrial STAT3 molecules[194]. One hypothesis is that STAT3 promotes the formation of respirasomes or respiratory super-complexes, which incorporate multiple ETC complexes to increase efficiency and decrease ROS generation via physical proximity[195, 196]. In addition, mitochondrial STAT3 was reported to be able to inhibit the opening of the mitochondrial permeability transition pore (mPTP) by physical binding of cyclophilin D[197]. Mitochondrial STAT3 thereby prevents loss of mitochondrial membrane potential and subsequent mitochondrial swelling and induction of apoptosis[171, 197]. In line with this function, STAT3 was also reported to be associated with the

endoplasmic reticulum (ER) where it facilitates the degradation of inositol 1,4,5-trisphosphate receptor, type 3 (IP3R3) which is an important Ca^{2+} channel involved in transferring Ca^{2+} from the ER to mitochondria which eventually promotes opening of the mPTP followed by induction of apoptosis[198]. Overall, through these mechanisms, mitochondrial STAT3 plays a role for efficient mitochondrial metabolism as well as the inhibition of the mitochondrial apoptosis pathway[171].

Moreover, multiple studies report a role of STAT3 in the regulation of autophagy and lysosomal activities. Specifically, STAT3 was described to physically associate with protein kinase R (PKR) which is known to phosphorylate the pro-autophagic eukaryotic initiation factor 2α (eIF2α)[199]. Additionally, STAT3 was also reported to contribute to inhibition of autophagy through repression of transcription of *BECN1* (coding for beclin 1), which is involved in the autophagic process[200]. Further, at lysosomes, STAT3 was found to associate with the vacuolar H^+-ATPase and to increase its activity, contributing to preserving an alkaline cytosol[201]. In this context, it was interestingly reported that activity of the canonical STAT3 pathway is reduced upon cytosolic acidification which leads to increased STAT3 recruitment to the lysosomes to reequilibrate the intracellular pH[201].

Another non-canonical STAT3 function is its ability to repress transcription of various genes, at least partly through epigenetic mechanisms. For example, repression of transcription of *REDD1* (coding for regulated in development and DNA damage response 1) was found to crucially depend on Y705-phosphorylated STAT3 binding to non-canonical binding sites within the *REDD1* promoter leading to repression of promoter activity[179, 202]. Similarly, the above-mentioned repression of *BECN1* by STAT3 depends on STAT3 binding to the *BECN1* promotor in response to IL-6, followed by histone deacetylase 3 (HDAC3) recruitment[200]. Furthermore, repression of various tumor suppressor genes by STAT3 is associated with DNA methylation and was reported to depend on acetylated STAT3 followed by association with sin3 transcription regulator family member A (Sin3A) at promoter regions[178].

Furthermore, even though Y705 phosphorylation is generally considered to be a crucial factor determining binding of STAT3 to respective promoter regions, there are reports indicating that STAT3 can also affect transcription while being unphosphorylated[145, 203]. Interestingly, it was reported that Y705 phosphorylation is not necessarily required for dimerization of STAT3[204] and that unphosphorylated STAT3 can bind at least some of the same DNA motifs as Y705 phosphorylated STAT3[205, 206]. However, unphosphorylated STAT3 was found to bind these motifs with lower affinity only[205, 206] while being able to modulate transcription of a set of genes not responsive towards canonical Y705 phosphorylated STAT3[145, 207]. This can be at least partly explained due to physical interaction of unphosphorylated STAT3 with other factors such

as NfκB[145] and jun activation domain-binding protein 1 (JAB1)[203]. Moreover, unphosphorylated STAT3 was found to modulate chromatin structure[206-208], for example leading to inhibition of transcription of a range of pro-apoptotic genes[207]. Taken together, non-canonical functions of STAT3 can play prominent roles in various cellular contexts and therefore add another layer of complexity to the regulation and the cellular effects of STAT3.

1.3.4 STAT3 in disease

Since STAT3 is involved in a broad spectrum of key physiological and cellular processes, alterations of its activity have been implicated in many different diseases[121, 122]. One large set of non-malignant diseases with STAT3 involvement is linked to canonical STAT3 signaling and its prominent role for the immune system in response to cytokines. For example, aberrant pro-inflammatory STAT3 activity was reported to be a key component of autoimmune diseases such as psoriasis[209], diabetes mellitus type 1[210], inflammatory bowel diseases (e.g. Crohn's disease)[211] and multiple sclerosis[212]. In some patients, these diseases are associated with certain STAT3 single nucleotide polymorphisms (SNPs) or gain-of-function mutations leading to elevated basal and cytokine-induced STAT3 activity[210, 213]. Interestingly, hyperactive STAT3 is also a critical factor in coronavirus disease 2019 (COVID19), a particularly severe complication of SARS-CoV-2 infection with characteristics of aberrant immune cell activities[214]. *Vice versa*, reductions of STAT3 activity, in this case commonly through STAT3 loss-of-function mutations, can lead to establishment of the hyper-IgE syndrome, which is often associated with uncontrolled bacterial infections[142]. Another notable pathologic state in which STAT3 is a central player is cardiac injury through ischemia, e.g. via cardiac infarction, followed by reperfusion which often leads to exacerbated cardiac cell death[215]. In this setting, both canonical STAT3 signaling and non-canonical mitochondrial STAT3 functions are critical for survival of cardiac cells[215].

In addition, critical STAT3 involvement has been reported for many cancer entities[216]. This is not surprising since many of the processes regulated by STAT3, e.g. proliferation[216], survival[216], migration[216], invasion[158] and aberrant immune responses[121] (e.g. immunosuppression), represent hallmarks of cancer[217]. Aberrant canonical[216] and non-canonical activity[190] of STAT3 have been reported for many prevalent cancer types, including hematologic cancers[178], lung cancer[218], liver cancer[219], colorectal cancer[220], pancreatic cancer[221], glioblastoma[222], malignant melanoma[223, 224], breast cancer[168] as well as cancers associated with viral infection by Epstein-Barr virus (EBV) or HPV such as head & neck cancer[225] and cervical cancer (please refer to 1.3.5). Notably, there are also reports describing STAT3 as a factor associated with favorable prognosis, for example by suppression of migration and invasion in colorectal cancer[226, 227]. Similarly, high expression of STAT3 beta was reported to be associated with favorable prognosis in esophageal squamous cell

carcinoma and was shown to block the transcriptional activity of STAT3 alpha[228]. However, in most cancers, STAT3 is considered an oncogene[216, 229]. Overall, it is reported that STAT3 is constitutively active in over 70% of all cancers, often due to increased inflammatory and growth factor signaling or the loss of negative regulators[216]. Interestingly, only in the great minority of cancers or neoplastic diseases gain-of-function mutations of STAT3 or upstream kinases such as JAK2 have been described[141]. This is in particular the case for polycythemia vera[230] and T-cell large granular lymphocytic leukemia (T-LGL)[141, 144, 231]. As a consequence of abnormal STAT3 activity, cancer cells are often found to increasingly express common oncogenic drivers and pro-survival factors such as *MYC*, *SOX2*, *BCL2*, *BCL2L1*, *MCL1*, *BIRC5*, *CCND1*, members of the MMP family, various cytokines, *PD-L1* and many more[140, 216, 223, 224, 232, 233]. In virus-associated cancers such as cervical cancer, it was additionally reported that STAT3 is critically involved in promoting the expression of virus-derived oncogenes as described in detail below in section 1.3.5.

Furthermore, STAT3 has been reported to be a major resistance factor against both chemotherapy and targeted treatments. For example, canonical STAT3 signaling was found to be feedback-activated in response to many different inhibitors, targeting the PI3K-, MAPK- and c-MET pathways[223, 224, 234-241]. Similarly, increased levels of STAT3 signaling have been implicated in cells resistant to human epidermal growth factor receptor (HER)-family-targeting therapies[236, 242-244]. In the context of chemotherapeutics, pro-proliferative and anti-apoptotic factors which are under transcriptional control of constitutive STAT3 signaling are proposed to confer resistance to cancer cells[245, 246]. Collectively, STAT3 is considered to be a broadly relevant and highly promising therapeutic target for many diseases, in particular for autoimmunity-linked diseases and cancers.

1.3.5 STAT3 in cervical cancer

In cervical cancer, STAT3 has been associated with poor prognosis and metastasis[247] and is considered as an especially promising target due to its multifaceted activities[248-250]. Specifically, efficient expression of the HPV E6/E7 oncogenes, which are essential for the growth and survival of cervical cancer cells, has been proposed to critically depend on STAT3[251-253]. However, the underlying mechanism was not yet fully elucidated since inhibitors targeting canonical STAT3 signaling were found to repress E6/E7 levels[252, 253] while another study reported that the dependence of E6/E7 expression on STAT3 is not linked to transcriptional activity of STAT3 in keratinocytes harboring episomal HPV18 genomes[251]. Additionally, despite the presence of potential STAT3 binding sites in the HPV16 LCR, STAT3 binding to the LCR could not be detected[187]. Rather, it was reported that STAT3 associates with the AP-1 components c-JUN and c-FOS to promote HPV16 transcription[187], however this interaction increased upon IL-6 treatment[187] (which can activate canonical STAT3 signaling),

establishing a potential link to the above-referenced results reported with inhibitors of canonical STAT3 signaling. This is also compatible with a study reporting an activation of the HPV16 LCR by IL-10 induced STAT3 signaling, either through direct association of STAT3 with the LCR or via association with transcription factors that bind the LCR[254].

Vice versa, the HPV oncogenes have been proposed to activate STAT3 signaling[251, 253, 255]. Specifically, STAT3 Y705 phosphorylation was reported to be induced by HPV E6 in an protein kinase B/AKT and autocrine IL-6 dependent manner[251, 253]. This finding is compatible with immunohistochemical analyses showing that STAT3 Y705 phosphorylation levels (indicating STAT3 activation) are higher in cervical cancers than in the corresponding normal tissue[256]. Further, silencing of E6/E7 by RNAi in cervical cancer cell lines was described to repress of activation of STAT3[257]. However, even though IL-6 was found to be highly expressed in cervical cancer tissue[258-260], the importance of the IL-6/STAT3 axis for STAT3 activation in the cancer cells, as specified above, is challenged by other studies reporting a general loss of IL-6 receptor (IL-6R) expression in cervical cancer cells, possibly due to selective pressure to evade the immune system[261, 262]. Cervical cancer cells were thus found to be unresponsive to IL-6[261, 262] and only when IL-6R was reconstituted, for example via soluble IL-6Rs, the HPV18 LCR was responsive to IL-6 in a STAT3-dependent manner[263]. In line, the levels of Y705-phosphorylated STAT3 were found to increase from CIN1 to CIN3 but decreased upon further progression to invasive cervical cancer cells, when compared to adjacent CIN3 lesions in the same tissue sample[264]. Additionally, above-mentioned IL-6 mediated autocrine stimulation of STAT3 activity is challenged by a study that identified macrophages in the tumor stroma as the main source of IL-6 protein, while cervical cancer cells did not show any IL-6 staining[258].

Besides this postulated, mutually stimulatory interconnection with the E6/E7 oncogenes, STAT3 was reported to be essential for promoting the growth and survival of cervical cancer cells[252, 255, 256, 265-268], e.g. by transcriptional induction of putative oncogenic STAT3 target genes such as *BCL2*[267, 268], *BCL2L1*[247, 256, 267], *BIRC5*[256, 267], *MCL1*[267], and *CCND1*[253, 267]. In addition, in line with reports on other cancers, STAT3 was described to promote the migration of cervical cancer cells[268], to correlate with their stemness[269, 270] and to contribute to their therapy resistance, for example to cisplatin treatment[266, 271, 272]. This latter notion, however, has been challenged by other studies in cervical cancer cells, which unexpectedly obtained evidence for a pro-apoptotic role of STAT3 activation when combined with cisplatin treatment[264, 273].

Overall, despite remaining open questions regarding the mechanism of the induction of STAT3 Y705 phosphorylation by the HPV oncogenes or, *vice versa*, regarding the promotion of E6/E7 expression by STAT3 activity, E6/E7 and STAT3 are proposed to form a mutually stimulating feedback loop promoting the oncogenic activities of each other[249]. Thus, the current model of

STAT3 in cervical cancer considers STAT3 to be deeply intertwined with the HPV oncogenes and regards STAT3 as essential for the proliferation of cervical cancer cells[249]. Consequently, STAT3 is considered to represent a promising target for therapeutic intervention in cervical cancer cells.

1.3.6 Inhibition of STAT3 signaling

Since STAT3 is known as an important factor in many diseases[121, 122], various approaches to inhibit STAT3 were developed in the past and are still presently intensely investigated. Altogether, current strategies to inhibit STAT3 signaling or expression can be grouped in the following categories[216]:

(1) Small molecule inhibitors targeting STAT3 activity
(2) Small molecule inhibitors targeting upstream kinases which activate STAT3
(3) Small molecules reducing STAT3 protein stability
(4) Oligonucleotide-based molecules interfering with STAT3 expression or function
(5) Protein-based molecules targeting extracellular cytokines and growth factors involved in STAT3 activation

However, despite intense efforts, none of these approaches achieved regular clinical use yet, with the exception of upstream kinase inhibitors targeting, for example, JAK, and antibodies targeting cytokines, for example, IL-6[216]. These agents, however, were not solely developed to inhibit STAT3 signaling and can also affect activation of factors other than STAT3, resulting in limited specificity for STAT3. In contrast, direct chemical small molecule STAT3 inhibitors such as Stattic[274] or C188-9[275], in principle, possess the potential to be more selective for STAT3. However, the development of truly specific inhibitors turned out to be rather difficult since STAT3, as a transcription factor, functions mainly via interactions with DNA and other proteins occurring over large, flat areas, which makes it difficult to design small molecules that inhibit these interactions[276, 277]. In contrast, many potent and specific small molecule inhibitors target the enzymatic activity of kinases, which often occur in deep and specific pockets that can be targeted by small molecules[276, 277]. To target ‘undruggable’ proteins like STAT3, novel technologies are currently being developed, for example proteolysis targeting chimeras (PROTACs) which induce specific degradation of proteins which are difficult to target by conventional means[276, 277]. For STAT3, multiple PROTACs[278-280] were developed showing potent and specific degradation of STAT3 also *in vivo* [278, 279] as well as in a first clinical trial[281]. In comparison to inhibitors targeting upstream kinases or STAT3 signaling, targeted protein degradation has the potential advantage to additionally target non-canonical STAT3 functions, which do not necessarily depend on its phosphorylation state.

Another class of molecules to inhibit STAT3 are large biological molecules, for example antibodies and antisense oligonucleotides. Specifically, the antisense oligonucleotide AZD9150 was developed to leverage RNAi to inhibit STAT3 expression on the transcript level with early signs of clinical activity[282, 283]. On another level, decoy oligonucleotides harboring STAT3 binding sites can be used to outcompete STAT3 binding sites in the genome[284-286]. However, these approaches are complicated in terms of drug delivery and stability[285, 286]. In contrast, protein-based large molecules such as the antibodies Tocilizumab[287] or Siltuximab[288] target the IL-6R or IL-6, respectively, and thereby block canonical STAT3 signaling. However, these, as mentioned above, lack specificity for STAT3 and do not necessarily block canonical STAT3 signaling altogether but instead only the fraction of STAT3 signaling which is induced by the targeted cytokine, IL-6. Collectively, despite a broad range of available STAT3 inhibitors, further research has to be conducted to finally yield a specific and effective STAT3 inhibitor for clinical use[216].

1.4 Research objectives

The STAT3 protein is currently discussed to represent a highly promising therapeutic target for cervical cancer therapy, since it has been reported to be essential for the proliferation of HPV-positive cancer cells. In addition, STAT3 has been described to undergo mutually stimulatory interactions with the HPV E6/E7 oncogenes, which are the key drivers of HPV-induced carcinogenesis. In this light, recent findings revealing that the iron chelator CPX potently blocks proliferation while inducing the degradation of the STAT3 protein in cervical cancer cells are of high interest. Therefore, my thesis focuses on addressing the following major open questions:

(1) Is the anti-proliferative effect of CPX related to the degradation of the STAT3 protein in HPV-positive cancer cells? Is the CPX-induced downregulation of E6/E7 functionally linked to STAT3?
(2) Which factors could potentially mediate the degradation of STAT3 by CPX? Is this proteolytic effect limited to HPV-positive cancer cells or observed in other cells as well?
(3) Is STAT3 a decisive factor for the proliferation of HPV-positive cancer cells? Which potential downstream targets are responsive to STAT3 in these cells?
(4) Do STAT3 and the viral E6/E7 genes undergo a functional crosstalk in HPV-positive cancer cells, i.e. are STAT3 activities depending on the viral oncogenes and *vice versa*?
(5) Can inhibition of STAT3 sensitize HPV-positive cancer cells to drugs which are employed for targeted therapies?

Overall, this thesis aims to illuminate the role of STAT3 for the malignant phenotype of HPV-positive cancer cells and to obtain insights into the interplay between STAT3 and the HPV oncogenes. On the one hand, it is hoped that these investigations improve our understanding of the functional relevance of STAT3 in HPV-positive cancer cells and the significance of its interaction with oncogenic HPVs. On the other hand, the results of the planned studies should be informative for the prevailing concept that inhibiting STAT3 represents a highly attractive therapeutic strategy in HPV-positive cancer cells.

CHAPTER 2

Results

2. Results

2.1 Investigation of the destabilization of STAT3 by CPX-induced iron chelation

In view of the pronounced anti-tumorigenic effects of the iron chelator CPX in cervical cancer cells[86, 87], it was of high interest to gain mechanistic insights into the underlying process. Since STAT3 was reported to be an essential factor for stimulating proliferation[252, 255, 256, 265-268] and efficient viral E6/E7 oncogene expression[187, 251-253] in cervical cancer cells, I aimed to investigate whether destabilization of STAT3[119] is responsible for the anti-proliferative and E6/E7-inhibitory effects of CPX[86], and further, to gain first insights into the mechanism of STAT3 destabilization by CPX.

Because of STAT3's reported importance for many diseases[121, 122], including HPV-independent malignant and non-malignant diseases with high need for novel therapeutic options, I first assessed whether the repression of STAT3 by CPX is independent of HPV and whether it is conserved across cells of different histologic backgrounds. Thus, HPV-negative MeWo melanoma, HCT116 colorectal cancer, and FaDu and Cal27 head and neck squamous cell carcinoma (HNSCC) cells were treated with CPX, revealing that the effect on STAT3 is indeed HPV-independent, as STAT3 was clearly downregulated after 48 h in all investigated cell lines (Figure 2A). Additionally, I tested whether CPX could also downregulate STAT3 levels in non-cancerous cells, normal oral keratinocytes (NOKs)[289]. Comparable to the tested cancer cell lines, STAT3 protein levels were downregulated in NOKs starting after 48 h of CPX treatment (Figure 2B). These results indicate that the mechanism of STAT3 repression by CPX is conserved across cells of different histologic origins and is independent of their HPV-status or malignancy.

STAT3 is known to translocate to the mitochondria where it is reported to play a substantial oncogenic role[171, 190]. To study whether the mitochondrial STAT3 pool is affected by CPX as well, protein fractionation was performed after 48 h of CPX treatment in HPV16-positive SiHa cells, revealing that mitochondrial STAT3 protein levels are also strongly decreased (Figure 2C). Notably, the mitochondrial marker cytochrome C (cyt. C) is also found in the cytosolic protein fraction after CPX treatment, possibly due to mitochondrial release of cyt. C during apoptosis[290] which indeed can be induced by CPX treatment[86]. Thus, not only the cytosolic but also the mitochondrial pool of STAT3 with oncogenic potential[171, 190] is reduced by CPX.

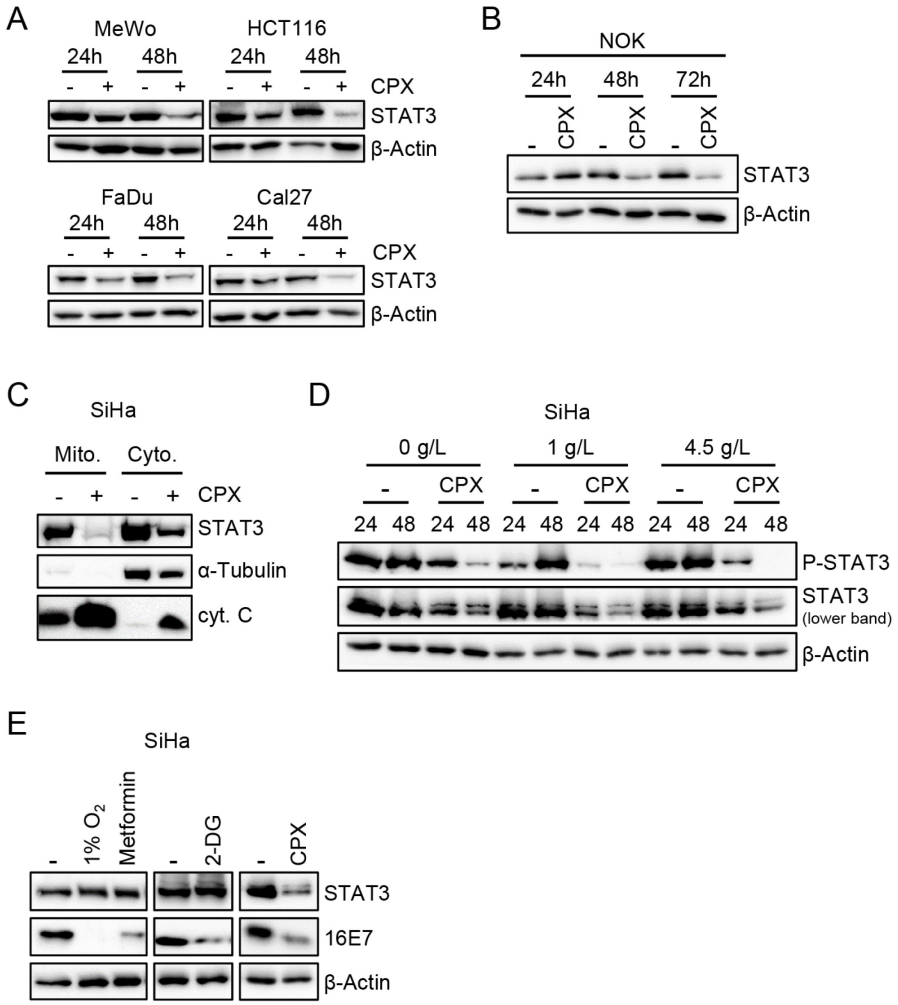

Figure 2: Downregulation of STAT3 protein levels by CPX. (A) *HPV-negative MeWo, HCT116, FaDu and Cal27 cells were treated for the indicated time periods with 10 µM CPX or solvent control (-) and analyzed by immunoblot for STAT3 protein levels. β-Actin, loading control. FaDu and Cal27 experiments were performed in cooperation with Maria Weber.* ***(B)*** *NOKs were treated and analyzed as in (A) for 24, 48 and 72h.* ***(C)*** *SiHa cells were treated as in (A) for 48 h followed by fractionation of mitochondrial proteins and analysis by immunoblot for STAT3 protein levels. α-Tubulin, cytosolic marker. cyt. C, mitochondrial marker.* ***(D)*** *SiHa cells were treated as in (A) for 24 or 48 h with glucose concentrations of 0 g/L, 1 g/L or 4.5 g/L and analyzed by immunoblot for P-STAT3 (Y705) and STAT3 protein levels. β-Actin, loading control.* ***(E)*** *SiHa cells were exposed to hypoxia (1 % O_2), 2.5 mM Metformin, 5 mg/mL 2-DG, 10 µM CPX or solvent control (normoxic conditions, 21% O_2) (-) for 24 h and analyzed by immunoblot for STAT3 and HPV 16E7 protein levels. β-Actin, loading control. Subfigure (A) and corresponding legend from Strobel et al., 2023[119].*

CPX as an iron chelator strongly affects the cellular metabolism and supplementation with high amounts of glucose can strongly influence the effects of CPX treatment[87]. Therefore, the question arose whether the repression of STAT3 might be linked to glucose-linked metabolic alterations in cervical cancer cells. However, in contrast to the CPX-induced repression of HPV E6/E7 oncogene expression, which can be counteracted by high glucose concentrations of 4.5 g/L[87], downregulation of total STAT3 and phosphorylated STAT3 Y705 levels by CPX treatment in SiHa cells was observed under all tested glucose concentrations of 4.5 g/L, 1 g/L

(standard cell culture concentration) and 0 g/L after 48 h (Figure 2D). These results indicate that the repression of STAT3 by CPX is largely independent of glucose availability.

Additionally, cells were investigated under further experimental conditions that can strongly affect the cellular metabolic state. In addition to the glycolysis inhibiting glucose analogue 2-DG[291], hypoxia and Metformin were employed which repress OXPHOS[292, 293] alike iron chelators such as CPX[87, 294]. Importantly, whereas all these conditions suppress HPV E6/E7 expression (Figure 2E), as seen for CPX[86] (Figure 2E), STAT3 protein levels were affected only by CPX treatment (Figure 2E). These latter results show that the inhibition of OXPHOS or glycolysis is not sufficient to induce the downregulation of STAT3 and, furthermore, also indicate that the repression of E6/E7 is not linked to a reduction of STAT3 protein levels.

Besides the metabolic similarities between hypoxia and iron chelator treatment, iron chelators are often used as hypoxia mimetics[295-298] due to the stabilizing action of iron insufficiency on the hypoxia inducible factor 1 alpha (HIF1α) protein[299]. Furthermore, both iron chelators, including CPX, as well as hypoxia induce upregulation of glycolytic genes[87] and inhibit mTOR signaling[86]. Yet, despite these similarities, application of CPX results in downregulation of STAT3 protein levels while hypoxia does not (Figure 2E). Therefore, existing proteome signatures of SiHa cells exposed to hypoxia or CPX[86] were systematically analyzed and compared with respect to factors and gene sets potentially involved in STAT3 degradation by CPX.

In line with above mentioned similarities between hypoxia and CPX treatment, gene set enrichment analyses[300] (GSEA) of the proteome data clearly shows an upregulation of hypoxia-linked proteins (gene set: HALLMARK_HYPOXIA) under both conditions (Figure 3A). Further, I identified in total 12 proteins by direct comparison of hypoxia and CPX proteome datasets with respect to proteins which are involved in protein degradation processes and are at the same time differentially expressed after CPX treatment but not under hypoxia. These factors could therefore potentially be involved in destabilization of the STAT3 protein (Figure 3B). Among them are one downregulated proteasome inhibitor protein, seven upregulated proteins with deubiquitinase activity, and four proteins linked to E3-ligase activity which are upregulated after CPX treatment but not under hypoxia. Additionally, GSEA was performed on gene sets involving processes potentially involved in protein degradation. Interestingly, I found the gene set REACTOME_SUMOYLATION_OF_UBIQUITINYLATION_PROTEINS as well as the gene set REACTOME_SUMOYLATION to be positively enriched in the CPX proteome screen compared to hypoxia (Figure 3C). This indicates that SUMOylation processes, which can generally be involved in protein stability[301], might be more active or involved factors at least increasingly expressed under CPX treatment compared to hypoxia.

A

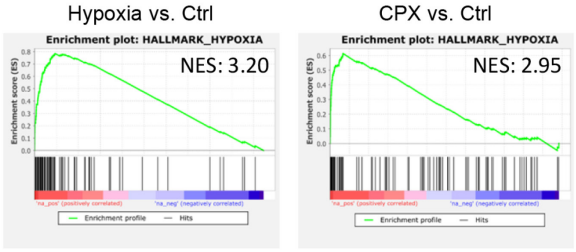

B

Symbol	Function	CPX	Hypoxia
STAT3	Transcr. factor	-1.47	0.23
PSMF1	Proteasome	-1.07	0.15
UCHL3	Deubiquitinase	-0.83	0.23
UCHL1		-1.04	-0.01
OTUB1		-0.76	0.23
USP5		-0.59	0.22
USP14		-0.67	0.13
USP15		-0.68	0.02
USP24		-0.80	-0.09
UHRF2	E3 ligase	0.86	0.20
RNF34		0.71	-0.08
RNF2		0.91	-0.24
DTL		0.86	-0.47

log2FC: 1 | 0 | -1

C

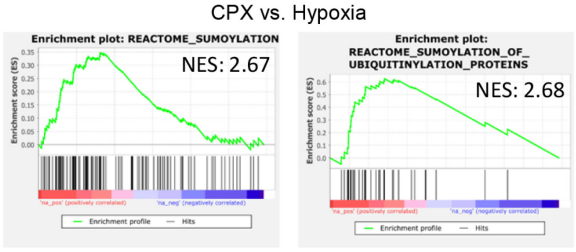

Figure 3: SUMOylation pathways and proteins involved in protein ubiquitination are differentially expressed after CPX compared to hypoxia treatment. (A) *GSEA was performed on existing proteome data[86] derived from SiHa cells treated with hypoxia (1% O_2) or CPX for 48 h for the indicated gene set.* ***(B)*** *proteome data as described in (A) was comparatively analyzed for proteins which are involved in ubiquitination and protein degradation processes and are differentially expressed under CPX treatment but not under hypoxia.* ***(C)*** *GSEA was performed as described in (A) for the indicated gene sets.*

The identification of these differentially regulated protein degradation-linked factors (Figure 3B) as well as the observed effects on SUMOylation (Figure 3C) could represent starting points for future studies investigating the destabilization of STAT3 on a mechanistic level in more detail.

Collectively, these findings indicate that the destabilization of the STAT3 protein by CPX' iron chelating activity effectively depletes cells of their total and mitochondrial STAT3 pool. The underlying mechanism is independent of the HPV status, is not affected by glucose and is conserved between cells of different histological origin. These observations indicate that CPX could be a highly interesting drug candidate to treat various STAT3-dependent diseases.

2.2 Assessment of the functional significance of STAT3 for cervical cancer cell proliferation

In view of the literature, which reports that STAT3 is an essential factor for the proliferation of cervical cancer cells[252, 255, 256, 265-268], I next aimed to elucidate whether the powerful anti-proliferative action of CPX[86, 87] in these cells might be linked to the destabilization of STAT3[119].

2.2.1 Chemical STAT3 inhibitors induce heterogeneous effects

Small molecule inhibitors of STAT3 are often used to investigate the oncogenic function of STAT3 in cancer cells[216]. I thus applied the commonly employed STAT3 inhibitors BP-1-102, C188-9, Cryptotanshinone, Niclosamide, Stattic and WP1066 and assessed their effect on the growth and cellular morphology of SiHa and HeLa cervical cancer cells by live-cell imaging at comparable concentrations or, due to observed strong toxicities in initial experiments, at concentrations lower than used in the literature[187, 251, 253], respectively. Concentrations of inhibitors, for which an application was not yet reported for cervical cancer cells, were titrated to inhibit STAT3 Y705 phosphorylation while inducing phenotypes similar to the phenotypes reported upon STAT3 inhibition in cervical cancer cells[251-253, 255, 265] with other small molecule inhibitors.

Each inhibitor, apart from BP-1-102 in HeLa cells, led to a strong reduction of proliferation in a time- and dose-dependent manner (Figure 4), as is found for CPX treatment[86, 87]. Notably, however, considerably variable time courses of growth inhibition (Figure 4) as well as different cellular morphologies were noted for individual inhibitors (Figure 5A, B). For example, the most widely used STAT3 inhibitor Stattic induced cell death and inhibited proliferation immediately after starting the treatment while C188-9 did only mildly affect HeLa and SiHa cells in the first 24-48 h followed by a sharp increase in its anti-proliferative activity (Figure 4). This was followed by the induction of cell death (Figure 5A, B) coinciding with its delayed anti-proliferative effect. Furthermore, even though growth curves of Cryptotanshinone, Niclosamide and BP-1-102 look similar in SiHa cells (Figure 4, upper panel), the cellular morphologies after treatment with these compounds looked vastly different (Figure 5A).

In view of these disparities, I additionally employed the well-established and clinically used JAK1/2 inhibitor Ruxolitinib[122], as JAK2 is known to be an important activator of STAT3 signaling and was shown to phosphorylate STAT3 at Y705 in cervical cancer cells[266]. If STAT3 signaling could be blocked by Ruxolitinib, I expected to observe a strong anti-proliferative effect, similar to the effects observed with direct STAT3 inhibitors as described above (Figure 4).

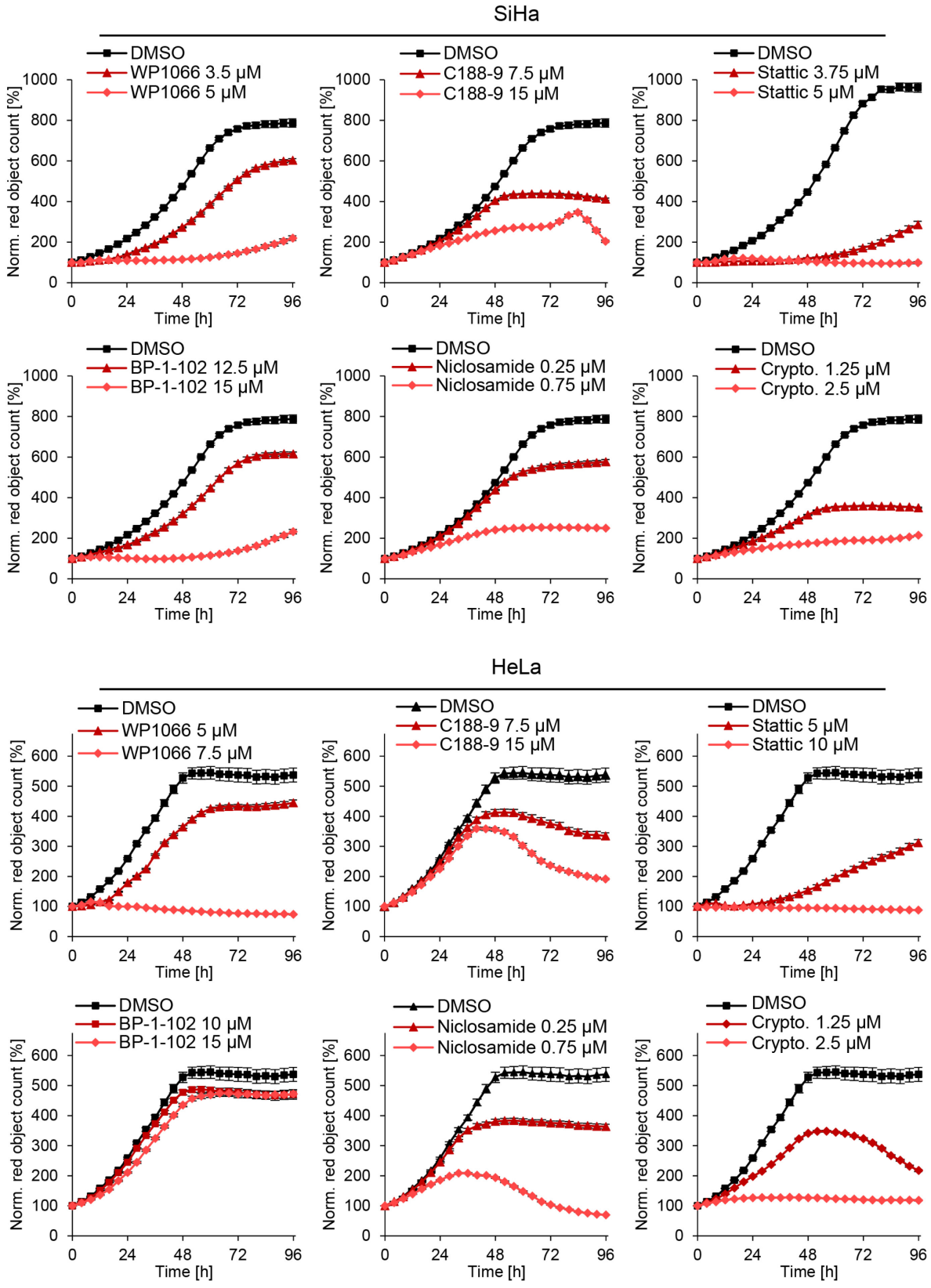

Figure 4: Small molecule STAT3 inhibitors induce heterogeneous effects on cervical cancer cell proliferation. *SiHa-mKate2 and HeLa-mKate2 cells were treated 48 h after seeding in 96-well plates (time point 0) with the indicated concentrations of different STAT3 inhibitors or solvent control for up to 96 h and imaged using the Incucyte® S3 live-cell imaging system. Image analysis and red object quantification (cell counts) were performed using the Incucyte® software package. Figure and legend from Strobel et al., 2023[119].*

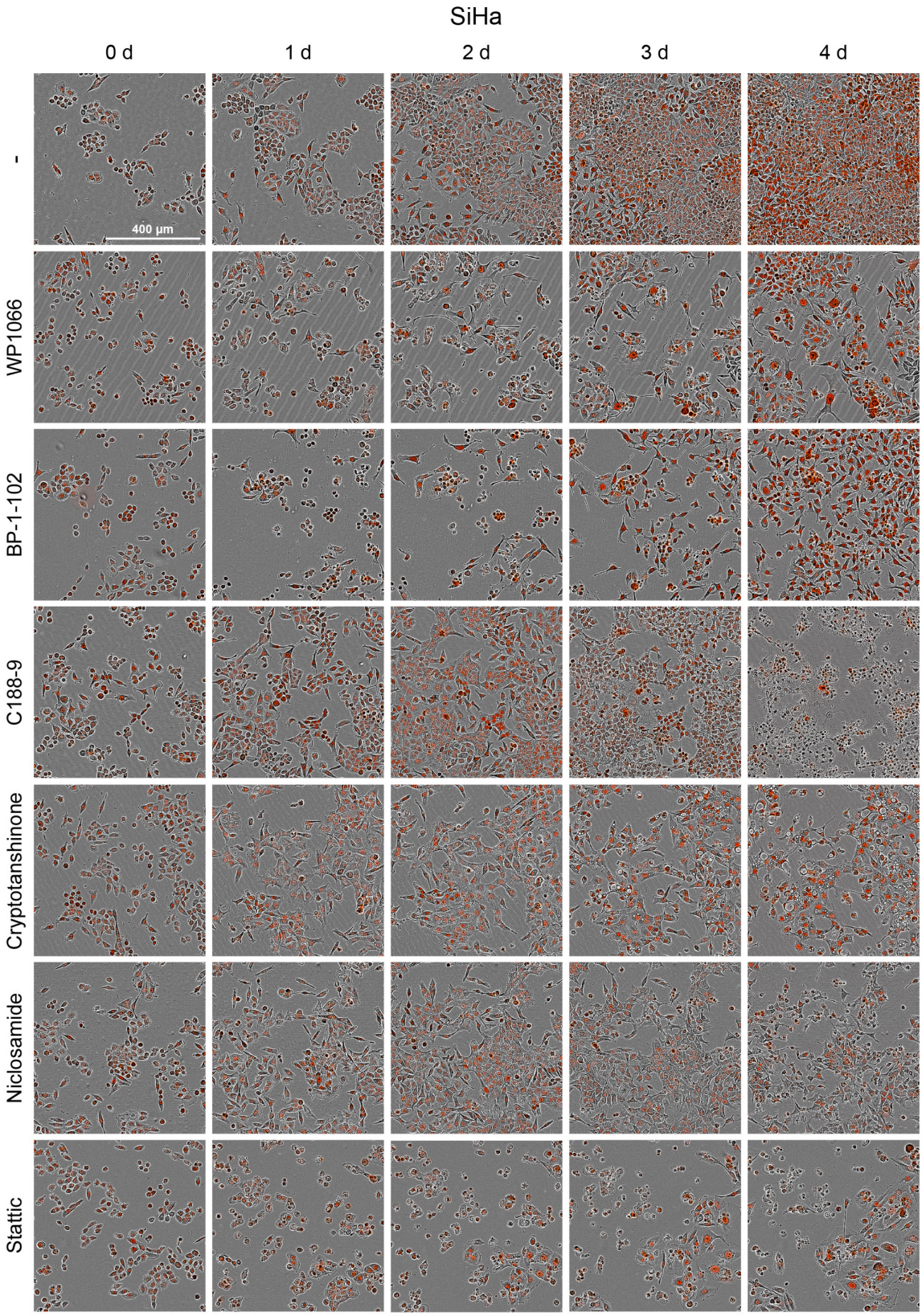
SiHa
0 d
1 d
2 d
3 d
4 d
-
WP1066
BP-1-102
C188-9
Cryptotanshinone
Niclosamide
Stattic
400 µm

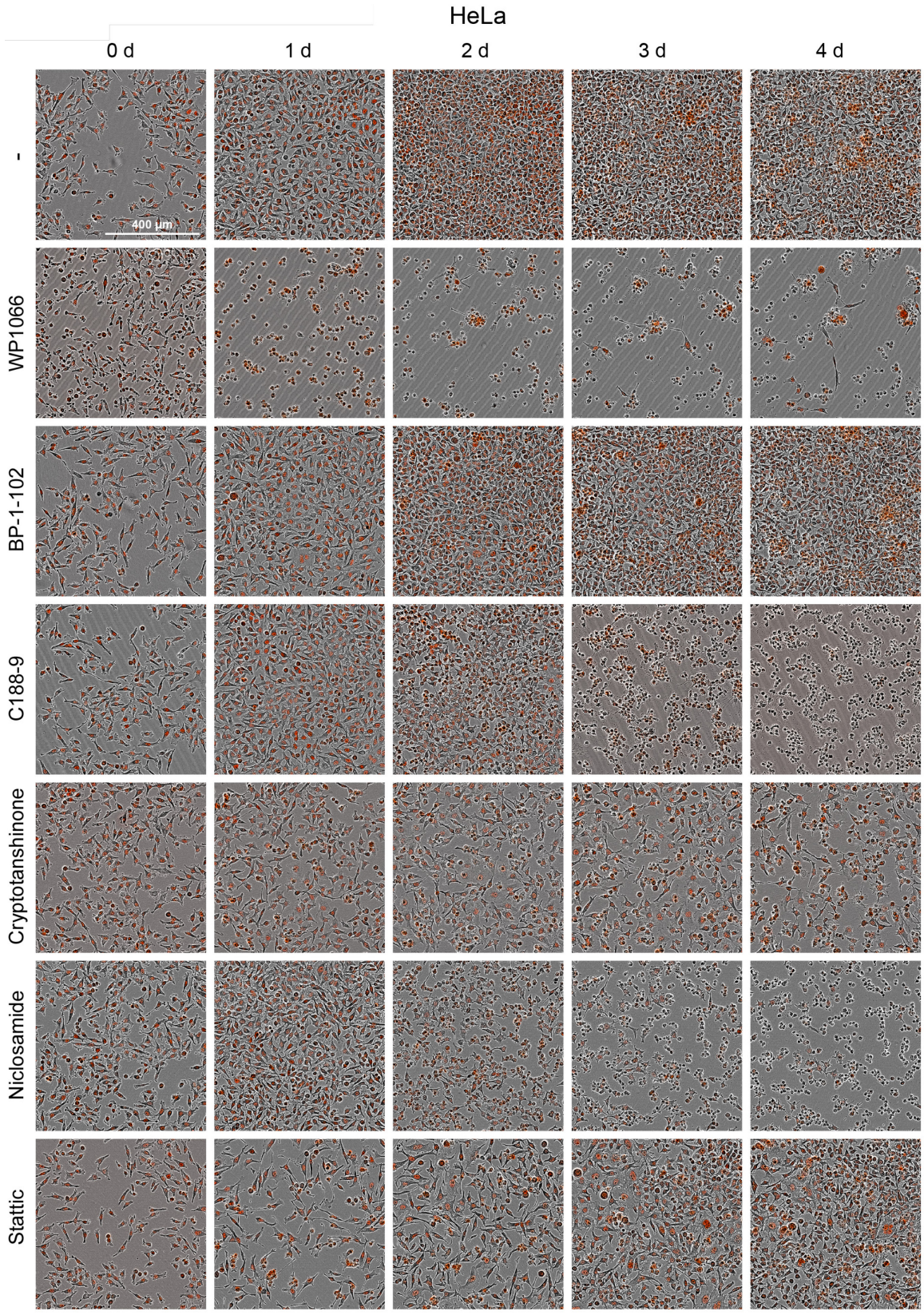

Figure 5 (incl. previous page): Chemical STAT3 inhibitors induce heterogeneous effects on cervical cancer cell morphology. *SiHa-mKate2 and HeLa-mKate2 cells were treated 48 h after seeding (time point 0) with 5 µM (SiHa) or 7.5 µM (HeLa) WP1066, 15 µM BP-1-102, 15 µM C188-9, 2.5 µM Cryptotanshinone, 0.75 µM Niclosamide, 3.75 µM (SiHa) or 5 µM (HeLa) Stattic, or solvent control (-), for up to 96 h and imaged using the Incucyte® S3 live-cell imaging system. Scale bar: 400 µm. Figure and legend from Strobel et al., 2023[119].*

Surprisingly, although STAT3 Y705 phosphorylation, which is integral for activation of canonical STAT3 signaling[126], was repressed with high efficacy by Ruxolitinib treatment (Figure 6A), growth curves obtained using live-cell imaging were unaffected in SiHa, CaSki and HeLa cells over a time span of up to 96 h (Figure 6B). Importantly, the cells retained their normal morphology during Ruxolitinib treatment and showed no signs of cell death (Figure 7) despite the depletion of phosphorylated STAT3 Y705.

Additionally, to assess if efficient inhibition of JAK/STAT3 signaling for an extended time period might influence growth or survival of cervical cancer cells, colony formation assays (CFAs) were performed in the presence of Ruxolitinib for 10-14 days. However, colony formation rate was unchanged for SiHa, CaSki and HeLa cells treated with Ruxolitinib, compared to solvent control (Figure 6C). Furthermore, concentrations of Ruxolitinib exceeding those needed to efficiently block STAT3 Y705 phosphorylation were tested to investigate whether these show an effect on proliferation, however this was not the case either (Figure 6D). These concentrations of up to 10 µM did also not induce any signs of cell death and did not severely alter cellular morphologies (not shown) which is in stark contrast to the tested small molecule STAT3 inhibitors (Figure 5A, B). In conclusion, these findings reveal striking differences for different small molecule STAT3 inhibitors regarding their effect on proliferation and cell morphology of cervical cancer cells. Moreover, the JAK1/2 inhibitor Ruxolitinib showed no effect on short- or long-term proliferation or cellular morphology of cervical cancer cells despite efficiently blocking STAT3 Y705 phosphorylation.

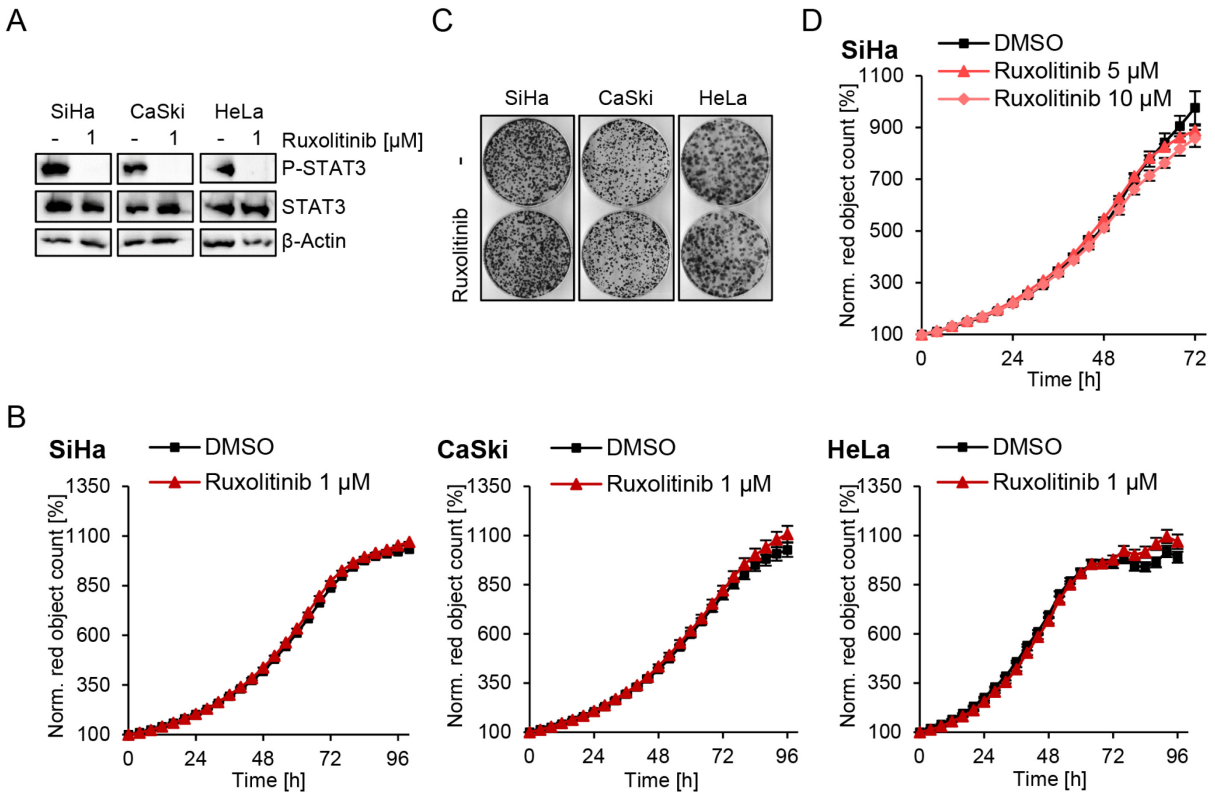

Figure 6 (previous page): Inhibition of STAT3 Y705 phosphorylation by Ruxolitinib does not affect cervical cancer cell proliferation. (A) *SiHa, CaSki and HeLa cells were treated with 1 µM Ruxolitinib or solvent control (-) for 96 h and analyzed by immunoblot for P-STAT3 Y705 and total STAT3 protein levels. β-Actin, loading control.* ***(B)*** *SiHa-mKate2, CaSki-mKate2 and HeLa-mKate2 cells were treated 48 h after seeding in 96-well plates with 1 µM Ruxolitinib (time point 0) or solvent control for up to 96 h and imaged using the Incucyte® S3 live-cell imaging system. Image analysis and red object quantification (cell counts) were performed using the Incucyte® software package.* ***(C)*** *3000 SiHa, CaSki or HeLa cells were seeded in 6 cm plates followed by treatment with 1 µM Ruxolitinib or solvent control (-) starting 48 h after seeding. Every 3-4 days, the cell culture medium was exchanged with fresh medium containing 1 µM Ruxolitinib. Colonies were fixed and stained after 14-15 days.* ***(D)*** *SiHa-mKate2 were treated and analyzed as in (A) with 5 µM or 10 µM Ruxolitinib, or solvent control, for up to 72 h. Figure and legend from Strobel et al., 2023[119].*

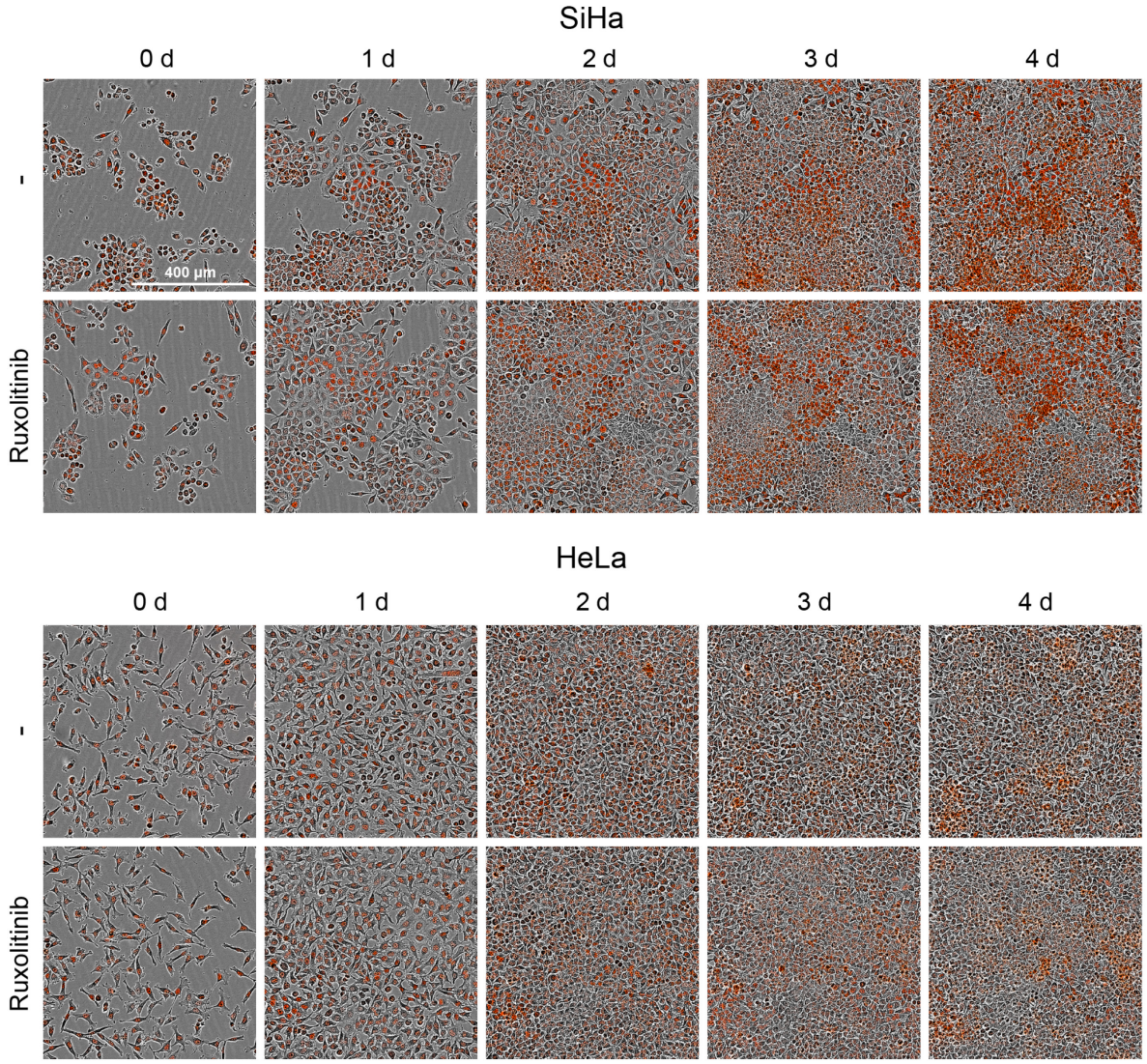

Figure 7: Cervical cancer cell morphology is not affected by Ruxolitinib treatment. *SiHa-mKate2 (upper panels) and HeLa-mKate2 (lower panels) cells were treated 48 h after seeding (time point 0) with 1 µM Ruxolitinib or solvent control (-) for up to 96 h and imaged using the Incucyte® S3 live-cell imaging system. Scale bar: 400 µm. Figure and legend from Strobel et al., 2023[119].*

Since members of the HER-family such as EGFR are reported to activate STAT3[132, 133], I also tested if HERs might participate in regulating STAT3 activity in cervical cancer cells. Further,

to assess whether HER activity might affect proliferation, potentially through STAT3, HeLa and SiHa cells were treated with the HER1/2/3 inhibitor Sapitinib[302] and analyzed using live-cell imaging.

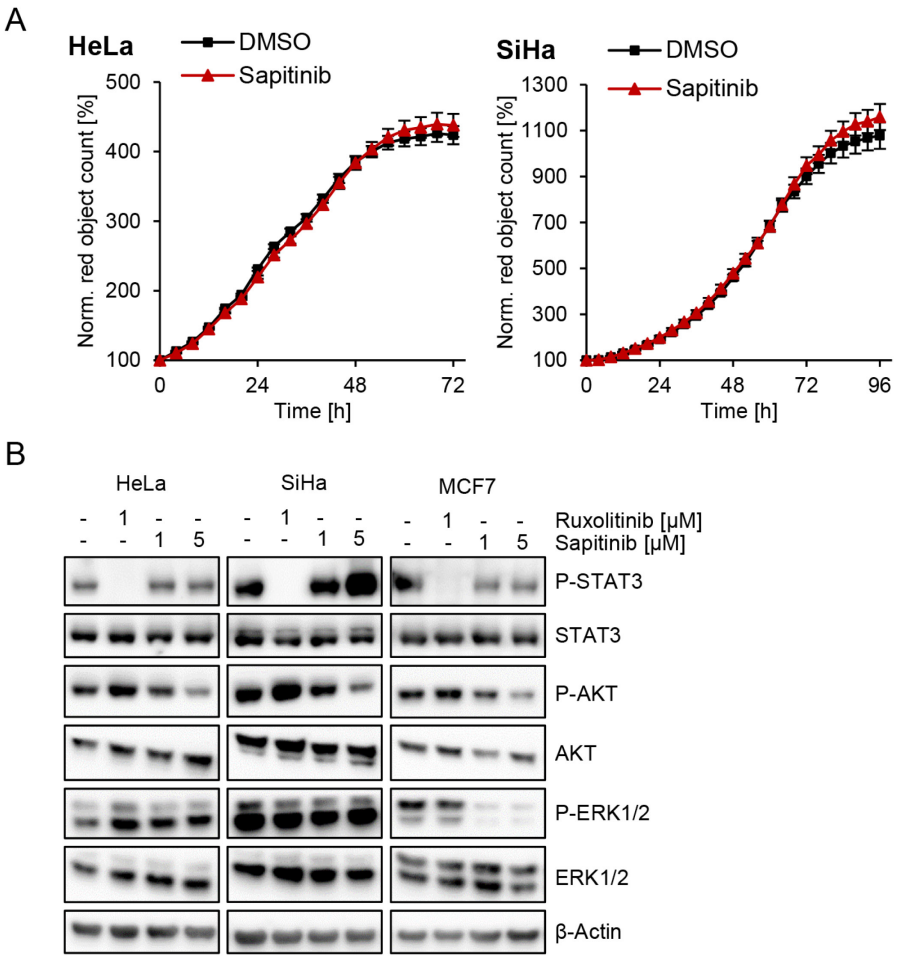

Figure 8: Inhibition of HER1/2/3 by Sapitinib does not affect STAT3 Y705 phosphorylation and proliferation in cervical cancer cells. (A) *HeLa-mKate2 and SiHa-mKate2 cells were treated 48 h after seeding in 96-well plates with 5 µM Sapitinib (time point 0) or solvent control for up to 96 h and imaged using the Incucyte® S3 live-cell imaging system. Image analysis and red object quantification (cell counts) were performed using the Incucyte® software package.* ***(B)*** *HeLa, SiHa and MCF7 cells were treated with 1 µM Ruxolitinib, 1 or 5 µM Sapitinib or solvent control (-) for 96 h and analyzed by immunoblot for P-STAT3 Y705, total STAT3, P-AKT S473, total AKT, P-ERK1/2 T202/Y204 and total ERK1/2 protein levels. β-Actin, representative loading control.*

Interestingly, despite the reported oncogenic role of EGFR in HPV infected cells[303] as well as invasive cervical cancer[304, 305], proliferation was unchanged in HeLa and SiHa cells after Sapitinib treatment (Figure 8A). Moreover, Sapitinib did neither block STAT3 Y705 phosphorylation nor phosphorylation of other targets further downstream of HERs such as EGFR, including extracellular signal-regulated kinase 1/2 (ERK1/2)[306] and protein kinase B/AKT[306] in HeLa and SiHa cells at 1 µM. Notably, at a higher concentration of 5 µM only phosphorylation of AKT was reduced (Figure 8B). As a positive control for the efficacy of

Sapitinib treatment, the breast cancer cell line MCF7 was analyzed, which is described to express moderate levels of EGFR[307]. In contrast to HeLa and SiHa cells, Sapitinib reduced phosphorylation of STAT3, AKT and ERK1/2 in MCF7 cells (Figure 8B), indicating that these effects are cell line dependent.

Consistent with my previous results, Ruxolitinib completely blocked STAT3 Y705 phosphorylation in all three analyzed cell lines while showing no inhibitory effect on the phosphorylation of other tested proteins (Figure 6, Figure 8B). These results indicate that HERs, including EGFR, do not play a major role for the regulation of STAT3 activity in HeLa and SiHa cells and thus, to efficiently block STAT3 signaling in these cells, Ruxolitinib was used in further experiments.

2.2.2 STAT3 repression by genetic interference does not influence proliferation

Considering the discordant observations for the tested small molecule STAT3 inhibitors (Figure 4, Figure 5) in comparison to Ruxolitinib (Figure 6), I utilized genetic techniques to further elucidate the role of STAT3 for proliferation in cervical cancer cells. To inhibit both canonical and non-canonical STAT3 functions I employed RNAi (Figure 9A, C) and CRISPR/Cas9 gene editing (Figure 9D). For RNAi, four distinct STAT3-targeting small interfering RNAs (siRNAs), each binding to different exons conserved in all, or almost all, respectively, known transcript classes were employed (please refer to 4.1.4). Notably, as seen for STAT3 inhibition by Ruxolitinib, cell proliferation was unaffected when these siRNAs were applied as pools in HeLa and SiHa cells (Figure 9A). In comparison, blocking expression of the growth-promoting[12, 308, 309] HPV E6/E7 oncogenes by RNAi virtually completely inhibited the proliferation of HeLa and SiHa cells under the same experimental conditions (Figure 9B). Although all individual STAT3-targeting siRNAs efficiently repressed STAT3 at the protein and RNA level in all three cell lines also when applied individually (Figure 10A), siRNAs #2 and #6 slightly repressed proliferation in SiHa and CaSki cells (Figure 9C). In HeLa cells, siRNA #6 did not affect proliferation but siRNA #2 induced cytotoxic effects in initial experiments (not shown). This indicates at most only minor STAT3-independent, siRNA-specific off-target effects on the proliferation of SiHa and CaSki cells for siRNA #2 and #6 while siRNA #2 was excluded for experiments with HeLa cells.

To further complement and extend these results to also investigate a long-term depletion of STAT3, I employed two independent STAT3 KO (knockout) single cell clones each of SiHa and HeLa parental origin, respectively. For establishing efficient STAT3 KO, the CRISPR/Cas9 technology with two distinct guide RNAs (gRNAs), each for one HeLa and one SiHa STAT3 KO clone, was used with the objective to reduce potential gRNA-specific off-target effects, which could lead to misinterpretations.

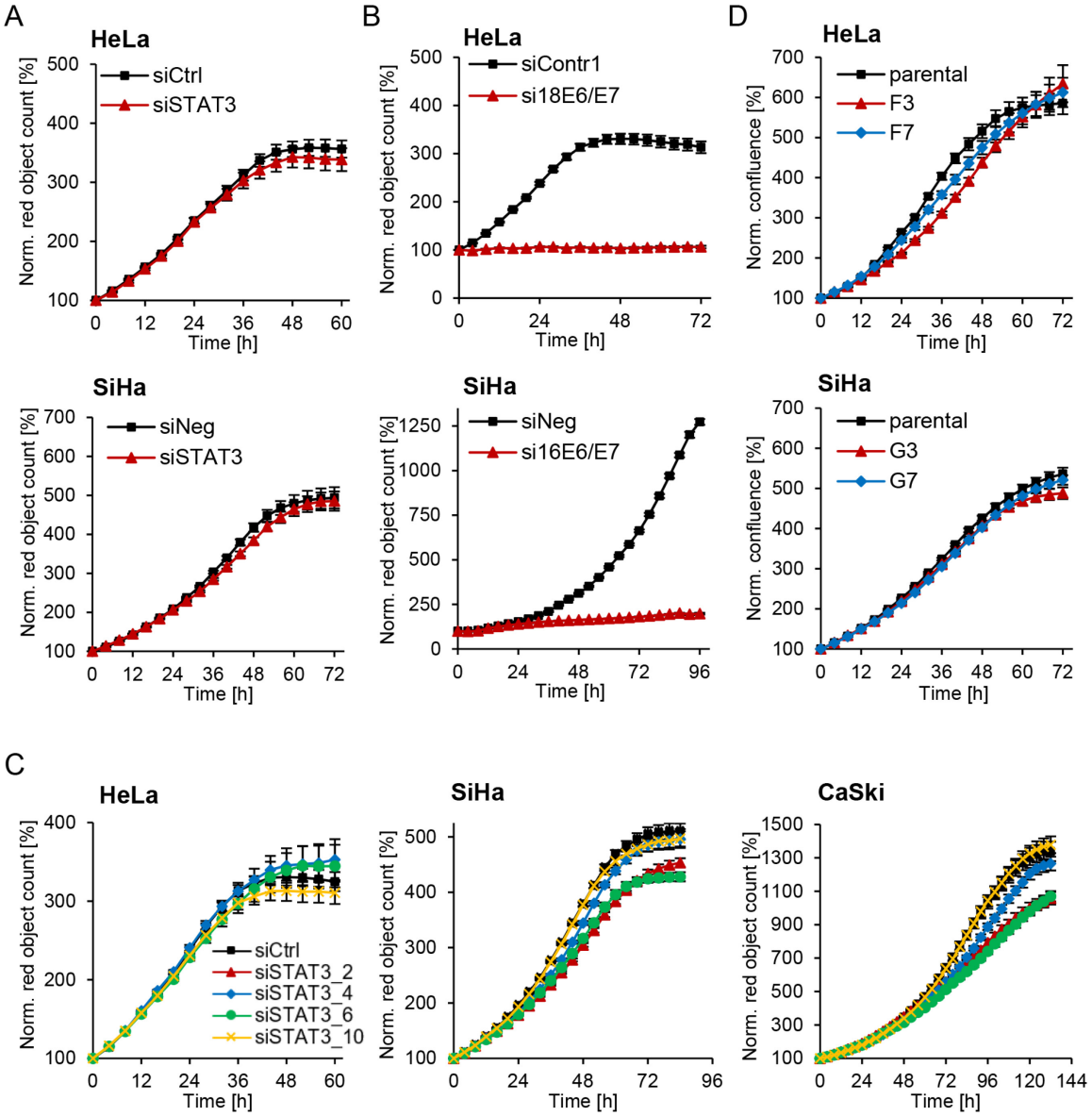

Figure 9: STAT3 depletion by genetic interference does not appreciably influence the proliferation of cervical cancer cells. (A) *HeLa-mKate2 and SiHa-mKate2 cells were reverse transfected in 96-well plates with a STAT3-targeting siRNA pool (siSTAT3) or control-siRNA (siCtrl, siNeg). Imaging started 48 h after transfection (time point 0) for up to 72 h using the Incucyte® S3 live-cell imaging system. Image analysis and red object quantification (cell counts) were performed using the Incucyte® software package.* ***(B)*** *HeLa-mKate2 and SiHa-mKate2 cells were reverse transfected with the indicated HPV16 or HPV18 E6/E7-targeting siRNA pools or control siRNAs and imaged and analyzed as in (A) for up to 96 h.* ***(C)*** *HeLa-mKate2, SiHa-mKate2 and CaSki-mKate2 cells were reverse transfected with the indicated STAT3-targeting or control siRNAs and imaged and analyzed as in (A) for up to 144 h.* ***(D)*** *Parental HeLa and SiHa cells, HeLa STAT3 KO cell clones F3 and F7 and SiHa STAT3 KO cell clones G3 and G7 were seeded in 96-well plates and imaged as in (A), starting 48 h after seeding (time point 0). Image analysis and cell confluence quantification were performed using the Incucyte® software package. SiHa STAT3 KO clones were generated in cooperation with Maria Weber. Figure content and corresponding legends from Strobel et al., 2023[119].*

Importantly, although I did not detect any STAT3 protein expression in all four established STAT3 KO single cell clones (Figure 10B), proliferation remained largely unchanged

compared to the corresponding parental cell lines (Figure 9D). These results are in line with those I obtained for the application of STAT3-targeting siRNAs (Figure 9A, C, D), collectively demonstrating that genetic depletion of STAT3 expression does not appreciably influence the proliferation of cervical cancer cells.

Despite the distinct functions for different STAT family members in cancer[310, 311], different STAT proteins can possess partly overlapping activities [312], can partly share the same target genes[313] and can be activated in response to the same cytokines[314, 315], especially upon loss of one STAT member[314, 315]. To exclude the possibility that the STAT3 KO clones might have adapted to compensate for the loss of STAT3 through upregulation of signaling via other STAT molecules such as STAT1 or STAT5A/B (STAT5), total protein as well as phosphorylation levels of STAT1 and STAT5 at Y701 or Y694/699, respectively, were determined by immunoblotting (Figure 10B). Interestingly, while total levels of STAT1 and STAT5 were, as expected, unaffected by STAT3 KO, levels of STAT5 Y694/699 phosphorylation were downregulated in all STAT3 KO clones of either SiHa or HeLa parental origin (Figure 10B). In contrast, phosphorylated STAT1 stayed largely unchanged, except for HeLa STAT3 KO clone F7 which showed a slight upregulation of STAT1 Y701 phosphorylation levels (Figure 10B). Collectively, these findings show that neither STAT1 nor STAT5 signaling are consistently or considerably upregulated to potentially compensate for the loss of STAT3. Rather, the downregulation of STAT5 Y694/699 phosphorylation in STAT3 KO clones indicates that activity of STAT5 signaling might be dependent on active STAT3 in cervical cancer cells.

Taken together, these findings demonstrate that the proliferation rate of cervical cancer cells does not depend on the expression or activation of STAT3 under the tested conditions of short- or long-term chemical (Ruxolitinib) or genetic (RNAi, CRISPR/Cas9 KO) STAT3 inhibition.

2.3 Investigation of the interconnection of STAT3 and the HPV E6/E7 oncogenes

Of particular interest for the field of HPV-induced carcinogenesis, STAT3 has been attributed to promote HPV *E6/E7* oncogene expression[187, 251-253], which is essential for the growth and survival of cervical cancer cells[12, 308, 309] (Figure 9B). *Vice versa*, expression of the E6/E7 oncogenes, particularly of E6, was described to induce the activation of STAT3[251, 253, 255], reportedly via increased IL6-induced STAT3 Y705 phosphorylation[253]. This crosstalk between viral oncoproteins and STAT3 is thus hypothesized to play a decisive role for driving the oncogenic phenotype of cervical cancer cells[248-250], which may also be important under therapeutic aspects.

2.3.1 The expression of HPV E6/E7 is not dependent on STAT3

In light of my findings that neither chemical (Ruxolitinib) nor genetic (RNAi, CRISPR/Cas9 KO) STAT3 inhibition reduced the proliferation of HPV-positive cancer cells, the reported dependence of E6/E7 expression on STAT3 signaling is surprising: Since the E6/E7 oncogenes are essential for cervical cancer cell proliferation, a downregulation of E6/E7 through STAT3 inhibition should consequently strongly impair proliferation.

However, in line with my findings that STAT3 is not a relevant factor for proliferation under the tested conditions while depletion of E6/E7 by RNAi strongly blocked proliferation, efficient RNAi-mediated silencing of STAT3 in SiHa, HeLa and CaSki cells using four different siRNAs did not lead to a considerable and consistent downregulation of HPV E6/E7 expression at both the protein (Figure 10A, upper panels) and the RNA level (Figure 10A, lower panels). In comparison, I observed a pronounced and significant reduction of transcript levels of the well-characterized STAT3 target *SOCS3*[149-151] in SiHa and CaSki cells after silencing of STAT3 expression (Figure 10A, lower panels), indicating that STAT3 signaling is in principle active and functional in these cells. In contrast, in HeLa cells, expression of *SOCS3* remained largely unaltered.

In addition, also in SiHa and HeLa STAT3 KO cells, E6/E7 protein expression did not considerably differ in comparison to the corresponding parental cell lines (Figure 10B). In line with this, *E6/E7* was unchanged on transcript levels in SiHa STAT3 KO cells (Figure 10C, left panel) as well, while in HeLa STAT3 KO cells, I observed a tendency towards slightly reduced *E6/E7* transcript levels (Figure 10C, right panel). To assess the regulation of E6/E7 expression by an unrelated strategy to modulate STAT3 activities, HeLa cells were transfected with either empty pcDNA3 expression vector (control), wildtype STAT3-encoding pcDNA3 or pcDNA3 encoding a dominant-negative variant of STAT3 (Y705F-mutated[316, 317]). As expected, ectopic

overexpression of wildtype STAT3 resulted in strongly increased STAT3 Y705 phosphorylation levels while ectopic overexpression of Y705F-mutated STAT3 resulted in modestly decreased levels (Figure 10D). However, both conditions also did not affect the expression of E6 or E7 (Figure 10D).

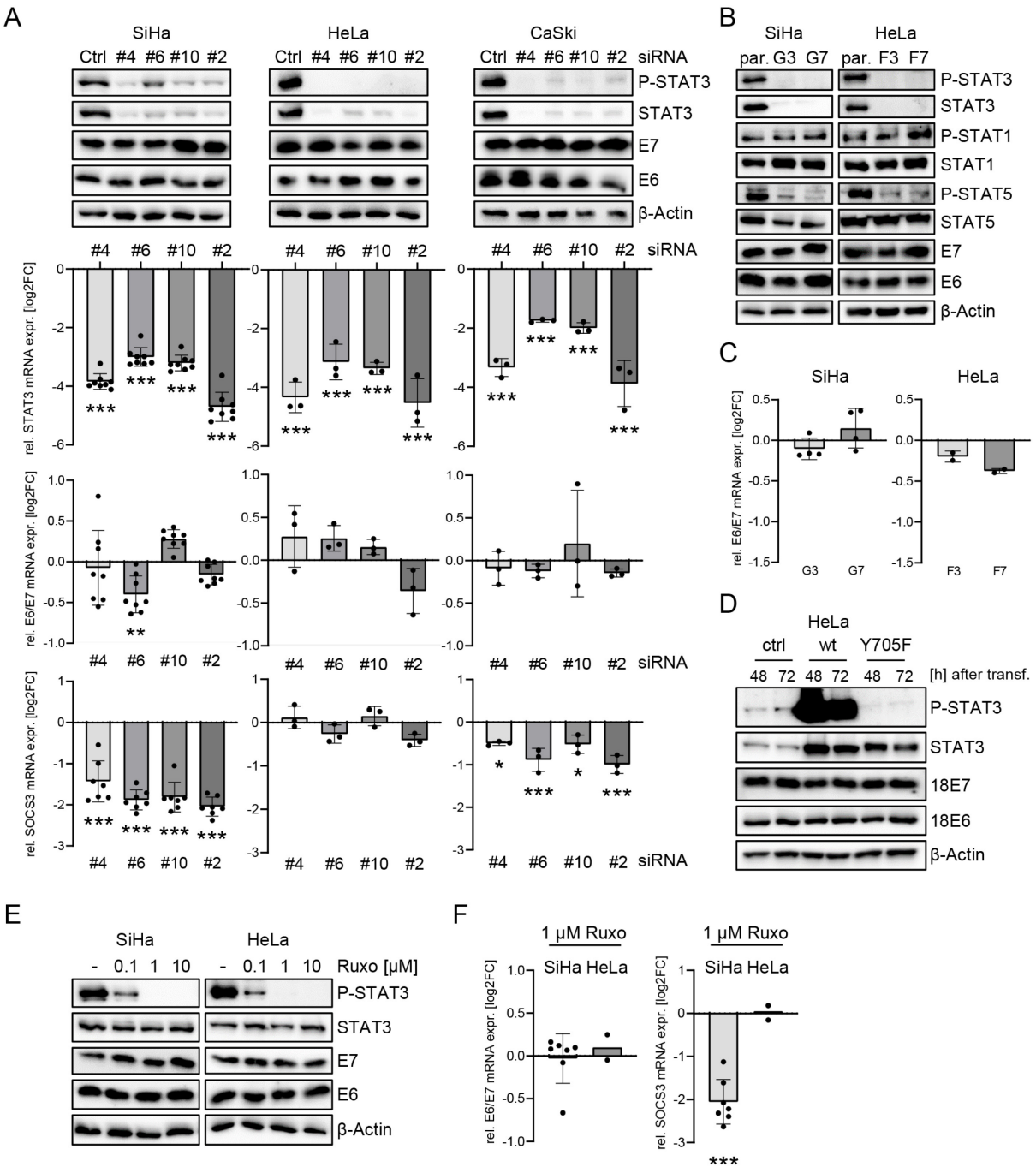

Figure 10: Inhibition, depletion or ectopic overexpression of STAT3 does not influence levels of E6/E7 in cervical cancer cells. (A) *SiHa, HeLa and CaSki cells were reverse transfected with the indicated STAT3-targeting siRNAs and analyzed by immunoblot for P-STAT3 Y705, total STAT3, HPV E6 and HPV E7 protein levels. β-Actin, representative loading control. STAT3 (upper panels), HPV E6/E7 (middle panels) and SOCS3 (lower panels) transcript levels were analyzed by qRT-PCR. Shown are the log_2-transformed fold changes (log_2FC) of mean expression with standard deviations. Statistically significant differences in cells transfected with siSTAT3 compared to control siRNA*

*($log_2FC = 0$) were determined by one-way ANOVA. *: $p < 0.05$, **: $p < 0.01$, ***: $p < 0.001$. **(B)** Parental (par.) SiHa and HeLa cells, SiHa STAT3 KO cell clones G3 and G7 and HeLa STAT3 KO cell clones F3 and F7 were analyzed 72 h after seeding by immunoblot for P-STAT3 Y705, total STAT3, P-STAT1 Y701, total STAT1, P-STAT5A/B Y 694/699, total STAT5A/B, HPV E6 and HPV E7 protein levels. β-Actin, representative loading control. **(C)** Transcript levels of HPV E6/E7 of cells treated as in (B) were analyzed by qRT-PCR. Shown are the log_2-transformed fold changes (log_2FC) of mean expression with standard deviations. Statistically significant differences in STAT3 KO cells compared to parental cell lines ($log_2FC = 0$) were determined by one-way ANOVA. **(D)** HeLa cells were transfected with pcDNA3-STAT3, pcDNA3-STAT3-Y705F or empty (control) pcDNA3 expression vector and analyzed by immuniblot for P-STAT3 Y705, total STAT3, HPV E6 and HPV E7 protein levels. β-Actin, representative loading control. **(E)** SiHa and HeLa cells were treated 24 h after seeding with indicated Ruxolitinib concentrations or solvent control (-) for 24 h and analyzed by immunoblot for P-STAT3 Y705, total STAT3, HPV E6 and HPV E7 protein levels. β-Actin, representative loading control. **(F)** Analysis of HPV E6/E7 and SOCS3 transcript levels of cells treated as in (E) by qRT-PCR. Shown are the log_2-transformed fold changes (log_2FC) of mean expression with standard deviations. Ruxolitinib- and solvent control-treated cells ($log_2FC = 0$) were analyzed for statistically significant differences by a two-tailed t-test. ***: $p < 0.001$. Subfigures (A), (B) and (F) as well as subfigures (D) and (E) and corresponding legends are from or extended from, respectively, Strobel et al., 2023[119].*

Corroborating these results, upon treatment of SiHa and HeLa cells with Ruxolitinib, E6/E7 protein (Figure 10E) and mRNA levels (Figure 10F, left panel) also remained unchanged despite efficient, dose-dependent inhibition of STAT3 Y705 phosphorylation (Figure 10E). In comparison, *SOCS3* transcript levels were strongly and significantly repressed in SiHa cells after Ruxolitinib treatment while they were unaffected in HeLa cells (Figure 10F, right panel), similar to the results obtained after STAT3 silencing by RNAi (Figure 10A).

Conversely, I assessed whether STAT3 might influence E6/E7 expression if the activity of STAT3 is elevated beyond its constitutive level. Therefore, I employed the cytokine Oncostatin M (OSM), which is known to strongly induce STAT3 Y705 phosphorylation in cervical cancer cells[264, 273]. As reported[318], and similar to ectopic STAT3 overexpression (Figure 10D), levels of STAT3 Y705 phosphorylation were strongly increased in SiHa and HeLa cells by OSM treatment for 1 h (Figure 11A). Despite this increase, however, E6 and E7 protein levels remained unchanged (Figure 11A). Moreover, HPV *E6/E7* transcript levels were also unaffected (Figure 11B, right panel) whereas mRNA levels of *SOCS3* were strongly and significantly elevated by OSM (Figure 11B, left panel) in both SiHa and HeLa cells. Additionally, it was tested whether proliferation rate of HeLa, SiHa or CaSki cells is increased when treated with OSM, however this was not the case either (Figure 11C). In summary, these results, obtained by using five different experimental methods to modulate STAT3 activity or expression, provide strong evidence that STAT3 does not play a major role in regulating the expression of HPV E6/E7 in cervical cancer cells, at least under standard *in vitro* conditions, in contrast to previous reports[187, 251-253].

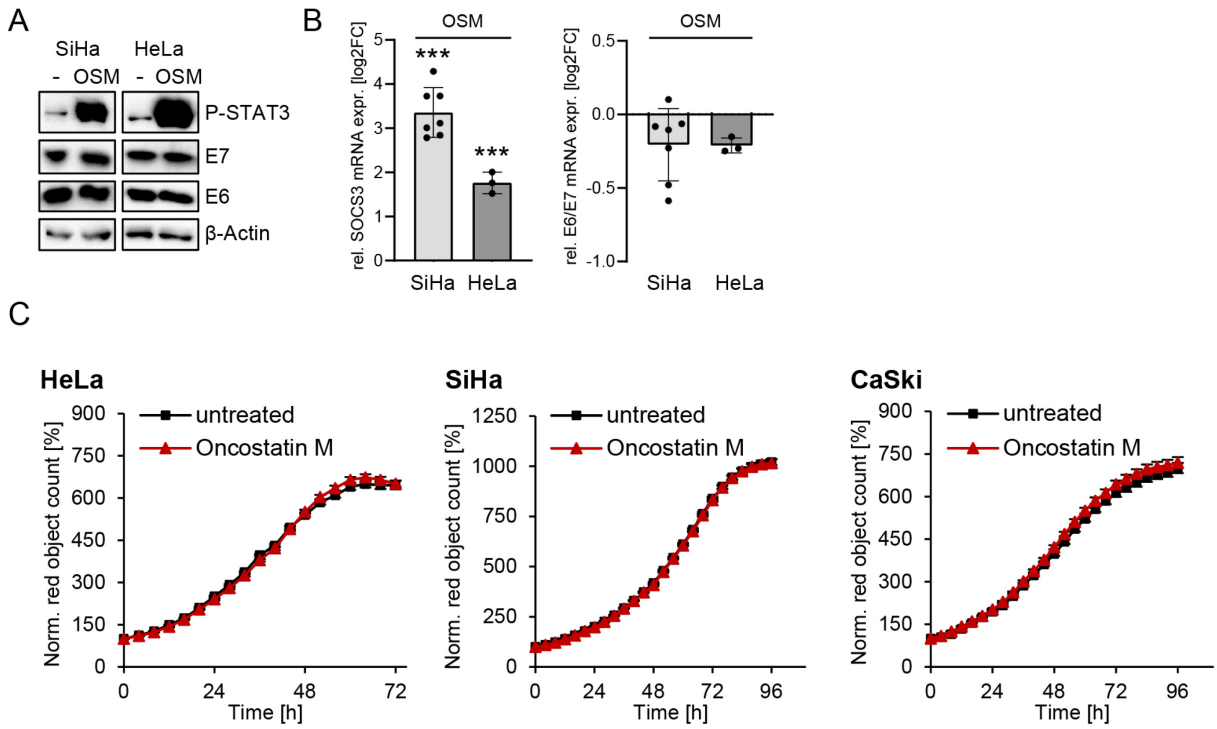

Figure 11: STAT3 activation by OSM treatment does not increase HPV E6/E7 expression or proliferation of cervical cancer cells. (A) *SiHa and HeLa cells were treated 48 h after seeding with 10 ng/mL OSM for 1 h and analyzed by immunoblot for P-STAT3 Y705, total STAT3, HPV E6 and HPV E7 protein levels. β-Actin, representative loading control.* ***(B)*** *SiHa and HeLa cells were treated as in (A), followed by analysis of SOCS3 and HPV E6/E7 transcript levels by qRT-PCR. Shown are the log_2-transformed fold changes (log_2FC) of mean expression with standard deviations. Statistically significant differences in cells treated with OSM compared to solvent control ($log_2FC = 0$) were determined by a two-tailed t-test. ***: $p < 0.001$.* ***(C)*** *HeLa-mKate2, SiHa-mKate2 and CaSki-mKate2 cells were treated with 10 ng/mL OSM or solvent control 48 h after seeding (time point 0) for up to 96 h and imaged using the Incucyte® S3 live-cell imaging system. Image analysis and red object quantification (cell counts) were performed using the Incucyte® software package. Figure content and corresponding legends from Strobel et al., 2023[119].*

2.3.2 Levels of STAT3 Y705 phosphorylation are not decreased by E6/E7 silencing

Vice versa, to analyze if the HPV oncogenes may activate STAT3 signaling in cervical cancer cells, RNAi was employed to deplete endogenous E6 or E6/E7 levels in HeLa and SiHa cells for 72 h. In contrast to previous reports[251, 253], STAT3 Y705 phosphorylation was not decreased despite efficient E6 silencing (Figure 12A). Interestingly, STAT3 Y705 phosphorylation levels were rather induced by combined silencing of E6 and E7 in HeLa cells while they stayed unchanged in SiHa cells (Figure 12A).

For further assessment of whether the downregulation of E6/E7 expression may generally lead to increased STAT3 Y705 phosphorylation levels, as seen in HeLa cells before (Figure 12A), cells were grown under hypoxia (1% O_2) or treated with Metformin (Figure 12B) - two conditions previously shown to strongly downregulate E6/E7 protein and transcript levels[84, 319, 320].

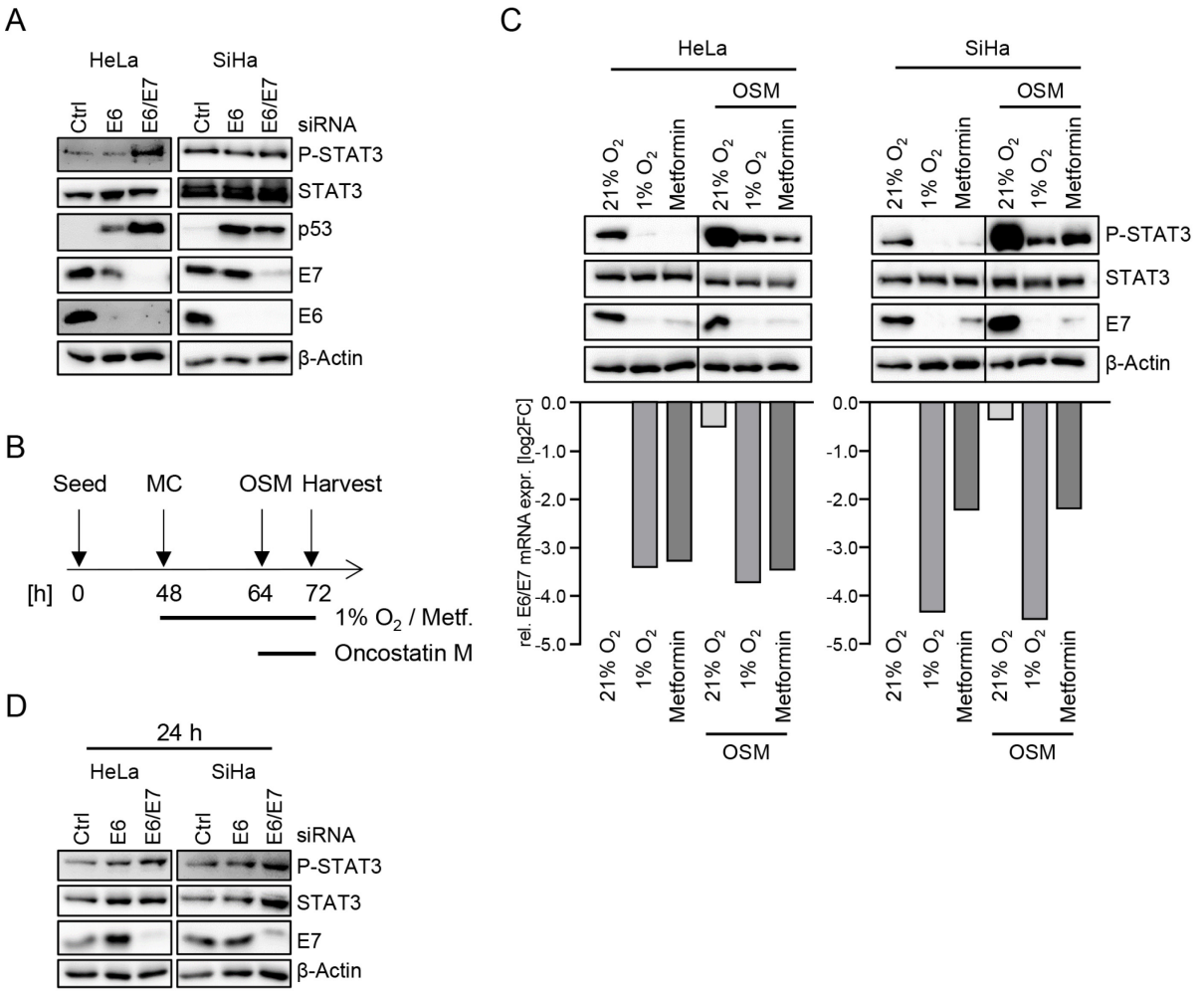

Figure 12: HPV E6/E7 downregulation by RNAi, hypoxia or Metformin does not affect STAT3 Y705 phosphorylation in a consistent manner in cervical cancer cells. (A) *HeLa and SiHa cells were transfected with siRNA targeting HPV E6 or E6/E7, or with control siRNA (siCtrl). P-STAT3 Y705, total STAT3, HPV E6, HPV E7 and p53 protein levels were analyzed by immunoblot 72 h after transfection. β-Actin, representative loading control.* ***(B)*** *Design of experiments performed for the results presented in (C). MC, medium exchange.* ***(C)*** *HeLa and SiHa cells were cultivated under hypoxia (1% O_2) or treated under normoxia (21% O_2, standard cell culture) with 2.5 mM Metformin, 10 ng/mL OSM or solvent control (normoxic conditions, 21% O_2) as visualized in (B) and analyzed by immunoblot (upper panels) for P-STAT3, total STAT3 and HPV E7 protein levels. β-Actin, representative loading control. Vertical lines between lanes indicate where original images of the same immunoblots were spliced for the purpose of presentation. Immunoblots for total STAT3, HPV E7 and β-Actin of SiHa cells have been already shown in Figure 2E and are reincluded here for didactic reasons. SOCS3 (middle panels) and HPV E6/E7 (lower panels) transcript levels were analyzed by qRT-PCR. Shown are log_2-transformed fold changes (log_2FC) of relative expression (solvent control (normoxic conditions, 21% O2): $log_2FC = 0$) corresponding to samples of the same cells also used for immunoblots (upper panels).* ***(D)*** *HeLa and SiHa cells were transfected as in (A). P-STAT3 Y705, total STAT3 and HPV E7 protein levels were analyzed by immunoblot 24 h after transfection. β-Actin, loading control. Subfigure (A) and correspondonding legend from Strobel et al., 2023[119].*

Interestingly, STAT3 Y705 phosphorylation levels were strongly reduced after both hypoxia or Metformin treatment in HeLa and SiHa cells while E7 levels were downregulated on protein and RNA level (Figure 12C) to a similar extent compared to E6/E7 silencing by RNAi

(Figure 12A). These findings thus differ from the results obtained after RNAi-mediated, selective silencing of E6/E7 expression under normoxia (Figure 12A), possibly due to the broad spectrum of additional cellular effects induced by hypoxia or metformin.

Notably, in contrast to metformin treatment or hypoxia, targeted repression of E6 and E7 leads to rapid induction of senescence[63, 64] which can, for example by using RNAi, already be clearly seen after 72 h[319] (not shown). Since senescence is often linked to the induction of the senescence associated secretory phenotype (SASP)[321] of which IL-6 is an important mediator and which can lead to the activation of STAT3[322, 323], the question arose whether the increased STAT3 Y705 phosphorylation in HeLa cells might be a secondary effect of siE6/E7-mediated senescence induction. To address this question, E6 or E6 and E7 were silenced for 24 h only (Figure 12D), after which clear phenotypic changes towards senescence are not yet observable (not shown) while E7 levels are already knocked down as evidenced by immunoblotting (Figure 12D). Interestingly, considering levels of total STAT3 and the β-Actin loading control, STAT3 Y705 phosphorylation remained largely unchanged or only minimally increased, respectively, under this condition (Figure 12D). This indicates that the increased STAT3 Y705 phosphorylation in HeLa cells seen after silencing E6/E7 for 72 h by RNAi might indeed be linked to secondary cellular effects, e.g. related to senescence induction.

Conversely, to assess whether the downregulation of E6/E7 under hypoxia or Metformin treatment might be related to the repression of STAT3 activity, cells were co-treated under these experimental conditions with OSM to activate STAT3 (Figure 12B). In line with my previous results indicating no effect of STAT3 activity on E6/E7 expression (Figure 10, Figure 11), OSM treatment under hypoxia and Metformin did not reactivate E6/E7 expression (Figure 12C). At the same time, STAT3 Y705 phosphorylation after OSM treatment under hypoxia or combined with Metformin treatment reached levels comparable to normoxic (21% O_2) control cells which express E6/E7 (Figure 12C). Collectively, these findings do not provide evidence for a substantial, mutual stimulatory interconnection between STAT3 and the E6/E7 oncogenes in cervical cancer cells.

2.3.3 STAT3 may influence senescence induction of HeLa cells after E6/E7 silencing

As STAT3 Y705 phosphorylation was induced in HeLa cells 72 h after E6/E7 silencing, but not in SiHa cells, and since STAT3 activity was previously described to be linked to senescence[322, 323], the question arose whether STAT3 might play a role for senescence induction after E6/E7 silencing in HeLa cells.

To investigate this question, SiHa and HeLa cells were co-transfected with siRNA pools targeting E6/E7 or STAT3, either alone or in combination (Figure 13A) for 72 h. Interestingly,

in CFAs (Figure 13B) of HeLa cells, around two times more clones grew out after co-silencing of E6/E7 and STAT3 (Figure 13C), compared to silencing E6/E7 alone.

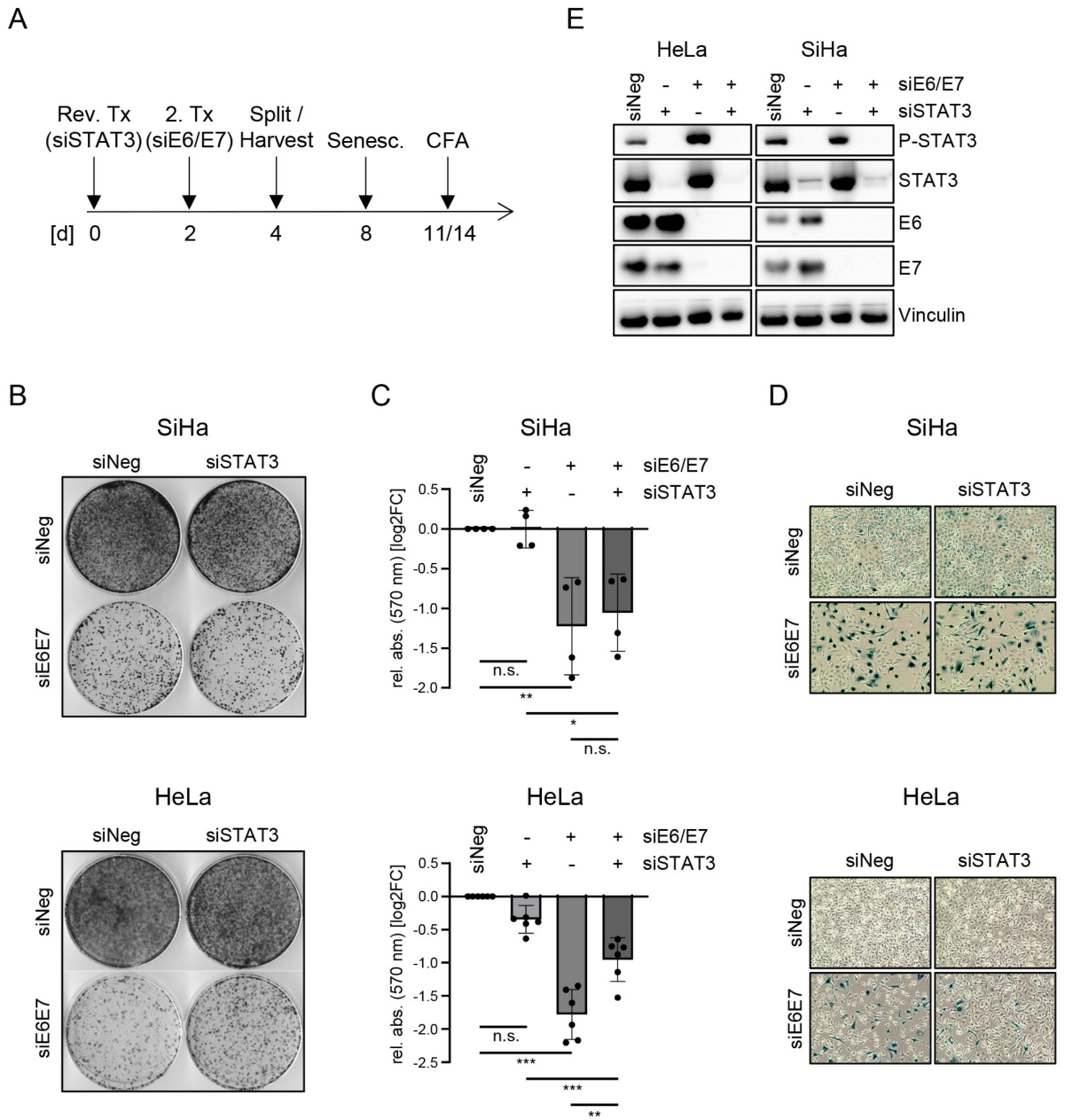

Figure 13: Knockdown of STAT3 increases colony formation rate after E6/E7 silencing by RNAi in HeLa cells. (A) *Experimental setup as performed in (B)-(E). SiHa and HeLa cells were co-transfected with pools of siRNAs targeting STAT3, E6/E7 or control siRNA (siNeg) as indicated.* ***(B)*** *Exemplary CFAs and* ***(C)*** *quantification of CFAs.* ***(D)*** *Senescence assays.* ***(E)*** *Analyses of P-STAT3 Y705, total STAT3, HPV E6 and HPV E7 by immunoblot. Vinculin, representative loading control.*

In senescence assays (Figure 13D), lower numbers of senescent HeLa cells, as indicated by blue staining[324, 325] (please refer to 4.1.7), were seen under the same condition while STAT3 Y705 phosphorylation was again found to be increased (Figure 13E). None of these effects were seen in SiHa cells as colony formation assays, senescence assays and STAT3 Y705 phosphorylation were largely unchanged when comparing E6/E7 silencing alone with

combined E6/E7 and STAT3 knockdown. These results thus correlate with previously observed levels of STAT3 Y705 phosphorylation after silencing of E6/E7 for 72 h which were induced in HeLa cells while they remained largely unchanged in SiHa cells (Figure 12A).

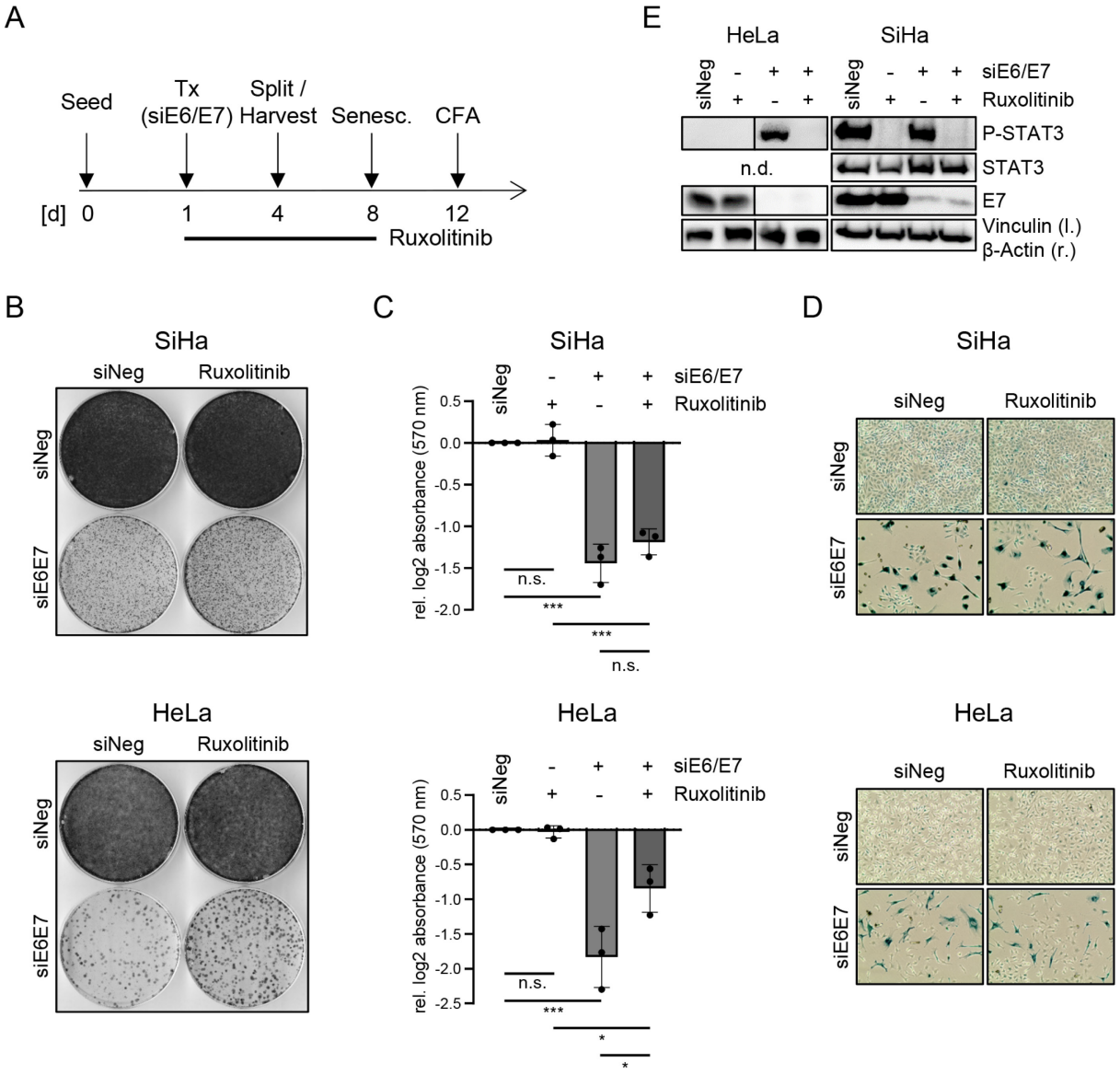

Figure 14: Inhibition of STAT3 activity by Ruxolitinib increases colony formation rate after E6/E7 silencing by RNAi in HeLa cells. (A) *Experimental setup as performed in (B)-(E). SiHa and HeLa cells were transfected with a pool of E6/E7-targeting siRNAs or control siRNA (siNeg) and co-treated with 1 µM Ruxolitinib as indicated.* ***(B)*** *Exemplary CFAs and* ***(C)*** *quantification of CFAs.* ***(D)*** *Senescence assays.* ***(E)*** *Analyses of P-STAT3 Y705, total STAT3, HPV E6 and HPV E7 protein levels by immunoblot. Vinculin, β-Actin, representative loading controls. Vertical lines between lanes indicate where original images of the same immunoblots were spliced for the purpose of presentation.*

I further validated my findings by transfection of SiHa and HeLa cells with E6/E7 targeting siRNA pools and co-treatment with Ruxolitinib to block STAT3 activity by chemical means instead of using STAT3-inhibitory siRNAs. To ensure continuous inhibition of STAT3 signaling, treatment with Ruxolitinib started from transfection until 7 days thereafter and was renewed on

day 4 (Figure 14A). Interestingly, in line with the results for combined RNAi-mediated E6/E7 and STAT3 silencing, a strong increase in the number of HeLa clones in CFAs was observed after combined E6/E7 knockdown and Ruxolitinib treatment (Figure 14B, C). Likewise, less HeLa cells stained positive in senescence assays (Figure 14D) under this condition. For SiHa cells, a similar trend in CFA analyses (Figure 14B) was observed, although this effect was less pronounced than in HeLa cells. At the same time however, no difference between E6/E7 silencing combined with Ruxolitinib treatment and E6/E7 silencing alone was seen in senescence assays for SiHa cells (Figure 14D). On the protein level, STAT3 Y705 phosphorylation was again induced after E6/E7 knockdown in HeLa cells while it remained unchanged in SiHa cells (Figure 14E). Ruxolitinib treatment efficiently inhibited STAT3 Y705 phosphorylation in both SiHa and HeLa cells (Figure 14E), as expected from my previous findings (Figure 5A, Figure 10E).

Collectively, these results demonstrate that in HeLa cells, levels of STAT3 Y705 phosphorylation correlate with the extent of senescence induction after knockdown of HPV E6/E7. However, whether this observation relies on a direct involvement of STAT3 in this process in HeLa cells must be further investigated in the future. In contrast to the finding in HeLa cells, no clear correlation between STAT3 Y705 phosphorylation and siE6/E7-mediated senescence induction was observed in SiHa cells, indicating a cell type-specific regulation.

2.4 Assessment of STAT3-independent effects of small molecule STAT3 inhibitors

Next, I addressed the question why all tested small molecule STAT3 inhibitors, many of which are binding directly to STAT3[275], induced anti-proliferative effects in cervical cancer cells in initial experiments (Figure 4). This finding has been linked in the literature to their repressing effects on E6/E7 expression[187, 251-253], which is in stark contrast to my results obtained on the JAK1/2 inhibitor Ruxolitinib (Figure 6) or genetic interference with STAT3 expression by RNAi or CRISPR/Cas9 gene editing (Figure 9). One possible explanation for this discrepancy could be provided by target-independent toxicities, which are often observed for anti-cancer small molecule inhibitors, even for those reaching clinical trials[326]. I therefore aimed to investigate whether off-target effects might potentially explain the diverse anti-proliferative effects of chemical STAT3 inhibitors observed in my experiments (Figure 4) as well as in the literature[251-253, 255, 265].

2.4.1 STAT3 small molecule inhibitors induce distinct cytotoxicities unrelated to STAT3

To this end, an approach inspired by Peretz et al.[327] was used: The employed inhibitors were analyzed in both parental SiHa and SiHa STAT3 KO cells by live-cell imaging, at the same concentration ranges as used in my previous experiments (Figure 4). Due to the inherent loss of STAT3 in KO cells, effects of STAT3 inhibitors on proliferation should not be observable if these effects are truly linked to inhibition of STAT3. In contrast, if the inhibitors induce the same effects in both parental SiHa and SiHa STAT3 KO cells, these effects are likely STAT3-independent.

Strikingly, all tested STAT3 inhibitors which acted growth-inhibiting in parental SiHa cells (Figure 4) also blocked the proliferation of SiHa STAT3 KO cells to a comparable extent (Figure 15A), indicating that their anti-proliferative effect is STAT3-independent. To complement these findings, cytotoxicity was analyzed by live-cell imaging using the Incucyte® Cytotox Green reagent (please refer to 4.1.6). Quantification of Cytotox-positive cells revealed the induction of cell death in both parental SiHa as well as SiHa STAT3 KO cells (Figure 15B) by all STAT3 inhibitors, apart from Niclosamide, which however induced a cellular morphology resembling cell death (Figure 16). Niclosamide might therefore induce a form of cell death not leading to staining of dead cells by the Cytotox Green reagent. Generally, however, all STAT3 inhibitors induced distinct morphologic alterations similar in both parental and STAT3 KO cells (Figure 16). In contrast, Ruxolitinib did not induce Cytotox-positive cell death or any morphologic alteration resembling cell death in neither parental nor STAT3 KO cells (Figure 17A, B). These results, demonstrating highly similar phenotypic responses of both

parental and STAT3 KO cells, support the notion that the tested STAT3 inhibitors can induce substantial STAT3-unrelated effects at commonly used concentrations.

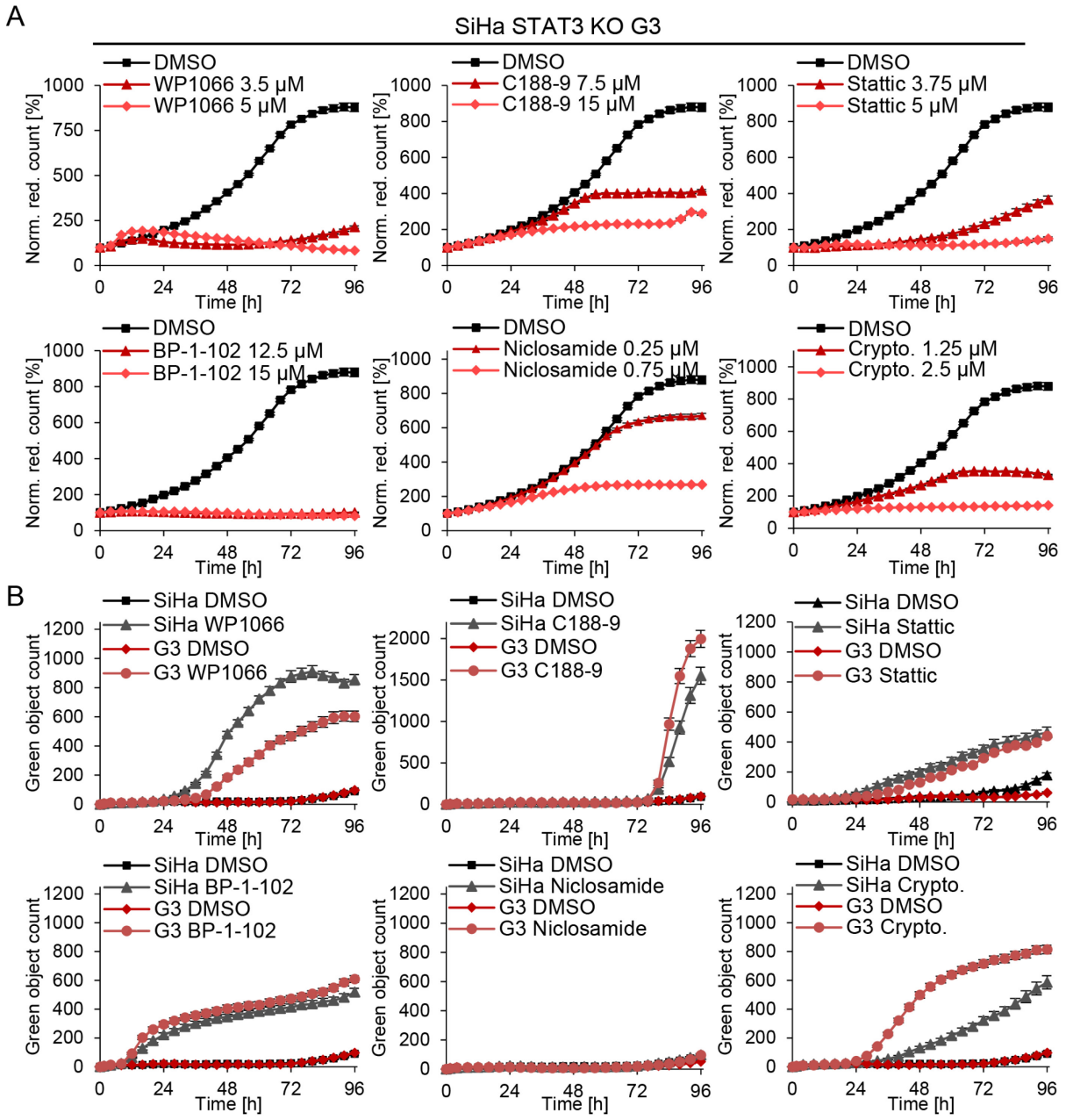

Figure 15: Small molecule inhibitors of STAT3 repress growth and induce cell-death in both parental SiHa and SiHa STAT3 KO cells. (A) *mKate2-labelled SiHa STAT3 KO G3 cells were treated 48 h after seeding in 96-well plates (time point 0) with the indicated STAT3 inhibitors or solvent control (-) at the depicted concentrations for up to 96 h and imaged by the Incucyte® S3 live-cell imaging system. Image analysis and red object quantification (cell counts) were performed using the Incucyte® software package.* ***(B)*** *Parental SiHa and SiHa STAT3 KO G3 cells were cultivated as in (A) with addition of 100 nM of the cell death marker Incucyte® Cytotox green. Figure content and corresponding legend from Strobel et al., 2023[119].*

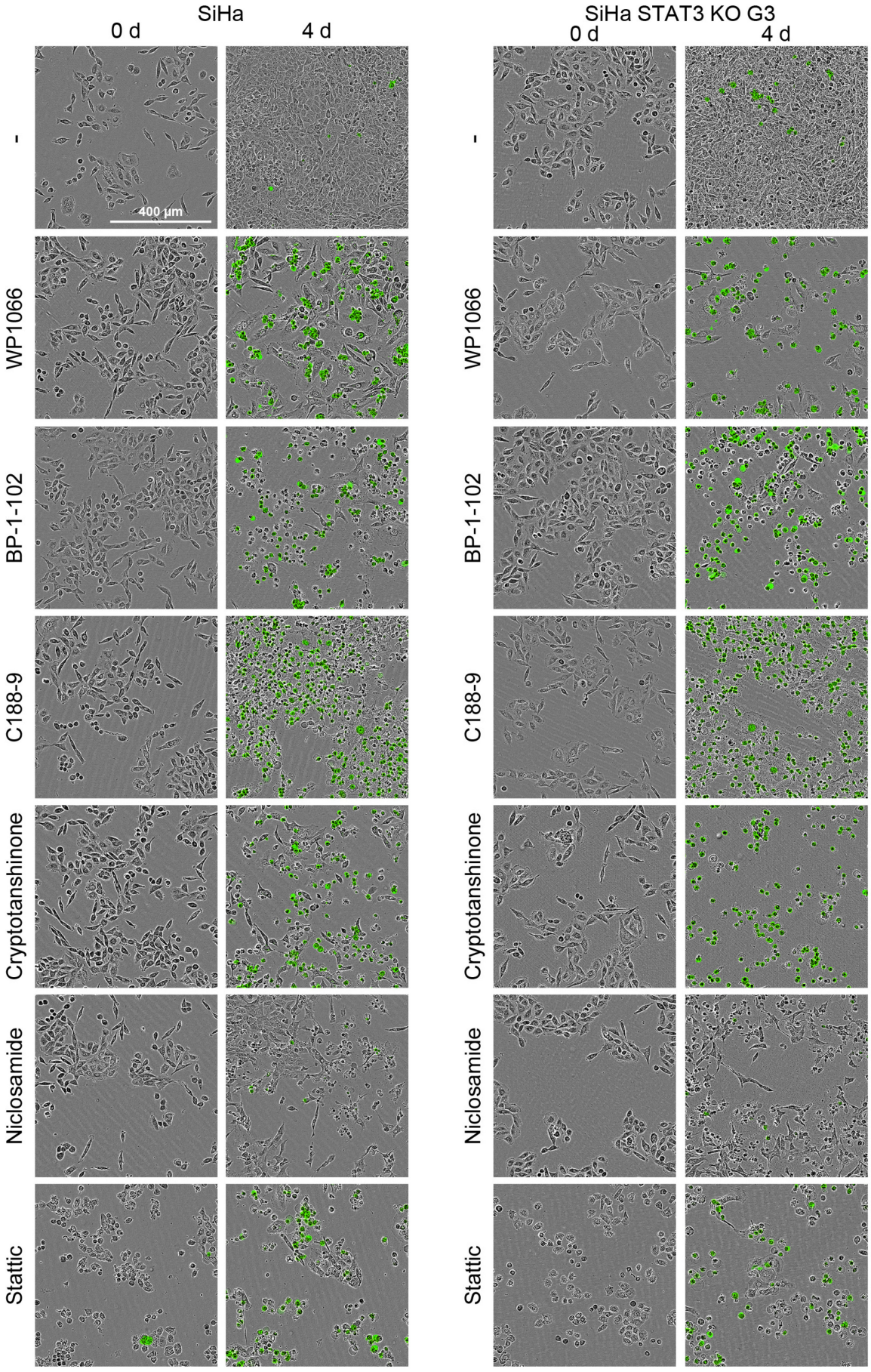
SiHa
0 d
4 d
SiHa STAT3 KO G3
0 d
4 d
-
WP1066
BP-1-102
C188-9
Cryptotanshinone
Niclosamide
Stattic
400 µm

Figure 16 (previous page): Small molecule inhibitors of STAT3 induce cell death and distinct morphologic alterations similar in both parental SiHa and SiHa STAT3 KO cells. *SiHa and SiHa STAT3 KO G3 cells were treated 48 h after seeding in 96-well plates (time point 0) with 5 µM WP1066, 15 µM BP-1-102, 10 µM C188-9, 5 µM Cryptotanshinone, 1.25 µM Niclosamide, 5 µM Stattic, or solvent control (-), for 96 h. Cytotox Green reagent was used at a concentration of 100 nM and added at the time of treatment. Images were acquired by the Incucyte® S3 live-cell imaging system. Scale bar: 400 µm. Figure and legend from Strobel et al., 2023[119].*

Moreover, I found that all tested small molecule STAT3 inhibitors affected activation of the cervical cancer-linked[39, 81-83, 328] PI3K/AKT/mTOR- or MAPK pathways or altered the expression of p53 or E6/E7 in parental SiHa cells (Figure 18 left panel). For example, C188-9, Niclosamide, Cryptotanshinone, BP-1-102, WP1066 and Stattic effectively reduced phosphorylation levels of AKT or 4E-BP1, indicative of inhibition of the PI3K/AKT/mTOR pathway. Similarly, Niclosamide blocked the phosphorylation of ERK while Cryptotanshinone and C188-9 treatment led to an induction of ERK phosphorylation levels. Further, C188-9, BP-1-102 and Niclosamide strongly downregulated the expression of p53. Overall, the different STAT3 inhibitors each affected a different combination of cervical cancer-linked pathways, indicating that these modulations are independent of their inhibitory effect on STAT3. Importantly, and in line with the literature[187, 251-253], all tested direct STAT3 inhibitors also repressed E6/E7 on the protein level.

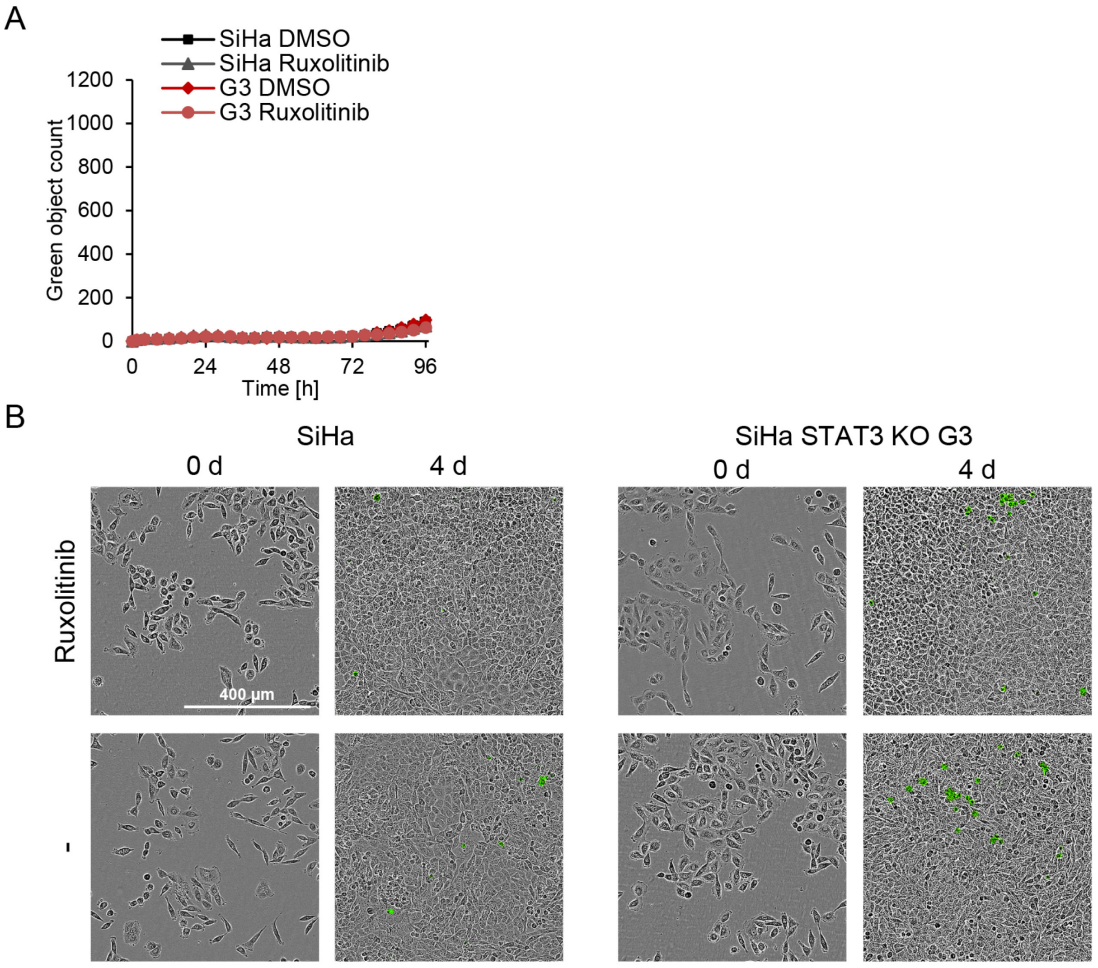

Figure 17 (previous page): Ruxolitinib treatment does not induce cell death in parental SiHa or SiHa STAT3 KO cells. *SiHa and SiHa STAT3 KO G3 cells were treated 48 h after seeding in 96-well plates (time point 0) with 1 µM Ruxolitinib or solvent control for 96 h. Cytotox Green reagent was used at a concentration of 100 nM and added at the time of treatment. Green cell counts **(A)** and images **(B)** were acquired by the Incucyte® S3 live-cell imaging system. Image analysis and green object quantification (dead cell counts) were performed using the Incucyte® software package. Scale bar: 400 µm. Figure and legend from Strobel et al., 2023[119].*

The only compound leading to inhibition of STAT3 Y705 phosphorylation that did not show any considerable modulations of the aforementioned cervical cancer-linked pathways as well as E6/E7 levels was Ruxolitinib (Figure 18 left panel). Interestingly, Ruxolitinib acts upstream of STAT3 on JAK1/2[329] and not on STAT3 directly but was highly effective in blocking STAT3 Y705 phosphorylation at much lower concentrations (Figure 6) than required for many direct small molecule STAT3 inhibitors. Because of the discrepant cellular responses induced by different inhibitors and the stark contrast to the effects of Ruxolitinib treatment, these results further support the notion that the tested direct STAT3 inhibitors can exert considerable effects on pathways other than JAK/STAT3 signaling.

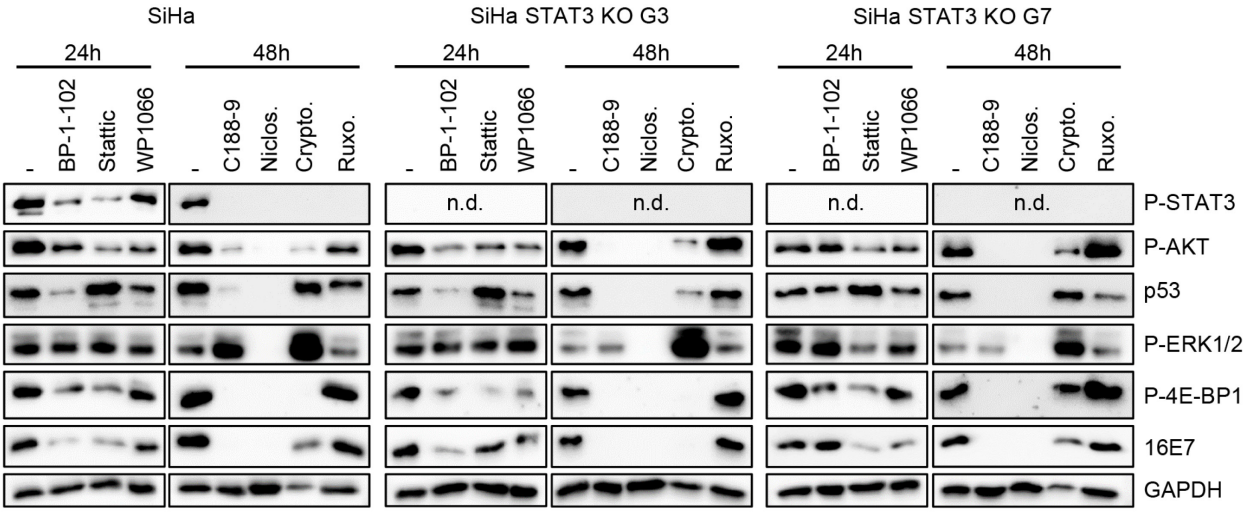

Figure 18: Small molecule inhibitors of STAT3 induce distinct alterations of cervical cancer-linked factors in both parental SiHa and STAT3 KO cells. *Parental SiHa or STAT3 KO G3 cells were treated 24 h after seeding with 20 µM BP-1-102, 10 µM Stattic, 7.5 µM WP1066, 15 µM C188-9, 2.5 µM Niclosamide (Niclo.), 5 µM Cryptotanshinone (Crypto.), 1 µM Ruxolitinib (Ruxo.) or solvent control (-) for 24 or 48 h, as indicated, and analyzed by immunoblot for P-STAT3 Y705, P-AKT S473, p53, P-ERK1/2 T202/Y204, P-4E-BP1 S65 or HPV16 E7 protein levels. GAPDH, representative loading control. n.d.: not detectable. Figure content and corresponding legend from Strobel et al., 2023[119].*

To further strengthen this hypothesis, all STAT3 inhibitors were again applied in SiHa STAT3 KO cells and analyzed by immunoblot (Figure 18 middle and right panel). If the findings described above in parental SiHa cells were due to the STAT3 inhibitors' effects on STAT3, none of these effects should be observable in SiHa STAT3 KO cells. Notably, however, all tested inhibitors acted again in a highly similar way on specific cervical cancer-linked pathways

as well as on E6/E7 expression in both SiHa STAT3 KO cells and parental SiHa cells (Figure 18 left panel).

Collectively, these observations provide strong experimental evidence that the tested small molecule STAT3 inhibitors can induce substantial off-target effects on cell growth, cell death or E6/E7 expression in cervical cancer cells, which are not linked to STAT3 inhibition.

2.4.2 Lower concentrations of small molecule STAT3 inhibitors induce fewer off-target effects but do not affect E6/E7 expression and fail to block OSM-induced STAT3 activity

To investigate the possibility that the observed off-target effects of STAT3 inhibitors are primarily due to high inhibitor concentrations, as they are also commonly employed in the literature[187, 251, 253], they were titrated with the aim to find the lowest possible concentration, which still considerably inhibits constitutive STAT3 Y705 phosphorylation (Figure 19).

At these titrated concentrations, no considerable or only weak effects, respectively, on ERK and AKT phosphorylation were seen (Figure 19, upper panel), indicating fewer off-target toxicities. Importantly however, the strong repression on E6/E7 levels, which was seen before (Figure 18), and is an essential finding reported in the literature[187, 251-253], was not observed anymore as well, despite efficient downregulation of constitutive STAT3 Y705 phosphorylation. In contrast, expression of the well characterized STAT3 target gene *SOCS3*[149-151] was downregulated by most tested STAT3 inhibitors under the same experimental conditions (Figure 19, lower panel), indicating that STAT3 activity is substantially inhibited. This further corroborates the notion that the previously observed effects of these inhibitors on cervical cancer-linked pathways (Figure 18) were likely due to off-target effects at higher concentrations. This applies also to their repressory effects on E6/E7 expression, which are highly likely not linked to STAT3 in line with my experiments questioning the mutual stimulatory interdependence of STAT3 and E6/E7 (please refer to 2.3).

Finally, the question arose whether the lower concentrations of STAT3 inhibitors described above are sufficient to block STAT3 signaling also after exogenic stimulation. Therefore, STAT3 was activated in SiHa cells using OSM in the presence of different small molecule STAT3 inhibitors (Figure 19). Interestingly, while constitutive STAT3 Y705 phosphorylation was blocked by most STAT3 inhibitors at lower concentrations, this was not the case for the strong induction of STAT3 Y705 phosphorylation through OSM treatment (Figure 19, upper panel). Furthermore, also the STAT3 target gene *SOCS3* was induced on transcript level in SiHa cells despite the presence of STAT3 inhibitors to levels comparable to treatment with OSM only (Figure 19, lower panel).

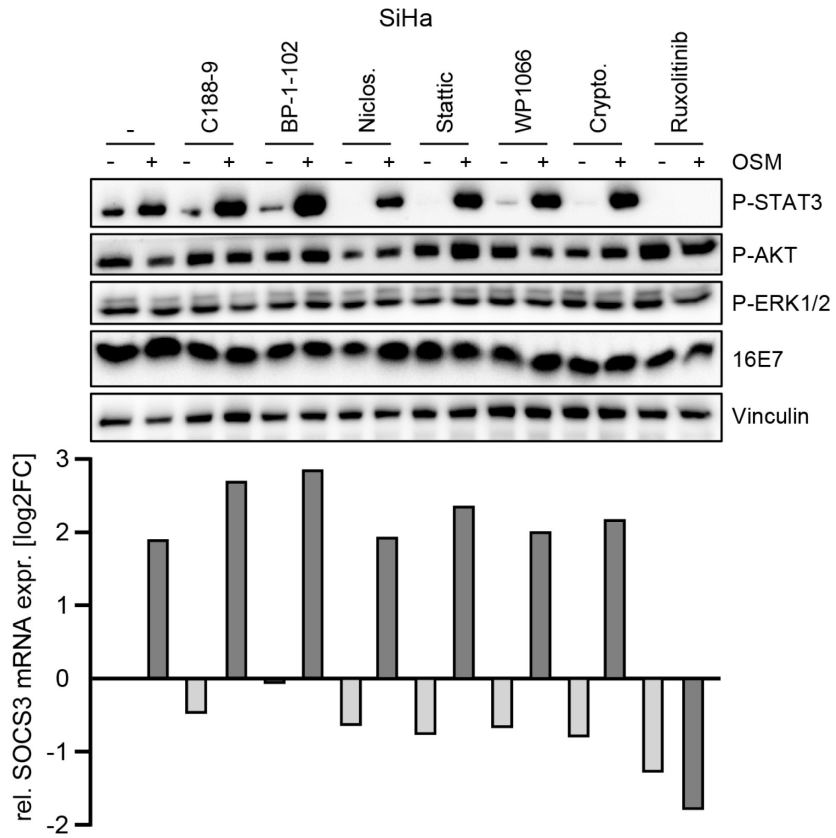

Figure 19: Lower concentrations of small molecule STAT3 inhibitors able to block constitutive STAT3 Y705 phosphorylation do not affect expression of cancer-linked factors in cervical cancer cells. *SiHa cells were treated 24 h after seeding with 10 µM BP-1-102, 2.5 µM Stattic, 2.5 µM WP1066, 5 µM C188-9, 0.25 µM Niclosamide (Niclo.), 1 µM Cryptotanshinone (Crypto.), 1 µM Ruxolitinib or solvent control (-) for 24 h, as indicated. 10 ng/mL OSM were added as indicated 1 h before harvest. Upper panel: Protein levels of P-STAT3 Y705, P-AKT S473, P-ERK1/2 T202/Y204 or HPV16 E7 were analyzed by immunoblot. Vinculin, representative loading control. Lower panel: SOCS3 transcript levels were analyzed by qRT-PCR. Shown are log_2-transformed fold changes (log_2FC) of relative expression (solvent control: $log_2FC = 0$) corresponding to samples of the same cells also used for immunoblots (upper panel).*

Notably, neither of these responses were observed under Ruxolitinib treatment, which efficiently repressed both constitutive and OSM-induced STAT3 Y705 phosphorylation and *SOCS3* expression (Figure 19). Therefore, these tested lower concentrations of STAT3 inhibitors are not sufficient to inhibit STAT3 activation upon stimulation with OSM. Collectively, these results show that the tested direct small molecule STAT3 inhibitors inherently only possess a narrow concentration range in cervical cancer cells in which they can efficiently block endogenous STAT3 Y705 phosphorylation without inducing substantial off-target effects.

2.5 Analysis of STAT3 transcriptional targets in cervical cancer cells

The results obtained so far indicate that STAT3 is not an essential factor, neither for proliferation nor efficient HPV E6/E7 oncogene expression in cervical cancer cells. This raises questions concerning the transcriptional activity of STAT3 and the regulation of additional putative STAT3 target genes besides *SOCS3* in these cells.

2.5.1 Transcript levels of its putative oncogenic target genes are not affected upon STAT3 knockdown in cervical cancer cells

According to the literature, genes involved in the regulation of apoptosis like *BIRC5* (coding for survivin) and *BCL2L1* (coding for BCL_{XL}), oncogenic transcription factors like *MYC* (coding for c-myc) and pro-proliferative factors such as *CCND1* (coding for cyclin D1) are cancer-linked transcriptional targets of STAT3[140], thereby mediating the proposed pro-proliferative activity of STAT3 also in cervical cancer cells[247, 253, 256, 267]. Since I did not observe a critical role of STAT3 for proliferation of cervical cancer cells, Affymetrix Clariom™ S transcriptome analyses were performed in cooperation with the "Genomics and Proteomics" core facility (DKFZ, Heidelberg) to gain a more comprehensive understanding of the functional significance of STAT3 and to identify genes controlled by endogenous STAT3 activity in cervical cancer cells.

Therefore, I transfected SiHa cells with four unique STAT3-targeting siRNAs, as the regulation of the well-established STAT3 target gene *SOCS3*[149-151] seemed to be the most pronounced in these cells (Figure 10, Figure 11B). Interestingly, despite efficient down-regulation of STAT3 by all four STAT3-targeting siRNAs (Figure 10A), the transcriptome analyses revealed varying counts of differentially expressed protein coding transcripts (Table 1). In particular, siRNA #10 resulted in substantially fewer differentially expressed transcripts compared to the other tested siRNAs, including control siRNA compared to mock transfection.

***Table 1: Numbers of differentially expressed transcripts after knockdown of STAT3 in SiHa cells**. Colors indicate log_2FC threshold, log_2FC of STAT3 given as reference for degree of STAT3 depletion.*

comparisons / log_2FC cutoff	siSTAT3_2 vs. siCtrl	siSTAT3_4 vs. siCtrl	siSTAT3_6 vs. siCtrl	siSTAT3_10 vs. siCtrl	Mock vs. siCtrl
$log_2FC > 1.5$	3	2	1	1	1
$log_2FC > 1.0$	14	13	30	4	5
$log_2FC > 0.58$	192	126	235	63	79
$log_2FC < -0.58$	395	305	330	86	128
$log_2FC < -1.0$	64	42	58	11	14
$log_2FC < -1.5$	7	9	14	4	4
log_2FC STAT3	-2.56	-2.58	-1.81	-1.77	-0.36

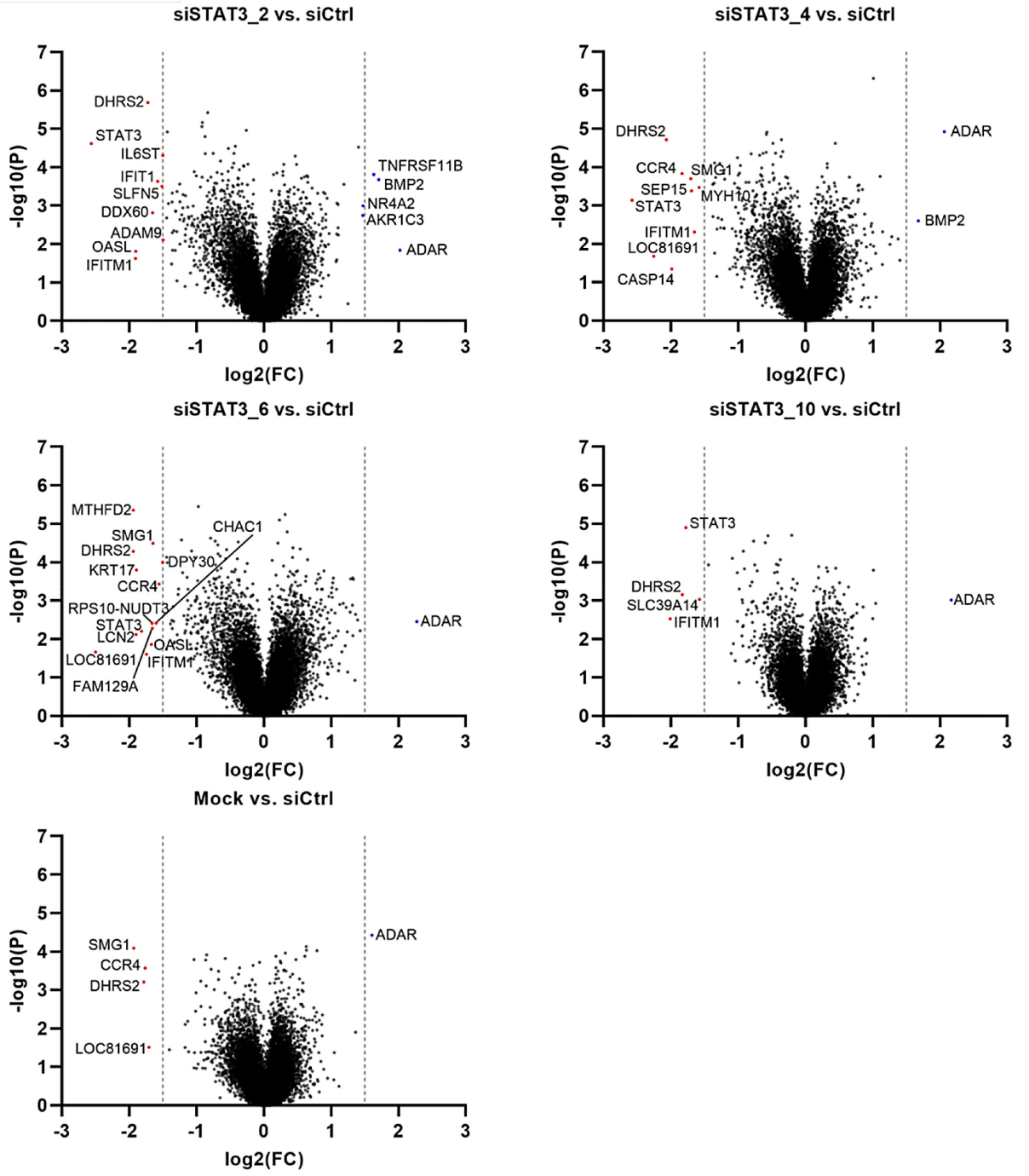

Figure 20: Transcriptome analysis reveals differences between the activities of STAT3-targeting siRNAs. *SiHa cells were reverse transfected with indicated siRNAs followed by Affymetrix Clariom™ S assay and volcano plot analysis using GraphPad Prism. Transcripts reaching the log_2FC threshold (vertical dashed lines) are annotated. Red: Transcripts with $log_2FC \leq -1.5$, blue: Transcripts with $log_2FC \geq 1.5$.*

Next, I filtered the data (for details, please refer to 4.2.3) to identify transcripts that are consistently differentially expressed after knockdown of STAT3 by each of the four siRNAs but not by the control siRNA (siCtrl). For example, transcripts of genes like *ADAR* and *DHRS2* were filtered out as these are not only regulated by all STAT3-targeting siRNAs but are also differentially expressed to comparable extent in the siCtrl vs. mock condition as can be seen

in volcano plots (Figure 20). Surprisingly, filtering resulted in only 5 out of 19525 evaluable protein coding transcripts being classified as consistently differentially expressed after STAT3 knockdown, besides the *STAT3* mRNA itself (Figure 21A). This suggests a strong influence by the transfection process itself and/or by effects specifically linked to individual siRNAs in comparison to the effect of STAT3 depletion on the transcriptome.

A

siRNA / Symbol	#2	#4	#6	#10	mock
IFITM1	-2.95	-1.65	-1.74	-2.01	-0.87
STAT3	-2.48	-2.58	-1.81	-1.77	-0.36
CHAC1	-1.24	-1.01	-1.60	-0.87	-0.57
ETS2	-1.06	-0.76	-1.20	-0.75	-0.21
FAM84B	-0.74	-0.78	-0.66	-0.73	-0.12
TGFBR3	0.75	0.75	1.12	0.69	0.06

C

siRNA / Symbol	#2	#4	#6	#10
STAT3	-2.48	-2.58	-1.81	-1.77
FOS	0.00	-0.17	0.22	-0.08
HIF1A	-0.33	-0.31	-0.16	-0.22
MYC	-0.03	-0.80	0.13	-0.48
SOX2	0.18	0.18	0.26	0.22
NANOG	0.01	-0.07	0.10	-0.08
BCL2	-0.09	0.29	-0.16	0.17
MCL1	-0.11	-0.43	0.13	-0.09
BCL2L1	-0.33	-0.42	-0.46	-0.39
BIRC5	0.35	-0.02	-0.08	0.36
BIRC2	-0.30	0.24	0.50	-0.02
CCND1	-0.42	-0.72	0.85	-0.71
PIM1	0.37	-0.18	0.36	0.20

log2FC				
2	1	0	-1	-2

B

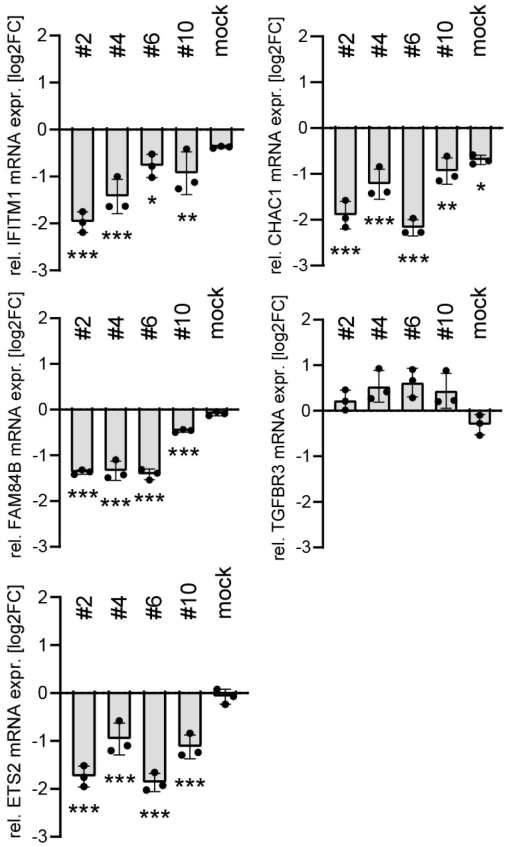

Figure 21: Expression of oncogenic putative STAT3 target genes are mostly unaffected upon silencing STAT3 expression in cervical cancer cells. (A) *SiHa cells were reverse transfected with the indicated STAT3-targeting siRNAs (#2, #4, #6, #10) or control siRNA (siCtrl) followed by Affymetrix Clariom™ S assay 72 h after transfection and subsequent filtering of protein coding transcripts as described in section 4.3.2. Shown are log_2FC values of consistently differentially expressed transcripts.* ***(B)*** *Concomitantly prepared RNA was used to determine transcript levels of IFITM1, CHAC1, FAM84B, TGFBR3 and ETS2 by qRT-PCR. Shown are the log_2-transformed fold changes (log_2FC) of mean expression with standard deviations. Statistically significant differences in cells transfected with siSTAT3 (#2, #4, #6, #10) or mock transfection compared to siCtrl (log_2FC = 0) were determined by one-way ANOVA. *: $p < 0.05$, **: $p < 0.01$, ***: $p < 0.001$.* ***(C)*** *Shown are log_2FC values of select transcripts in the transcriptome data from (A) without filtering. Subfigures (A) and (C) and corresponding legends from Strobel et al., 2023[119].*

In a second step, expression of the five differentially expressed genes was validated via qRT-PCR after STAT3 silencing (Figure 21B). As anticipated, transcripts of all five genes were found to be regulated in a similar manner as found in the transcriptome screen. However, while this was highly significant for *IFITM1*, *CHAC1*, *ETS2* and *FAM84B*, it did not reach significance for *TGFBR3* (Figure 21B). It is further interesting that the expression of a broad array of pro-

proliferative putative STAT3 target genes[140] was not impaired upon STAT3 knockdown in cervical cancer cells. These include pro-survival factors such as *BCL2*, *BCL2L1* and *BIRC5*, oncogenic transcription factors like *MYC*, and genes linked to cell-cycle progression like *CCND1* (Figure 21C) – some of which have been reported to be important STAT3 target genes in cervical cancer cells[247, 253, 256, 267, 268]. This observation is consistent with my results indicating that STAT3 is not an essential factor for cervical cancer cell proliferation, at least under the tested conditions.

2.5.2 GSEA reveals a lack of consistently regulated gene sets after silencing of STAT3

Next, GSEA using all "GO", "BIOCARTA" and "HALLMARK" gene sets of the molecular signatures database (MSigDB) v2023.1.Hs was applied to the transcriptome data obtained after STAT3 knockdown in SiHa cells. In general, the effect of STAT3 silencing on its putative target genes was only of modest intensity (Figure 21), if considerable at all. It thus was aimed to detect sets of genes or pathways, which may be – as a whole – consistently up- or downregulated after STAT3 silencing, even though fold change values of individual transcripts might only be weakly affected. Consistent with individual differentially expressed transcripts (Table 1), the number of positively or negatively enriched gene sets was variable for different siRNAs, with siRNA #10 resulting in the least and siRNA #6 in the most enriched gene sets (Table 2).

Table 2: Counts of enriched gene sets after knockdown of STAT3 in SiHa cells.

	siSTAT3_2 vs. siCtrl	siSTAT3_4 vs. siCtrl	siSTAT3_6 vs. siCtrl	siSTAT3_10 vs. siCtrl	Mock vs. siCtrl
Pos. enriched gene sets (FDR < 0.25)	405	333	618	208	41
Neg. enriched gene sets (FDR < 0.25)	477	566	458	59	320

To find out which gene sets are consistently regulated by all four siRNAs without being affected by the transfection process itself (mock vs. siCtrl), the top 10 up- and downregulated gene sets of each condition (Supplementary Table 1 to Supplementary Table 5) were assessed, resulting in 80 unique gene sets across all conditions. These 80 gene sets were then clustered (for details, please refer to 4.2.3) (Supplementary Table 6), eventually yielding six clusters of gene sets. However, none of these clusters is consistently regulated across all STAT3 siRNAs while being fully unaffected in the mock vs. siCtrl condition. Out of all the tested individual gene sets only GOBP_CARDIAC_EPITHELIAL_TO_MESENCHYMAL_TRANSITION, GOBP_FATTY_ ACYL_COA_BIOSYNTHETIC_PROCESS, GOBP_FORELIMB_ MORPHOGENESIS as well as the GOBP_ENDODERM_FORMATION gene set were positively enriched by all four STAT3

siRNAs while being rather close to unchanged or negatively enriched in the mock vs. siCtrl condition.

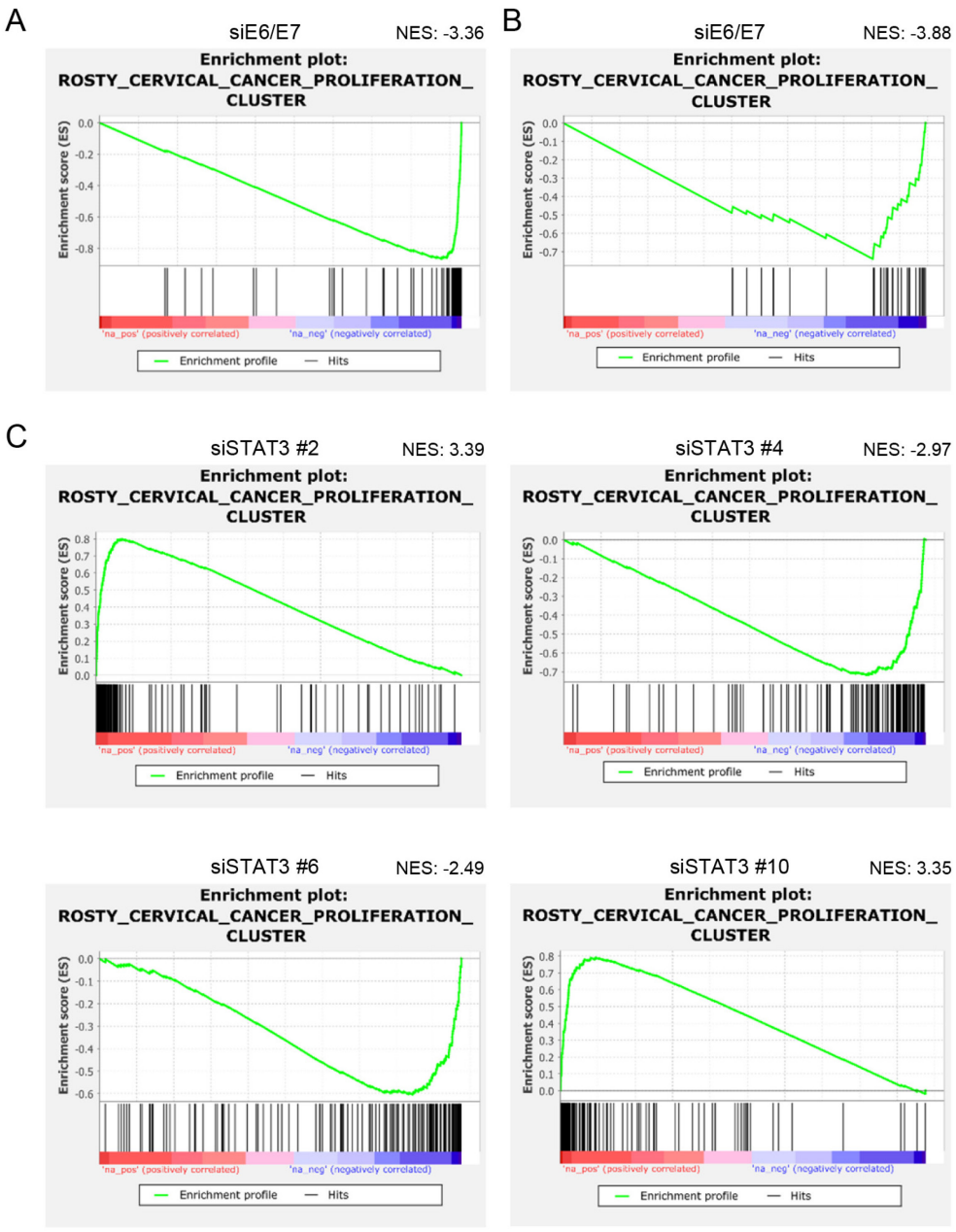

Figure 22: A cervical cancer proliferation signature gene set is consistently downregulated by silencing of E6/E7 but not of STAT3. (A) *GSEA was applied on unpublished proteomic data of SiHa cells 72 h after transfection of E6/E7-targeting siRNAs.* ***(B)*** *GSEA was applied as in (A) on available microarray-based transcriptomic data of HeLa cells[330] 72 h after transfection of E6/E7-targeting siRNAs.* ***(C)*** *SiHa cells were reverse transfected with the indicated STAT3-targeting siRNAs or control siRNA (siCtrl) followed by Affymetrix Clariom™ S mRNA analysis 72 h after transfection. GSEA was performed on the gene set ROSTY_CERVICAL_CANCER_PROLIFERATION_CLUSTER for each condition in each subfigure.*

Finally, I extended the analysis to further gene sets beyond the “GO”, “BIOCARTA” and “HALLMARK” groups. Specifically, I assessed enrichment of a cervical cancer signature gene set containing genes, which are strongly associated with E6/E7 expression and cervical cancer

cell proliferation[331] (ROSTY_CERVICAL_CANCER_PROLIFERATION_CLUSTER). To validate this gene set, I performed GSEA on proteome data of SiHa cells (Figure 22A, unpublished data) and on microarray-based transcriptome data of HeLa cells[330] (Figure 22B) after E6/E7 silencing. Under these conditions of efficient E6/E7 depletion, this gene set is clearly negatively enriched. Similarly, in previous work of our laboratory on Metformin, which downregulates E6/E7[84] (Figure 12C), corresponding proteomic alterations were found as well[84].

Meanwhile, in my transcriptome data obtained after STAT3 silencing by RNAi, regulation of this gene set is comparable to cluster #2 and #5 (Supplementary Table 6), i.e. positively enriched by STAT3-targeting siRNAs #2 and #10 while being negatively enriched by siRNAs #4 and #6 (Figure 22A). Together with my previous results, these inconsistent enrichments are another indication that STAT3 is likely not directly involved in the regulation of proliferation and E6/E7 expression in cervical cancer cells. Rather, these results indicate that siRNA-specific effects are stronger determinants of enrichment of this gene set than the depletion of STAT3.

Altogether, my results corroborate the notion that the expression of a range of well-defined oncogenic STAT3 target genes is not under control of constitutive STAT3 activity in cervical cancer cells and that STAT3 is not essential for the expression of these factors, at least under the tested conditions. Further, these data are in line with my findings on the lack of a substantial role of STAT3 for proliferation and E6/E7 expression in cervical cancer cells.

2.5.3 Most transcript levels of its putative oncogenic target genes are not affected upon induction of STAT3 activity in cervical cancer cells

These findings also raised the question whether the elevation of STAT3 activity beyond the constitutive level in cervical cancer cells might be necessary to stimulate the expression of putative oncogenic STAT3 target genes. To investigate this issue and validate potential hits at the same time, parental SiHa and HeLa as well as corresponding STAT3 KO clones were treated with OSM for 1 h. Subsequently, I analyzed expression of select oncogenic STAT3 target genes as well as the five newly identified potential STAT3 targets described above using qRT-PCR (Figure 23).

As expected, OSM strongly induced STAT3 Y705 phosphorylation in immunoblot analyses of both parental SiHa and HeLa cells while no signal was detectable in the respective STAT3 KO clones (Figure 23A). Expression of the STAT3 target gene *SOCS3* on RNA level was substantially increased by OSM treatment in parental SiHa and HeLa cells, while it remained unchanged in the respective STAT3 KO cell clones (except for SiHa STAT3 KO G3, in which it was induced as well, although to a weaker extent) (Figure 23B). In contrast, mRNA levels of

almost all other tested cancer-linked putative STAT3 target genes, namely *CCND1*, *BIRC5*, *BCL2* and *BCL2L1,* remained unchanged after OSM treatment (Figure 23B). The only exception was *MYC*, however its response to OSM treatment appeared to be cell line dependent. A modest increase of *MYC* transcript levels under OSM treatment was observed in parental SiHa cells but not in SiHa STAT3 KO cells, whereas *MYC* expression remained unchanged in both parental HeLa and HeLa STAT3 KO cells (Figure 23B). Therefore, except for *MYC* in SiHa cells, even strongly elevated levels of phosphorylated STAT3 Y705 do not lead to considerably increased transcript levels of genes that have been reported to be relevant cancer-linked STAT3 targets in cervical cancer cells[247, 253, 256, 267, 268].

Of the five newly identified potential STAT3 targets in SiHa cells (Figure 23A, B), only *ETS2* was convincingly and significantly upregulated by OSM treatment in parental SiHa and, to a lesser extent, in parental HeLa cells, while the induction was absent or weaker and not significant in SiHa and HeLa STAT3 KO cells (Figure 23C), similar to regulation of *SOCS3* transcripts (Figure 23B). In contrast, regulation of all four other potential STAT3 targets, namely *FAM84B*, *CHAC1*, *TGFBR3* and *IFITM1* exhibited pronounced interexperimental variability or remained largely unchanged. Notably, *FAM84B* transcripts were undetectable in HeLa cells altogether.

Interestingly, in above-described experiments, some transcripts like *SOCS3* or *ETS2* seemed to be influenced by OSM treatment in STAT3 KO cells as well (Figure 23B, C). Thus, I speculated whether these somewhat heterogeneous results upon OSM treatment might be due to effects on other STAT transcription factors, such as STAT1 or STAT5. Indeed, it has been shown that for example STAT1 activity is induced in response to IL-6 upon loss of STAT3[315]. Notably, for all STAT3 KO clones except for HeLa clone F7, STAT1 Y701 phosphorylation was largely not altered by OSM treatment, while immunoblotting revealed strongly induced STAT5 Y694/699 phosphorylation after OSM treatment, especially in SiHa clone G3 as well as in HeLa clone F3 (Figure 23D). It thus will be interesting to explore in future analyses whether this finding might explain the STAT3-independent induction of *SOCS3* or *ETS2* in SiHa STAT3 KO G3 cells (Figure 23B, C). These results underline the complexity of STAT signaling and indicate that most of the five identified potentially STAT3-dependent target genes in cervical cancer cells, are not upregulated by OSM-induced STAT3 activation and require further experiments to validate whether they are truly under transcriptional control of STAT3.

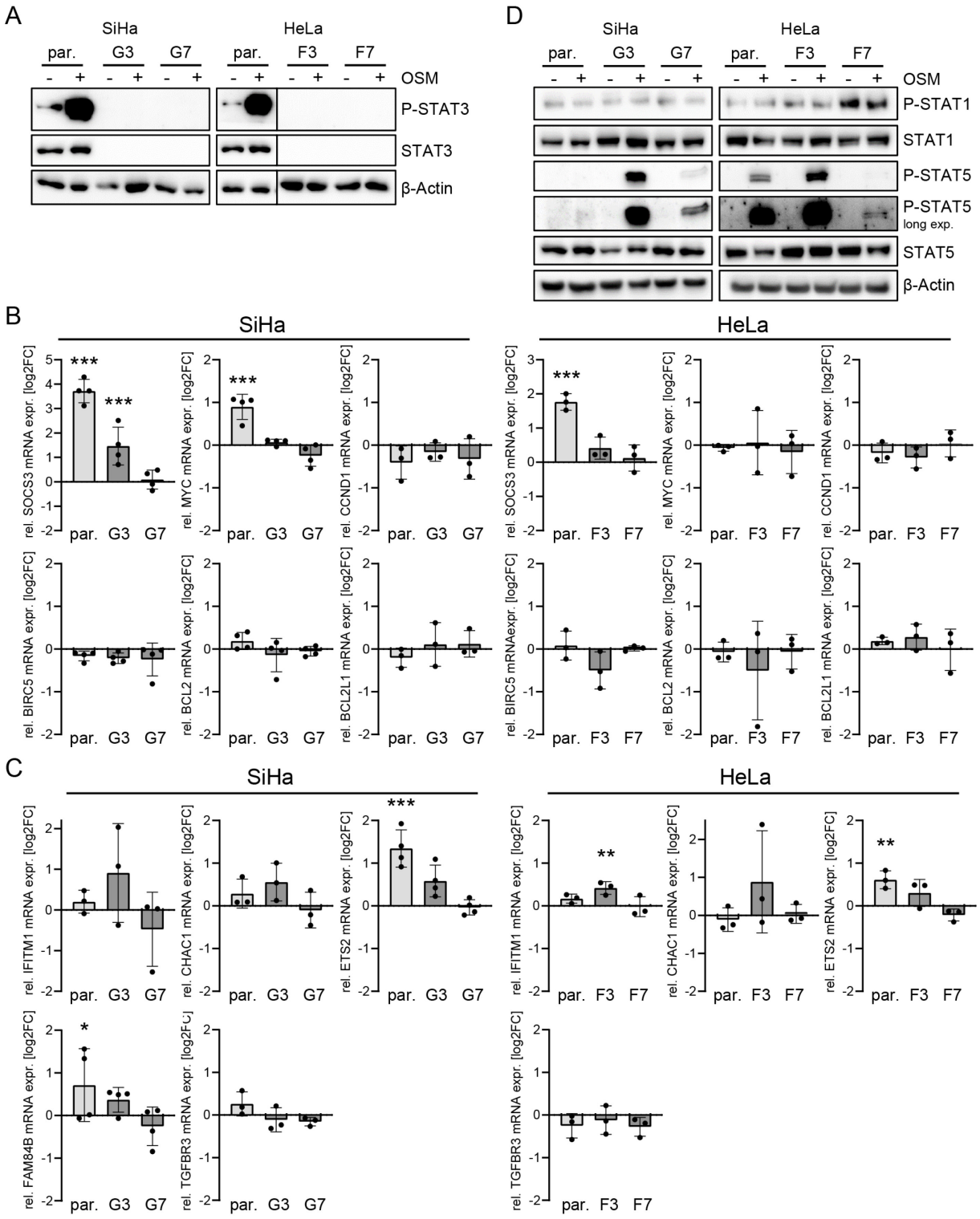

Figure 23: Expression of oncogenic putative STAT3 target genes remains mostly unaffected upon increasing STAT3 activity in cervical cancer cells. (A) *Parental (par.) SiHa and HeLa and respective STAT3 KO cells were treated with 10 ng/mL OSM for 1 h and analyzed by immunoblot for P-STAT3 Y705 and total STAT3 protein levels. β-Actin, representative loading control. Vertical lines between lanes indicate where original images of the same immunoblot were spliced for the purpose of presentation.* ***(B)*** *Parental SiHa, HeLa and respective STAT3 KO cells were treated as described for (A), followed by analysis of transcript levels of SOCS3, MYC, CCND1, BIRC5, BCL2 and BCL2L1 by qRT-PCR. Shown are log_2-transformed fold changes (log_2FC) of mean expression with standard deviations. Statistically significant differences in cells treated with OSM compared to solvent control*

*(log$_2$FC = 0) were determined by one-way ANOVA. ***: p < 0.001. **(C)** SiHa, HeLa and respective STAT3 KO cells were treated as described for (A), followed by analysis of transcript levels of IFITM1, CHAC1, ETS2, FAM84B and TGFBR3 by qRT-PCR. Shown are the log$_2$-transformed fold changes (log$_2$FC) of mean expression with standard deviations. Statistically significant differences in cells treated with OSM compared to solvent control (log$_2$FC = 0) were determined by one-way ANOVA. *: p < 0.05, **: p < 0.01, ***: p < 0.001. **(D)** SiHa, HeLa and respective STAT3 KO cells were treated as described for (A) and analyzed by immunoblot for P-STAT1 Y701, total STAT1, P-STAT5A/B Y694/699 and total STAT5A/B protein levels. β-Actin, representative loading control. Subfigures (A) and (B) and corresponding legends from Strobel et al., 2023[119].*

Additionally, to rule out the possibility that the induction of STAT3 Y705 phosphorylation by OSM for 1 h is too brief to induce an effect on STAT3 target genes, SiHa cells were treated with OSM for 1, 3 and 6 h (Figure 24). Despite strongly increased STAT3 Y705 phosphorylation after 6 h of OSM treatment (Figure 12C), again none of the tested STAT3 target genes was considerably upregulated on RNA level after neither 3 nor 6 h compared to either solvent control or the 1 h time point of OSM treatment (Figure 24). In contrast, the strongest responses for both *SOCS3* and *MYC* were observed at the 1 h time point (Figure 24).

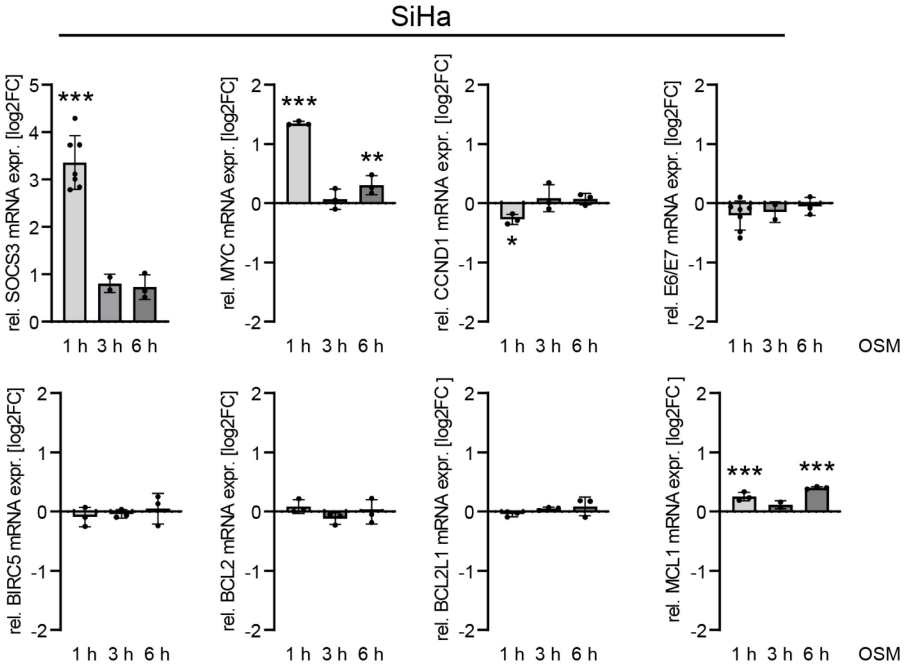

Figure 24: Several putative, cancer-linked STAT3 target genes are not considerably upregulated after extended stimulation of STAT3 activity by OSM. *SiHa cells were treated with 10 ng/mL OSM for 1, 3 or 6 h and analyzed for SOCS3, MYC, CCND1, HPV E6/E7, BIRC5, BCL2, BCL2L1 and MCL1 transcript levels by qRT-PCR. Shown are the log$_2$-transformed fold changes (log$_2$FC) of mean expression with standard deviations. Statistically significant differences in cells treated with OSM compared to solvent control (log$_2$FC = 0) were determined by one-way ANOVA. *: p < 0.05, **: p < 0.01, ***: p < 0.001. Transcript levels of SOCS3 and HPV E6/E7 after 1 h of OSM stimulation are also depicted in Figure 11B for didactic reasons. Figure content and legend partly from Strobel et al., 2023[119].*

Importantly, also the transcript levels of the HPV *E6/E7* oncogenes remained unchanged after 3 and 6 h of OSM treatment (Figure 24) as they were after 1 h (Figure 11, Figure 24),

further arguing against the idea that the activation of STAT3 signaling is a crucial stimulus for the expression of the HPV oncogenes. Thus, the lack of a response of transcript levels of putative STAT3 target genes, including HPV *E6/E7*, towards increased STAT3 Y705 phosphorylation can likely not be explained by a delayed response to OSM, which would not yet be observable at the 1 h time point.

2.6 Evaluation of the role of STAT3 for drug resistance in cervical cancer cells

In the literature, feedback activation of STAT3 Y705 phosphorylation, as illustrated in Figure 25, is reported in response to various treatments and has been described as an important resistance mechanism to targeted therapies in certain cancer models[234-244].

Thus, the significance of STAT3 for resistance to prospective targeted therapies discussed for cervical cancer treatment was investigated. Specifically, I examined whether STAT3 signaling might affect cervical cancer cell growth or survival if additional stressors such as anti-proliferative drugs targeting specific oncogenic pathways or the more broadly acting iron chelator CPX are applied.

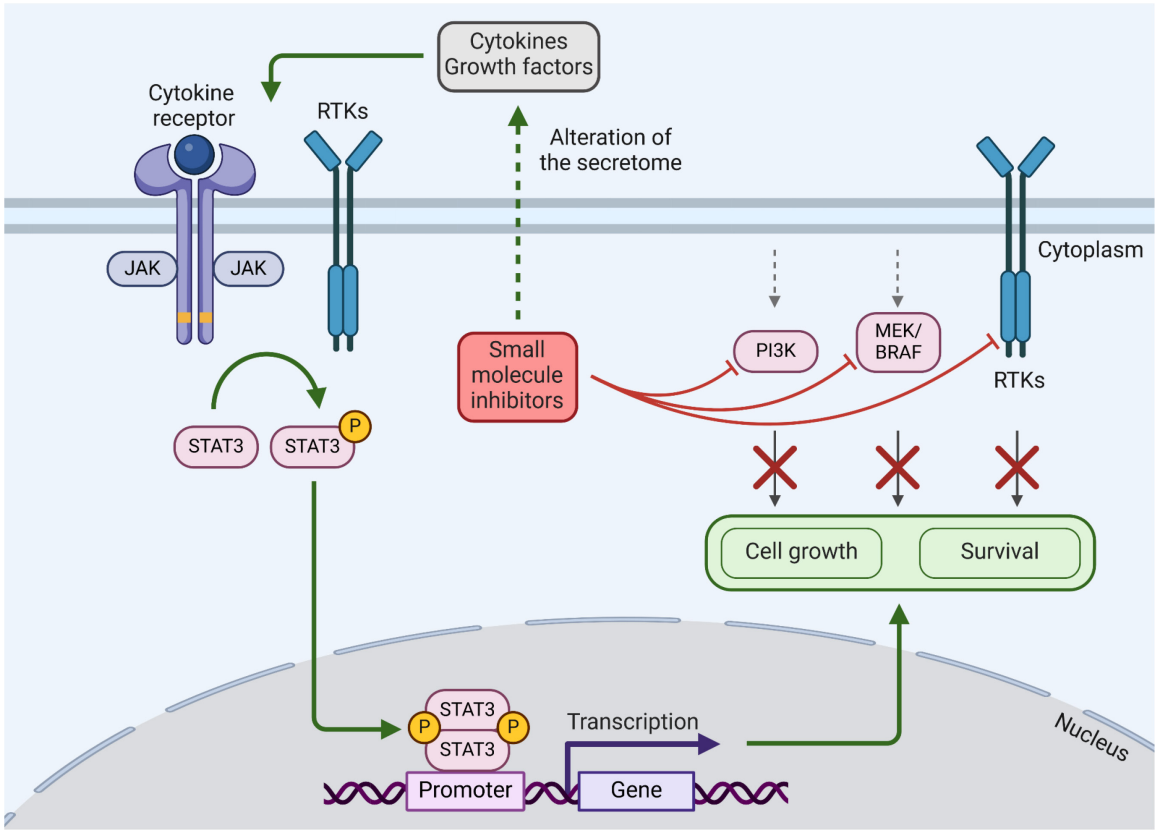

Figure 25: Potential mechanism of STAT3 activation in response to targeted treatments. *Small molecule inhibitors targeting oncogenic factors such as PI3K/AKT, BRAF/MEK or receptor tyrosine kinases (RTKs) efficiently block cell growth and survival mediated by these pathways in certain cancer models[234-236, 238, 332]. This can be linked to rapid alterations of the composition of the secretome followed by increased RTK (e.g. HERs) or cytokine receptor signaling and induction of STAT3 activity through autocrine stimulation[235, 236, 238]. Increased STAT3 activity then proposedly leads to transcriptional activation of pro-proliferative factors, thereby mediating drug resistance[235, 236, 238]. BRAF: v-Raf murine sarcoma viral oncogene homolog B, MEK: mitogen-activated protein kinase kinase. Figure created with BioRender.com.*

2.6.1 Inhibition of PI3K- and MAPK pathways induces STAT3 Y705 phosphorylation

Both the PI3K- and MAPK pathways have been reported to play a critical role for the malignant phenotype of cervical cancer cells[82, 328], yet the individual inhibition of both pathways yielded only insufficient efficacy in a clinical trial[333]. In addition, resistance-inducing feedback activation of STAT3, as depicted in Figure 25, was reported for the inhibition of PI3K-[235, 236] and MAPK-linked[236, 237, 239-241] signaling pathways in certain cancer cells. Thus, the question arose whether STAT3 Y705 phosphorylation might be induced in response to PI3K- or MAPK-pathway inhibition in cervical cancer cells as well and whether it consequently might play a role for resistance to these treatments.

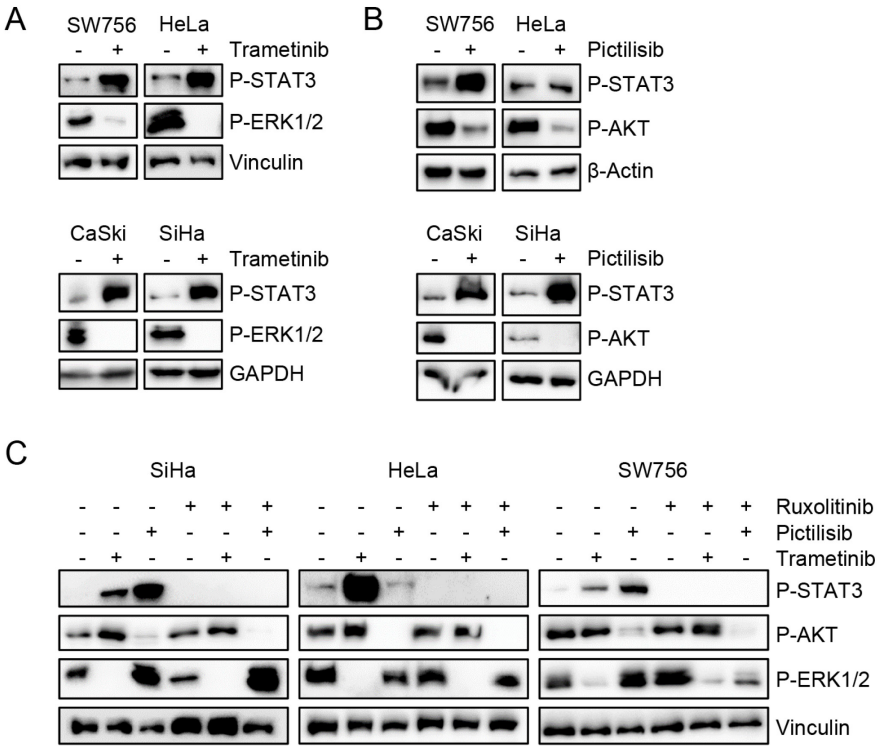

Figure 26: STAT3 Y705 phosphorylation is induced upon inhibition of PI3K- or MEK-linked signaling pathways in a JAK1/2-dependent manner. *SW756, HeLa, CaSki and SiHa cells were treated 24 h after seeding with* ***(A)*** *100 nM Trametinib or* ***(B)*** *7.5 µM (HeLa) or 10 µM (SW756, CaSki, SiHa) Pictilisib, or solvent control (-), and analyzed by immunoblot for P-STAT3 Y705, P-ERK1/2 T202/Y204 or P-AKT S473 protein levels. β-Actin, GAPDH and Vinculin, representative loading controls.* ***(C)*** *SiHa, HeLa and SW756 cells were treated and analyzed as described for subfigures (A) and (B), respectively, with addition of 1 µM Ruxolitinib as indicated. Figure content and corresponding legends from Strobel et al., 2023[119].*

In response to the clinically used mitogen-activated protein kinase kinase (MAPKK; MEK) inhibitor Trametinib, STAT3 Y705 phosphorylation was strongly upregulated in SW756, HeLa, CaSki and SiHa cervical cancer cells while phosphorylation of the MEK downstream target ERK1/2 was efficiently inhibited (Figure 26A). Comparably, in response to the PI3K inhibitor Pictilisib, STAT3 Y705 phosphorylation levels were strongly elevated in SW756, CaSki and

SiHa cells, but not in HeLa cells (Figure 26B). Collectively, these results show that some form of feedback activation of STAT3 in response to these targeted treatments is intact in cervical cancer cells.

Feedback activation of STAT3 is often reported to be mediated by autocrine secretion of cytokines or growth factors, followed by stimulation of JAK or HER family signaling which leads to increased STAT3 Y705 phosphorylation levels, as illustrated in Figure 25[235, 236, 238]. Importantly, in cervical cancer cells, the induction of STAT3 Y705 phosphorylation after both Trametinib and Pictilisib treatment could be completely blocked by co-inhibition of JAK1/2 with Ruxolitinib (Figure 26C) while inhibition of HER1/2/3 with Sapitinib treatment did not show any effect (not shown). This therefore indicates that the observed induction of STAT3 Y705 phosphorylation is JAK1/2 dependent and independent of HER1/2/3 activity.

2.6.2 Feedback induction of STAT3 activity does not affect selected STAT3 target genes in cervical cancer cells

Next, I investigated whether the strongly increased STAT3 Y705 phosphorylation after Trametinib or Pictilisib treatment (Figure 26) translates into increased transcript levels of putative STAT3 target genes, as was reported for resistance-inducing STAT3 feedback activation in other cancers[234-236]. Interestingly though, in both HeLa and SiHa cells, transcript levels of most investigated putative STAT3 target genes did not increase with Trametinib or Pictilisib treatment despite the increase in STAT3 Y705 phosphorylation, and the addition of Ruxolitinib did not considerably affect these transcript levels further (Figure 27).

As the only one of all tested putative STAT3 targets, the non-oncogenic *SOCS3* was upregulated by Pictilisib treatment in SiHa cells, and this upregulation could be counteracted by combination with Ruxolitinib (Figure 27). In contrast, in HeLa cells *SOCS3* was unchanged after Pictilisib treatment (Figure 27). All other tested STAT3 target genes, including the putative target HPV *E6/E7*, did not exhibit a differential expression pattern that would indicate a STAT3-dependent induction after Pictilisib or Trametinib treatment as well as a subsequent block of this induction through concomitant Ruxolitinib treatment (Figure 27).

Collectively, my findings indicate that the observed induction of STAT3 signaling does not lead to increased expression of putatively STAT3-reponsive factors frequently reported to promote growth or survival of cervical cancer cells[247, 253, 256, 267, 268] and neither that STAT3 activity could thereby possibly counteract PI3K- or MAPK pathway inhibition and mediate resistance.

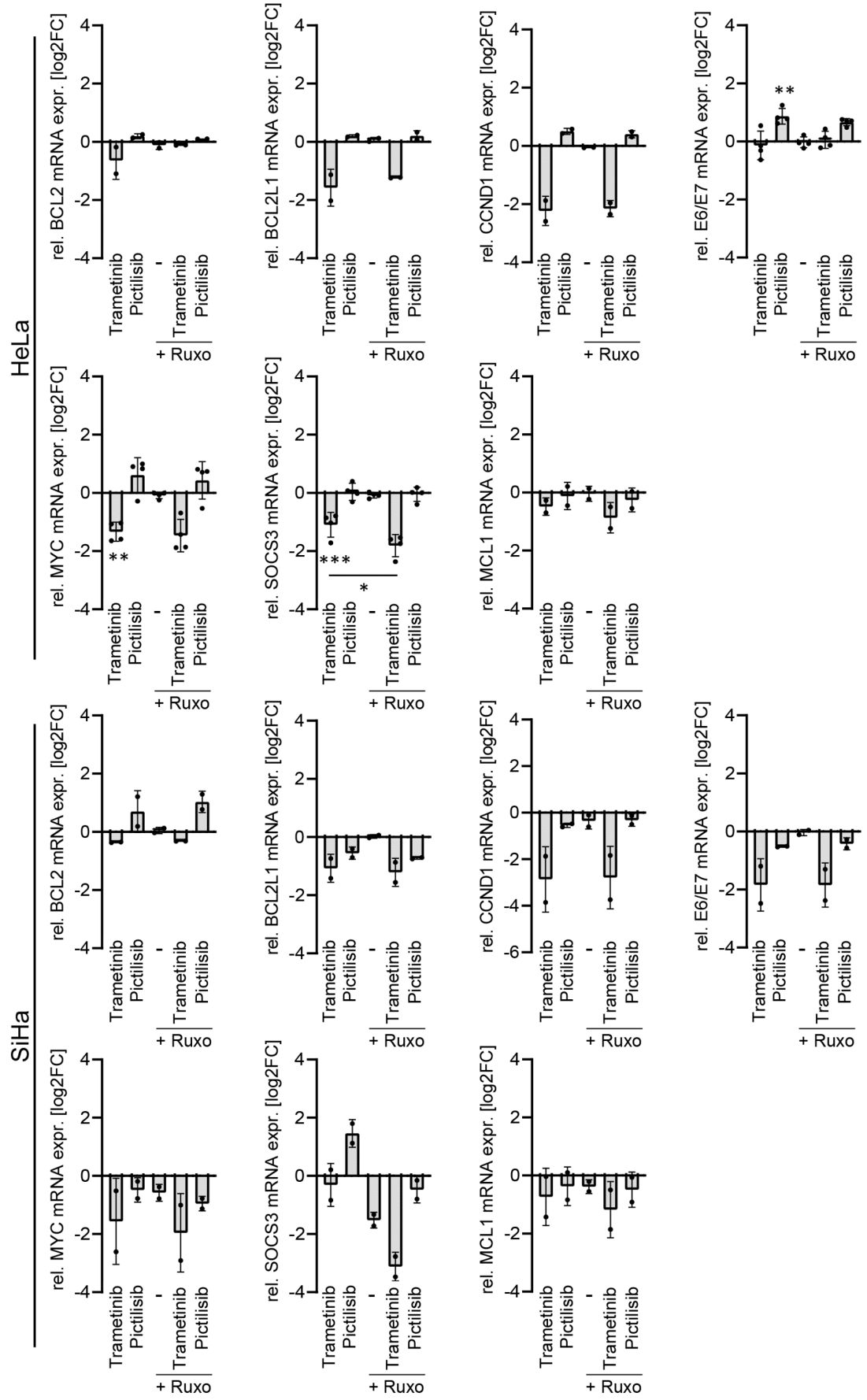
HeLa
SiHa
rel. BCL2 mRNA expr. [log2FC]
rel. MYC mRNA expr. [log2FC]
rel. BCL2L1 mRNA expr. [log2FC]
rel. SOCS3 mRNA expr. [log2FC]
rel. CCND1 mRNA expr. [log2FC]
rel. MCL1 mRNA expr. [log2FC]
rel. E6/E7 mRNA expr. [log2FC]
Trametinib
Pictilisib
-
Trametinib
Pictilisib
+ Ruxo
+ Ruxo

Figure 27 (previous page): Transcript levels of putative STAT3 target genes are not increased after PI3K- or MAPK pathway inhibition in cervical cancer cells. *HeLa and SiHa cells were treated 24 h after seeding with 100 nM Trametinib or 7.5 µM (HeLa) or 10 µM (SiHa) Pictilisib, or solvent control (-) with addition of 1 µM Ruxolitinib as indicated and analyzed for BCL2, BCL2L1, CCND1, HPV E6/E7, MYC, SOCS3, MCL1 transcript levels by qRT-PCR. Shown are the log_2-transformed fold changes (log_2FC) of mean expression with standard deviations. If three or more data points were available, statistically significant differences in treated cells compared to solvent control ($log_2FC = 0$) were determined by one-way ANOVA. *: $p < 0.05$, **: $p < 0.01$, ***: $p < 0.001$.*

Of additional note, multiple of the tested putative STAT3 targets like *MYC*, *BCL2L1* or *CCND1* were substantially downregulated on transcript level by treatment with Trametinib alone in both HeLa and SiHa cells (Figure 27), despite the strong induction of STAT3 Y705 phosphorylation (Figure 26). This indicates that, under the tested conditions, the MAPK pathway plays a greater role for the expression of these genes than the JAK/STAT3 pathway.

2.6.3 Inhibition of STAT3 does not sensitize cells to PI3K- or MAPK pathway inhibitors

Finally, to directly assess a possible role of STAT3 for the therapy resistance of cervical cancer cells, I tested whether inhibition of STAT3 activity leads to an increased sensitivity of cervical cancer cells to Trametinib or Pictilisib. As expected, and in line with the discovery that multiple pro-proliferative factors such as *MYC* or *CCND1* are downregulated by Trametinib (Figure 27), treatment with Trametinib, but also with Pictilisib, slowed the proliferation of both SiHa and HeLa cells substantially, as assessed by live cell imaging (Figure 28). This observation is supported by studies reporting that PI3K- and MAPK pathways are critical growth promoting factors in cervical cancer cells[82, 328].

In contrast to Trametinib and Pictilisib, Ruxolitinib treatment alone did not result in any reduction in proliferation of both SiHa and HeLa cells (Figure 28A), as expected from my previous results (Figure 6B). Remarkably however, even though STAT3 Y705 phosphorylation is virtually completely inhibited (Figure 26C), combined treatment of Ruxolitinib with Trametinib or Pictilisib did not affect the growth curves of both SiHa and HeLa cells in combination treatments (Figure 28A).

Likewise, depletion of STAT3 by RNAi did not considerably affect proliferation curves *per se*, as observed before (Figure 9A, C). Largely in line with the results obtained for Ruxolitinib, STAT3-targeting siRNAs also largely did not effectively enhance sensitivity of SiHa and HeLa cells towards Trametinib or Pictilisib treatment (Figure 28B). However, minimal combinatorial effects were visible in SiHa cells, when treated with Trametinib or Pictilisib and in HeLa cells when treated with Pictilisib, each combined with STAT3-targeting siRNAs (Figure 28B).

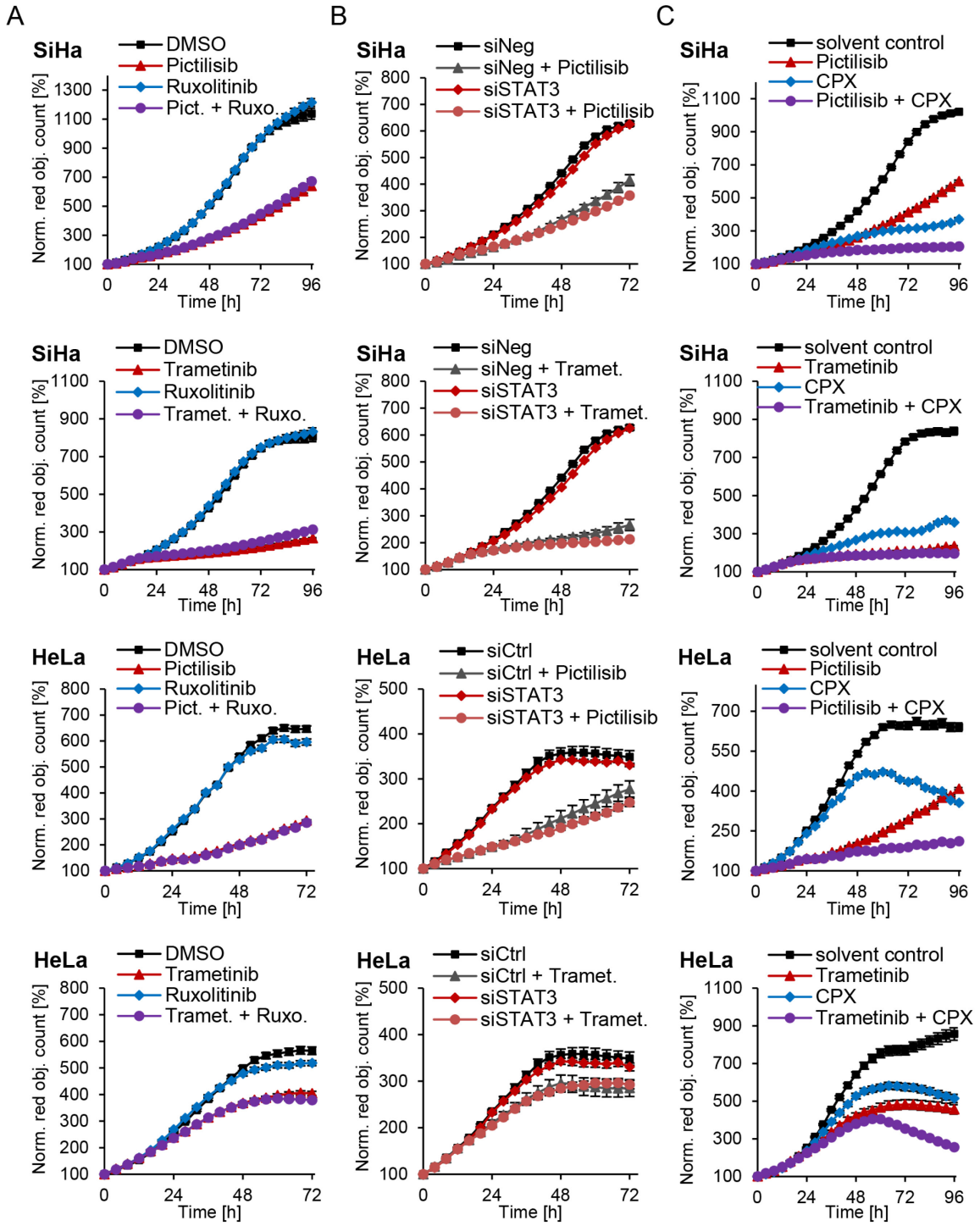

Figure 28: Co-treatment of PI3K- or MAPK pathway inhibitors with Ruxolitinib or STAT3 RNAi-mediated silencing does not lead to considerable combinatorial effects in cervical cancer cells. *SiHa-mKate2 and HeLa-mKate2 cells were treated 48 h after seeding or reverse transfection with indicated siRNAs, respectively, into a 96-well plate with 100 nM Trametinib, 7.5 µM (HeLa) or 10 µM (SiHa) Pictilisib or solvent control and imaged using the Incucyte® S3 live-cell imaging system for up to 96 h. Image analysis and red object quantification (cell counts) were performed using the Incucyte® software package.* ***(A)*** *SiHa-mKate2 and HeLa-mKate2 cells were co-treated with 1 µM Ruxolitinib or solvent control (DMSO), as indicated.* ***(B)*** *SiHa-mKate2 and HeLa-mKate2 were reverse transfected with pools of STAT3 targeting siRNAs (siSTAT3) or control siRNAs (siCtrl, siNeg), as indicated.* ***(C)*** *SiHa-mKate2 and HeLa-mKate2 cells were co-treated with 1.2 µM CPX or solvent control, as indicated. Subfigures (A) and (B) and corresponding legends from Strobel et al., 2023[119].*

In addition, I employed CPX as a third method to block STAT3 activity (Figure 28C). Interestingly, the combination of Pictilisib or Trametinib with CPX more effectively repressed proliferation of both SiHa and HeLa cells than either treatment alone. However, in contrast to Ruxolitinib or STAT3 silencing by RNAi, CPX strongly reduced proliferation of both SiHa and HeLa cells already when applied as a single treatment (Figure 28C), indicating that the cooperative effects between Pictilisib or Trametinib, respectively, and CPX may be independent of STAT3.

To validate whether the small cooperative effects seen with STAT3 silencing and Trametinib or Pictilisib treatment as well as the substantial cooperative effects seen with CPX treatment in conjunction with either Trametinib or Pictilisib can in fact be attributed to concomitant STAT3 inhibition, the same validation approach as employed in my previous experiments (Figure 15) was used: The same treatment conditions, including the transfection of STAT3-targeting siRNAs or the treatment with CPX, were applied to SiHa STAT3 KO and HeLa STAT3 KO cells. Due to the inherent loss of STAT3 in these cells, the effects of the combination treatments should not differ from Trametinib or Pictilisib treatment alone, respectively, if the observed cooperative effects seen in parental SiHa and HeLa cells are indeed linked to concurrent STAT3 inhibition.

Of note, for both STAT3 silencing by RNAi (Figure 29A) as well as CPX treatment (Figure 29B), the cooperative effects seen in parental SiHa and HeLa cells could as well be observed in STAT3 KO clones, indicating that they are independent of concurrent STAT3 inhibition. Moreover, and importantly, also CPX treatment alone leads to comparable anti-proliferative effects in STAT3 KO cells and parental cells (please compare Figure 28C and Figure 29B), indicating that the anti-proliferative effect of CPX is likely unrelated to its destabilizing effect on STAT3 as well.

Finally, in order to assess if the inhibition of the induction of STAT3 Y705 phosphorylation upon PI3K- or MAPK pathway inhibition may lead to substantial sensitization upon prolonged treatment, SiHa, HeLa and CaSki cells were cultured in the presence of Trametinib or Pictilisib and in combination with or without STAT3 inhibition in CFAs for 10-14 days. For this purpose, Ruxolitinib was used to inhibit STAT3 signaling as it exerted the least STAT3-unrelated effects on proliferation compared to STAT3 siRNAs or CPX treatment in previous experiments. In this setup, as in previous long-term inhibition experiments (Figure 6), the medium was refreshed along with the treatments every 72-96 h.

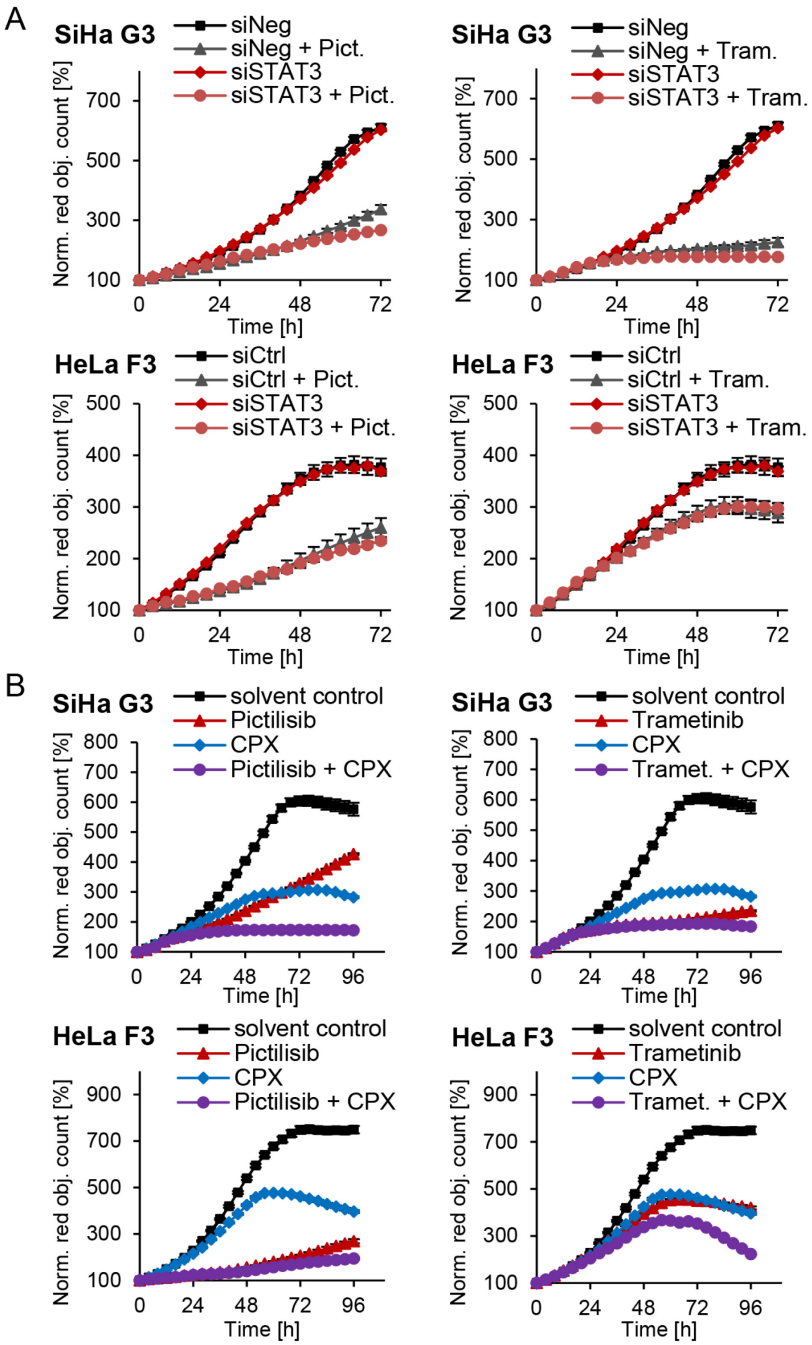

Figure 29: STAT3 does not confer treatment resistance against PI3K- or MAPK pathway inhibitors in cervical cancer cells. (A) *SiHa STAT3 KO G3-mKate2 and HeLa STAT3 KO F3-mKate2 cells were reverse transfected in 96-well plates with pools of STAT3 targeting siRNAs (siSTAT3) or control siRNA (siCtrl, siNeg). Cells were treated 48 h after transfection (time point 0) with 100 nM Trametinib and 7.5 µM (HeLa) or 10 µM (SiHa) Pictilisib, or solvent control, for up to 72 h and imaged using the Incucyte® S3 live-cell imaging system. Image analysis and red object quantification (cell counts) were performed using the Incucyte® software package.* ***(B)*** *SiHa STAT3 KO G3-mKate2 and HeLa STAT3 KO F3-mKate2 cells were treated 48 h after seeding (time point 0) into a 96-well plate with 100 nM Trametinib, 7.5 µM (HeLa) or 10 µM (SiHa) Pictilisib, 1.2 µM CPX, solvent control or a combination thereof, as indicated. Image acquisition and analysis was performed as in (A).*

In line with my results obtained from short-term proliferation assays (Figure 28), Trametinib as well as Pictilisib treatment showed strong anti-proliferative effects on all cervical cancer cell

lines (Figure 30) with Trametinib being especially effective in SiHa cells and inducing a senescence-like morphology with large, flat cells. In CaSki cells, Pictilisib was particularly effective, which was expected because of a driving gain-of-function mutation in *PIK3CA* in these cells[334]. In contrast, treatment with Ruxolitinib alone did not lead to any effects on colony formation or cell morphology, as expected (Figure 6C, Figure 7). Furthermore, colony formation was virtually unaffected in all cell lines when Trametinib or Pictilisib was combined with Ruxolitinib compared to each treatment alone (Figure 30). Similarly, although clone and cell morphology differed strongly between Trametinib or Pictilisib and solvent control treatment, addition of Ruxolitinib did not further alter morphology (Figure 30).

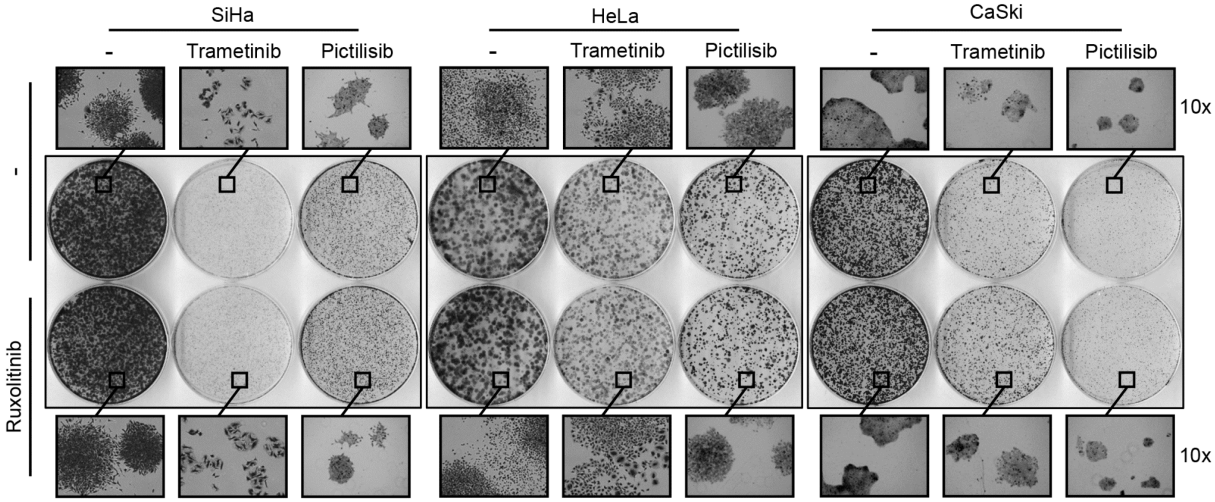

Figure 30: Long-term co-treatment of Ruxolitinib with Pictilisib or Trametinib does not provide evidence for STAT3-induced treatment resistance. *3000 SiHa, HeLa and CaSki cells were seeded in 6 cm plates followed by treatment with 0.75 µM (CaSki), 2.5 µM (HeLa) or 5 µM (SiHa) Pictilisib, 100 nM Trametinib, 1 µM Ruxolitinib, solvent control or a combination thereof, as indicated, 48 h after seeding. Every 3-4 days, the cell culture medium was exchanged with fresh medium containing the respective drugs. Colonies were fixed and stained after 14-15 days. Cell and colony morphology images were acquired using a brightfield light microscope with 10× magnification. Figure content and legend from Strobel et al., 2023[119].*

Taken together, these results do not provide evidence that the observed induction of STAT3 Y705 phosphorylation after application of inhibitors of the PI3K- and MAPK pathways is a considerable resistance mechanism in cervical cancer cells. Other than suggested for certain other cancer entities[234-236], these findings thus do not support the idea that the therapeutic sensitivity of cervical cancer cells to the tested specific pathway inhibitors (targeted therapy) can be considerably enhanced by concomitantly blocking STAT3.

2.6.4 Combinatorial effects of CPX and Decitabine treatment are independent of STAT3

Another promising therapeutic agent that is being investigated for the treatment of HPV-induced cancers such as cervical cancer is the demethylating agent Decitabine (DAC)[335]. Interestingly, I found that CPX strongly enhances the effectiveness of DAC treatment in CFAs

(Figure 31A) and senescence assays in SiHa cells (Figure 31B) as well as HeLa cells (not shown). Since CPX treatment leads to the degradation of STAT3[119], the question arose whether this combinatorial effect might be linked to STAT3.

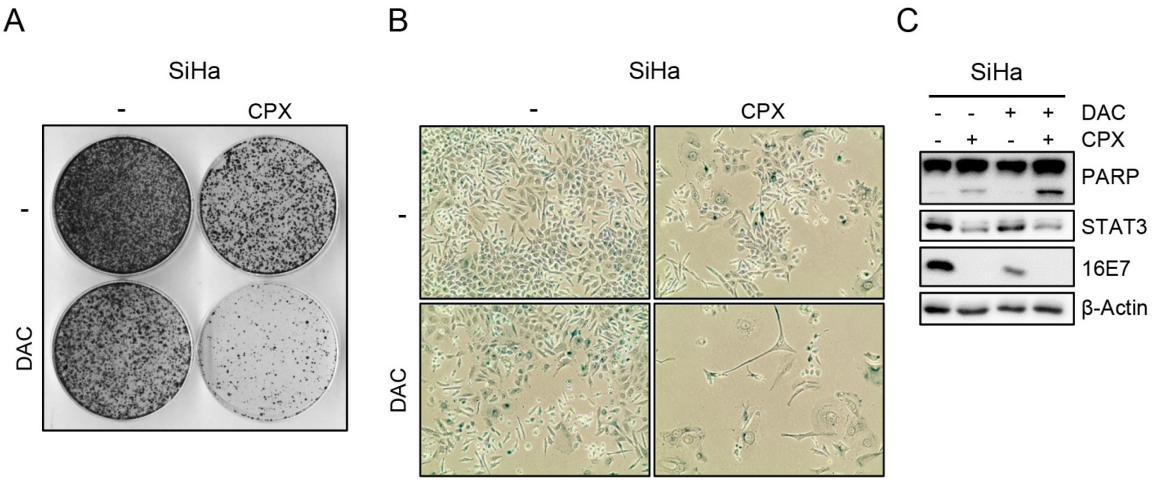

Figure 31: Ciclopirox strongly sensitizes SiHa cells to Decitabine treatment. *SiHa cells were treated 48 h after seeding with 1 µM DAC, 2.5 µM CPX, solvent control (-) or a combination thereof, as indicated, for 48 h followed by* ***(A)*** *CFAs,* ***(B)*** *senescence assays or* ***(C)*** *analysis of PARP, total STAT3, HPV 16E7 or Ferritin protein levels by immunoblot. β-Actin, representative loading control.*

Initial investigations led to the finding that this combinatorial effect is likely due to both increased induction of a senescence-resembling phenotype (large, flattened, non-proliferating cells, Figure 31B), as well as an increased induction of apoptosis as evidenced by increased levels of the commonly used apoptosis marker cleaved poly-(ADP-ribose)-polymerase (PARP)[336, 337] compared to either CPX or DAC treatment alone (Figure 31C).

Next, to assess whether STAT3 repression by CPX is involved in the observed combinatorial effect, the same approach as in my previous experiments (Figure 15, Figure 29) was utilized: If the same combinatorial effect can be observed in STAT3 KO cells, STAT3 is highly unlikely to be relevant for the phenomenon. Using live-cell imaging, I found that DAC and CPX treatment as well as the combination of both acted highly similar in SiHa STAT3 KO cells and parental SiHa cells (Figure 32A). This again indicates that not only the combinatorial effect, but also the anti-proliferative effect of CPX *per se* is not linked to STAT3 repression. Additionally, I exchanged CPX as an STAT3 repressor for the JAK1/2 pathway inhibitor Ruxolitinib to block STAT3 signaling. This combination also resulted in similar growth curves in both parental and SiHa STAT3 KO cells and did not lead to the same effects observed when CPX and DAC are combined (Figure 32B), further pointing towards a CPX-specific, but STAT3-independent, combinatorial effect.

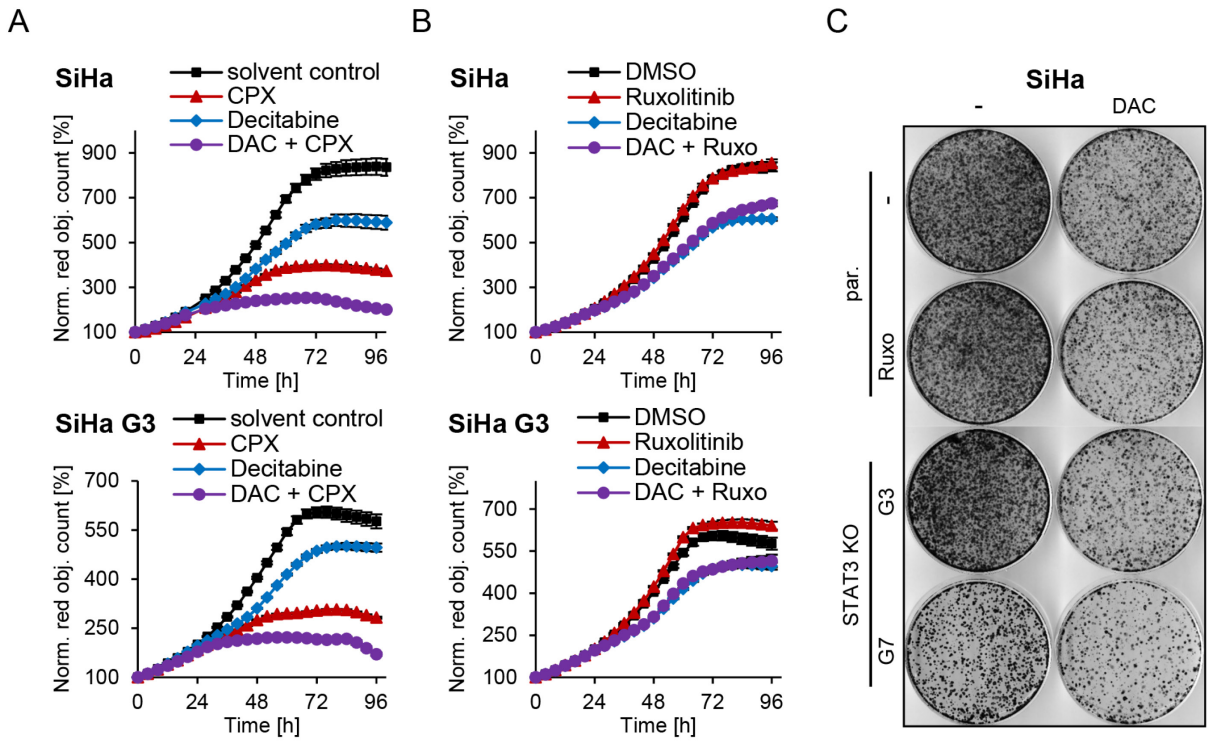

Figure 32: Combinatorial effects of Ciclopirox and Decitabine treatment are independent of STAT3. *SiHa-mKate2 cells were treated 48 h after seeding (time point 0) into a 96-well plate with 1 µM DAC or solvent control combined with* ***(A)*** *1.2 µM CPX or* ***(B)*** *1 µM Ruxolitinib, as indicated, for 96 h and imaged by the Incucyte® S3 live-cell imaging system. Image analysis and red object quantification (cell counts) were performed using the Incucyte® software package.* ***(C)*** *SiHa and SiHa STAT3 KO cells were treated 48 h after seeding with 1 µM DAC, 1 µM Ruxolitinib, solvent control (-) or a combination thereof, as indicated, for 48 h followed by CFAs.*

Finally, since DAC treatment led to a slight induction of senescence at the applied concentrations (Figure 31B), it was tested whether STAT3 might affect the outgrowth of colonies similar as it was observed after combination of STAT3 inhibition by RNAi or Ruxolitinib with senescence-inducing siRNAs targeting E6 and E7 (Figure 13, Figure 14). In line with the results obtained in live-cell imaging assays (Figure 32A, B) DAC treatment did not result in less colony outgrowth when combined with Ruxolitinib or when applied in STAT3 KO cells compared to parental SiHa cells (Figure 32C). Only in STAT3 KO G7 cells, slightly fewer colonies are visible after DAC treatment. However, this is already the case in untreated STAT3 KO G7 cells (Figure 32C). In conclusion, these results show that STAT3 highly likely does not play a role for the combinatorial effect observed when treating cells with CPX and DAC concurrently.

Taken together, the obtained results indicate that STAT3 does neither play a considerable role for resistance to the drug DAC nor for resistance to agents employed for targeted therapy, like Pictilisib or Trametinib, at least under the tested conditions.

2.6.5 Ectopic overexpression of STAT3 does not confer resistance to CPX treatment

Finally, returning to the starting point of my investigations, I further assessed whether STAT3 plays a major role for the anti-proliferative effects of CPX in cervical cancer cells. The results showing that CPX is similarly effective as an anti-proliferative agent in STAT3 KO cells and parental cells (Figure 29B, Figure 32A) already strongly indicate that STAT3 is not a critical determinant of the CPX-mediated effects in cervical cancer cells.

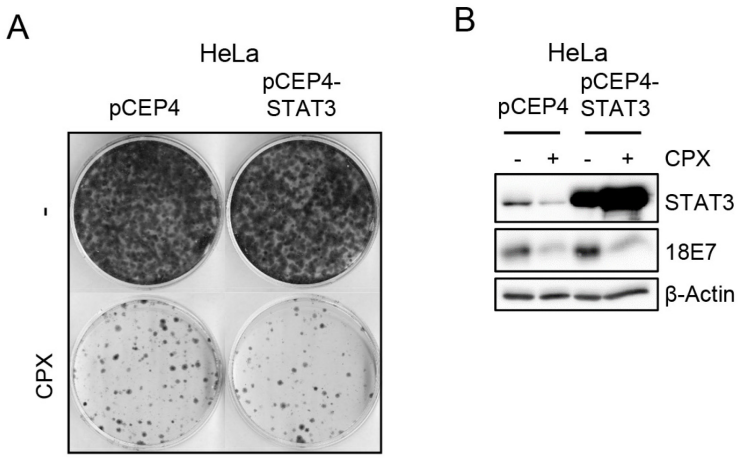

Figure 33: The repressory effects of CPX on cervical cancer cell proliferation and viral oncogene expression are not affected by ectopic overexpression of STAT3. *HeLa cells were transfected with the indicated plasmids 24 h after seeding followed by treatment after further 24 h with 10 µM CPX or solvent control (-) for 48 h. Cells were then processed for* ***(A)*** *CFAs (solvent control (-) cells: split 1:200, CPX treated cells: split 1:50) or* ***(B)*** *analysis of total STAT3 and HPV 18E7 protein levels by immunoblot. β-Actin, loading control.*

This is further supported by experiments in which I ectopically overexpressed STAT3 in HeLa cells followed by treatment with CPX (Figure 33). If the downregulation of STAT3 by CPX is a critical determinant of CPX' anti-proliferative and E6/E7-repressing effects, it was expected that overexpression of STAT3 might at least partially counteract these effects.

However, in line with live-cell imaging results indicating that STAT3 downregulation is not a major determinant of the anti-proliferative effects of CPX (Figure 29B, Figure 32A), ectopic overexpression of STAT3 did not confer resistance to CPX treatment in CFAs (Figure 33A). Furthermore, it did also not counteract the CPX-induced downregulation of HPV18 E7 levels (Figure 33B). Although these results have to be interpreted with caution due to potential unspecific effects of ectopic protein overexpression in general[338], they also do not provide evidence that the repressing effects of CPX on cervical cancer cell proliferation or on HPV E6/E7 oncogene expression critically depend on CPX-linked STAT3 inactivation.

CHAPTER 3

Discussion

3. Discussion

Despite the introduction of effective prophylactic vaccines targeting the most common high-risk HPV types[68-70], HPV-induced cancers will likely remain a major burden for public health systems, with especially high incidence in developing countries[18]. Therefore, novel therapeutic options for HPV-induced cancers as well as pre-neoplastic lesions are urgently needed. One promising possibility could be the iron chelator CPX, which is already in clinical use with an excellent safety profile since several decades for the topical treatment of fungal infections[89]. Previously, CPX was found to block proliferation as well as expression of the HPV E6/E7 oncogenes in cervical cancer cells[86, 87]. Interestingly, CPX induces the destabilization of STAT3[119] – a transcription factor reported to be essential for promotion of proliferation[252, 255, 256, 265-268] and efficient HPV E6/E7 expression[187, 251-253] in cervical cancer cells. *Vice versa*, E6 is described to induce the induction of STAT3 activity[251, 253, 255], reportedly in an IL-6 dependent manner[253], resulting in a critical oncogenic positive feedback loop. Due to this interconnection, STAT3 is proposed to be a highly promising therapeutic target to interfere with cervical cancer cell proliferation as well as E6/E7 expression simultaneously. In my thesis I therefore aimed to assess whether STAT3 plays a critical role for cervical cancer cell proliferation, HPV oncogene expression and treatment resistance and consequently, whether the destabilization of STAT3 is a critical contributor to the anti-proliferative effects of CPX.

After identification of potential factors that could serve as starting points for further investigations addressing the destabilization of STAT3 by CPX treatment, I obtained several surprising results with respect to the role of STAT3 in cervical cancer cells. While small molecule STAT3 inhibitors blocked proliferation and E6/E7 expression in cervical cancer cells, genetic modulation of STAT3 expression by RNAi, CRISPR/Cas9 and ectopic overexpression as well as modulation of the JAK1/2-STAT3 signaling axis by Ruxolitinib or OSM treatment, respectively, did not yield any evidence pointing to a critical role of STAT3 in HPV-positive cervical cancer cells for their proliferation, treatment resistance or E6/E7 expression. Subsequently, I showed that the effects of CPX as well as various small molecule STAT3 inhibitors are independent of STAT3 in cervical cancer cells. Taken together, my results thus question the prevailing concept that STAT3 serves as a highly promising therapeutic target to directly inhibit proliferation and viral E6/E7 oncogene expression in cervical cancer cells. My findings further highlight the need for carefully controlled, multi-methodological studies when assessing the potential of STAT3 to serve as a therapeutic target.

3.1 Anti-proliferative effects of the iron chelator Ciclopirox

3.1.1 CPX-induced anti-proliferative effects are independent of STAT3

In view of CPX' therapeutic potential for HPV-related diseases[86, 87], initially the question arose whether CPX' anti-proliferative effects depend on the destabilization of the STAT3 protein. Importantly, most commonly used STAT3 inhibitors only address canonical STAT3 signaling by inhibition of dimerization or Y705 phosphorylation, which is essential for STAT3's canonical function as a transcription factor[126]. In addition to canonical STAT3 signaling, however, there are multiple non-canonical functions of STAT3 with strong oncogenic potential[190]. By inducing the degradation of total STAT3 protein, CPX is in principle not only able to block canonical but also all non-canonical functions of STAT3, as also indicated by the observed degradation of mitochondrial STAT3. CPX could therefore be especially promising in comparison to conventional STAT3 inhibitors.

In cervical cancer cells, I found that the anti-proliferative effect of CPX is comparable to various STAT3 inhibitors. Importantly however, I could observe this anti-proliferative effect of CPX to a similar extent also in STAT3 KO cells. As illustrated in Figure 34, using STAT3 KO cells for target validation, it was essentially expected that CPX would be inactive in STAT3 KO cells if its effects could be purely attributed to the destabilization of STAT3, since these cells proliferate without detectable STAT3 expression and thus targeting STAT3 through CPX should have had no effect. Furthermore, I found that also ectopic overexpression of STAT3 did not counteract the inhibition of colony formation as well as E6/E7 repression by induced by CPX. Similarly, I found that, in contrast to the anti-proliferative and E6/E7 repressing effects of CPX[87], the destabilization of STAT3 by CPX was not counteracted by high glucose supplementation. These findings therefore strongly indicate that the major determinants underlying the anti-proliferative activity of CPX in cervical cancer cells are independent of STAT3. This notion is further supported, as discussed in more detail in the following chapters, by various genetic (Figure 9, Figure 10) and non-genetic methods (Figure 6, Figure 10, Figure 11) which I used to modulate STAT3 expression and activity. They collectively did not yield any evidence for an essential role of STAT3 for proliferation or efficient viral oncogene expression in cervical cancer cells, strongly indicating that the observed effects of CPX on these parameters are not linked to its destabilizing effect on STAT3.

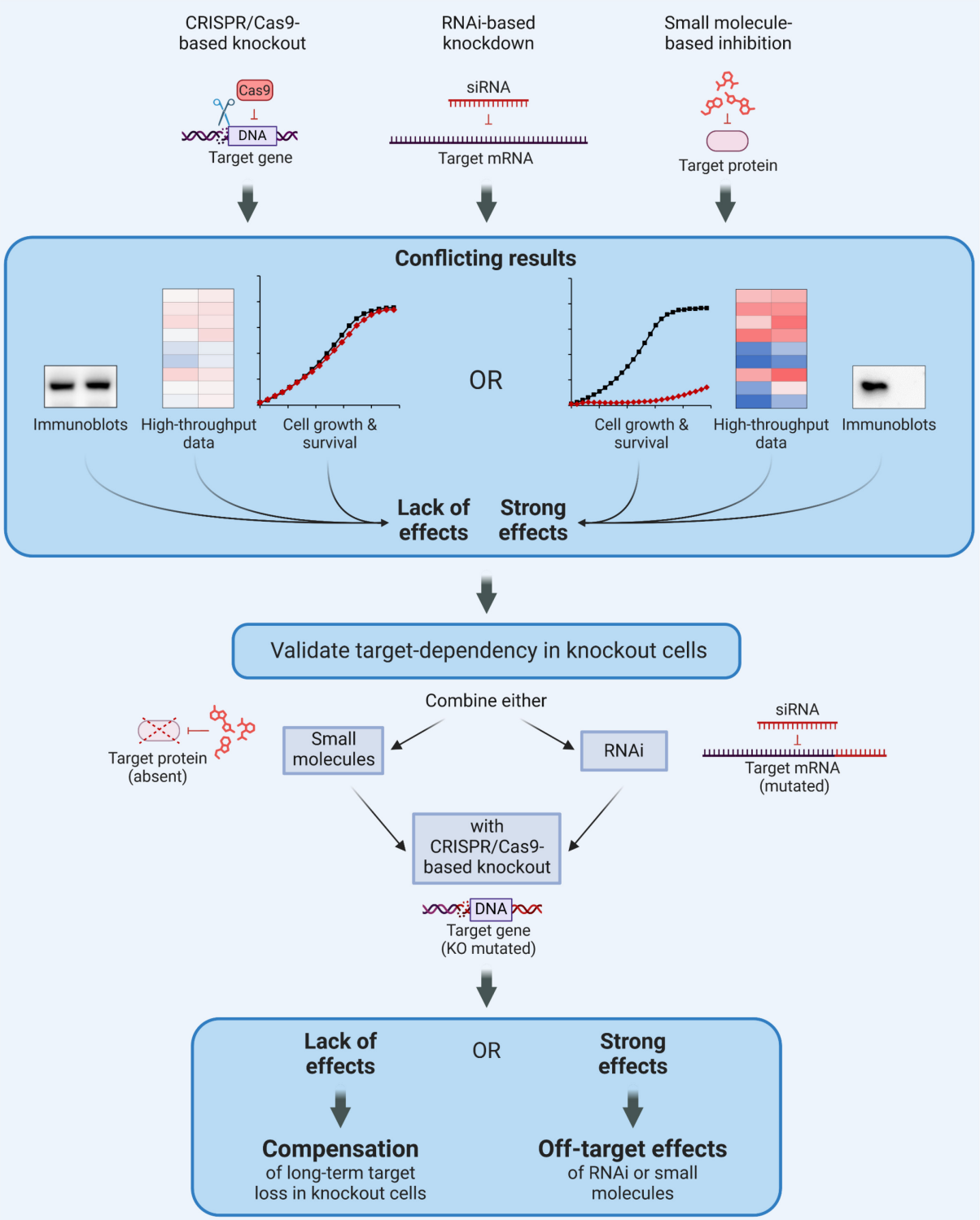

Figure 34: Target validation strategy employed in this thesis. *CRISPR/Cas9-based KO, RNAi-based knockdown or small molecule-based inhibition are often employed to investigate the function of prospective drug targets. These methods not always yield consistent results leading to uncertainty regarding whether the protein in question is truly critical and thus a promising target for potential future therapies or whether it is dispensable and thus neglectable and a non-optimal target. If viable and validated CRISPR/Cas9-based KO cells are available, a reliable strategy to assess this issue is the application of aforementioned small molecule inhibitors or RNAi techniques in KO cells. If RNAi or small molecules do not induce any effects in KO cells, it is likely that their effects in parental cells are target specific and that KO cells adapted to long-term target loss. If, in contrast, the same effects can be*

observed in both KO and parental cells, it is highly likely that these effects are not target specific but instead represent off-target effects of small molecules or RNAi. Target validation strategy inspired and adapted from Peretz et al.[327]. Figure created with BioRender.com.

Nonetheless, CPX – which is in clinical use since decades with an excellent safety profile for topical treatment of fungal infections[89] – could still possess great therapeutic potential in the context of HPV-induced diseases. Since CPX strongly downregulates the expression of E6/E7[86, 87] it could for example have potential for the treatment of preneoplastic CIN lesions which are often easily accessible and may thus possibly be treated via topical CPX application. Further, CPX may have potential to be utilized for the topical treatment of reportedly STAT3-dependent diseases such as psoriasis[209]. In this regard, it is a promising finding that CPX treatment leads to STAT3 downregulation in non-cervical cancer cells and non-malignant keratinocytes as well. For systemic cancer treatment, toxicity of iron chelation as well as unfavorable pharmacokinetics of CPX could pose a challenge[339]. To address the latter, fosciclopirox was developed to allow oral application[339] and possibly enable treatment of STAT3-dependent systemic diseases[121, 122]. For example, T-LGL often harbors STAT3 mutations and is dependent on constitutively active STAT3 signaling[141, 144, 231]. T-LGL could thus be particularly sensitive to CPX if systemic concentrations sufficient to induce STAT3 destabilization can be reached.

In addition, CPX has strong potential for effective combination therapies[87]. In this regard, combination with DAC could be especially promising since DAC is currently being developed for the treatment of HPV-induced cancers[335] and showed encouraging cooperative potential with CPX in cervical cancer cells in my experiments (Figure 31, Figure 32). Furthermore, the strong effects observed for CPX combined with Pictilisib or Trametinib (Figure 28) indicate that iron chelation might be a promising strategy to enhance the efficacy of anti-proliferative treatments in cervical cancer cells in general. Importantly, the concentrations of CPX required to achieve effective cooperative results were almost considerably lower than the CPX concentrations required to fully block growth of cervical cancer cells as a single agent[86, 87]. Thus, if CPX as a single agent will prove to be too toxic, combination regimens could be the key to therapeutically exploit the anti-proliferative effects of CPX in the future.

Notably, similar to applying CPX as a single agent, all tested combination treatments – DAC, Pictilisib or Trametinib combined with CPX – yielded highly similar results in parental and STAT3 KO cervical cancer cells, again highlighting the independence of the observed effects from STAT3. Due to the plethora of cellular functions that directly or indirectly depend on intracellular iron availability, it is likely that the effects of CPX as a single agent as well as the cooperative effects seen with CPX are linked to other biological consequences of iron chelation. For example, inhibition of OXPHOS is considered to alleviate treatment resistance[340]

while application of mTOR inhibitors is a known anti-cancer strategy[341]. Importantly, iron chelation in cancer cells similarly affects these processes[86, 294, 342] – the above-mentioned alterations could thus explain the anti-proliferative and combinatorial potential of CPX. Notably, also other metabolic conditions and drugs such as hypoxia, Metformin or 2-DG share some of these effects with CPX and downregulate E6/E7 expression as well[84, 85, 319, 320]. Which features of iron chelation – besides inhibition of OXPHOS[87] – are the most critically determining factors for CPX' anti-proliferative activity will have to be elucidated in the future. In cervical cancer cells however, the destabilization of STAT3 highly likely does not play an appreciable role for the anti-proliferative effects of CPX.

3.1.2 Mechanistic insights into the destabilization of STAT3 by CPX

Nonetheless, it will be of high interest to investigate the detailed mechanism of STAT3 destabilization by CPX in the future. Factors involved in this process could potentially be targeted to induce STAT3 destabilization without iron chelation-induced side effects of CPX treatment. This could possibly yield a new class of STAT3 inhibitors, which may be broadly applicable also to the diverse array of STAT3-linked diseases.

To this end, I found that expression of factors involved in SUMOylation is enriched after CPX treatment. SUMOylation was described to be able to induce protein degradation[301] and interestingly, one of the most strongly differentially expressed SUMOylation-related factors in the proteome data[86] investigated in my thesis is the deSUMOylating isopeptidase 1 (DESI1) which may thus be involved in STAT3 destabilization. First tests however revealed that downregulation of DESI1 is only observed in SiHa cells (not shown), questioning whether DESI1 is a causative factor for STAT3 destabilization, which was observed in all tested cervical cancer cell lines. Further, I identified 12 proteins involved in ubiquitination and degradation of polyubiquitinylated proteins which could hypothetically contribute to the reduced half-life of STAT3 after CPX treatment. However, since protein degradation is a highly complex process involving the interplay of protein complexes via protein-protein interactions[343], a mechanism independent of any of these factors is certainly plausible as well. For example, also post-translational modifications are known to further affect the function of proteins linked to proteolysis[344] and post-translational modification changes are not identified by the utilized proteomics methodology.

The identification of factors involved in the degradation of STAT3 by CPX will likely be a comprehensive long-term research project on its own. This project could start with analyzing the factors that I identified to be potentially involved in STAT3 degradation and could apply the conditions that I identified to retain STAT3 protein levels despite similarities to CPX treatment. For example, 2-DG, hypoxia and Metformin treatment block E6/E7 expression[85, 86, 319] and, in

the case of hypoxia and Metformin, induce similar metabolic alterations by blocking OXPHOS[292, 293] and mTOR signaling[84, 319]. Despite these similarities, I found that STAT3 is not repressed under any of these conditions. Hypoxia in particular closely resembles CPX treatment since it also upregulates proteins involved in glycolysis[87] and stabilizes HIF transcription factors[299]. In fact, iron chelators are often utilized as hypoxia mimetics due to their similarities[295-298]. These circumstances could be exploited to delineate specific differences between hypoxia and CPX, which are responsible for the observed STAT3 destabilization. For example, immune precipitation of STAT3 followed by identification and quantification of proteins and their post-translational modifications by mass spectrometry could be employed to discover post-translational modifications or further candidate proteins that differentially interact with STAT3 or are differentially present, respectively, in cells treated with CPX, hypoxia or a combination thereof. Eventually, the identified candidate proteins will have to be validated using techniques like RNAi, CRISPR/Cas9 or the ectopic expression of certain mutants of candidate proteins and of STAT3.

Notably, it was reported that CPX also induces the destabilization of cell division cycle 25 homolog A (CDC25A)[345, 346] and cyclin D1[108]. It might thus also be possible that STAT3 is not the only protein degraded upon iron chelation. This would potentially undermine the therapeutic potential of a prospective future drug targeting the mechanism of iron chelation-induced STAT3 degradation since the degradation of other proteins besides STAT3 by the same mechanism could lead to an unfavorable safety profile. To investigate this, quantitative mass spectrometry in combination with pulse-chase metabolic labelling could be employed to systematically identify proteins that are (de)stabilized and to determine their extent of (de)stabilization, i.e. their half-life, upon CPX treatment.

Overall, this part of my thesis provides valuable first insights into the destabilization of STAT3 in cervical cancer cells by iron chelators such as CPX, which could lead to the development of new therapies for STAT3-dependent diseases in the future. However, in view of my unexpected findings on the functional significance of STAT3 in HPV-positive cancer cells, I focused a large part of my studies on this latter aspect, since it should have a strong impact on the prevailing concept that STAT3 serves as a key therapeutic target in HPV-induced cancers.

3.2 Endogenous STAT3 as a therapeutic target in cervical cancer

3.2.1 Discordant effects of small molecule STAT3 inhibitors on cellular proliferation

During the investigation of the functional significance of STAT3 in cervical cancer cells, multiple surprising results were obtained. While STAT3 inhibition by application of commonly used small molecule STAT3 inhibitors strongly repressed proliferation and induced cell death, inhibition of the JAK1/2 kinases upstream of STAT3 by Ruxolitinib did not affect growth or viability of cervical cancer cells. Additionally, I observed highly variable changes in cellular morphologies as well as differing kinetics of growth inhibition and cell death induction for different small molecule STAT3 inhibitors but not for Ruxolitinib. Thus, the question arose whether these discrepancies may possibly be explained by STAT3-independent effects in a manner similar to CPX.

Considering the discussions around 'undruggable' proteins[276, 347], it can be speculated whether the relatively high concentrations which are frequently employed for the application of small molecule STAT3 inhibitors[187, 251, 255] might possibly be linked to the scarcity of deep binding pockets in many transcription factors such as STAT3, thereby complicating development of potent and specific small molecule inhibitors[276]. Accordingly, many oncogenic transcription factors such as c-myc, BRD4 (bromodomain-containing protein 4) as well as STAT3 have been classified as 'undruggable' in a sense that it proved to be rather difficult to design inhibitors with high specificity and potency[276, 277]. Intriguingly, a recent report showed that the anti-proliferative effects induced by one of the most commonly used small molecule STAT3 inhibitors, Stattic, cannot be solely attributed to inhibition of STAT3. Instead the cytotoxic effects of Stattic are at least partly due to inhibition of histone acetylation[348], inhibition of glutathione reductase[349] and by acting as an alkylating agent on multiple different STATs and on NUDT5 (nucleoside diphosphate-linked moiety X motif 5)[350]. Similarly, substantial off-target effects or unexpected modes-of-action were reported for BP-1-102[350] and further STAT3 inhibitors such as OBP-51602[351, 352], Cpd188[350] and JSI124[353], for example by activation of NfκB[353] or by mitochondrial alteration through formation of toxic STAT3 aggregates[351]. Interestingly, and provocatively, a comprehensive investigation reported considerable off-target effects for a wide range of small molecule inhibitors, which already entered the clinical trial phases, providing a potential explanation for unacceptable toxicities observed for some of these compounds[326].

To evaluate whether the observed effects of small molecule STAT3 inhibitors investigated in this thesis might be attributable to off-target toxicities, the validation strategy illustrated in Figure 34 was employed. If small molecule STAT3 inhibitors induce the same effects in STAT3 KO cells, a mode-of-action independent of STAT3 is highly likely. Indeed, I found that all tested

STAT3 inhibitors are also active in STAT3 KO cells. Specifically, compared to parental SiHa cells, I found that application of these STAT3 inhibitors in SiHa STAT3 KO cells (1) repressed proliferation to a similar extent, (2) resulted in comparable levels of cell death and (3) induced similar cellular morphologies. Furthermore, (4) several pathways and factors of critical relevance in cervical cancer[39, 65, 82, 328] were affected by all tested STAT3 inhibitors in STAT3 KO as well as in parental cells. Importantly, none of these effects was visible under treatment with Ruxolitinib. Taken together, these four major findings strongly suggest that the observed effects of the tested STAT3 inhibitors in cervical cancer cells can largely be attributed to off-target toxicities. Of note, it is plausible that at least part of these effects could be linked to the observed modulation of p53 or the investigated PI3K and MAPK pathways. In further support of the hypothesis that most of the effects exerted by the tested STAT3 inhibitors in HPV-positive cancer cells were unrelated to STAT3, blockage of STAT3 expression through genetic methods such as RNAi and CRISPR/Cas9 did not affect their proliferation despite efficient downregulation or depletion of STAT3, respectively. Neither did treatment with OSM have an impact on the growth of HPV-positive cancer cells, even though STAT3 activity was strongly induced.

Collectively, these results strongly question the prevailing concept that STAT3 is an essential factor for the proliferation of cervical cancer cells. Although this finding is surprising in light of the general idea that STAT3 is an important growth-promoting factor in many cancers, it is noteworthy that my findings are not exclusive to cervical cancer. For example, a study reported that the targeted degradation of STAT3 in several acute myeloid leukemia and lymphoma cell lines did not result in growth suppression or cell death despite considerable constitutive activation of STAT3 in these cells[278]. Instead this study showed that only a subset of anaplastic large-cell lymphoma cells was highly responsive to STAT3 depletion[278].

What could potentially explain the discrepancy of my results to the studies reporting STAT3 as a critical player for cervical cancer cell proliferation? Besides employing off-target prone small molecule STAT3 inhibitors[187, 251-253, 256], other studies utilized RNAi[252, 253, 255], ectopic expression of dominant negative STAT3 mutants[251, 256] or the natural compound Curcumin[252, 255] to inhibit STAT3 activity and expression. It cannot be excluded that possible off-target effects of these methods may potentially contribute to the negative impact on cervical cancer cell proliferation. In fact, in initial experiments for this thesis (not shown), 10 different sequences were tested regarding their potential for specifically targeting STAT3 by RNAi. Of these, 2 were found to strongly affect proliferation (albeit in in a cell line-dependent manner), similar to aforementioned studies utilizing RNAi to inhibit STAT3 expression[252, 253, 255]. However, these 2 siRNAs were also effective in STAT3 KO cells, indicating that they exert STAT3-independent anti-proliferative effects. These initial experiments highlighted the need to thoroughly assess

the specificity of the different STAT3-targeting methods applied in my thesis. Notably, off-target effects of individual siRNAs are reported to be common[354] while in comparison, pooling of many siRNAs was shown to virtually completely eliminate off-target effects by allowing the application of lower concentrations of individual siRNAs[355].

Therefore, I employed pools of 3 or 4 siRNAs, depending on the cell line, in all key experiments. Individually, all these siRNAs were found to efficiently downregulate STAT3 expression while showing no indication of strong STAT3-independent toxicities. Consistently, these pools of siRNAs did not considerably affect proliferation of cervical cancer cells. In addition, the CRISPR/Cas9 technique was utilized to generate STAT3 KO clones, since this method is reported to be less prone to off-target effects than RNAi[354, 356]. Nevertheless, to still account for potential CRISPR/Cas9-related off-target effects as best as possible, I also employed two different gRNAs for the generation of STAT3 KO cells. In summary, I applied a range of different methods to modulate STAT3 activity or expression (Figure 35) as well as extensive validation strategies (Figure 34). In contrast, most above-referenced studies employed only one or few different methods to modulate STAT3, often involving very high small molecule or siRNA concentrations, and none of these studies addressed the issue of potential off-target effects experimentally.

Furthermore, my experimental results are also supported by published high-throughput data, which was generated without any bias for STAT3. According to the online database portal DepMap[357, 358] (https://depmap.org/portal), which comprises extensive RNAi and CRISPR/Cas9 high-throughput data on the cell growth-dependency of various cancer cell lines on specific genes, cervical cancer cell lines do not critically depend on the expression of STAT3 (Supplementary Figure 1). This is in stark contrast to the E6 interaction partner E6AP which is critical for facilitating p53 degradation[37, 38] in HPV-positive cancer cells and also scores in the datasets accessible via DepMap as an essential growth factor in cervical cancer cell lines (Supplementary Figure 1), underlining the validity of these datasets. Furthermore, my own transcriptome data of SiHa cells depleted of STAT3 by RNAi did not reveal any major influence on well-known oncogenic STAT3 target genes and gene sets that have been described to mediate the pro-proliferative action of STAT3 in cervical cancer cells. Moreover, even strongly inducing the activity of STAT3 by OSM treatment surprisingly only marginally affected the expression of oncogenic STAT3 target genes, if at all. Meanwhile, the non-oncogenic STAT3 target *SOCS3* was – cell line dependently – clearly responsive to OSM as well as STAT3 inhibition by RNAi or Ruxolitinib, demonstrating that STAT3 is in principle functional and active in cervical cancer cells. However, STAT3 apparently lacks the ability to efficiently induce transcription of pro-proliferative candidate target genes in these cells under the different tested experimental conditions.

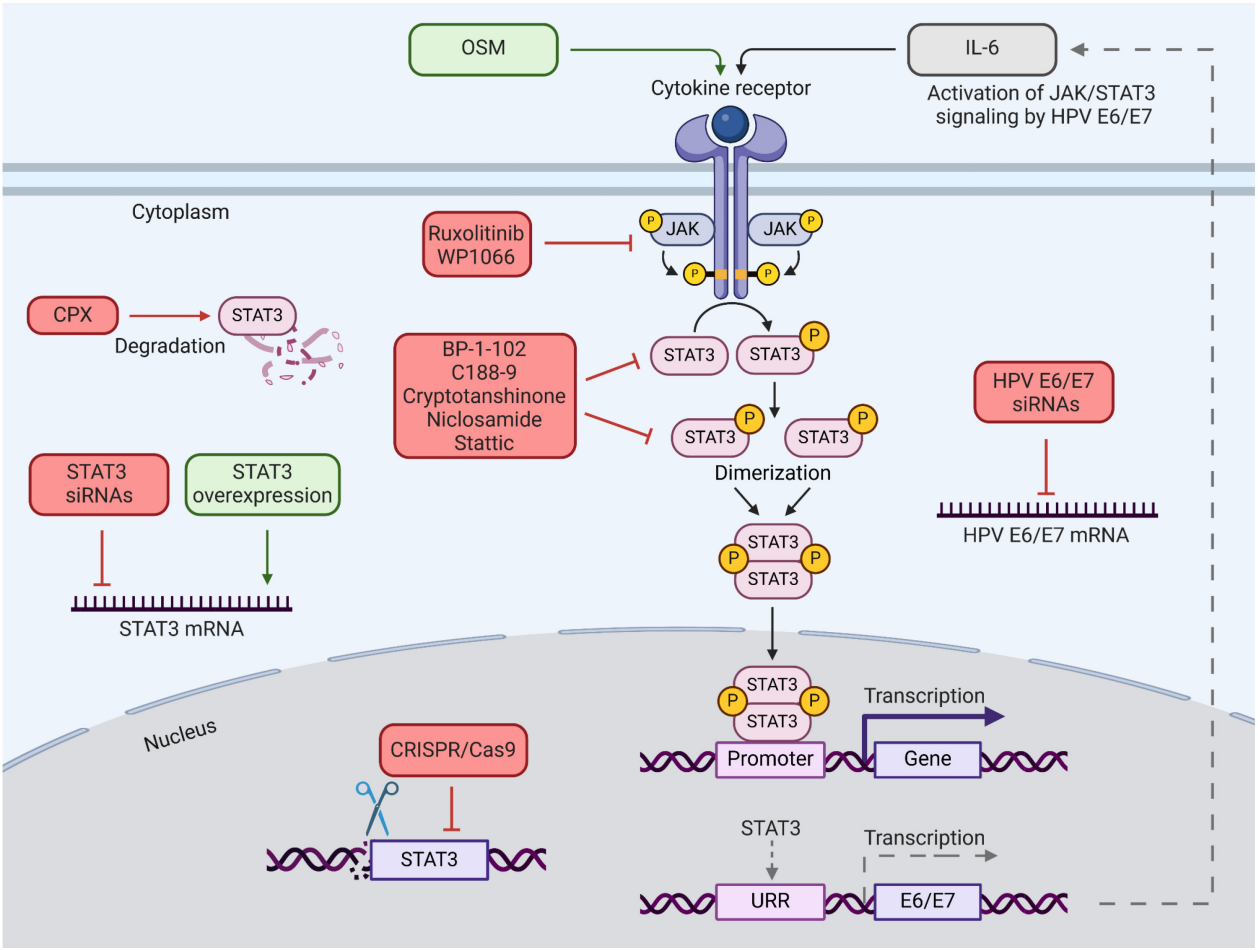

Figure 35: Experimental strategies employed in this thesis. *During canonical activation of STAT3 signaling, e.g. through cytokines like IL-6, STAT3 can become phosphorylated by Janus Kinases (JAKs), dimerizes, translocates from the cytoplasm to the nucleus, where it can transcriptionally activate growth-promoting target genes by binding to specific recognition motifs in their transcriptional promoters. The dashed lines indicate the proposed action of STAT3 in HPV-positive cancer cells. STAT3 has been reported to increase HPV E6/E7 oncogene expression through poorly characterized mechanisms, which may not require direct binding of STAT3 to the viral transcriptional control region (Upstream Regulatory Region, URR) [187, 251-253]. Further, STAT3 signaling has been reported to be activated in cervical cancer cells by an E6-dependent induction of an IL-6-linked autocrine loop[251-253] and by phosphorylation through JAK2 activity[266]. The inhibitory experimental strategies employed in this study analyzing STAT3 and its postulated crosstalk with the HPV oncogenes are indicated in red (chemical JAK and STAT3 inhibitors, CPX, siRNAs, CRISPR/Cas9 KO), activatory strategies are depicted in green (OSM, ectopic STAT3 overexpression). Adapted from the templates "PI3K/AKT, RAS/MAPK, JAK/STAT Signaling" and "Cytokine Signaling through the JAK-STAT Pathway", by BioRender.com (2023). Template retrieved from https://app.biorender.com/biorender-templates. Figure and legend from Strobel et al., 2023[119].*

Finally, I observed that lower concentrations of the tested small molecule STAT3 inhibitors resulted in far weaker off-target toxicities when titrated to find the minimal effective concentration sufficient for inhibition of STAT3 Y705 phosphorylation. This finding further argues against an uncritical use of small molecule STAT3 inhibitors to study the phenotypic effects of STAT3 inhibition, since apparently, at least in cervical cancer cells, many of the tested inhibitors possess only a small therapeutic window in which they inhibit constitutive

activity of STAT3 without inducing pronounced off-target effects. However, at these lower, active concentrations, the tested small molecule STAT3 inhibitors are unable to reduce the OSM-induced high levels of STAT3 Y705 phosphorylation while Ruxolitinib is efficiently able to do so. It is likely that the potential of STAT3 inhibitors to induce off-target effects is not restricted to cervical cancer cells. Therefore, their use in clinical trials, as already done for other cancers with rather limited success[359] (for example by treatment with WP1066[359] or TTI-101[360], also known as C188-9[361]), should be very cautiously evaluated beforehand.

3.2.2 The role of STAT3 for treatment resistance

The absence of a detectable growth-response of cervical cancer cells to the inhibition of STAT3 activity or expression under the tested conditions raised the question whether additional stress factors might be required to reveal a pro-proliferative potential of STAT3 in HPV-positive cancer cells. In other tumor models, STAT3 was reported to confer resistance to targeted treatments such as inhibitors of the PI3K-[235, 236], MAPK-[236, 237, 239-241] or HER-family[236, 242-244] pathways. As illustrated in Figure 25, one major cause of this resistance was reported to be an autocrine feedback loop in which inhibition of the oncogenic driver induces a change in composition of the secretome, which subsequently activates STAT3 signaling through cytokine or growth factor receptors[235, 236, 238]. This was described to be followed by STAT3-mediated induction of transcription of oncogenic target genes promoting cell growth and survival and thus treatment resistance[235, 236, 238]. An alternative possibility for STAT3 activation in response to targeted treatments, in particular in response to MEK inhibitors, is the downregulation of negative regulators of STAT3 signaling, such as *SOCS3*, leading to increased STAT3 activity[239].

Since both PI3K- as well as MAPK pathways are important factors also for cervical cancer cell proliferation[82, 328] and inhibitors of these were tested in an early clinical trial[333], I focused on the investigation of a potential sensitization of cervical cancer cells by concurrent inhibition of STAT3 and PI3K- or MAPK pathways, respectively. I found that JAK1/2-dependent STAT3 Y705 phosphorylation is strongly induced by inhibition of PI3K or MEK, respectively, indicating that some form of this regulation (illustrated in Figure 25) is conserved in cervical cancer cells. Interestingly, however, this induction of STAT3 activity did not translate into increased expression of putative oncogenic target genes, such as *CCND1*, *BCL2L1*, *BCL2*, *MCL1* or *MYC*, which were reported to be mediators of STAT3-induced resistance in other cancer models[238, 244] and in addition were reported to be under control of STAT3 in cervical cancer cells[247, 253, 256, 267, 268]. Moreover, neither did expression of these genes decrease through concurrent inhibition of STAT3 and PI3K- or MAPK pathways. Instead, the tested putative STAT3 target genes *MYC*, *CCND1* and *BCL2L1* were far more responsive to MEK inhibition

than to STAT3 inhibition, despite the strong induction of STAT3 activity. In line with these findings, combined inhibition of STAT3 and PI3K or MEK did not sensitize cervical cancer cells in short- and long-term proliferation assays. Importantly, the induction of weak cooperative effects, which I observed when RNAi was employed to inhibit STAT3 in combination with PI3K or MEK, were also observed in STAT3 KO cells, indicating slight STAT3-independent effects of the used siRNAs under these particular conditions. Thus, similar to untreated cervical cancer cells, STAT3 activity does not affect proliferation or provide resistance under conditions where PI3K- or MEK inhibitors are applied as additional stressors, despite high activation levels of STAT3. Further, these results indicate that the mechanism responsible for the impaired influence of STAT3 on putative oncogenic target genes is conserved in HPV-positive cervical cancer cells under multiple experimental conditions.

In this context, it is also noteworthy that some of the above-referenced studies reporting that STAT3 provides resistance to targeted treatments, such as PI3K or MEK inhibitors, in certain cancer models use small molecule STAT3 inhibitors such as Stattic[235, 239], which can induce anti-proliferative off-target effects[348-350]. Additionally, similar to my results, another well-controlled study on the treatment resistance of melanoma cells to BRAF inhibitors[224] also reported an absence of STAT3-linked regulation of putative oncogenic target genes such as *MYC*, *BCL2*, *MCL1* and *BIRC5*, indicating that this phenomenon is not restricted to cervical cancer cells. Interestingly, this latter study instead identified another factor, *SOX2*, to be under control of STAT3, mediating resistance to BRAF inhibition[224]. Since I did not observe any sensitizing effect of STAT3 inhibition on growth curves as well as on *SOX2* transcript levels upon STAT3 silencing, it is however unlikely that *SOX2* mediates resistance also in my experimental settings.

In addition to Trametinib and Pictilisib, inhibitors of KRAS, which is occasionally found to be gain-of-function-mutated in cervical cancer cells[83, 362], as for example also in the SW756 cell line[363], as well as inhibitors of the cervical cancer-linked[304, 305, 364] HER1/2/3, and c-MET pathways, were tested alone and in combination with Ruxolitinib (not shown). Importantly, alike my findings using PI3K and MEK inhibitors, none of these combination schedules showed cooperative potential with STAT3 inhibition. However, unlike PI3K and MEK inhibitors, most of these additionally tested inhibitors did not affect proliferation of cervical cancer cells *per se*, underlining the importance of PI3K- and MAPK pathways for cervical cancer cells. In principle, since STAT3 signaling in cervical cancer cells is sensitive to Ruxolitinib treatment, high-throughput cellular assays could be employed to investigate a broader range of drugs with regard to their cooperative potential in combination with Ruxolitinib in the future. However, given that under all my tested conditions, increased STAT3 activities in response to drug treatments did not translate into the stimulation of target genes which could mediate treatment

resistance in cervical cancer cells, it seems questionable whether this strategy will be successful.

Besides providing resistance towards different forms of targeted therapy, STAT3 is reported to also play a role for resistance against different chemotherapeutics in various cancers[245, 246]. Since Cisplatin represents one of the most commonly used chemotherapeutic drugs in cervical cancer[71], I also investigated whether STAT3 may confer resistance to Cisplatin. In the literature, there exist discrepant results regarding this question since there are studies reporting a sensitization to Cisplatin by JAK/STAT3 inhibition[266] as well as studies reporting a sensitization to Cisplatin by JAK/STAT3 activation[264, 273]. In my experiments, depending on the STAT3-targeting siRNA or the STAT3 KO clone, somewhat varying results were obtained, but the effects were generally rather small and ranged from slight enhancement to slight attenuation of Cisplatin resistance (not shown). Moreover, our group has found that two major forms of hypoxia present in cancers, chronic and cycling hypoxia provide resistance to chemotherapy[319, 320], however I did not detect an appreciable effect of STAT3 modulation on Cisplatin resistance also under these conditions (not shown). Thus, my results do not point to a major role of constitutive STAT3 activity for Cisplatin resistance in cervical cancer cells.

A promising drug which is currently under investigation to be repurposed for HPV-induced cancers is the demethylating agent DAC[335]. Interestingly, I found that the concurrent application of DAC and CPX induced substantial combinatorial effects. However, as discussed in section 3.1.1, these effects were independent of STAT3, since substitution of CPX with Ruxolitinib or STAT3 KO did not result in cooperative effects when combined DAC.

Collectively, despite a substantial induction of STAT3 phosphorylation in response to the investigated drugs used for targeted therapy, my findings do not provide evidence that this regulatory phenomenon results in increased treatment resistance of cervical cancer cells.

3.2.3 The postulated interdependence of STAT3 and the HPV E6/E7 oncogenes

In addition to an essential role of STAT3 for cervical cancer cell proliferation, a functional interdependence between STAT3 and the HPV E6/E7 oncogenes has been reported[248-250] (Figure 35), however the exact mechanism has not yet been fully elucidated in these studies. On the one hand, STAT3 has been reported to activate expression of E6/E7, since the natural compound Curcumin (which can inhibit JAK/STAT3 signaling) as well as the small molecule JAK/STAT3 pathway inhibitor AG490 were described to block E6/E7 expression in SiHa cells[252]. On the other hand, a study assessing the dependence of the HPV life-cycle on STAT3 function in keratinocytes harboring episomal HPV18 genomes reported that STAT3-targeting siRNAs as well as Cryptotanshinone treatment downregulated E6/E7 protein levels[251]. Interestingly, these authors also reported that the transcriptional activity of

STAT3 is not required to promote E6/E7 expression[251]. In addition, a study described an activation of the HPV16 LCR through IL-10-induced STAT3 signaling[254], while another study could not detect direct binding of STAT3 to the LCR and instead proposed, using IL-6 and Stattic to modulate STAT3 signaling, an indirect mechanism through association of STAT3 with c-JUN and c-FOS[187].

Importantly, however, several of these published studies may have faced experimental limitations. For example, the JAK/STAT3 inhibitor AG490 is not specific for the JAK/STAT3 pathway since it can affect numerous other factors, such as EGFR and HER2[365-367], HIF1α through inhibition of hydroxylation[368] and guanylyl cyclases[369] as well. Accordingly, the specificity of AG490 as an JAK/STAT3 inhibitor has been challenged by a study indicating that data solely relying on AG490 should be interpreted with caution[370]. Similarly, the high concentrations of Cryptotanshinone employed[251, 253] were highly toxic to cervical cancer cells in my own experiments – by a mechanism which appeared to be independent of STAT3. Furthermore, although four different STAT3-targeting siRNAs were used in one of these studies[251], they only modestly downregulated the expression of STAT3 on RNA level by around 50%[251], while STAT3 silencing resulted in my experiments in highly efficient repression of STAT3 transcript levels by approximately 90-95%, without affecting E6/E7 levels. Further, the study reporting an activation of the HPV16 LCR in response to IL-10[254] might possibly reflect a special biological condition, since it did not assess the role of constitutive endogenous STAT3 signaling on basal E6/E7 expression. Finally, my own experiments, in line with published data[348-350], show that Stattic is likely not a reliable tool for specific STAT3 inhibition at the employed concentrations in the report cited above[187], due to substantial off-target toxicities.

These discrepancies and uncertainties warranted the investigation of the functional significance of STAT3 for E6/E7 expression in more detail and in a carefully controlled manner. Furthermore, since E6/E7 expression is essential for cervical cancer cell proliferation[12, 63-65], the absence of an anti-proliferative effect, which I observed upon STAT3 inhibition, was unexpected if STAT3 is truly a key driver of E6/E7 expression. Indeed, and in contrast to the studies referenced above, I found no evidence for a critical role of STAT3 for promoting E6/E7 expression in cervical cancer cells, despite highly efficient inhibition or activation of STAT3, respectively, and the use of five different methods to modulate STAT3 activity or expression in short- and long-term assays (Figure 35). Further, stimulation of STAT3 signaling by OSM treatment did also not counteract the repression of E6/E7 by hypoxia[319] or Metformin[84] treatment. In addition, I obtained evidence that the inhibitory effects of small molecule STAT3 inhibitors on E6/E7 expression may be related to off-target toxicities when applied at high concentrations, as discussed in detail in section 3.2.1. Taken together, the results of my experiments, applying a broad range of different methods to modulate expression or activity of

STAT3, do not support the notion that the endogenous, constitutive STAT3 activity in HPV-positive cervical cancer cells is directly or indirectly playing a substantial role for efficient viral E6/E7 oncogene expression.

Vice versa, a study ectopically expressing HPV E5, E6 or E7 in HPV-negative keratinocytes described increased levels of STAT3 Y705 phosphorylation[251]. This induction of STAT3 activity by the HPV oncogenes was suggested to be caused by a deregulation of Let-7a and miR-21 microRNAs[255] and by an autocrine stimulation with IL-6 followed by the induction of JAK activity[253] – both of which mechanisms have been reported to depend on the viral E6 protein. This latter scenario, though, is not supported by previous studies showing that cervical cancer cells are largely unresponsive to IL-6, since expression of the IL6-receptor, IL-6R, is strongly reduced in these cells[261-263].

In contrast to the above referenced studies, silencing of the E6 oncogene for 72 h by RNAi in both HeLa and SiHa cells did not affect STAT3 Y705 phosphorylation in my experiments. To limit the possibility of siRNA-specific off-target effects, pools of three HPV16 E6- or HPV18 E6-specific siRNAs were employed. Likewise, to assess the possibility of temporary effects and to mitigate secondary phenotypes induced by long-term knockdown of E6 for 72 h, I also assessed STAT3 Y705 phosphorylation levels at 24 h after E6 knockdown in both HeLa and SiHa cells. Notably and in line with my observations after 72 h of E6 silencing, STAT3 Y705 phosphorylation levels were unchanged also after short-term silencing of E6 for 24 h by RNAi, despite efficient knockdown of E6. These findings indicate that STAT3 activation levels, as indicated by STAT3 Y705 phosphorylation, are not directly linked to the expression of the E6 oncoprotein is in cervical cancer cells.

Extending my investigations on concurrent silencing of both E6 and E7 by RNAi, I interestingly found that under these conditions, STAT3 Y705 phosphorylation levels were also not reduced but were instead even increased in HeLa cells while they remained largely unchanged in SiHa cells, indicating a cell line specific regulation. In contrast, I could not observe a substantial induction of STAT3 Y705 phosphorylation upon silencing of E6/E7 in HeLa (and SiHa) cells for a shorter time period of 24 h. Notably, at the 24 h time point, the induction of senescence through E6/E7 silencing[319], which is microscopically detectable after 72 h, is not yet observable. Interestingly, it was reported, that senescence-induced secretome alterations can affect the activity of STAT3[323], indicating that the observed induction of STAT3 Y705 phosphorylation in HeLa cells after silencing of E6/E7 for 72 h might be a secondary effect of senescence induction and not a direct effect of the downregulation of E6/E7. Similarly, it is plausible that my findings on the repression of STAT3 Y705 phosphorylation in HeLa and SiHa cells cultivated under hypoxia or treated with Metformin, which both efficiently downregulate

E6/E7[84, 319], may also be confounded by secondary effects of these treatments. For example, both conditions inhibit OXPHOS[292, 293] and mTOR-signaling[84, 319] while additionally, hypoxia was also reported to induce a change of the secretome composition[371].

Collectively, my results do thus not provide experimental evidence for a substantial, mutually stimulatory crosstalk or an interdependence of E6/E7 and STAT3 in cervical cancer cells: Neither did the modulation of STAT3 activity or expression by five different methods considerably influence the expression levels of E6 and E7 nor did the silencing of E6 or E6/E7 primarily influence the levels of STAT3 activation.

3.2.4 Why is the stimulation of STAT3 target genes impaired in cervical cancer cells?

Overall, I found that STAT3 is dispensable for efficient E6/E7 expression, proliferation and treatment resistance in cervical cancer cells under the tested conditions – despite detectable constitutive STAT3 Y705 phosphorylation, indicative of activation. Hence, in view of the literature describing STAT3 as a powerful oncogene in cancer[216], including cervical cancer[248-250], the question emerged as to why the oncogenic capacity of STAT3 as a transcriptional activator of cancer-linked genes is not detectable in cervical cancer cells under all different experimental conditions employed in my studies.

In principle, I found that STAT3 is active and functional in cervical cancer cells as both constitutive as well as induced STAT3 activity translated into functional impact on transcript levels of the well-characterized STAT3 target gene *SOCS3*. However, no considerable influence on the expression of a number of putative oncogenic STAT3 target genes was observed in my experimental settings. These include genes which also have been linked to cervical cancer [247, 253, 256, 267, 268] and were reported to mediate the effects of STAT3 on the proliferation and treatment resistance in cervical cancer cells[247, 253, 256, 267, 268].

One possible explanation for the impairment of STAT3-dependent transactivation in cervical cancer cells may relate to reports indicating that certain post-translational modifications are required for this activity[166], with the most prominent example being the phosphorylation at Y705, which was thoroughly investigated in my thesis. Another important phosphorylation site is S727, which was described to be required for full transcriptional activity of STAT3[168, 170, 172]. In initial experiments, I analyzed STAT3 S727 phosphorylation as well and found that it is detectable under standard cell culture conditions in both HeLa and SiHa cells (not shown). Apart from phosphorylation, a range of further post-translational modifications such as acetylation[174, 175], methylation[176] and oxidation[177], were shown to modulate the transcriptional activity of STAT3. Thus, there are multiple potential post-translational modifications which can increase or decrease STAT3-mediated transcriptional transactivation and may underlie the apparent impairment of STAT3-dependent transactivation of its oncogenic target genes.

However, since I also found that *SOCS3* is responsive to STAT3, one would have to assume that the transactivation of *SOCS3* by STAT3 does require a different set of post-translational modifications than the unresponsive oncogenic STAT3 target genes.

Another possibility could be epigenetic silencing of the investigated STAT3 target genes in cervical cancer cells, resulting in very low expression levels. However, this seems unlikely, since transcripts of most of these genes were readily detectable in my qRT-PCR experiments and their expression is detectable on protein and/or RNA level in the cervical cancer cell lines used in this thesis[247, 253, 256, 267, 268] as well as cell lines of other cancers[238]. Additionally, some of these targets such as *BIRC5* or *CCND1* were independently reported to be overexpressed in cervical cancer[372]. Overall, these findings do not provide evidence for a general silencing of the investigated STAT3 target genes. It can however not be formally excluded that their promoters may be only partially silenced, for example at or around STAT3 binding sites, thereby specifically interfering with STAT3-mediated transactivation. To the best of my knowledge, however, there is no published example of this mechanism for the control of these STAT3-regulated genes.

Alternatively, negative regulators of STAT3 could be responsible for the impairment of STAT3-mediated transactivation in HPV-positive cancer cells. For example, SOCS3[147, 148] or PIAS3[146, 152] are known to inhibit STAT3 activation or DNA binding capacity, respectively. Whereas I found that *SOCS3* is indeed induced in response by STAT3 in cervical cancer cells, it seems unlikely to be responsible for the impairment of STAT3-mediated transactivation, since SOCS3 acts upstream of STAT3[373] and should diminish STAT3 Y705 phosphorylation levels, which however was not observed in my experiments even after 6 h of OSM treatment. At this time point the induction of *SOCS3* itself in response to OSM treatment was almost back at baseline levels while elevated levels of STAT3 Y705 phosphorylation were still present. In this context, it is also noteworthy that the type of cytokine initially stimulating JAK/STAT signaling could play an important role in determining the transcriptional response[180]. It thus cannot be formally excluded that the stimulation of STAT3 by a cytokine other than OSM might have resulted in a different effect on STAT3 target genes. However, for my thesis, I chose to work with OSM since OSM was shown to potently activate STAT3 in cervical cancer cells previously[264, 273], and, additionally, overexpression of the OSM receptor is associated with poor survival of cervical cancer patients[374, 375], indicative of an oncogenic role of OSM in cervical cancer cells. This is further in line with a study reporting that HPV16 E6/E7 can induce the upregulation of OSM[376].

Interestingly, it was also reported that certain cellular pathways such as PI3K- or MAPK signaling, can suppress STAT3 activity[377]. In cervical cancer, both pathways are important

oncogenic factors[82, 328] and are occasionally mutated, as are some regulators of these pathways[83, 362]. For example, multiple cervical cancer cell lines, such as HeLa and SiHa, harbor deletions of *STK11* (coding for liver kinase B1, LKB1) leading to a deregulation of mTOR[378], which acts downstream of the PI3K pathway. Furthermore, *PIK3CA* in CaSki cells[334] and *KRAS* in SW756 cells[363] harbor gain-of-function-mutations. In line with the importance of these pathways in cervical cancer cells and their suppressive role on STAT3 activity[377], I observed that inhibition of PI3K or MEK strongly induced STAT3 Y705 phosphorylation in most tested cervical cancer cell lines. However, this fails to explain the impaired response of oncogenic STAT3 target genes when PI3K- or MAPK pathways are inhibited and STAT3 activity is induced. *Vice versa*, in other cancer models it was reported that signaling through the MAPK pathway can be induced by inhibition of STAT3 and that MAPK signaling can thereby partly compensate the inhibition of oncogenic functions of STAT3[379, 380]. However, this scenario is rather unlikely to explain my observations, since Ruxolitinib treatment, as well as knockdown of STAT3 by RNAi (not shown), did not consistently increase the levels of phosphorylated ERK1/2 throughout my experiments, which would have been expected from the reported MAPK pathway activation. Similarly, small molecule STAT3 inhibitors, applied at concentrations, which do not cause appreciable off-target toxicities, did not increase the levels of phosphorylated ERK1/2.

Further, despite the distinct functions of different STAT family members in cancer[310, 311], different STAT proteins can possess partly overlapping activities[312], can partly share the same target genes[313] and can be activated in response to the same cytokines[314, 315], especially upon loss of one STAT member[314, 315]. Thus, it could be possible that another STAT protein can functionally compensate for STAT3 inhibition, thereby maintaining the expression of STAT3-responsive genes. In this context, STAT5 could be particularly interesting, which also is reported to play an oncogenic role in multiple cancer entities[310], including cervical cancer[266]. However, at least in the STAT3 KO cells tested here, a compensatory STAT5 activation was not observed and, surprisingly, STAT5 Y694/699 phosphorylation levels were instead strongly diminished. This finding indicates that STAT5 activity might be dependent on STAT3 in cervical cancer cells and, further, that STAT5 may be neglectable for proliferation and E6/E7 expression. This latter result is noteworthy since one of the same studies reporting an important role of STAT3 also described STAT5 to be a critical pro-proliferative factor in cervical cancer cells[266].

The third cancer-linked STAT family member, besides STAT3 and STAT5, is STAT1[311]. In contrast to STAT5, I found that STAT1 Y701 phosphorylation levels remained largely unchanged in untreated STAT3 KO cells with the exception of a slight induction in HeLa STAT3 KO clone F7. Since it was reported that expression of some shared STAT1/STAT3 target

genes were only downregulated if both STAT3 and STAT1 were depleted[313], the maintained levels of STAT1 Y701 phosphorylation in STAT3 KO cells could therefore possibly mask the effect of STAT3 on these target genes. However, this would be counterintuitive for the expression of the oncogenic STAT3 target genes I focused on, since high STAT1 levels were described to be associated with longer survival[381] and increased sensitivity to radio-[382] and chemoradiotherapy[383] in cervical cancer, suggesting an anti-tumorigenic function.

Generally, the literature describing that STAT3 and other pathways are able to compensate for each other are in line with the notion that proliferation pathways can be redundant and/or work in parallel[384]. For example, different rat sarcoma (RAS) proteins as well as many different receptor tyrosine kinases (RTKs) and JAK/STAT pathways are all able to promote proliferation and were found to be important drivers in certain cancer entities[384]. Since not all of them are active at the same time in every cancer cell of every cancer entity, inhibition of a critical proliferation pathway may be compensated by activation of another pathway, for example through the promotion of expression of shared downstream targets by the compensating pathway[384, 385]. In cervical cancer cells, E6 and E7 are highly potent oncogenes, modulating a plethora of cancer hallmarks for driving carcinogenesis[386]. Additionally, as mentioned above, it is known that the PI3K- and MAPK pathways are oncogenic key factors[82, 328] and are often mutated[83, 362]. Possibly, due to the contribution of multiple different pathways to the malignant phenotype of HPV-positive cancer cells, additional STAT3 signaling might be redundant and inhibition of STAT3 could thus be without major consequences.

The pathways that actively promote proliferation in a certain context are specific for cell types and states[384] and thus also depend on the biological consequences of signaling through a certain pathway besides the promotion of proliferation. Since JAK/STAT3 signaling is known to also control transcription of a broad range of genes involved in immune responses[121, 122, 140], the impairment of the transactivation function of STAT3 in cervical cancer cells might stem from evolutionary adaptation processes to escape anti-viral and/or anti-tumor immune responses. Supporting this hypothesis, it was reported that cervical cancer cells lack expression of the IL-6R[261, 262] to avoid induction of the chemokine MCP-1 (monocyte chemoattractant protein-1) attracting mononuclear immune cells[262, 387]. Since STAT3 is one of the major downstream effectors of IL-6 signaling[216], it could be possible that cervical cancer cells adapt to avoid expression or functional activation of factors such as IL-6R and STAT3 to evade detection and elimination by the immune system. The role of STAT3 for the expression of immune system-related factors in cervical cancer cells is further supported by two studies reporting the STAT3-dependent induction of interferon regulatory factor 1 (IRF1) by OSM treatment, leading to increased Cisplatin sensitivity[264, 273]. Of note, IRF1 was also found to be targeted for inactivation by the E7 oncogene during carcinogenesis to promote immune

evasion[388-390]. Furthermore, in my own transcriptome screen, one of the factors identified as a potential STAT3 target gene was *IFITM1*, coding for interferon-inducible transmembrane protein 1. Interestingly, IFITM1 is downregulated in cervical cancer tissue[391] and loss of IFITM1 in cervical cancer cells is associated with reduced protein expression of interferon-inducible factors and components of the major histocompatibility complex (MHC) class 1 in response to interferon-γ[392]. Further, IFITM1 inversely correlates with metastatic cervical cancer, possibly due to the reduced expression of MHC class 1, aiding immune escape[392]. In line with these reports, high risk HPVs were described to downregulate *IFITM1* expression in infected keratinocytes to withstand the immune response and avoid growth-inhibitory effects of interferon-γ[393].

These considerations raise the possibility that for cervical cancer cells, exploiting alternative oncogenic pathways such as the PI3K- or MAPK pathways[82, 328] to drive carcinogenesis in addition to E6 and E7 may be more advantageous than relying on the JAK/STAT3 pathway which can lead to the induction of factors involved in anti-viral and/or anti-tumor immune responses. Viewed from a different perspective, cervical cancers with high levels of STAT3 signaling in the tumor cells might possibly be eliminated early, in line with a report showing that activation of STAT3 is reduced in invasive cervical cancer tissue in comparison to precursor lesions (CIN3), in the same tissue sample[264]. It thus will be interesting for future analyses to investigate whether cervical cancer cells might be selected to exploit alternative pro-proliferative pathways due to the induction of factors involved in the immune response by STAT3. This will require experimental models which also incorporate the interplay of HPV-positive cancer cells with the tumor microenvironment, including animal models for papillomavirus-induced carcinogenesis[394].

3.2.5 Influence of STAT3 signaling on the senescence response to E6/E7 repression

Interestingly, during the investigation of a potential interdependence of STAT3 and E6/E7, I found that in HeLa cells, inhibition of STAT3 activity or expression attenuated the induction of senescence after silencing of E6/E7 by RNAi. Further, the induction of senescence in HeLa cells correlated with the increase of STAT3 Y705 phosphorylation upon E6/E7 silencing for 72 h and was not observed after a shorter duration of E6/E7 silencing for 24 h after which no senescence-like phenotype was observed yet. In the literature, STAT3 has been reported to be activated in response to senescence[322, 323] and was also described to be causally involved in IL-6-induced premature senescence of fibroblasts[395]. Thus, my findings indicate that STAT3 might possibly be a modulator of senescence induction in response to E6/E7 silencing in HeLa cells.

Since future therapies for cervical cancer, as well as other HPV-induced malignancies, might rely on the anti-proliferative effect of E6/E7 inhibition[12], identifying factors influencing the phenotype of cells depleted of E6/E7 is of high interest. Future experiments could firstly aim to validate whether STAT3 is indeed causally involved in the induction of senescence in HeLa cells in response to E6/E7 silencing. To this end, a similar strategy as for other parts of my thesis using STAT3 KO cells could be employed (Figure 34). If STAT3-targeting siRNAs or Ruxolitinib show no senescence-attenuating effect after E6/E7 silencing in STAT3 KO HeLa cells, this effect is likely indeed dependent on STAT3. Additionally, since I did not observe these effects to a considerable extent in SiHa cells, it will be of high interest to investigate whether the observed alleviation of the senescence induction is specific to HeLa cells upon E6/E7 silencing or whether it is also conserved in additional cervical cancer cells and for other senescence-inducing stimuli such as chemotherapy.

Secondly, if the observed phenotype proves to be STAT3-dependent, it will be interesting to elucidate the underlying mechanism. One factor that may potentially be involved is ETS2, since *ETS2* transcripts were downregulated by STAT3 silencing in my transcriptome screen and since ETS2 can reportedly induce expression of $p16^{INK4A}$ [396], a tumor suppressor which can mediate senescence induction[396, 397] and was speculated to also contribute to senescence induction upon E6/E7 repression[63]. Furthermore, STAT3 could also be causally involved via IL-6-induced reactive oxygen species generation followed by p53 induction, similar to how it was reported for fibroblasts undergoing premature senescence[395]. Alternatively, non-canonical functions of STAT3 may be relevant for the attenuating effect of STAT3 inhibition on E6/E7 silencing-induced senescence, for example via the impact of STAT3 on mitochondria[171, 190], since mitochondria can play a crucial role for senescence induction[398]. However, since I observed senescence alleviation also with Ruxolitinib treatment, this latter hypothesis is rather unlikely, as Ruxolitinib primarily blocks canonical STAT3 signaling rather than non-canonical functions of STAT3 in mitochondria.

3.2.6 Therapeutic implications: STAT3 as a therapeutic target in HPV-positive cancers?

Despite the introduction of effective prophylactic vaccines for most cancer-linked HPV types, incidences of HPV-induced malignancies will likely remain high in the future, primarily due to the long course of carcinogenesis, typically taking decades from infection to cancer, as well as the low vaccination rates, especially affecting less-developed regions[12, 18, 68-70]. Moreover, the prognosis of advanced disease is still poor[71], including for cervical cancers, which worldwide constitute the majority of HPV-induced cancers. Thus novel and effective therapeutic strategies for the treatment of HPV-induced cancers are urgently required.

Currently, STAT3 is under intense discussion to serve as one of the most promising targets of prospective treatment strategies for cervical cancer[248-250] , a therapeutic approach which is also considered for other HPV-linked cancer entities such as oropharyngeal HNSCC[399]. Likewise, due to many reports indicating its multi-faceted oncogenic functions[216], STAT3 is also thought to be a promising therapeutic target in multiple other cancer entities[216] such as non-small-cell lung cancer[400]. Therefore, various pharmacological strategies have been developed to inhibit STAT3 activities, including small molecule inhibitors[216], anti-sense[283] and decoy oligonucleotides[284] as well as PROTACs[278]. However, the therapeutic benefit in early clinical trials evaluating STAT3 inhibition for cancer treatment was rather limited[283, 359, 401-407], mainly due to a lack of efficacy in the great majority of treated solid cancer patients and/or pronounced treatment-related toxicities.

In the field of cervical cancer, the prevailing concept considers STAT3 as an especially promising target since it was reported to be essential for promoting proliferation[252, 255, 256, 265-268] while also being critically involved in inducing the expression of the E6/E7 oncogenes through mutually stimulatory interactions[251-253, 255]. Therefore, as the E6/E7 oncogenes are potent drivers of cervical carcinogenesis[12], interfering with this duality of STAT3 activities may theoretically even provide some degree of treatment specificity for HPV-positive cancer cells and lead to a particularly pronounced efficacy of STAT3-targeting therapies in cervical cancer.

Importantly, however, the concept of viewing STAT3 as a promising therapeutic target in cervical cancer is based on studies attributing a critical role to STAT3 signaling in HPV-positive cancer cells. My results strongly question this basis and, in contrast, reveal that constitutively active STAT3 in cervical cancer cells is neither an essential factor for their proliferation, nor was any evidence for a substantial crosstalk between STAT3 and the viral E6/E7 oncogenes obtained. In addition, and in line with two studies which observed a reduced activity of STAT3 in HPV-positive compared to HPV-negative HNSCC[408, 409], initial experiments indicated that STAT3 may also be dispensable for HPV-positive HNSCC cells (not shown). It will thus be of high interest to further investigate whether the absence of a substantial role of STAT3 for cell proliferation and viral oncogene expression is also conserved in cancer cells representing other HPV-positive cancer entities.

Yet, whereas my results strongly question the idea that targeting constitutive STAT3 signaling in HPV-positive cancer cells directly is a powerful therapeutic strategy, it is still possible that STAT3 inhibition may be of value for cervical cancer treatment, for example by reshaping the tumor microenvironment. Specifically, in the cervical tumor stroma STAT3 activity was reported to support carcinogenesis by instructing non-malignant cells to establish a pro-tumorigenic and

immunosuppressive microenvironment, primarily mediated via paracrine IL-6 stimulation[410]. In this context, IL-6/JAK/STAT3 signaling was shown to impair dendritic cell function[411] and to stimulate accumulation of M2 macrophages[412], which are considered to be pro-tumorigenic and express PD-L1 to prevent cytotoxic T-cell activation[410]. Additionally, STAT3 signaling, partly induced by IL-6, instructs stromal fibroblasts to recruit immunosuppressive Th17 cells via chemokine (C-C motif) ligand 20 (CCL20) secretion[413] while in stromal monocytes STAT3 activity induces the expression of MCP-1, which subsequently leads to matrix metalloprotease 9 (MMP-9) expression, triggering angiogenesis[410, 414]. Furthermore, OSM secreted by macrophages in the cervical cancer stroma reportedly stimulates STAT3 signaling in cervical cancer cells to upregulate genes that are for example involved in wound healing, the inflammatory response and angiogenesis while downregulating differentiation signatures[415]. This latter study[415] thereby indicates an oncogenic role of STAT3 in cervical cancer cells which is different from the prevailing concept of oncogenic STAT3 activities. Thus, it will be of high interest to investigate these aspects, especially the role of STAT3 for the interaction of cancer cells with mesenchymal and immune cells, in recently developed animal models, which allow to study papillomavirus-induced carcinogenesis in natural hosts[394].

Collectively, my findings provide novel insights into the functional role of STAT3 in HPV-positive cancer cells. By employing multiple different experimental approaches and extensive control experiments, my results strongly argue against the prevailing concept that constitutively active STAT3 signaling is essential for the proliferation of cervical cancer cells. They also put into question the reported mutually stimulatory crosstalk between STAT3 and the HPV oncogenes. Further, no evidence was obtained for a role of STAT3 as a resistance factor against multiple different anti-cancer drugs in cervical cancer cells. It is hoped that these unexpected results regarding a factor thus far considered to be essential for the growth of cervical cancer cells will not only add to our understanding of the molecular pathogenesis of cervical cancer, but will also reshape the ongoing discussions suggesting that inhibiting STAT3 in these cells could serve as a highly promising future therapeutic strategy.

CHAPTER 4

Materials & Methods

4. Materials & Methods

All experiments were conducted in a well-controlled manner including appropriate technical and biological replicates to ensure high reproducibility of each individual result. Individual experiments that failed due to technical reasons were disregarded for final analysis. If not indicated differently, all buffers were set up using distilled H_2O.

Whenever feasible and available, molecular biology grade reagents where utilized. All standard laboratory materials and reagents not specified in detail below were sourced from AppliChem (Darmstadt, Germany), BD Biosciences (Franklin Lakes, NJ, USA), Bio-Rad Laboratories (Hercules, CA, USA), Biozym Scientific (Hessisch Oldendorf, Germany), Carl Roth (Karlsruhe, Germany), Corning (Corning, NY, USA), Enzo Life Sciences (Farmingdale, NY, USA), Eppendorf (Hamburg, Germany), GE Healthcare (Chicago, IL, USA), Gerbu Biotechnik (Heidelberg, Germany), Greiner Bio-One (Kremsmünster, Austria), Merck (Darmstadt, Germany), New England Biolabs (Ipswich, NA, USA), Nerbe Plus (Winsen, Germany), Promega (Fitchburg, WI, USA), Sigma-Aldrich (St. Louis, MO, USA), Thermo Fisher Scientific (Waltham, MA, USA), Roche Diagnostics (Basel, Switzerland), Gabler-Saliter Milchwerk (Obergünzburg, Germany), Santa Cruz Biotechnology (Dallas, TX, USA), Sartorius (Göttingen, Germany) or Vector Laboratories (Newark, CA, USA). Manufacturers of other materials, compounds, systems or biologics are specified in the corresponding section or table below.

4.1 Cell-based methods

4.1.1 Cell culture

All cell lines (Table 3) were of human origin and were obtained from the German Cancer Research Center tumor bank (Heidelberg, Germany), were authenticated by single-nucleotide polymorphism (SNP) profiling (Multiplexion GmbH, Heidelberg, Germany) and were validated to be free of mycoplasma contamination.

Table 3: Overview of used cell lines, their properties and alterations. *AC: adeno carcinoma, SCC: squamous cell carcinoma.*

Cell line	Origin	HPV status	RRID	Modifications
SiHa	Cervical SCC	HPV16+	CVCL_0032	-
CaSki	Cervical SCC	HPV16+	CVCL_1100	-
HeLa	Cervical AC	HPV18+	CVCL_0030	-
SiHa-mKate2	Cervical SCC	HPV16+	-	nuclear mKate2
CaSki-mKate2	Cervical SCC	HPV16+	-	nuclear mKate2
HeLa-mKate2	Cervical AC	HPV18+	-	nuclear mKate2
SW756	Cervical SCC	HPV18+	CVCL_1727	-
Cal27	HNSCC	negative	CVCL_1107	-
FaDu	HNSCC	negative	CVCL_1218	-
HCT116	Colorectal AC	negative	CVCL_0291	-
MeWo	Malignant melanoma	negative	CVCL_0445	-
SiHa-STAT3 KO G3	Cervical SCC	HPV16+	-	STAT3 KO
SiHa-STAT3 KO G7	Cervical SCC	HPV16+	-	STAT3 KO
HeLa-STAT3 KO F3	Cervical AC	HPV18+	-	STAT3 KO
HeLa-STAT3 KO F7	Cervical AC	HPV18+	-	STAT3 KO
SiHa-STAT3 KO G3-mKate2	Cervical SCC	HPV16+	-	STAT3 KO + nuclear mKate2
HeLa-STAT3 KO F3-mKate2	Cervical AC	HPV18+	-	STAT3 KO + nuclear mKate2
NOK	Oral keratinocytes[289]	negative[289]	-	Spontaneous immortalization[289]

HeLa mKate2, SiHa mKate2 and CaSki mKate2 cells stably express a nuclear-restricted form of the fluorescent mKate2 protein and were generated as described before[87]. Spontaneously immortalized NOKs were established by Dr. Ruwen Yang, DKFZ, Heidelberg, Germany[289].

All cells except for NOK cells were cultivated in Dulbecco's minimal essential medium (DMEM, Gibco, Thermo Fisher Scientific) containing 1 g/L (5.5 mM) glucose, 10% fetal bovine serum (FBS, PAN-Biotech, Aidenbach, Germany) and supplemented with 100 U/mL Penicillin, 100 µg/mL Streptomycin, and 2 mM L-glutamine (all by Sigma-Aldrich) at 37 °C, 5% CO_2, and 21% O_2. NOK cells were kept in Keratinocyte-SFM (serum free medium; Gibco, Thermo Fisher Scientific) supplemented with human recombinant epidermal growth factor (EGF 1-53) and bovine pituitary extract (BPE) (Gibco, Thermo Fisher Scientific). For experiments involving hypoxic conditions, cells were cultured at 1% O_2 and 5% CO_2 in an Invivo$_2$ 400 physiological oxygen workstation (Ruskinn Technology, Bridgend, UK). For experiments requiring seeding of a certain number of cells, cell counting was performed using trypan blue and the Countess™ Automated Cell Counter (Invitrogen, Carlsbad, CA, USA).

4.1.2 Generation of KO cells

STAT3 KO cells were established from HeLa and SiHa cells using the CRISPR/Cas9 gene editing technology[416] with two distinct STAT3-specific guide RNAs (gRNAs). Plasmids encoding both Cas9 and a STAT3-specific gRNA (please refer to 4.1.4) were generated by cloning of DNA sequences coding for either one of the STAT3 specific gRNAs (Table 4) into pLenti-CRISPRv1 plasmids. Subsequently, plasmids were transfected into parental HeLa and SiHa cells[119].

Table 4: DNA sequences coding for gRNAs used for CRISPR/Cas9-based STAT3 KO.

Sense sequence	Antisense sequence	Clones
5'-CACCGAAAGTGGTAGAGAATCTCC-3'	5'-AAACGGAGATTCTCTACCACTTTC-3'	SiHa: G3 HeLa: F3
5'-CACCTGTACAGCACCGGCCGATGC-3'	5'-AAACGCATCGGCCGGTGCTGTACA-3'	SiHa: G7 HeLa: F7

Two days after transfection, 1 µg/mL Puromycin was added. Three days after transfection, cells were split 1:10 in 6 cm plates. Six days after transfection, cells were split and transferred into 96-well plates at densities of 0.5-10 cells per well to allow generation of single cell clones. Using the Incucyte® live-cell imaging system (Sartorius), single cell clones were confirmed and subsequently expanded. Clones with successful STAT3 KO and harboring mutations incompatible with expression of functional full-length STAT3 protein were identified using immunoblotting as well as sequencing (Table 5, Eurofins Scientific, Luxembourg City,

Luxembourg) of the corresponding region of the STAT3 gene. SiHa STAT3 KO clones G3 and G7 were generated in cooperation with Maria Weber, DKFZ.

Table 5: Sequences of primers used for amplification and subsequent sequencing of the STAT3 gene after CRISPR/Cas9-based KO.

Forward sequence	Reverse sequence	Clones
Amplification: 5'-GGCTCCTTTGAGGACCCGTA-3' Sequencing: 5'-CCCGCCTTAAGATCTAAACAGA-3'	Amplification: 5'-AAGCCTCGGGCAGGGAG-3' Sequencing: 5'-GCCTTCTCTTGGGGATACTGC-3'	SiHa: G3 HeLa: F3
Amplification: 5'-GCAACAAATTTCAACCCCGCA-3' Sequencing: 5'-CCACACCTGGAAAGAATGACCC-3'	Amplification: 5'-CCCAACATGGTGAAAAATTCCTCTT-3' Sequencing: 5'-ATCCTTGTCCCTTTCCCTCATCTA-3'	SiHa: G7 HeLa: F7

4.1.3 Generation of mKate2 expressing STAT3 KO cells

Expression of the nuclear restricted red fluorescent protein mKate2 enables efficient quantification of cell counts by live-cell imaging (please refer to 4.1.6). Generation of mKate2 expressing STAT3 KO cells was performed as described before for the generation of mKate2 expressing HeLa, SiHa and CaSki cells[87]. Briefly, STAT3 KO single cell clones were first assessed regarding their resistance to Puromycin treatment, since the generation of mKate2 expressing cells requires Puromycin-based selection of transduced cells. Sensitivity of SiHa STAT3 KO clone G3 and HeLa STAT3 KO clone F3 to Puromycin treatment was determined to be comparable to the respective parental cell lines. Next, SiHa STAT3 KO clone G3 and HeLa STAT3 KO clone F3 were lentivirally transduced in 24-well plates with the Incucyte® NucLight Lentivirus reagent (Sartorius) according to the manufacturer's instructions. Lentiviruses were utilized at a multiplicity of infection of 3, supplemented with 8 µg/mL polybrene in DMEM. Puromycin-based selection was started 48 h after viral transduction to eliminate non-transduced cells. After expansion of Puromycin resistant cells, successful integration of nuclear mKate2 was assessed using the Incucyte® live-cell imaging system as described in section 4.1.6. After confirmation of nuclear mKate2 positivity, cells were cryopreserved in liquid nitrogen for future use.

4.1.4 Transfection, RNA interference and ectopic overexpression

Synthetic siRNAs (Silencer® Select, Thermo Fisher Scientific) were reverse transfected using Lipofectamine RNAiMAX (Invitrogen, Thermo Fisher Scientific) to reach a final siRNA concentration of 30 nM if not specified otherwise. All transfections were performed using 5 µL

RNAiMAX in 2.5 mL final volume in 6 cm plates according to the instructions of the manufacturer. Medium was exchanged 24 h after transfection.

Table 6: Employed siRNAs and their target sequences.

siRNA	Target sequence
siNeg (negative control; no target)	5′-UACGACCGGUCUAUCGUAG-3′
siCtrl (negative control; no target)	5′-CAGUCGCGUUUGCGACUGG-3′
siSTAT3_2	5’-GGCUGGACAAUAUCAUUGA-3’
siSTAT3_4	5’-GGACAUCAGCGGUAAGACC-3’
siSTAT3_6	5’-GCAGCAGAUGCUGGAGCAG-3’
siSTAT3_10	5’-GCUUCCUGCAAGAGUCGAA-3’
si16E6/E7_1	5’-CCGGACAGAGCCCAUUACA-3’
si16E6/E7_2	5’- CACCUACAUUGCAUGAAUA-3’
si16E6/E7_3	5’- CAACUGAUCUCUACUGUUA-3’
si18E6/E7_1	5’-CCACAACGUCACACAAUGU-3’
si18E6/E7_2	5’-CAGAGAAACACAAGUAUAA-3’
si18E6/E7_3	5’-UCCAGCAGCUGUUUCUGAA-3’
si16E6_1	5′-ACCGUUGUGUGAUUUGUUA-3′
si16E6_2	5′-GGGAUUUAUGCAUAGUAUA-3′
si16E6_3	5′-UUAGUGAGUAUAGACAUUA-3′
si18E6_1	5′-GACAUUAUUCAGACUCTGU-3′
si18E6_2	5′-CAGACUCUGUGUAUGGAGA-3′
si18E6_3	5′-CUCUGUGUAUGGAGACACA-3′

For reverse transfection of siRNAs in 96-well plates, 0.2 µL RNAiMAX per well were used for HeLa, SW756 and CaSki cells in a total volume of 100 µL. In SiHa cells, RNAiMAX was titrated to 0.15 µL per well to reduce toxicity of the transfection. Additionally, for all cell lines, instead of exchanging the medium after 24 h, 200 µL fresh medium were added to each well to avoid loss of cells exhibiting incomplete adherence after 24 h. Medium was then exchanged 48 h after transfection to 200 µL per well.

All STAT3 siRNAs (Table 6) target distinct exons (Table 7) and cover all known and predicted transcript variants of STAT3 according to the NCBI RefSeq database[417], except for siRNA #6, which does not bind to transcript variant 17 (NM_001384989.1). If not indicated otherwise, STAT3 siRNAs were used in pools to reduce the risk of potential off-target effects. For SiHa and SiHa-derived cells, the employed siSTAT3pool contained siRNAs #2, #4, #6 and #10 while

the siSTAT3pool only contained siRNAs #4, #6 and #10 when used in HeLa or HeLa-derived cells to avoid STAT3-independent cytotoxicities of siRNA #2, which were exclusively observed in HeLa cells for siRNA #2.

The siRNAs targeting E6 or E6/E7 (siE6; siE6/E7) of HPV16 or HPV18 have been used in pools of three each. The negative control siRNAs siCtrl and siNeg harbor four or more mismatches to transcripts of all known human genes[418].

Table 7: Transcript coverage of STAT3 siRNAs.

siRNA	Targeted STAT3 transcripts	Targeted exon (of variant #1)
siSTAT3_2	All known and predicted transcript variants according to the NCBI RefSeq database[417].	Exon 19
siSTAT3_4		Exon 20/21 (junction spanning)
siSTAT3_10		Exon 3
siSTAT3_6	All variants, except for variant 17 (NM_001384989.1)	Exon 5

Table 8: Utilized plasmids and their purpose.

Plasmid	Purpose	Provider
pLenti-CRISPRv1	Base vector for CRISPR/Cas9	kind gift from Feng Zhang, Addgene plasmid #49535
pLenti-CRISPRv1-gRNA5	pLenti-CRISPRv1 expression vector for Cas9 and gRNA5 or gRNA6	generated in cooperation with Maria Weber
pLenti-CRISPRv1-gRNA6		
pcDNA3	Base vector for transient expression	Invitrogen, Carlsbad, CA, USA
pcDNA3-STAT3	pcDNA3 expression vector for wildtype human STAT3	kind gift from Jie Chen, Addgene plasmid #74433
pcDNA3-STAT3-Y705F	pcDNA3 expression vector for Y705F-mutated human STAT3	kind gift from Jie Chen, Addgene plasmid #74434
pCEP4	Base vector for episomal expression	Invitrogen, Carlsbad, CA, USA
pCEP4-STAT3	pCEP4 expression vector for wildtype human STAT3	generated in cooperation with Claudia Lohrey

Plasmids (Table 8) used for ectopic overexpression of wildtype STAT3 and Y705F-mutated STAT3 as well as plasmids used for the generation of STAT3 KO clones were transfected using the calcium phosphate coprecipitation technique[419]. The pCEP4-STAT3 plasmid was established by transfer of STAT3 cDNA from pcDNA3-STAT3 into the pCEP4 vector.

Generation of pLenti-CRISPRv1-gRNA5 and pLenti-CRISPRv1-gRNA6 expression vectors is described in section 4.1.2.

4.1.5 Drug Treatment

Treatment of cells with the listed compounds (Table 9) was performed alone or in combination using the concentrations and time spans indicated in corresponding text or figure legend.

Table 9: Compounds and their corresponding solvents and manufacturers.

Drug	Solvent	Manufacturer
Ciclopirox olamine (CPX)	EtOH	Santa Cruz Biotechnology
Niclosamide (Niclo.)	DMSO	
Deferoxamine mesylate	DMSO	Sigma-Aldrich
2-deoxy-D-glucose (2-DG)	DMEM	
Ruxolitinib (Ruxo.)	DMSO	MedChemExpress, South Brunswick, NJ, USA
Sapitinib	DMSO	
Decitabine (DAC)	DMSO	
Pictilisib (Pict.)	DMSO	Selleck Chemicals, Houston, TX, USA
Cryptotanshinone (Crypto.)	DMSO	
Trametinib (Tram./Tramet.)	DMSO	Cayman Chemical, Ann Arbor, MI, USA
Stattic	DMSO	
C188-9	DMSO	AdooQ BioScience, Irvine, CA, USA
WP1066	DMSO	
BP-1-102	DMSO	TargetMol Chemicals, Boston, MA, USA
Metformin	DMEM	Enzo Life Sciences
Oncostatin M (OSM)	H_2O	GenScript Biotech, Piscataway, NJ, USA

If not indicated otherwise, medium was always exchanged immediately before addition of the drug treatment. Solvent controls were used at a maximum final concentration of 0.1% in the medium, which did not result in any detrimental effects on cell growth or viability. Oncostatin M was generally used at a concentration of 10 ng/mL.

4.1.6 Live-cell imaging

Live-cell imaging was employed for proliferation assays as previously[420] to precisely track cell counts and enable detection even of small differences in proliferation upon treatment. If possible, live-cell imaging experiments employing the Incucyte® S3 system (Sartorius) were performed with mKate2-labelled cells to enable determination of red object counts (= red nuclei

counts, corresponding to cell counts). Per well, 3000 cells were seeded into 96-well plates and treated after 48 h or as specified in the corresponding section. When siRNAs were reverse transfected, 6000 cells were seeded to account for slightly slower initial proliferation rates due to the transfection process, followed by drug treatment 48 h after reverse transfection. Every 4 h, four images were taken of each well with 10× magnification. Each experimental condition was assessed in triplicates resulting in 12 images per condition per time point. Shown are the average cell counts or confluences, respectively, of these 12 images for each time point and condition. To analyze proliferation rates, viable cell numbers (red objects) were assessed using the Incucyte® 2019B Rev2 software over a course of 96 h, if not stated otherwise. To account for slight variations in seeded cell counts between wells, growth curves were normalized to the first time point (0 h), i.e. the time point at drug treatment or 48 h after transfection, respectively.

For determining dead cell counts, the Incucyte® Cytotox Green Dye (Sartorius, Cat. No. 4633) was employed at a concentration of 100 nM over a course of 96 h and was added to the medium along with the indicated drug treatment. The Cytotox Green Dye permeates impaired plasma membranes and subsequently stains DNA, thereby enabling determination of cells undergoing cell death (green objects). Representative images of phase, red, green and/or merged channels, respectively, were exported by using the Incucyte® 2019B Rev2 software (Sartorius) at 10× magnification. The scale bars indicate 400 µM.

4.1.7 Senescence assay

For identification of senescent cells, activity of the senescence-associated β-galactosidase (SA-β-gal) was assessed. In senescent cells, detectable β-galactosidase activity at pH 6.0 is strongly induced, while in non-senescent cells β-galactosidase activity typically only occurs at pH 4.0 within lysosomes[324, 325]. The activity of SA-β-gal as a senescence marker was determined using X-gal (5-bromo-4-chloro-3-indolyl-β-D-galactopyranoside), an artificial chromogenic substrate resulting in a blueish staining of senescent cells while non-senescent cells typically remain unstained.

For SA-β-gal staining, cells were washed with phosphate buffered saline (PBS), fixed using 1 mL paraformaldehyde solution (2% PFA, 0.2% glutaraldehyde in PBS) for 3 min, washed with PBS again and subsequently incubated in 1.5 mL of senescence assay buffer (Table 10) at 37 °C for 24-48 h until staining of senescent cells could be clearly observed. Senescence assay buffer was then discarded, cells were washed with PBS followed by image acquisition using the EVOSxl Core Cell Imaging System (Invitrogen, Thermo Fisher Scientific) at a magnification of 20×.

Table 10: Senescence assay buffer ingredients.

Senescence assay buffer
• 40 mM citric acid • 150 mM NaCl • 2 mM $MgCl_2$ • 5 mM $K_3[Fe(CN_6)]$ • 5 mM $K_4[Fe(CN_6)]$ • 1 mg/mL X-gal in DMF • adjusted to pH 6.0 with Na_2HPO_4

4.1.8 Colony formation assay

Colony formation assays were performed in two variations as indicated in the corresponding text or figure legend, respectively. The first variant was employed to assess long-term proliferation and colony formation of cells under continuous presence of a compound. This assay thus aims to determine whether inhibition of the compound's target may affect proliferation or colony formation upon prolonged inhibition. In contrast, the second variant was employed to assess the remaining proliferative or colony formation capacity of a cell population after a certain treatment. This assay thus aims to determine whether and to what extent a certain treatment induces phenotypes that are not compatible with continued proliferation after the treatment, i.e. the induction of cell death or senescence.

For the first variant, cells were seeded at a density of 3000 cells per 6 cm plate followed by the indicated treatments 48 h after seeding to allow full attachment of cells before treatment application. Every 72-96 h, the medium was exchanged with fresh medium including the specified drug concentrations for a total of 14 days or as indicated in the corresponding text or figure legend, respectively, until colony size was sufficient for staining. Drug exposure was thus maintained throughout the colony growth phase.

In the second variant, $4x10^5$ to $8x10^5$ cells, depending on the cell line, were seeded and treated as indicated. After 48-72 h, depending on the experiment, cells were split 1:50, 1:100 and 1:200 and further incubated for 10-14 days without presence of the drug to allow outgrowth of cells without terminal phenotype to colonies. Medium was exchanged every 72-96 h.

For both colony formation assay variants, colonies were then washed with PBS and fixed and stained with 350 µL of formaldehyde-crystal violet solution (12 mM crystal violet, 29 mM NaCl, 3% formaldehyde, 22% EtOH) per 6 cm plate for 5 min followed by a washing step with PBS. Dried 6 cm plates were scanned using the Epson Perfection 4990 Photo Scanner (Epson, Suwa, Japan).

To obtain close images of individual colonies, plates were partly destained using 1 mL of 33% acetic acid solution on each plate for approximately 20 s followed by image acquisition using the EVOSxl Core Cell Imaging System (Invitrogen, Thermo Fisher Scientific) at a magnification of 20×. For colorimetric quantification of colony formation, stained colonies were destained as described above until no crystal violet was visibly bound to colonies anymore. Colorimetric extinction of the solution containing crystal violet was then measured at 570 nm using the SpectroStar Nano Photometer (BMG Labtech, Ortenberg, Germany).

4.2 RNA-based methods

4.2.1 RNA extraction

RNA extraction was performed according to the instructions of the PureLink™ RNA Mini Kit (Invitrogen, Thermo Fisher Scientific). Cells were treated according to the indicated experimental conditions in 6 cm plates followed by cell lysis using 600 µL of PureLink™ RNA Mini Kit lysis buffer. For 96-well plates, 100 µL lysis buffer were used per well. Optional washing and DNA digestion steps using the PureLink™ DNase set (Invitrogen, Thermo Fisher Scientific) were performed. Finally, total cellular RNA was eluted in nuclease free water followed by determination of each sample's RNA concentration using the NanoDrop ND-1000 spectrophotometer (Peqlab, Erlangen, Germany). Extracted RNA was stored at -80 °C for further use in Affymetrix Clariom™ S microarray analyses (please refer to 4.2.3) or cDNA generation for quantitative real-time PCR (please refer to 4.2.2).

4.2.2 Reverse transcription & quantitative real-time PCR

To generate cDNA suitable for subsequent use in quantitative real-time PCR (qRT-PCR) experiments, the previously extracted total cellular RNA was reverse transcribed using the ProtoScript® II First Strand cDNA Synthesis Kit (New England Biolabs) according to the instructions of the manufacturer. For each sample, 500 ng of RNA were reverse transcribed into cDNA using a 1:1 mixture of random and oligo-dT primers in the MJ Research PTC 200 Gradient Thermal Cycler (Marshall Scientific, NH, USA). Final cDNA samples were stored at -20 °C until further use.

Before use in qRT-PCR experiments, cDNA samples were diluted 1:5 with nuclease free water. Relative levels of indicated transcripts were determined in duplicates in 96-well qRT-PCR plates. Each well contained a mixture of 7.2 µL H_2O, 0.4 µL of forward and reverse primer each, 10 µL of SYBR® Green PCR master mix (Applied Biosystems, Thermo Fisher Scientific) and 2 µL of the diluted cDNA. Forward and reverse primers (Table 11) were used at a concentration of 5 pM each. The qRT-PCR was performed for 40 amplification cycles on a 7300 Real Time PCR System (Applied Biosystems, Thermo Fisher Scientific). Transcript levels were quantified relative to *TMBIM6* mRNA as an internal reference by applying the comparative ct ($2^{-\Delta\Delta Ct}$) method[421].

Table 11: Forward and reverse primer sequences for qRT-PCR.

Target	Forward primer	Reverse primer
STAT3	5'-GAAGCTGACCCAGGTAGC-3'	5'-CATCGGCAGGTCAATGGTA-3'
TMBIM6	5'-GTGGTCATGTGTGGCTTCGT-3'	5'-GGAAAGGCTGGATGGTCACT-3'
HPV16 E6/E7	5'-CAATGTTTCAGGACCCACAGG-3'	5'-CTCACGTCGCAGTAACTGTTG-3'
HPV18 E6/E7	5'-TTGGAACTTACAGAGGTGCC-3'	5'-TTGGAGTCGTTCCTGTCGTG-3'
SOCS3	5'-GTGGGACGATAGCAACCACA-3'	5'-CGAAGTGTCCCCTGTTTGGA-3'
MYC	5'-CAGATCAGCAACAACCGAAA-3'	5'-GGCCTTTTCATTGTTTTCCA-3'
CCND1	5'-CCTCCTCCTCGCACTTCTGT-3'	5'-CCGTCCATGCGGAAGATC-3'
BIRC5	5'-TTCTCAAGGACCACCGCATC-3'	5'-CCAAGTCTGGCTCGTTCTCA-3'
BCL2	5'-ATGTGTGTGGAGAGCGTCAACC-3'	5'-GCATCCCAGCCTCCGTTATC-3'
BCL2L1	5'-GATCCCCATGGCAGCAGTAAAGCAAG-3'	5'-CCCCATCCCGGAAGAGTTCATTCACT-3'
MCL1	5'-CCAAGGCATGCTTCGGAAA-3'	5'-TCACAATCCTGCCCCAGTTT-3'
IFITM1	5'-CCTACTCCGTGAAGTCTAGGG-3'	5'-GAGCCGAATACCAGTAACAGGA-3'
CHAC1	5'-GTTTCTGGCAGGGAGACACC-3'	5'-CCCAAGTGCAGCCCTCAT-3'
ETS2	5'-GCAGCGGCAGGATGAATGA-3'	5'-AATCCAAGCCTGTTGGCACT-3'
FAM84B	5'-TCTCCGCGGGTAGCCT-3'	5'-GCAAGGGGAGAAAGCGAAAC-3'
TGFBR3	5'-TGCACTTTCCTATCCCGCAA-3'	5'-TCAGGAGGCACACACTTAGG-3'

4.2.3 Microarray-based gene expression analysis

Microarray experiments were performed by the Microarray Unit of the Genomics and Proteomics core facility (DKFZ Heidelberg) using the RNA from my experiments. Briefly, Clariom™ S Assay GeneChips (Thermo Fisher Scientific), allowing the relative quantification of transcript levels of more than 20.000 well-annotated genes, were used to analyze the transcript expression of SiHa cells transfected with either control siRNA (siCtrl) or four different STAT3-targeting siRNAs (siSTAT3_*X*), or without siRNA (mock). Total cellular RNA was extracted, as described before in section 4.2.2, 72 h after transfection. Total cellular RNA was then reverse transcribed to cDNA followed by subsequent *in vitro* transcription to cRNA modified with biotin-tagged uracil bases. After random fragmentation of the cRNA into 30-400 nucleotide long pieces, the cRNA fragments were hybridized with oligonucleotide probes on the Clariom™ S GeneChips. Bound hybridized RNA was subsequently stained using Cy5-streptavidin and quantified by laser scanning. Transcript levels of all conditions were determined in biological triplicates. Quality of the Clariom™ S assay was monitored and validated by the Microarray Unit of the Genomics and Proteomics core facility at all times. The

Microarray Unit of the Genomics and Proteomics core facility provided basic data analysis, including basic relative quantification of transcript levels.

Upon receiving the microarray data, potential STAT3 target genes were identified. In total, 19525 protein-coding transcripts were evaluable across all conditions. In a first step, transcripts were filtered using a log_2-transformed fold change (log_2FC) cutoff of ±0.58 (1.5× fold change). Transcripts which did not consistently meet this criterion across each of the four STAT3 siRNAs compared to siCtrl were discarded, yielding 25 transcripts. Next, transcripts, which can likely be considered to be differentially expressed solely due to effects of the control siRNA (siCtrl) or the transfection reagents or process *per se,* were disregarded. For this, transcripts for which the absolute difference between the mean log_2FC of the four siSTAT3 vs. siCtrl conditions and the log_2FC of the mock transfection vs. siCtrl was smaller than 0.58 were filtered out. Overall, disregarding the STAT3 transcripts themselves, this process resulted in 5 genes which score as potential STAT3 targets.

Volcano plots of all conditions depicting all detected transcripts were prepared using GraphPad Prism 9.5.1 (GraphPad Software, CA, USA). All transcripts reaching a log_2FC of ≥ 1.5 were colored in blue while all transcripts reaching a log_2FC of ≤ -1.5 were colored in red. Individual symbols are depicted for all transcripts reaching a log_2FC of ≥ 1.5 or ≤ -1.5.

Gene set enrichment analysis[300] (GSEA) was performed using GSEA v. 4.0.3 and MSigDB v2023.1.Hs from which all gene sets belonging to the HALLMARK, BIOCARTA and GO family of gene sets were selected. From every condition, gene symbols and log_2FC values were loaded into the GSEA software to perform pre-ranked enrichment analysis. The following parameters were used: number of permutations, 1000; enrichment statistic, weighted; max size: exclude larger sets, 500; min size: exclude smaller sets, 15; normalization mode, meandiv; seed for permutation, timestamp. From these results the top 10 negatively and top 10 positively enriched gene sets according to the normalized enrichment score (NES) were selected for every condition. Then, doubles were removed, resulting in 80 gene sets for which a heatmap was generated based on the NES for each condition. This enabled assessing whether there are any gene sets among the most strongly enriched gene sets, which are similarly regulated after knockdown of STAT3 across all four STAT3-targeting siRNAs. Furthermore, these 80 gene sets were clustered in six distinct groups using K-means clustering with Euclidian distance based on the NES using the Morpheus software (Broad Institute, Cambridge, MA, USA). Additionally, the transcriptome datasets of the four siSTAT3-targeting conditions compared to the siCtrl condition as well as available microarray-based data of HeLa cells depleted of E6/E7 by RNAi[330] were analyzed regarding enrichment of the ROSTY_CERVICAL_CANCER_PROLIFERATION_ CLUSTER[331] gene set.

4.3 Protein-based methods

4.3.1 Cell harvest and protein extraction

For all protein-based methods, cells were cultured in standard 6 cm plates. For protein extraction cells were washed with ice cold PBS once. Then, cells were scraped in ice cold PBS and pelleted in a microreaction tube by centrifugation at 13.200 rcf for approximately 15 s at 4 °C. The cell pellet was then resuspended and incubated on ice for 30 min in 20-100 µL CSK-1 buffer (Table 12), depending on the size of the pellet. Afterwards, the lysed cells were centrifuged at 13.200 rcf for 5 min at 4 °C followed by transfer of the protein containing supernatant into a new microreaction tube. To determine protein concentration, 1 µL of each sample was transferred into semi-micro cuvettes containing 1 mL of Bradford solution (Bio-Rad Laboratories), followed by assessment of the absorption at 595 nm using a photometer (Eppendorf). Each sample was finally mixed with the respective volume of 4x SDS-PAGE loading buffer (Table 12), heated to 95 °C for 5 min to denature all proteins. Final samples were stored at -80 °C until further use.

Table 12: CSK1 lysis and 4x loading buffer ingredients.

CSK1 lysis buffer	4x loading buffer
• 10 mM PIPES (pH 6.8) • 300 mM NaCl • 1 mM EDTA • 300 mM sucrose • 1 mM MgCl2 • 0.5% Triton X-100 900 µL CSK-1 were freshly supplemented with: • 100 µL of PhosSTOP phosphatase inhibitor cocktail (Roche Diagnostics, Switzerland; one tablet per 1 mL stock) • 25 µL of 100 mM Pefablock (Merck) • 10 µL of P8340 protease inhibitor cocktail (Sigma-Aldrich)	• 8% SDS • 250 mM Tris-HCl (pH 6.8) • 20% β-mercaptoethanol • 40% glycerol • 0.008% Bromophenol

4.3.2 SDS-PAGE and Western blot

Sodium dodecyl sulfate-polyacrylamide gel electrophoresis (SDS-PAGE) separates proteins depending to their electrophoretic mobility, which correlates with molecular weight due to the binding of SDS to denatured proteins. Gels were manually casted and prepared according to Table 13. Per lane, 20 µg of total protein were separated at 100 V for approximately 3 h, depending on the size of the investigated protein. The PageRuler™ Prestained Protein Ladder (Thermo Fisher Scientific) was used as a marker. Following SDS-PAGE, the proteins

underwent semi-dry electrotransfer onto a PVDF membrane. The membrane was activated by soaking in methanol, while Whatman filter paper was soaked in Towbin transfer buffer (Table 14). The membrane was then positioned below the gel in the Trans-Blot® system (Bio-Rad Laboratories), with four Whatman papers placed below and above. Electroblotting onto the membrane took place at 20 V for 1 h.

Table 13: Ingredients of 5% and 12.5% acrylamide gels for SDS-PAGE.

Chemical	Stacking gel (5%)	Resolving gel (12.5%)
H_2O	2 mL	5.7 mL
30% acrylamide	620 µL	6.4 mL
0.47 M Tris-HCl (pH 6.7)	1200 µL	n.a.
3 M Tris-HCl (pH 8.9)	n.a.	1.8 mL
10% SDS	45.8 µL	137.5 µL
10% APS	183.3 µL	176 µL
TEMED	1.8 µL	3.4 µL

Table 14: Towbin transfer buffer ingredients.

Towbin transfer buffer (pH 8.3)
• 2.5 mM Tris • 19.2 mM glycine • 20% methanol

Subsequently, the membrane was incubated in 5% skim milk and 1% BSA in 0.2 % PBS-T at room temperature for 1 h. Depending on the protein to be analyzed, the membrane was cut into distinct pieces, guided by the protein marker for orientation. The membrane was then incubated overnight at 4 °C with the primary antibody according to Table 15. The following day, the membrane was washed at least thrice for 10 min each in 0.2 % PBS-T and subsequently incubated with the corresponding secondary antibody (Table 15) at room temperature for 1 h. The primary and secondary antibodies were diluted in 5% skim milk and 1% BSA in 0.2 % PBS-T. After incubation with the secondary antibody, the membrane was washed again at least thrice, 10 min each, in 0.2 % PBS-T.

Finally, Western blots were analyzed using the enhanced chemiluminescence (ECL) system (ECL Prime Western Blotting Detection Reagent, Cytiva, Marlborough, MA, USA and WesternBright Sirius HRP Substrate, Advansta, San Jose, CA, USA) and utilizing secondary antibodies coupled to horseradish peroxidase (HRP), which catalyzes the oxidation of luminol to 3-aminophthalate (3-AP). The light emitted through decay of 3-AP was then detected using the Fusion SL Gel Detection System (Vilber Lourmat, Eberhardzell, Germany).

Table 15: Primary and secondary antibodies and their corresponding properties.

Target	Dilution	Source	Clone	Product	Supplier
β-Actin	1:50000	mouse	C4	sc-47778	Santa Cruz Biotechnology
GAPDH	1:4000	rabbit	FL335	sc-25778	
Vinculin	1:4000	mouse	7F9	sc-73614	
STAT3	1:1000	rabbit	n.a.	sc-482	
phospho-STAT1 (Y701)	1:500	mouse	A-2	sc-8394	
p53	1:1000	mouse	DO-1	sc-126	
Cytochrome C	1:1000	mouse	A-8	sc-13156	
anti-chicken IgY-HRP	1:5000	goat	n.a.	sc-2428	
phospho-AKT (S473)	1:1000	rabbit	193H12	#4058	Cell Signaling Technology (Boston, MA, USA)
AKT	1:1000	rabbit	n.a.	#9272	
phospho-p44/42 ERK1/2 (T202/Y204)	1:1000	rabbit	n.a.	#9101	
p44/42 ERK1/2	1:1000	mouse	L34F12	#4696	
phospho-4E-BP1 (S65)	1:1000	rabbit	n.a.	#9451	
STAT1	1:1000	rabbit	D1K9Y	#14994	
phospho-STAT3 (Y705)	1:500	mouse	3E2	#9138	
STAT5A/B	1:1000	rabbit	D2O6Y	#94205	
phospho-STAT5A/B (Y694/Y699)	1:500	rabbit	D47E7	#4322	
PARP, cleaved Asp214	1:1000	mouse	19F4	#9546	
HPV16 E7	1:1000	mouse	NM2	n.a.	Prof. Dr. Martin Müller (DKFZ)
HPV18 E7	1:1000	chicken	E7C	n.a.	Prof. Dr. Hanswalter Zentgraf (DKFZ)
HPV18 E6	1:2000	mouse	AVC 399	n.a.	Dr. Johannes Schweizer (Arbor Vita, Fremont, CA, USA)
HPV16 E6	1:3000	mouse	AVC 843	n.a.	
α-tubulin	1:5000	mouse	CP06	CP06	Calbiochem, Darmstadt, Germany
anti-mouse IgG-HRP	1:10000	goat	n.a.	W4021	Promega Fitchburg, WI, USA
anti-rabbit IgG-HRP	1:10000	goat	n.a.	W4011	

4.3.3 Mitochondrial protein fractionation

For analysis of mitochondrial protein levels, fractionation was performed. Cells were seeded in 10 cm plates, treated after 48 h and harvested after 96 h. At harvest, cells were washed in PBS, centrifuged at 4000 rpm for 4 min at 4 °C and resuspended in 200 µL of 10 mM HEPES at pH 7.4, 0.25 M sucrose and 1 mM EGTA, as well as protease inhibitors as described in section 4.3.1. The homogenized cell solution was then processed 50 times in a 2 mL douncer on ice and centrifuged at 2000 rcf for 15 min at 4 °C. The remaining supernatant was transferred into a new tube followed by centrifugation at 10000 rcf for 15 min at 4 °C. The remaining supernatant was then transferred into a new tube, corresponding to the cytosolic protein fraction. The pellet, corresponding to the mitochondrial protein fraction, was lysed as described in section 4.3.1 using CSK1 buffer and protease inhibitors. Both fractions were further processed and utilized for SDS-PAGE and Western blot as described in section 4.3.2.

4.3.4 Proteome-based gene expression analysis

Analysis of previously published proteome data[86] of CPX treated or hypoxic SiHa cells was performed to identify factors involved in protein degradation. All genes of the KEGG_UBIQUITIN_MEDIATED_PROTEOLYSIS, REACTOME_DEUBIQUITINATION, REACTOME_PROTEIN_ UBIQUITINATION and GO_POLYUBIQUITINATION gene sets of the MSigDB v2023.1.Hs were assessed. Detected proteins were filtered for $\log_2$FC ≥ 0.58 or ≤ -0.58 in CPX treated cells while being largely unaffected ($\log_2$FC ≤ 0.58 or ≥ -0.58) under hypoxia. Proteins, which differential expression pattern was not compatible with the hypothesis of increased protein degradation through CPX treatment in view of each proteins specific function, were disregarded. Furthermore, GSEA was performed of the aforementioned and on the REACTOME_SUMOYLATION, REACTOME_SUMOYLATION_OF_UBIQUITINATION_ PROTEINS and GO_SUMOYLATION gene sets with parameters as described in section 4.2.3. GSEA Analysis of unpublished proteome data of SiHa cells depleted of E6/E7 by RNAi was performed to as described in section 4.2.3 on the gene set ROSTY_CERVICAL_CANCER_ PROLIFERATION_CLUSTER[331].

4.4 Statistical analysis

To assess statistical significance, GraphPad Prism 9.5.1 (GraphPad Software) was used. For statistical analysis of qRT-PCR experiments, values were transformed logarithmically (log_2) followed by statistical comparison of relative log_2 values via two-sided paired t-tests or one-way analysis of variance (ANOVA) tests. For statistical analysis of CFA quantification, obtained values were normalized to the corresponding control followed by log_2 transformation and assessment of statistical significance by one-way ANOVA. For ANOVA, Sidak's multiple comparisons test was applied if selected pairs of means were compared while Dunnett's multiple comparisons was performed if every mean was compared to a control mean. Generally, (adjusted) p-values ≤ 0.05 (*), ≤ 0.01 (**) and ≤ 0.001 (***) were considered statistically significant.

Appendix

Appendix

Supplementary figures

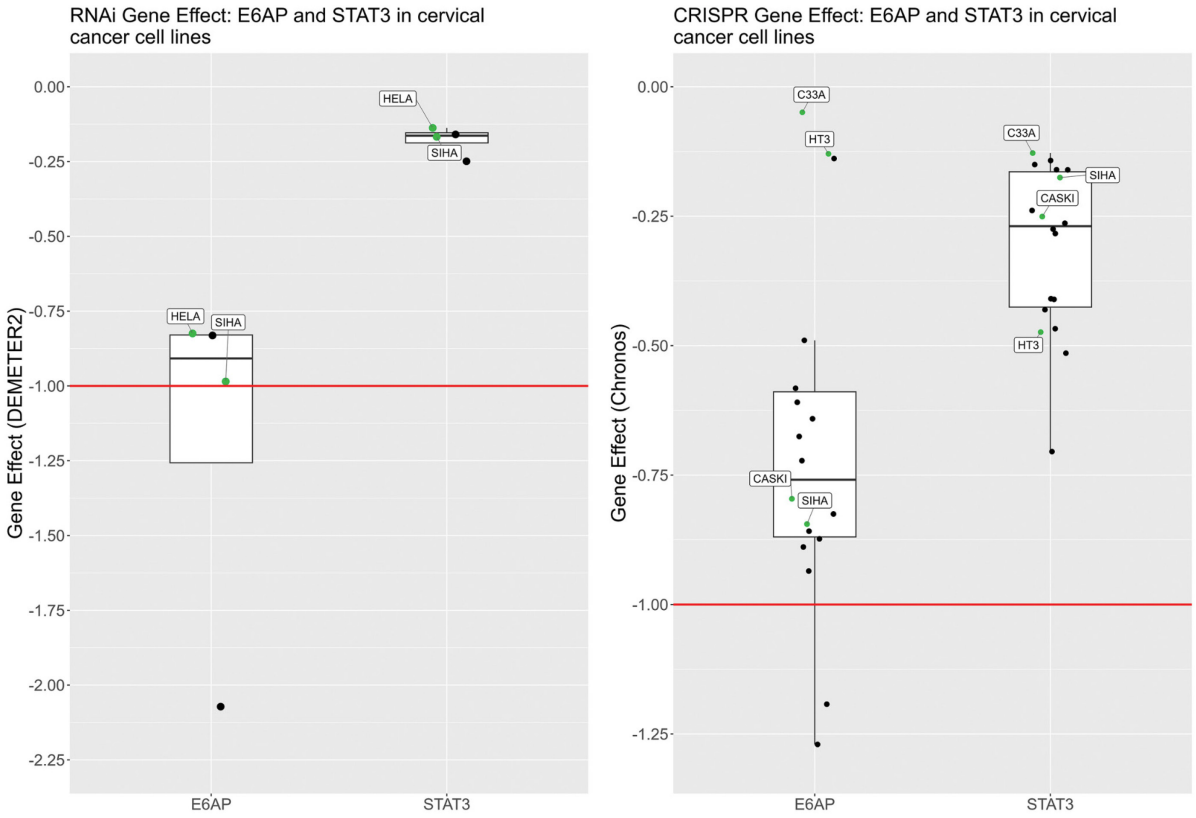

Supplementary Figure 1: Cell growth dependency scores DEMETER2 and Chronos are considerably higher for STAT3 than for E6AP in cervical cancer cell lines. *Cell growth dependency gene effect scores DEMETER2 (left panel) or Chronos (right panel), respectively, for UBE3A (E6AP) and STAT3 in cervical cancer cell lines were plotted as downloaded from the DepMap[357, 358] database portal using R Statistical Software[422-424]. For cell growth dependency based on RNAi-based gene depletion experiments, the "RNAi (Achilles+DRIVE+Marcotte, DEMETER2)" dataset was used while for CRISPR-based gene-depletion experiments, the "CRISPR (DepMap Public 24Q2+Score, Chronos)" dataset was used. The red line indicates a score of -1.0, corresponding to the median score of all pan-essential genes. Accordingly, a score of 0 indicates that a gene is non-essential for the respective cell line. If present in the dataset, the cell lines HeLa, SiHa and CaSki as well as the HPV-negative cervical cancer cell lines C33A and HT3 are labelled in green. Boxes range from the 25th to the 75th percentile, the horizontal black line in each box indicates the median. If applicable, vertical black lines range indicate the 1.5 fold of the inter-quartile range extending below the 25th and above the 75th percentile, respectively.*

Supplementary tables

Supplementary Table 1: Top 10 positively and negatively enriched gene sets in transcriptome data obtained from Affymetrix mRNA analysis in SiHa cells transfected with siSTAT3 #2 compared to siCtrl.

siSTAT3 #2 vs. siCtrl			
Gene Set	NES	P-value	FDR
HALLMARK E2F TARGETS	2.96	< 0.001	< 0.0001
GOCC CONDENSED CHROMOSOME CENTROMERIC REGION	2.63	< 0.001	< 0.0001
GOBP CHROMOSOME SEPARATION	2.62	< 0.001	< 0.0001
GOCC CONDENSED CHROMOSOME	2.60	< 0.001	< 0.0001
GOCC CHROMOSOME CENTROMERIC REGION	2.60	< 0.001	< 0.0001
GOBP REGULATION OF CHROMOSOME SEGREGATION	2.59	< 0.001	< 0.0001
HALLMARK G2M CHECKPOINT	2.59	< 0.001	< 0.0001
GOBP CHROMOSOME CONDENSATION	2.57	< 0.001	< 0.0001
GOBP MITOTIC SISTER CHROMATID SEGREGATION	2.54	< 0.001	< 0.0001
GOBP KINETOCHORE ORGANIZATION	2.50	< 0.001	< 0.0001
GOBP NEGATIVE REGULATION OF VIRAL LIFE CYCLE	-2.34	< 0.001	0.0011
HALLMARK INTERFERON ALPHA RESPONSE	-2.30	< 0.001	0.0005
GOBP NEGATIVE REGULATION OF VIRAL ENTRY INTO HOST CELL	-2.28	< 0.001	0.0007
HALLMARK UNFOLDED PROTEIN RESPONSE	-2.27	< 0.001	0.0005
GOCC TRANS GOLGI NETWORK	-2.21	< 0.001	0.0017
GOBP CELLULAR RESPONSE TO ZINC ION	-2.20	< 0.001	0.0014
HALLMARK INTERFERON GAMMA RESPONSE	-2.16	< 0.001	0.0024
GOBP REGULATION OF VIRAL ENTRY INTO HOST CELL	-2.12	< 0.001	0.0050
BIOCARTA IL6 PATHWAY	-2.08	< 0.001	0.0095
GOMF ATPASE COUPLED INTRAMEMBRANE LIPID TRANSPORTER ACTIVITY	-2.06	< 0.001	0.0122

Supplementary Table 2: Top 10 positively and negatively enriched gene sets in transcriptome data obtained from Affymetrix mRNA analysis in SiHa cells transfected with siSTAT3 #4 compared to siCtrl.

siSTAT3 #4 vs. siCtrl			
Gene Set	NES	P-value	FDR
GOBP EMBRYONIC FORELIMB MORPHOGENESIS	2.20	< 0.001	0.0151
GOBP POSITIVE REGULATION OF OSSIFICATION	2.13	< 0.001	0.0248
GOMF ANTIGEN BINDING	2.11	< 0.001	0.0201
GOBP GLANDULAR EPITHELIAL CELL DIFFERENTIATION	2.11	< 0.001	0.0167
GOBP PROTEOGLYCAN METABOLIC PROCESS	2.09	< 0.001	0.0186
GOBP FORELIMB MORPHOGENESIS	2.04	< 0.001	0.0362
GOBP GLANDULAR EPITHELIAL CELL DEVELOPMENT	2.03	< 0.001	0.0328
GOBP CARDIAC ATRIUM MORPHOGENESIS	2.01	< 0.001	0.0438
GOBP POSITIVE REGULATION OF BONE MINERALIZATION	1.98	< 0.001	0.0603
GOBP POSITIVE REGULATION OF ANIMAL ORGAN MORPHOGENESIS	1.97	< 0.001	0.0611
HALLMARK E2F TARGETS	-3.02	< 0.001	< 0.0001
HALLMARK G2M CHECKPOINT	-2.76	< 0.001	< 0.0001
GOBP MITOTIC SPINDLE ORGANIZATION	-2.46	< 0.001	< 0.0001
GOCC NUCLEAR CHROMOSOME	-2.44	< 0.001	< 0.0001
GOBP DNA TEMPLATED DNA REPLICATION	-2.43	< 0.001	< 0.0001
GOCC SPINDLE POLE	-2.38	< 0.001	< 0.0001
GOMF SINGLE STRANDED DNA BINDING	-2.35	< 0.001	< 0.0001
GOBP MICROTUBULE CYTOSKELETON ORGANIZATION INVOLVED IN MITOSIS	-2.34	< 0.001	0.0001
GOBP SIGNAL TRANSDUCTION IN RESPONSE TO DNA DAMAGE	-2.33	< 0.001	0.0001
GOBP DNA REPLICATION INITIATION	-2.31	< 0.001	0.0001

Supplementary Table 3: Top 10 positively and negatively enriched gene sets in transcriptome data obtained from Affymetrix mRNA analysis in SiHa cells transfected with siSTAT3 #6 compared to siCtrl.

siSTAT3 #6 vs. siCtrl			
Gene Set	NES	P-value	FDR
GOBP PHARYNGEAL SYSTEM DEVELOPMENT	2.08	< 0.001	0.0728
GOBP LONG CHAIN FATTY ACYL COA BIOSYNTHETIC PROCESS	2.07	< 0.001	0.0532
GOBP CARDIAC EPITHELIAL TO MESENCHYMAL TRANSITION	2.06	< 0.001	0.0444
GOBP FATTY ACYL COA BIOSYNTHETIC PROCESS	2.06	< 0.001	0.0336
GOBP COLLAGEN FIBRIL ORGANIZATION	2.05	< 0.001	0.0311
BIOCARTA ALK PATHWAY	2.04	< 0.001	0.0282
GOBP NUCLEOSIDE BISPHOSPHATE BIOSYNTHETIC PROCESS	2.04	< 0.001	0.0262
GOBP THIOESTER BIOSYNTHETIC PROCESS	2.03	< 0.001	0.0250
GOBP ENDODERM FORMATION	2.03	< 0.001	0.0224
GOMF PEPTIDE ANTIGEN BINDING	2.01	0.002	0.0246
HALLMARK E2F TARGETS	-2.60	< 0.001	< 0.0001
GOCC MITOTIC SPINDLE	-2.25	< 0.001	0.0018
GOBP MITOTIC SPINDLE ORGANIZATION	-2.21	< 0.001	0.0021
HALLMARK G2M CHECKPOINT	-2.16	< 0.001	0.0064
GOBP SPINDLE ORGANIZATION	-2.15	< 0.001	0.0066
BIOCARTA IL6 PATHWAY	-2.13	< 0.001	0.0063
GOBP ATTACHMENT OF SPINDLE MICROTUBULES TO KINETOCHORE	-2.11	< 0.001	0.0093
GOBP INTERLEUKIN 6 MEDIATED SIGNALING PATHWAY	-2.07	< 0.001	0.0157
GOCC SPINDLE POLE	-2.07	< 0.001	0.0164
GOBP RESPONSE TO INTERLEUKIN 6	-2.05	< 0.001	0.0177

Supplementary Table 4: Top 10 positively and negatively enriched gene sets in transcriptome data obtained from Affymetrix mRNA analysis in SiHa cells transfected with siSTAT3 #10 compared to siCtrl.

siSTAT3 #10 vs. siCtrl			
Gene Set	NES	P-value	FDR
HALLMARK E2F TARGETS	2.79	< 0.001	< 0.0001
GOBP MITOTIC SISTER CHROMATID SEPARATION	2.60	< 0.001	< 0.0001
GOBP KINETOCHORE ORGANIZATION	2.49	< 0.001	< 0.0001
GOBP CELL CYCLE DNA REPLICATION	2.48	< 0.001	< 0.0001
GOBP REGULATION OF MITOTIC NUCLEAR DIVISION	2.46	< 0.001	< 0.0001
GOBP CHROMOSOME SEPARATION	2.46	< 0.001	< 0.0001
GOBP CENTROMERE COMPLEX ASSEMBLY	2.43	< 0.001	< 0.0001
GOBP REGULATION OF MITOTIC SISTER CHROMATID SEGREGATION	2.42	< 0.001	< 0.0001
GOBP NEGATIVE REGULATION OF NUCLEAR DIVISION	2.39	< 0.001	< 0.0001
GOBP MEIOTIC CHROMOSOME SEGREGATION	2.36	< 0.001	< 0.0001
BIOCARTA IL6 PATHWAY	-2.18	< 0.001	0.0389
GOBP CLEAVAGE INVOLVED IN RRNA PROCESSING	-2.00	< 0.001	0.3359
BIOCARTA MET PATHWAY	-1.96	< 0.001	0.3501
GOBP ENDONUCLEOLYTIC CLEAVAGE INVOLVED IN RRNA PROCESSING	-1.94	0.002	0.3380
BIOCARTA ERK PATHWAY	-1.94	< 0.001	0.2732
GOBP INTRACELLULAR STEROL TRANSPORT	-1.92	< 0.001	0.2978
GOBP REGULATION OF TOLL LIKE RECEPTOR 4 SIGNALING PATHWAY	-1.92	0.002	0.2634
GOBP MATURATION OF 5 8S RRNA FROM TRICISTRONIC RRNA TRANSCRIPT SSU RRNA 5 8S RRNA LSU RRNA	-1.92	0.002	0.2384
GOMF MONOATOMIC ANION MONOATOMIC CATION SYMPORTER ACTIVITY	-1.91	< 0.001	0.2322
GOBP NEGATIVE REGULATION OF VIRAL LIFE CYCLE	-1.90	0.006	0.2199

Supplementary Table 5: Top 10 positively and negatively enriched gene sets in transcriptome data obtained from Affymetrix mRNA analysis in SiHa cells mock transfected compared to siCtrl.

Mock vs. siCtrl			
Gene Set	NES	P-value	FDR
GOBP REGULATION OF MITOTIC CELL CYCLE SPINDLE ASSEMBLY CHECKPOINT	2.21	< 0.001	0.0081
GOBP NEGATIVE REGULATION OF NUCLEAR DIVISION	2.14	< 0.001	0.0122
GOBP REGULATION OF MITOTIC SISTER CHROMATID SEGREGATION	2.13	< 0.001	0.0097
GOBP CHROMOSOME SEPARATION	2.13	< 0.001	0.0077
GOBP MITOTIC SISTER CHROMATID SEPARATION	2.13	< 0.001	0.0063
GOBP REGULATION OF MITOTIC NUCLEAR DIVISION	2.02	< 0.001	0.0307
GOBP REGULATION OF CELL CYCLE CHECKPOINT	1.95	0.002	0.0611
GOBP POSITIVE REGULATION OF CHROMOSOME SEPARATION	1.95	< 0.001	0.0558
GOBP POSITIVE REGULATION OF MITOTIC SISTER CHROMATID SEPARATION	1.94	0.004	0.0603
GOBP POSITIVE REGULATION OF CELL CYCLE CHECKPOINT	1.93	< 0.001	0.0610
GOCC ENDOPLASMIC RETICULUM EXIT SITE	-2.20	< 0.001	0.0209
HALLMARK PROTEIN SECRETION	-2.13	< 0.001	0.0402
GOBP GOLGI ORGANIZATION	-2.13	< 0.001	0.0323
HALLMARK UNFOLDED PROTEIN RESPONSE	-2.07	< 0.001	0.0585
GOBP NLS BEARING PROTEIN IMPORT INTO NUCLEUS	-2.03	< 0.001	0.1027
HALLMARK UV RESPONSE DN	-2.03	< 0.001	0.0900
GOBP NEGATIVE REGULATION OF RHO PROTEIN SIGNAL TRANSDUCTION	-2.02	0.002	0.0829
GOBP CIRCADIAN REGULATION OF GENE EXPRESSION	-2.01	< 0.001	0.0875
HALLMARK TNFA SIGNALING VIA NFKB	-2.01	< 0.001	0.0815
GOBP CELL SUBSTRATE JUNCTION ORGANIZATION	-1.99	< 0.001	0.0876

Supplementary Table 6: Clustered top 10 positively and negatively enriched gene sets of each condition after STAT3 knockdown in SiHa cells.

Gene set	Clust.	NES #02	NES #04	NES #06	NES #10	NES Mock
GOBP NEGATIVE REGULATION OF VIRAL LIFE CYCLE	1	-2.3	-1.5	-1.6	-1.9	-1.3
GOBP NEGATIVE REGULATION OF VIRAL ENTRY INTO HOST CELL	1	-2.3	-1.6	-1.6	-1.9	-1.3
HALLMARK UNFOLDED PROTEIN RESPONSE	1	-2.3	-1.6	-1.8	-1.6	-2.1
GOCC TRANS GOLGI NETWORK	1	-2.2	-1.4	-1.2	-1.4	-1.7
GOBP REGULATION OF VIRAL ENTRY INTO HOST CELL	1	-2.1	-1.6	-1.4	-1.7	-1.2
BIOCARTA IL6 PATHWAY	1	-2.1	-1.9	-2.1	-2.2	-2.0
GOBP RESPONSE TO INTERLEUKIN 6	1	-1.8	-1.7	-2.1	-1.9	-1.4
GOBP REGULATION OF TOLL LIKE RECEPTOR 4 SIGNALING PATHWAY	1	-1.8	-1.7	-0.9	-1.9	-1.4
GOBP INTERLEUKIN 6 MEDIATED SIGNALING PATHWAY	1	-1.8	-1.8	-2.1	-1.9	-1.8
HALLMARK TNFA SIGNALING VIA NFKB	1	-1.6	-1.6	-1.6	-1.9	-2.0
GOBP INTRACELLULAR STEROL TRANSPORT	1	-1.5	-1.0	-1.0	-1.9	-1.4
BIOCARTA ERK PATHWAY	1	-1.5	-1.8	-1.6	-1.9	-1.6
GOBP GOLGI ORGANIZATION	1	-1.5	-1.3	-1.4	-1.5	-2.1
GOBP CIRCADIAN REGULATION OF GENE EXPRESSION	1	-1.3	-1.4	-1.2	-1.7	-2.0
BIOCARTA MET PATHWAY	1	-1.3	-1.8	-1.4	-2.0	-1.6
GOBP MATURATION OF 5 8S RRNA FROM TRICISTRONIC RRNA TRANSCRIPT SSU RRNA 5 8S RRNA LSU RRNA	1	-0.7	-1.5	-1.2	-1.9	-1.4
GOBP CLEAVAGE INVOLVED IN RRNA PROCESSING	1	-0.7	-1.4	-1.4	-2.0	-1.4
GOBP ENDONUCLEOLYTIC CLEAVAGE INVOLVED IN RRNA PROCESSING	1	1.1	-1.2	-0.6	-1.9	-1.2
GOBP SIGNAL TRANSDUCTION IN RESPONSE TO DNA DAMAGE	1	1.4	-2.3	-1.6	-1.3	-1.4
GOMF SINGLE STRANDED DNA BINDING	2	1.7	-2.4	-1.9	1.5	-1.3
GOBP MITOTIC SPINDLE ORGANIZATION	2	1.9	-2.5	-2.2	1.7	1.2
GOCC SPINDLE POLE	2	1.9	-2.4	-2.1	1.6	1.2
GOCC MITOTIC SPINDLE	2	1.9	-2.2	-2.3	1.7	1.2
GOBP SPINDLE ORGANIZATION	2	2.0	-2.3	-2.2	1.7	1.2
GOBP MICROTUBULE CYTOSKELETON ORGANIZATION INVOLVED IN MITOSIS	2	2.0	-2.3	-1.9	1.7	1.2
GOBP DNA REPLICATION INITIATION	2	2.1	-2.3	-1.8	2.1	1.1
GOBP CELL CYCLE DNA REPLICATION	2	2.2	-2.3	-1.9	2.5	1.4
GOCC NUCLEAR CHROMOSOME	2	2.2	-2.4	-1.9	1.8	-1.0
GOBP ATTACHMENT OF SPINDLE MICROTUBULES TO KINETOCHORE	2	2.3	-2.0	-2.1	2.0	1.5
GOBP DNA TEMPLATED DNA REPLICATION	2	2.5	-2.4	-1.9	2.3	1.4
GOBP MITOTIC SISTER CHROMATID SEGREGATION	2	2.5	-2.2	-2.0	2.2	1.5
HALLMARK G2M CHECKPOINT	2	2.6	-2.8	-2.2	2.4	1.6
GOCC CHROMOSOME CENTROMERIC REGION	2	2.6	-2.2	-1.9	2.1	1.3
GOCC CONDENSED CHROMOSOME	2	2.6	-2.2	-1.8	2.2	1.4
GOCC CONDENSED CHROMOSOME CENTROMERIC REGION	2	2.6	-2.2	-1.9	2.2	1.4
HALLMARK E2F TARGETS	2	3.0	-3.0	-2.6	2.8	1.9

Gene set	Clust.	NES #02	NES #04	NES #06	NES #10	NES Mock
HALLMARK INTERFERON ALPHA RESPONSE	3	-2.3	-1.5	1.1	-1.3	-1.6
GOBP CELLULAR RESPONSE TO ZINC ION	3	-2.2	1.7	-0.5	-0.8	-1.2
HALLMARK INTERFERON GAMMA RESPONSE	3	-2.2	-1.4	1.2	-1.2	-1.3
GOMF ATPASE COUPLED INTRAMEMBRANE LIPID TRANSPORTER ACTIVITY	3	-2.1	-1.4	1.2	-1.6	-1.6
HALLMARK PROTEIN SECRETION	3	-1.6	-1.1	1.2	0.6	-2.1
HALLMARK UV RESPONSE DN	3	-1.4	1.2	1.2	-1.2	-2.0
GOCC ENDOPLASMIC RETICULUM EXIT SITE	3	-1.2	-0.8	1.2	-1.1	-2.2
GOBP NEGATIVE REGULATION OF RHO PROTEIN SIGNAL TRANSDUCTION	3	-0.9	-1.6	0.8	-1.4	-2.0
GOMF MONOATOMIC ANION MONOATOMIC CATION SYMPORTER ACTIVITY	3	-0.9	1.3	1.3	-1.9	-0.9
GOMF ANTIGEN BINDING	4	0.8	2.1	1.9	1.1	1.3
GOBP FORELIMB MORPHOGENESIS	4	0.9	2.0	1.6	0.8	-1.0
GOMF PEPTIDE ANTIGEN BINDING	4	1.0	1.9	2.0	1.2	1.1
GOBP EMBRYONIC FORELIMB MORPHOGENESIS	4	1.1	2.2	1.8	0.8	0.9
GOBP COLLAGEN FIBRIL ORGANIZATION	4	1.1	1.2	2.1	-1.0	1.0
GOBP GLANDULAR EPITHELIAL CELL DEVELOPMENT	4	1.1	2.0	1.3	-0.9	-1.1
GOBP POSITIVE REGULATION OF ANIMAL ORGAN MORPHOGENESIS	4	1.1	2.0	1.8	1.2	1.3
GOBP CARDIAC ATRIUM MORPHOGENESIS	4	1.2	2.0	1.7	1.0	1.0
GOBP PROTEOGLYCAN METABOLIC PROCESS	4	1.2	2.1	1.5	1.0	1.3
GOBP POSITIVE REGULATION OF BONE MINERALIZATION	4	1.2	2.0	1.5	1.4	1.2
GOBP PHARYNGEAL SYSTEM DEVELOPMENT	4	1.2	1.6	2.1	1.2	1.4
GOBP POSITIVE REGULATION OF OSSIFICATION	4	1.2	2.1	1.5	1.5	1.1
GOBP GLANDULAR EPITHELIAL CELL DIFFERENTIATION	4	1.6	2.1	1.4	0.8	1.1
BIOCARTA ALK PATHWAY	4	1.6	1.9	2.0	1.3	1.3
GOBP REGULATION OF MITOTIC CELL CYCLE SPINDLE ASSEMBLY CHECKPOINT	5	1.7	-1.3	-1.1	2.3	2.2
GOBP POSITIVE REGULATION OF MITOTIC SISTER CHROMATID SEPARATION	5	1.9	-1.0	-1.3	2.0	1.9
GOBP REGULATION OF CELL CYCLE CHECKPOINT	5	1.9	-1.8	-1.7	2.1	2.0
GOBP MEIOTIC CHROMOSOME SEGREGATION	5	2.2	-1.8	-1.5	2.4	1.3
GOBP POSITIVE REGULATION OF CHROMOSOME SEPARATION	5	2.2	-1.5	-1.8	2.2	2.0
GOBP REGULATION OF MITOTIC SISTER CHROMATID SEGREGATION	5	2.4	-1.7	-1.6	2.4	2.1
GOBP NEGATIVE REGULATION OF NUCLEAR DIVISION	5	2.4	-1.6	-1.6	2.4	2.1
GOBP MITOTIC SISTER CHROMATID SEPARATION	5	2.4	-1.7	-1.6	2.6	2.1
GOBP REGULATION OF MITOTIC NUCLEAR DIVISION	5	2.4	-1.5	-1.5	2.5	2.0
GOBP CENTROMERE COMPLEX ASSEMBLY	5	2.5	-1.7	-1.6	2.4	1.8
GOBP KINETOCHORE ORGANIZATION	5	2.5	-1.9	-1.7	2.5	1.8
GOBP CHROMOSOME CONDENSATION	5	2.6	-1.6	-1.2	1.9	1.5
GOBP REGULATION OF CHROMOSOME SEGREGATION	5	2.6	-1.8	-2.0	2.2	1.8
GOBP CHROMOSOME SEPARATION	5	2.6	-1.7	-1.8	2.5	2.1
GOBP LONG CHAIN FATTY ACYL COA BIOSYNTHETIC PROCESS	6	-0.8	-0.6	2.1	1.0	-1.1
GOBP ENDODERM FORMATION	6	1.1	1.4	2.0	1.0	-1.8
GOBP NUCLEOSIDE BISPHOSPHATE BIOSYNTHETIC PROCESS	6	1.1	-1.0	2.0	0.8	0.7
GOBP THIOESTER BIOSYNTHETIC PROCESS	6	1.2	-1.0	2.0	0.9	-0.6
GOBP CARDIAC EPITHELIAL TO MESENCHYMAL TRANSITION	6	1.3	1.1	2.1	1.0	-0.9
GOBP FATTY ACYL COA BIOSYNTHETIC PROCESS	6	1.3	0.8	2.1	1.2	-0.8
GOBP NLS BEARING PROTEIN IMPORT INTO NUCLEUS	6	1.5	-0.9	1.4	0.8	-2.0

Clusters	
1	4
2	5
3	6

Color scale				
-3.0	-1.5	0.0	1.5	3.0

List of figures

Experimental results and/or illustrations and corresponding figure legends, or parts of these, respectively, which are presented in Figures 2, 4, 5, 6, 7, 9, 10, 11, 12, 15, 16, 17, 18, 21, 23, 24, 26, 28, 30 and 35 were taken and/or extended and/or adapted, respectively, from Strobel et al., 2023[119] as indicated in the corresponding figure legend.

List of supplementary figures

List of tables

List of supplementary tables

Abbreviations

Abbreviation	Meaning
2-DG	2-Deoxy-D-glucose
3-AP	3-aminophthalate
AC	adeno carcinoma
AKT	AKT serine/threonine kinase 1/protein kinase B
ANOVA	analysis of variance
AP-1	activator protein 1
APRF	acute phase response factor
BPE	bovine pituitary extract
BRAF	v-Raf murine sarcoma viral oncogene homolog B
BRD4	bromodomain-containing protein 4
CCL20	chemokine (C-C motif) ligand 20
CDC25A	cell division cycle 25 homolog A
CDK	cyclin dependent kinase
cDNA	complementary DNA
CFA	colony formation assay
CIN	cervical intraepithelial neoplasia
COP1	constitutive photomorphogenic protein 1
COVID19	coronavirus disease 2019
CPX	Ciclopirox
cRNA	complementary RNA
Crypto.	Cryptotanshinone
cyt. C	cytochrome C
DAC	Decitabine
DESI1	desumoylating isopeptidase 1
DMEM	Dulbecco’s minimal essential medium
DMSO	Dimethyl sulfoxide
DREAM	dimerization partner, Rb-like, E2F and MuvB complex
E6AP	E6-associated protein
EBV	Epstein-Barr virus
ECL	enhanced chemiluminescence
EGF	epidermal growth factor
EGFR	epidermal growth factor receptor
eIF2α	eukaryotic initiation factor 2α
ER	endoplasmic reticulum
ERK	extracellular signal-regulated kinase
ETC	electron transport chain
EtOH	Ethanol

FAM57A	family with sequence similarity 57 member A
FBS	fetal bovine serum
FBW7	F-box and WD repeat domain containing 7
FDR	false discovery rate
GAS	gamma activated sequences
gRNA	guide RNA
GSEA	gene set enrichment analysis
HDAC3	histone deacetylase 3
HER	human epidermal growth factor receptor
HIF1α	hypoxia inducible factor 1 alpha
HNSCC	head and neck squamous cell carcinoma
HPV	Human papillomavirus
HRP	horseradish peroxidase
IL	interleukin
IL-6R	interleukin 6 receptor
IP3R3	inositol 1,4,5-trisphosphate receptor, type 3
IRE	iron responsive element
IRF1	interferon regulatory factor 1
IRP	iron regulatory protein
JAB1	jun activation domain-binding protein 1
JAK	janus kinase
KO	knockout
KRAS	Kirsten rat sarcoma virus
LCR	long control region
LIF	leukemia inhibitory factor
LKB1	liver kinase B1
log2FC	log2(fold change)
MAGEC2	melanoma-associated antigen C2
MAPK	mitogen-activated protein kinase
MAPKK	mitogen-activated protein kinase kinase
MCP-1	monocyte chemoattractant protein-1
MEK	mitogen-activated protein kinase kinase
MHC1	major histocompatibility complex 1
MMP-9	matrix metalloprotease 9
mPTP	mitochondrial permeability transition pore
MSigDB	molecular signatures database
mTOR	mechanistic target of rapamycin
mTORC1	mechanistic target of rapamycin complex 1
NES	normalized enrichment score
NfκB	nuclear factor κB

Niclo.	Niclosamide
NOK	normal oral keratinocytes
NUDT5	nucleoside diphosphate-linked moiety X motif 5
ORF	open reading frame
OSM	oncostatin M
OXPHOS	oxidative phosphorylation
PARP	poly-(ADP-ribose)-polymerase
PBS	phosphate buffered saline
PCR	polymerase chain reaction
PD-1	programmed cell death protein 1
PDLIM2	PDZ and LIM domain protein 2
PDZ	post synaptic density protein, drosophila disc large tumor suppressor, and zonula occludens-1 protein
PFA	paraformaldehyde
PI3K	phosphatidylinositol 3-kinase
PIAS3	protein inhibitor of activated STAT3
Pict.	Pictilisib
PKB	protein kinase B
PKR	protein kinase R
pRb	retinoblastoma protein
PROTAC	proteolysis targeting chimera
PTP	protein tyrosine phosphatase
PTPRD	protein tyrosine phosphatase receptor-type D
qRT-PCR	quantitative real-time PCR
RAS	rat sarcoma virus
RNAi	RNA interference
RTK	receptor tyrosine kinase
Ruxo.	Ruxolitinib
SASP	senescence-associated secretory phenotype
SA-β-gal	senescence-associated β-galactosidase
SCC	squamous cell carcinoma
SDS-PAGE	Sodium dodecyl sulfate-polyacrylamide gel electrophoresis
SH2	src-homology 2
Sin3A	sin3 transcription regulator family member A
siRNA	small interfering RNA
SNP	single nucleotide polymorphism
SOCS3	suppressor of cytokine signaling 3
STAT1	signal transducer and activator of transcription 1
STAT3	signal transducer and activator of transcription 3
STAT5	signal transducer and activator of transcription 5 A/B

TERT	telomerase reverse transcriptase
T-LGL	T cell large granular lymphocytic leukemia
TRAF6	tumor necrosis factor receptor associated factor 6
Tram.	Trametinib
Tramet.	Trametinib
UBE3A	ubiquitin-protein ligase E3A
URR	upstream regulatory region
USP28	ubiquitin-specific peptidase 28
VEGF	vascular endothelial growth factor
Wnt	wingless and int-1
X-gal	5-bromo-4-chloro-3-indolyl-β-D-galactopyranoside

Units

Symbol	Unit
°C	degree celsius
ct	cycle threshold
Da	dalton
g	gram
h	hour
L	liter
m	meter
min	minutes
rcf	relative centrifugal force
rpm	rounds per minute
s	second
U	enzymatic activity unit
V	volt

References

1. Gelbard MK, Munger K. Human papillomaviruses: Knowns, mysteries, and unchartered territories. Journal of Medical Virology. 2023;95(10):e29191.

2. Muñoz N, Bosch FX, de Sanjosé S, Herrero R, Castellsagué X, Shah KV, et al. Epidemiologic classification of human papillomavirus types associated with cervical cancer. The New England journal of medicine. 2003;348(6):518-527.

3. Smotkin D, Wettstein FO. Transcription of human papillomavirus type 16 early genes in a cervical cancer and a cancer-derived cell line and identification of the E7 protein. Proc Natl Acad Sci U S A. 1986;83(13):4680-4684.

4. Thierry F, Howley PM. Functional analysis of E2-mediated repression of the HPV18 P105 promoter. The New biologist. 1991;3(1):90-100.

5. Graham SV. Human papillomavirus: gene expression, regulation and prospects for novel diagnostic methods and antiviral therapies. Future microbiology. 2010;5(10):1493-1506.

6. Bergvall M, Melendy T, Archambault J. The E1 proteins. Virology. 2013;445(1):35-56.

7. McBride AA. The papillomavirus E2 proteins. Virology. 2013;445(1-2):57-79.

8. Doorbar J. The E4 protein; structure, function and patterns of expression. Virology. 2013;445(1-2):80-98.

9. Venuti A, Paolini F, Nasir L, Corteggio A, Roperto S, Campo MS, et al. Papillomavirus E5: the smallest oncoprotein with many functions. Mol Cancer. 2011;10:140.

10. Hwang ES, Nottoli T, Dimaio D. The HPV16 E5 protein: expression, detection, and stable complex formation with transmembrane proteins in COS cells. Virology. 1995;211(1):227-233.

11. Schwarz E, Freese U, Gissmann L, Mayer W, Roggenbuck B, Stremlau A, et al. Structure and transcription of human papillomavirus sequences in cervical carcinoma cells. Nature. 1985;314(6006):111-114.

12. Hoppe-Seyler K, Bossler F, Braun JA, Herrmann AL, Hoppe-Seyler F. The HPV E6/E7 Oncogenes: Key Factors for Viral Carcinogenesis and Therapeutic Targets. Trends in microbiology. 2018;26(2):158-168.

13. Buck CB, Day PM, Trus BL. The papillomavirus major capsid protein L1. Virology. 2013;445(1-2):169-174.

14. Wang JW, Roden RB. L2, the minor capsid protein of papillomavirus. Virology. 2013;445(1-2):175-186.

15. Schiller JT, Day PM, Kines RC. Current understanding of the mechanism of HPV infection. Gynecologic oncology. 2010;118(1 Suppl):S12-17.

16. Pyeon D, Pearce SM, Lank SM, Ahlquist P, Lambert PF. Establishment of human papillomavirus infection requires cell cycle progression. PLoS Pathog. 2009;5(2):e1000318.

17. Doorbar J, Quint W, Banks L, Bravo IG, Stoler M, Broker TR, et al. The Biology and Life-Cycle of Human Papillomaviruses. Vaccine. 2012;30:F55-F70.

18. Bray F, Laversanne M, Sung H, Ferlay J, Siegel RL, Soerjomataram I, et al. Global cancer statistics 2022: GLOBOCAN estimates of incidence and mortality worldwide for 36 cancers in 185 countries. CA: a cancer journal for clinicians. 2024;74(3):229-263.

19. de Martel C, Georges D, Bray F, Ferlay J, Clifford GM. Global burden of cancer attributable to infections in 2018: a worldwide incidence analysis. The Lancet Global health. 2020;8(2):e180-e190.

20. zur Hausen H. Papillomaviruses and cancer: from basic studies to clinical application. Nature reviews Cancer. 2002;2(5):342-350.

21. Smith JS, Lindsay L, Hoots B, Keys J, Franceschi S, Winer R, et al. Human papillomavirus type distribution in invasive cervical cancer and high-grade cervical lesions: a meta-analysis update. Int J Cancer. 2007;121(3):621-632.

22. Schiffman M, Castle PE, Jeronimo J, Rodriguez AC, Wacholder S. Human papillomavirus and cervical cancer. Lancet (London, England). 2007;370(9590):890-907.

23. Schiffman M, Doorbar J, Wentzensen N, de Sanjosé S, Fakhry C, Monk BJ, et al. Carcinogenic human papillomavirus infection. Nature reviews Disease primers. 2016;2:16086.

24. Martin CM, O'Leary JJ. Histology of cervical intraepithelial neoplasia and the role of biomarkers. Best Practice & Research Clinical Obstetrics & Gynaecology. 2011;25(5):605-615.

25. Münger K, Werness BA, Dyson N, Phelps WC, Harlow E, Howley PM. Complex formation of human papillomavirus E7 proteins with the retinoblastoma tumor suppressor gene product. Embo j. 1989;8(13):4099-4105.

26. Boyer SN, Wazer DE, Band V. E7 protein of human papilloma virus-16 induces degradation of retinoblastoma protein through the ubiquitin-proteasome pathway. Cancer Res. 1996;56(20):4620-4624.

27. Huh K, Zhou X, Hayakawa H, Cho JY, Libermann TA, Jin J, et al. Human papillomavirus type 16 E7 oncoprotein associates with the cullin 2 ubiquitin ligase complex, which contributes to degradation of the retinoblastoma tumor suppressor. Journal of virology. 2007;81(18):9737-9747.

28. Nevins JR. E2F: a link between the Rb tumor suppressor protein and viral oncoproteins. Science. 1992;258(5081):424-429.

29. Khleif SN, DeGregori J, Yee CL, Otterson GA, Kaye FJ, Nevins JR, et al. Inhibition of cyclin D-CDK4/CDK6 activity is associated with an E2F-mediated induction of cyclin kinase inhibitor activity. Proc Natl Acad Sci U S A. 1996;93(9):4350-4354.

30. Li Y, Nichols MA, Shay JW, Xiong Y. Transcriptional repression of the D-type cyclin-dependent kinase inhibitor p16 by the retinoblastoma susceptibility gene product pRb. Cancer Res. 1994;54(23):6078-6082.

31. Giarrè M, Caldeira S, Malanchi I, Ciccolini F, Leão MJ, Tommasino M. Induction of pRb degradation by the human papillomavirus type 16 E7 protein is essential to efficiently overcome p16INK4a-imposed G1 cell cycle Arrest. Journal of virology. 2001;75(10):4705-4712.

32. Klaes R, Friedrich T, Spitkovsky D, Ridder R, Rudy W, Petry U, et al. Overexpression of p16(INK4A) as a specific marker for dysplastic and neoplastic epithelial cells of the cervix uteri. Int J Cancer. 2001;92(2):276-284.

33. Rashid NN, Rothan HA, Yusoff MS. The association of mammalian DREAM complex and HPV16 E7 proteins. American journal of cancer research. 2015;5(12):3525-3533.

34. Münger K, Howley PM. Human papillomavirus immortalization and transformation functions. Virus research. 2002;89(2):213-228.

35. Seavey SE, Holubar M, Saucedo LJ, Perry ME. The E7 oncoprotein of human papillomavirus type 16 stabilizes p53 through a mechanism independent of p19(ARF). Journal of virology. 1999;73(9):7590-7598.

36. Stott FJ, Bates S, James MC, McConnell BB, Starborg M, Brookes S, et al. The alternative product from the human CDKN2A locus, p14(ARF), participates in a regulatory feedback loop with p53 and MDM2. Embo j. 1998;17(17):5001-5014.

37. Huibregtse JM, Scheffner M, Howley PM. A cellular protein mediates association of p53 with the E6 oncoprotein of human papillomavirus types 16 or 18. Embo j. 1991;10(13):4129-4135.

38. Scheffner M, Huibregtse JM, Vierstra RD, Howley PM. The HPV-16 E6 and E6-AP complex functions as a ubiquitin-protein ligase in the ubiquitination of p53. Cell. 1993;75(3):495-505.

39. Vogt M, Butz K, Dymalla S, Semzow J, Hoppe-Seyler F. Inhibition of Bax activity is crucial for the antiapoptotic function of the human papillomavirus E6 oncoprotein. Oncogene. 2006;25(29):4009-4015.

40. Thomas M, Banks L. Human papillomavirus (HPV) E6 interactions with Bak are conserved amongst E6 proteins from high and low risk HPV types. Journal of General Virology. 1999;80(6):1513-1517.

41. Filippova M, Song H, Connolly JL, Dermody TS, Duerksen-Hughes PJ. The Human Papillomavirus 16 E6 Protein Binds to Tumor Necrosis Factor (TNF) R1 and Protects Cells from TNF-induced Apoptosis*. Journal of Biological Chemistry. 2002;277(24):21730-21739.

42. Ganti K, Broniarczyk J, Manoubi W, Massimi P, Mittal S, Pim D, et al. The Human Papillomavirus E6 PDZ Binding Motif: From Life Cycle to Malignancy. Viruses. 2015;7(7):3530-3551.

43. Katzenellenbogen RA, Egelkrout EM, Vliet-Gregg P, Gewin LC, Gafken PR, Galloway DA. NFX1-123 and poly(A) binding proteins synergistically augment activation of telomerase in human papillomavirus type 16 E6-expressing cells. Journal of virology. 2007;81(8):3786-3796.

44. Doorbar J, Egawa N, Griffin H, Kranjec C, Murakami I. Human papillomavirus molecular biology and disease association. Reviews in medical virology. 2015;25 Suppl 1(Suppl Suppl 1):2-23.

45. Lo Cigno I, Calati F, Albertini S, Gariglio M. Subversion of Host Innate Immunity by Human Papillomavirus Oncoproteins. Pathogens (Basel, Switzerland). 2020;9(4):292.

46. Perea SE, Massimi P, Banks L. Human papillomavirus type 16 E7 impairs the activation of the interferon regulatory factor-1. International journal of molecular medicine. 2000;5(6):661-666.

47. Niebler M, Qian X, Höfler D, Kogosov V, Kaewprag J, Kaufmann AM, et al. Post-translational control of IL-1β via the human papillomavirus type 16 E6 oncoprotein: a novel mechanism of innate immune escape mediated by the E3-ubiquitin ligase E6-AP and p53. PLoS Pathog. 2013;9(8):e1003536.

48. Hasan UA, Bates E, Takeshita F, Biliato A, Accardi R, Bouvard V, et al. TLR9 expression and function is abolished by the cervical cancer-associated human papillomavirus type 16. Journal of immunology (Baltimore, Md : 1950). 2007;178(5):3186-3197.

49. Duensing S, Münger K. Mechanisms of genomic instability in human cancer: insights from studies with human papillomavirus oncoproteins. Int J Cancer. 2004;109(2):157-162.

50. Hashida T, Yasumoto S. Induction of chromosome abnormalities in mouse and human epidermal keratinocytes by the human papillomavirus type 16 E7 oncogene. J Gen Virol. 1991;72 (Pt 7):1569-1577.

51. Steenbergen RD, Hermsen MA, Walboomers JM, Meijer GA, Baak JP, Meijer CJ, et al. Non-random allelic losses at 3p, 11p and 13q during HPV-mediated immortalization and concomitant loss of terminal differentiation of human keratinocytes. Int J Cancer. 1998;76(3):412-417.

52. Duensing S, Münger K. The human papillomavirus type 16 E6 and E7 oncoproteins independently induce numerical and structural chromosome instability. Cancer Res. 2002;62(23):7075-7082.

53. Zwerschke W, Mazurek S, Massimi P, Banks L, Eigenbrodt E, Jansen-Dürr P. Modulation of type M2 pyruvate kinase activity by the human papillomavirus type 16 E7 oncoprotein. Proc Natl Acad Sci U S A. 1999;96(4):1291-1296.

54. Martínez-Ramírez I, Carrillo-García A, Contreras-Paredes A, Ortiz-Sánchez E, Cruz-Gregorio A, Lizano M. Regulation of Cellular Metabolism by High-Risk Human Papillomaviruses. Int J Mol Sci. 2018;19(7):1839.

55. Honegger A, Schilling D, Bastian S, Sponagel J, Kuryshev V, Sültmann H, et al. Dependence of intracellular and exosomal microRNAs on viral E6/E7 oncogene expression in HPV-positive tumor cells. PLoS Pathog. 2015;11(3):e1004712.

56. Mittal S, Banks L. Molecular mechanisms underlying human papillomavirus E6 and E7 oncoprotein-induced cell transformation. Mutation research. 2017;772:23-35.

57. Pett M, Coleman N. Integration of high-risk human papillomavirus: a key event in cervical carcinogenesis? The Journal of pathology. 2007;212(4):356-367.

58. Cullen AP, Reid R, Campion M, Lörincz AT. Analysis of the physical state of different human papillomavirus DNAs in intraepithelial and invasive cervical neoplasm. Journal of virology. 1991;65(2):606-612.

59. McBride AA, Warburton A. The role of integration in oncogenic progression of HPV-associated cancers. PLoS Pathog. 2017;13(4):e1006211.

60. Kim K, Garner-Hamrick PA, Fisher C, Lee D, Lambert PF. Methylation patterns of papillomavirus DNA, its influence on E2 function, and implications in viral infection. Journal of virology. 2003;77(23):12450-12459.

61. Bhattacharjee B, Sengupta S. CpG methylation of HPV 16 LCR at E2 binding site proximal to P97 is associated with cervical cancer in presence of intact E2. Virology. 2006;354(2):280-285.

62. Hall AH, Alexander KA. RNA interference of human papillomavirus type 18 E6 and E7 induces senescence in HeLa cells. Journal of virology. 2003;77(10):6066-6069.

63. Goodwin EC, Yang E, Lee CJ, Lee HW, DiMaio D, Hwang ES. Rapid induction of senescence in human cervical carcinoma cells. Proc Natl Acad Sci U S A. 2000;97(20):10978-10983.

64. Wells SI, Francis DA, Karpova AY, Dowhanick JJ, Benson JD, Howley PM. Papillomavirus E2 induces senescence in HPV-positive cells via pRB- and p21(CIP)-dependent pathways. Embo j. 2000;19(21):5762-5771.

65. Goodwin EC, DiMaio D. Repression of human papillomavirus oncogenes in HeLa cervical carcinoma cells causes the orderly reactivation of dormant tumor suppressor pathways. Proc Natl Acad Sci U S A. 2000;97(23):12513-12518.

66. Butz K, Ristriani T, Hengstermann A, Denk C, Scheffner M, Hoppe-Seyler F. siRNA targeting of the viral E6 oncogene efficiently kills human papillomavirus-positive cancer cells. Oncogene. 2003;22(38):5938-5945.

67. Butz K, Denk C, Ullmann A, Scheffner M, Hoppe-Seyler F. Induction of apoptosis in human papillomaviruspositive cancer cells by peptide aptamers targeting the viral E6 oncoprotein. Proc Natl Acad Sci U S A. 2000;97(12):6693-6697.

68. Harper DM, DeMars LR. HPV vaccines - A review of the first decade. Gynecologic oncology. 2017;146(1):196-204.

69. Wang R, Pan W, Jin L, Huang W, Li Y, Wu D, et al. Human papillomavirus vaccine against cervical cancer: Opportunity and challenge. Cancer Lett. 2020;471:88-102.

70. Markowitz LE, Naleway AL, Klein NP, Lewis RM, Crane B, Querec TD, et al. Human Papillomavirus Vaccine Effectiveness Against HPV Infection: Evaluation of One, Two, and Three Doses. The Journal of infectious diseases. 2020;221(6):910-918.

71. Liontos M, Kyriazoglou A, Dimitriadis I, Dimopoulos MA, Bamias A. Systemic therapy in cervical cancer: 30 years in review. Critical reviews in oncology/hematology. 2019;137:9-17.

72. Cohen PA, Jhingran A, Oaknin A, Denny L. Cervical cancer. Lancet (London, England). 2019;393(10167):169-182.

73. Tewari KS, Sill MW, Penson RT, Huang H, Ramondetta LM, Landrum LM, et al. Bevacizumab for advanced cervical cancer: final overall survival and adverse event analysis of a randomised, controlled, open-label, phase 3 trial (Gynecologic Oncology Group 240). Lancet (London, England). 2017;390(10103):1654-1663.

74. Chung HC, Ros W, Delord JP, Perets R, Italiano A, Shapira-Frommer R, et al. Efficacy and Safety of Pembrolizumab in Previously Treated Advanced Cervical Cancer: Results From the Phase II KEYNOTE-158 Study. Journal of clinical oncology : official journal of the American Society of Clinical Oncology. 2019;37(17):1470-1478.

75. Tan S, de Vries EG, van der Zee AG, de Jong S. Anticancer drugs aimed at E6 and E7 activity in HPV-positive cervical cancer. Current cancer drug targets. 2012;12(2):170-184.

76. Duncan CL, Gunosewoyo H, Mocerino M, Payne AD. Small Molecule Inhibitors of Human Papillomavirus: A Review of Research from 1997 to 2021. Current medicinal chemistry. 2023;31(33):5308-5350.

77. Jung HS, Rajasekaran N, Ju W, Shin YK. Human Papillomavirus: Current and Future RNAi Therapeutic Strategies for Cervical Cancer. Journal of clinical medicine. 2015;4(5):1126-1155.

78. Guo KY, Han L, Li X, Yang AV, Lu J, Guan S, et al. Novel proteasome inhibitor delanzomib sensitizes cervical cancer cells to doxorubicin-induced apoptosis via stabilizing tumor suppressor proteins in the p53 pathway. Oncotarget. 2017;8(69):114123-114135.

79. Kruse S, Büchler M, Uhl P, Sauter M, Scherer P, Lan TCT, et al. Therapeutic vaccination using minimal HPV16 epitopes in a novel MHC-humanized murine HPV tumor model. Oncoimmunology. 2019;8(1):e1524694.

80. Blatnik R, Mohan N, Bonsack M, Falkenby LG, Hoppe S, Josef K, et al. A Targeted LC-MS Strategy for Low-Abundant HLA Class-I-Presented Peptide Detection Identifies Novel Human Papillomavirus T-Cell Epitopes. Proteomics. 2018;18(11):e1700390.

81. Voutsadakis IA. PI3KCA Mutations in Uterine Cervix Carcinoma. Journal of clinical medicine. 2021;10(2):220.

82. Luna AJ, Sterk RT, Griego-Fisher AM, Chung JY, Berggren KL, Bondu V, et al. MEK/ERK signaling is a critical regulator of high-risk human papillomavirus oncogene expression revealing therapeutic targets for HPV-induced tumors. PLoS Pathog. 2021;17(1):e1009216.

83. Wright AA, Howitt BE, Myers AP, Dahlberg SE, Palescandolo E, Van Hummelen P, et al. Oncogenic mutations in cervical cancer: genomic differences between adenocarcinomas and squamous cell carcinomas of the cervix. Cancer. 2013;119(21):3776-3783.

84. Hoppe-Seyler K, Herrmann AL, Däschle A, Kuhn BJ, Strobel TD, Lohrey C, et al. Effects of Metformin on the virus/host cell crosstalk in human papillomavirus-positive cancer cells. Int J Cancer. 2021;149(5):1137-1149.

85. Maehama T, Patzelt A, Lengert M, Hutter KJ, Kanazawa K, Hausen H, et al. Selective down-regulation of human papillomavirus transcription by 2-deoxyglucose. Int J Cancer. 1998;76(5):639-646.

86. Braun JA, Herrmann AL, Blase JI, Frensemeier K, Bulkescher J, Scheffner M, et al. Effects of the antifungal agent ciclopirox in HPV-positive cancer cells: Repression of viral E6/E7 oncogene expression and induction of senescence and apoptosis. Int J Cancer. 2020;146(2):461-474.

87. Herrmann AL, Kuhn BJ, Holzer A, Krijgsveld J, Hoppe-Seyler K, Hoppe-Seyler F. Delineating the Switch between Senescence and Apoptosis in Cervical Cancer Cells under Ciclopirox Treatment. Cancers (Basel). 2021;13(19):4995.

88. Corcoran C, Jacobs TF. Metformin. Treasure Island (FL): StatPearls Publishing LLC; 2023.

89. Subissi A, Monti D, Togni G, Mailland F. Ciclopirox: recent nonclinical and clinical data relevant to its use as a topical antimycotic agent. Drugs. 2010;70(16):2133-2152.

90. Williams RJ. Iron in evolution. FEBS letters. 2012;586(5):479-484.

91. Abbaspour N, Hurrell R, Kelishadi R. Review on iron and its importance for human health. Journal of research in medical sciences : the official journal of Isfahan University of Medical Sciences. 2014;19(2):164-174.

92. Vashchenko G, MacGillivray R. Multi-copper oxidases and human iron metabolism. Nutrients. 2013;5(7):2289-2313.

93. Anderson E, Shah Y. Iron homeostasis in the liver. Comprehensive Physiology. 2013;3(1):315-330.

94. Cheng Y, Zak O, Aisen P, Harrison S, Walz T. Structure of the human transferrin receptor-transferrin complex. Cell. 2004;116(4):565-576.

95. Ohgami R, Campagna D, Greer E, Antiochos B, McDonald A, Chen J, et al. Identification of a ferrireductase required for efficient transferrin-dependent iron uptake in erythroid cells. Nature Genetics. 2005;37(11):1264-1269.

96. Sirlin CB, Reeder SB. Magnetic resonance imaging quantification of liver iron. Magnetic resonance imaging clinics of North America. 2010;18(3):359-381.

97. Pantopoulos K. Iron metabolism and the IRE/IRP regulatory system: an update. Annals of the New York Academy of Sciences. 2004;1012:1-13.

98. Paul B, Manz D, Torti F, Torti S. Mitochondria and Iron: Current Questions. Expert Review of Hematology. 2007;10(1):65-79.

99. Warner MJ, Kamran MT. Iron Deficiency Anemia. Treasure Island (FL): StatPearls Publishing LLC; 2023.

100. Thelander L, Gräslund A. Mechanism of inhibition of mammalian ribonucleotide reductase by the iron chelate of 1-formylisoquinoline thiosemicarbazone. Destruction of the tyrosine free radical of the enzyme in an oxygen-requiring reaction. J Biol Chem. 1983;258(7):4063-4066.

101. Puig S, Ramos-Alonso L, Romero AM, Martínez-Pastor MT. The elemental role of iron in DNA synthesis and repair. Metallomics : integrated biometal science. 2017;9(11):1483-1500.

102. Wu Y, Brosh RM, Jr. DNA helicase and helicase-nuclease enzymes with a conserved iron-sulfur cluster. Nucleic Acids Res. 2012;40(10):4247-4260.

103. Dong C, Zhang H, Xu C, Arrowsmith CH, Min J. Structure and function of dioxygenases in histone demethylation and DNA/RNA demethylation. IUCrJ. 2014;1(Pt 6):540-549.

104. Kuang Y, Guo W, Ling J, Xu D, Liao Y, Zhao H, et al. Iron-dependent CDK1 activity promotes lung carcinogenesis via activation of the GP130/STAT3 signaling pathway. Cell Death & Disease. 2019;10(4):297.

105. Xue X, Ramakrishnan SK, Weisz K, Triner D, Xie L, Attili D, et al. Iron Uptake via DMT1 Integrates Cell Cycle with JAK-STAT3 Signaling to Promote Colorectal Tumorigenesis. Cell metabolism. 2016;24(3):447-461.

106. Park MH, Nishimura K, Zanelli CF, Valentini SR. Functional significance of eIF5A and its hypusine modification in eukaryotes. Amino acids. 2010;38(2):491-500.

107. Kim YS, Kang KR, Wolff EC, Bell JK, McPhie P, Park MH. Deoxyhypusine hydroxylase is a Fe(II)-dependent, HEAT-repeat enzyme. Identification of amino acid residues critical for Fe(II) binding and catalysis [corrected]. J Biol Chem. 2006;281(19):13217-13225.

108. Nurtjahja-Tjendraputra E, Fu D, Phang JM, Richardson DR. Iron chelation regulates cyclin D1 expression via the proteasome: a link to iron deficiency-mediated growth suppression. Blood. 2007;109(9):4045-4054.

109. Torti SV, Manz DH, Paul BT, Blanchette-Farra N, Torti FM. Iron and Cancer. Annual review of nutrition. 2018;38:97-125.

110. Fonseca-Nunes A, Jakszyn P, Agudo A. Iron and cancer risk--a systematic review and meta-analysis of the epidemiological evidence. Cancer epidemiology, biomarkers & prevention : a publication of the American Association for Cancer Research, cosponsored by the American Society of Preventive Oncology. 2014;23(1):12-31.

111. Fenton HJH. LXXIII.—Oxidation of tartaric acid in presence of iron. Journal of the Chemical Society, Transactions. 1894;65(0):899-910.

112. Wu KJ, Polack A, Dalla-Favera R. Coordinated regulation of iron-controlling genes, H-ferritin and IRP2, by c-MYC. Science. 1999;283(5402):676-679.

113. Mizuuchi H, Kudo R, Tamura H, Tsukahara K, Tsumura N, Kumai K, et al. Identification of transferrin receptor in cervical and endometrial tissues. Gynecologic oncology. 1988;31(2):292-300.

114. Alkhateeb AA, Connor JR. The significance of ferritin in cancer: anti-oxidation, inflammation and tumorigenesis. Biochim Biophys Acta. 2013;1836(2):245-254.

115. Siegel EM, Patel N, Lu B, Lee JH, Nyitray AG, Huang X, et al. Circulating biomarkers of iron storage and clearance of incident human papillomavirus infection. Cancer epidemiology, biomarkers & prevention : a publication of the American Association for Cancer Research, cosponsored by the American Society of Preventive Oncology. 2012;21(5):859-865.

116. Ibrahim O, O'Sullivan J. Iron chelators in cancer therapy. Biometals : an international journal on the role of metal ions in biology, biochemistry, and medicine. 2020;33(4-5):201-215.

117. Morales M, Xue X. Targeting iron metabolism in cancer therapy. Theranostics. 2021;11(17):8412-8429.

118. Abrams BB, Hänel H, Hoehler T. Ciclopirox olamine: a hydroxypyridone antifungal agent. Clinics in dermatology. 1991;9(4):471-477.

119. Strobel TD, Weber M, Heber N, Holzer A, Hoppe-Seyler K, Hoppe-Seyler F. Revisiting the role of endogenous STAT3 in HPV-positive cervical cancer cells. Journal of Medical Virology. 2023;95(11):e29230.

120. Lim CP, Cao X. Structure, function, and regulation of STAT proteins. Molecular bioSystems. 2006;2(11):536-550.

121. Wang Y, Shen Y, Wang S, Shen Q, Zhou X. The Role of STAT3 in Leading the Crosstalk between Human Cancers and the Immune System. Cancer Letters. 2018;415:117-128.

122. Hu X, li J, Fu M, Zhao X, Wang W. The JAK/STAT signaling pathway: from bench to clinic. Signal Transduction and Targeted Therapy. 2021;6(1):402.

123. Takeda K, Noguchi K, Shi W, Tanaka T, Matsumoto M, Yoshida N, et al. Targeted disruption of the mouse Stat3 gene leads to early embryonic lethality. Proc Natl Acad Sci U S A. 1997;94(8):3801-3804.

124. Wegenka UM, Buschmann J, Lütticken C, Heinrich PC, Horn F. Acute-phase response factor, a nuclear factor binding to acute-phase response elements, is rapidly activated by interleukin-6 at the posttranslational level. Molecular and cellular biology. 1993;13(1):276-288.

125. Wegenka UM, Lütticken C, Buschmann J, Yuan J, Lottspeich F, Müller-Esterl W, et al. The interleukin-6-activated acute-phase response factor is antigenically and functionally related to members of the signal transducer and activator of transcription (STAT) family. Molecular and cellular biology. 1994;14(5):3186-3196.

126. Zhong Z, Wen Z, Darnell JE, Jr. Stat3: a STAT family member activated by tyrosine phosphorylation in response to epidermal growth factor and interleukin-6. Science. 1994;264(5155):95-98.

127. Rose-John S. Interleukin-6 Family Cytokines. Cold Spring Harbor perspectives in biology. 2018;10(2):a028415.

128. Delgoffe GM, Vignali DA. STAT heterodimers in immunity: A mixed message or a unique signal? Jak-stat. 2013;2(1):e23060.

129. Horvath CM, Wen Z, Darnell JE. A STAT protein domain that determines DNA sequence recognition suggests a novel DNA-binding domain. Genes & Development. 1995;9(8):984-994.

130. Darnell JE, Jr., Kerr IM, Stark GR. Jak-STAT pathways and transcriptional activation in response to IFNs and other extracellular signaling proteins. Science. 1994;264(5164):1415-1421.

131. Xu X, Sun YL, Hoey T. Cooperative DNA binding and sequence-selective recognition conferred by the STAT amino-terminal domain. Science. 1996;273(5276):794-797.

132. Park OK, Schaefer TS, Nathans D. In vitro activation of Stat3 by epidermal growth factor receptor kinase. Proc Natl Acad Sci U S A. 1996;93(24):13704-13708.

133. Olayioye MA, Beuvink I, Horsch K, Daly JM, Hynes NE. ErbB Receptor-induced Activation of Stat Transcription Factors Is Mediated by Src Tyrosine Kinases *. Journal of Biological Chemistry. 1999;274(24):17209-17218.

134. Chen SH, Murphy DA, Lassoued W, Thurston G, Feldman MD, Lee WM. Activated STAT3 is a mediator and biomarker of VEGF endothelial activation. Cancer biology & therapy. 2008;7(12):1994-2003.

135. Zong CS, Chan J, Levy DE, Horvath C, Sadowski HB, Wang L-H. Mechanism of STAT3 Activation by Insulin-like Growth Factor I Receptor*. Journal of Biological Chemistry. 2000;275(20):15099-15105.

136. Turkson J, Bowman T, Garcia R, Caldenhoven E, De Groot RP, Jove R. Stat3 activation by Src induces specific gene regulation and is required for cell transformation. Molecular and cellular biology. 1998;18(5):2545-2552.

137. Garcia R, Bowman TL, Niu G, Yu H, Minton S, Muro-Cacho CA, et al. Constitutive activation of Stat3 by the Src and JAK tyrosine kinases participates in growth regulation of human breast carcinoma cells. Oncogene. 2001;20(20):2499-2513.

138. Schreiner SJ, Schiavone AP, Smithgall TE. Activation of STAT3 by the Src family kinase Hck requires a functional SH3 domain. J Biol Chem. 2002;277(47):45680-45687.

139. Rauluseviciute I, Riudavets-Puig R, Blanc-Mathieu R, Castro-Mondragon Jaime A, Ferenc K, Kumar V, et al. JASPAR 2024: 20th anniversary of the open-access database of transcription factor binding profiles. Nucleic Acids Res. 2023;52(D1):D174-D182.

140. Carpenter RL, Lo HW. STAT3 Target Genes Relevant to Human Cancers. Cancers (Basel). 2014;6(2):897-925.

141. Shahmarvand N, Nagy A, Shahryari J, Ohgami RS. Mutations in the signal transducer and activator of transcription family of genes in cancer. Cancer Sci. 2018;109(4):926-933.

142. Holland SM, DeLeo FR, Elloumi HZ, Hsu AP, Uzel G, Brodsky N, et al. STAT3 mutations in the hyper-IgE syndrome. The New England journal of medicine. 2007;357(16):1608-1619.

143. Vogel TP, Leiding JW, Cooper MA, Forbes Satter LR. STAT3 gain-of-function syndrome. Frontiers in pediatrics. 2022;10:770077.

144. Masle-Farquhar E, Jackson KJL, Peters TJ, Al-Eryani G, Singh M, Payne KJ, et al. STAT3 gain-of-function mutations connect leukemia with autoimmune disease by pathological NKG2D(hi) CD8(+) T cell dysregulation and accumulation. Immunity. 2022;55(12):2386-2404.e2388.

145. Yang J, Liao X, Agarwal MK, Barnes L, Auron PE, Stark GR. Unphosphorylated STAT3 accumulates in response to IL-6 and activates transcription by binding to NFkappaB. Genes Dev. 2007;21(11):1396-1408.

146. Wu M, Song D, Li H, Yang Y, Ma X, Deng S, et al. Negative regulators of STAT3 signaling pathway in cancers. Cancer Manag Res. 2019;11:4957-4969.

147. Sasaki A, Yasukawa H, Suzuki A, Kamizono S, Syoda T, Kinjyo I, et al. Cytokine-inducible SH2 protein-3 (CIS3/SOCS3) inhibits Janus tyrosine kinase by binding through the N-terminal kinase inhibitory region as well as SH2 domain. Genes to cells : devoted to molecular & cellular mechanisms. 1999;4(6):339-351.

148. Kershaw NJ, Laktyushin A, Nicola NA, Babon JJ. Reconstruction of an active SOCS3-based E3 ubiquitin ligase complex in vitro: identification of the active components and JAK2 and gp130 as substrates. Growth factors (Chur, Switzerland). 2014;32(1):1-10.

149. Starr R, Willson TA, Viney EM, Murray LJ, Rayner JR, Jenkins BJ, et al. A family of cytokine-inducible inhibitors of signalling. Nature. 1997;387(6636):917-921.

150. Minamoto S, Ikegame K, Ueno K, Narazaki M, Naka T, Yamamoto H, et al. Cloning and functional analysis of new members of STAT induced STAT inhibitor (SSI) family: SSI-2 and SSI-3. Biochemical and biophysical research communications. 1997;237(1):79-83.

151. Zhang L, Badgwell DB, Bevers JJ, 3rd, Schlessinger K, Murray PJ, Levy DE, et al. IL-6 signaling via the STAT3/SOCS3 pathway: functional analysis of the conserved STAT3 N-domain. Molecular and cellular biochemistry. 2006;288(1-2):179-189.

152. Chung C, Liao J, Liu B, Rao X, Jay P, Berta P, et al. Specific inhibition of Stat3 signal transduction by PIAS3. Science. 1997;278(5344):1803-1805.

153. Caldenhoven E, van Dijk TB, Solari R, Armstrong J, Raaijmakers JAM, Lammers J-WJ, et al. STAT3β, a Splice Variant of Transcription Factor STAT3, Is a Dominant Negative Regulator of Transcription*. Journal of Biological Chemistry. 1996;271(22):13221-13227.

154. Maritano D, Sugrue ML, Tininini S, Dewilde S, Strobl B, Fu X, et al. The STAT3 isoforms alpha and beta have unique and specific functions. Nature immunology. 2004;5(4):401-409.

155. Zhang H-X, Yang P-L, Li E-M, Xu L-Y. STAT3beta, a distinct isoform from STAT3. The International Journal of Biochemistry & Cell Biology. 2019;110:130-139.

156. Laudisi F, Cherubini F, Monteleone G, Stolfi C. STAT3 Interactors as Potential Therapeutic Targets for Cancer Treatment. Int J Mol Sci. 2018;19(6):1787.

157. Li P, Huang Z, Wang J, Chen W, Huang J. Ubiquitin-specific peptidase 28 enhances STAT3 signaling and promotes cell growth in non-small-cell lung cancer. Onco Targets Ther. 2019;12:1603-1611.

158. Song X, Hao J, Wang J, Guo C, Wang Y, He Q, et al. The cancer/testis antigen MAGEC2 promotes amoeboid invasion of tumor cells by enhancing STAT3 signaling. Oncogene. 2017;36(11):1476-1486.

159. Wurster KD, Hummel F, Richter J, Giefing M, Hartmann S, Hansmann ML, et al. Inactivation of the putative ubiquitin-E3 ligase PDLIM2 in classical Hodgkin and anaplastic large cell lymphoma. Leukemia. 2017;31(3):602-613.

160. Dallavalle C, Albino D, Civenni G, Merulla J, Ostano P, Mello-Grand M, et al. MicroRNA-424 impairs ubiquitination to activate STAT3 and promote prostate tumor progression. The Journal of clinical investigation. 2016;126(12):4585-4602.

161. Wei J, Yuan Y, Jin C, Chen H, Leng L, He F, et al. The ubiquitin ligase TRAF6 negatively regulates the JAK-STAT signaling pathway by binding to STAT3 and mediating its ubiquitination. PLoS One. 2012;7(11):e49567.

162. Yao S, Xu F, Chen Y, Ge Y, Zhang F, Huang H, et al. Fbw7 regulates apoptosis in activated B-cell like diffuse large B-cell lymphoma by targeting Stat3 for ubiquitylation and degradation. Journal of experimental & clinical cancer research : CR. 2017;36(1):10.

163. Tanaka T, Yamamoto Y, Muromoto R, Ikeda O, Sekine Y, Grusby MJ, et al. PDLIM2 inhibits T helper 17 cell development and granulomatous inflammation through degradation of STAT3. Sci Signal. 2011;4(202):ra85.

164. Oda A, Wakao H, Fujita H. Calpain is a signal transducer and activator of transcription (STAT) 3 and STAT5 protease. Blood. 2002;99(5):1850-1852.

165. Darnowski JW, Goulette FA, Guan YJ, Chatterjee D, Yang ZF, Cousens LP, et al. Stat3 cleavage by caspases: impact on full-length Stat3 expression, fragment formation, and transcriptional activity. J Biol Chem. 2006;281(26):17707-17717.

166. Tesoriere A, Dinarello A, Argenton F. The Roles of Post-Translational Modifications in STAT3 Biological Activities and Functions. Biomedicines. 2021;9(8):956.

167. Chung J, Uchida E, Grammer TC, Blenis J. STAT3 serine phosphorylation by ERK-dependent and -independent pathways negatively modulates its tyrosine phosphorylation. Molecular and cellular biology. 1997;17(11):6508-6516.

168. Tkach M, Rosemblit C, Rivas MA, Proietti CJ, Díaz Flaqué MC, Mercogliano MF, et al. p42/p44 MAPK-mediated Stat3Ser727 phosphorylation is required for progestin-induced full activation of Stat3 and breast cancer growth. Endocrine-related cancer. 2013;20(2):197-212.

169. Gough DJ, Koetz L, Levy DE. The MEK-ERK pathway is necessary for serine phosphorylation of mitochondrial STAT3 and Ras-mediated transformation. PLoS One. 2013;8(11):e83395.

170. Yokogami K, Wakisaka S, Avruch J, Reeves SA. Serine phosphorylation and maximal activation of STAT3 during CNTF signaling is mediated by the rapamycin target mTOR. Current biology : CB. 2000;10(1):47-50.

171. Garama DJ, White CL, Balic JJ, Gough DJ. Mitochondrial STAT3: Powering up a potent factor. Cytokine. 2016;87:20-25.

172. Wen Z, Zhong Z, Darnell JE, Jr. Maximal activation of transcription by Stat1 and Stat3 requires both tyrosine and serine phosphorylation. Cell. 1995;82(2):241-250.

173. Wakahara R, Kunimoto H, Tanino K, Kojima H, Inoue A, Shintaku H, et al. Phospho-Ser727 of STAT3 regulates STAT3 activity by enhancing dephosphorylation of phospho-Tyr705 largely through TC45. Genes to cells : devoted to molecular & cellular mechanisms. 2012;17(2):132-145.

174. Zhuang S. Regulation of STAT signaling by acetylation. Cell Signal. 2013;25(9):1924-1931.

175. Ma L, Huang C, Wang XJ, Xin DE, Wang LS, Zou QC, et al. Lysyl Oxidase 3 Is a Dual-Specificity Enzyme Involved in STAT3 Deacetylation and Deacetylimination Modulation. Mol Cell. 2017;65(2):296-309.

176. Dasgupta M, Dermawan JK, Willard B, Stark GR. STAT3-driven transcription depends upon the dimethylation of K49 by EZH2. Proc Natl Acad Sci U S A. 2015;112(13):3985-3990.

177. Sobotta MC, Liou W, Stöcker S, Talwar D, Oehler M, Ruppert T, et al. Peroxiredoxin-2 and STAT3 form a redox relay for H2O2 signaling. Nature chemical biology. 2015;11(1):64-70.

178. Gambi G, Di Simone E, Basso V, Ricci L, Wang R, Verma A, et al. The Transcriptional Regulator Sin3A Contributes to the Oncogenic Potential of STAT3. Cancer Res. 2019;79(12):3076-3087.

179. Köhler N, Wundrack N, Schulz S, Bartonitz F, Schaper F, Dittrich A. Non-canonical STAT3 function reduces REDD1 transcription. Febs j. 2023;290(7):1765-1781.

180. Murray PJ. The JAK-STAT Signaling Pathway: Input and Output Integration1. The Journal of Immunology. 2007;178(5):2623-2629.

181. Niemand C, Nimmesgern A, Haan S, Fischer P, Schaper F, Rossaint R, et al. Activation of STAT3 by IL-6 and IL-10 in Primary Human Macrophages Is Differentially Modulated by Suppressor of Cytokine Signaling 3 1. The Journal of Immunology. 2003;170(6):3263-3272.

182. Braun DA, Fribourg M, Sealfon SC. Cytokine Response Is Determined by Duration of Receptor and Signal Transducers and Activators of Transcription 3 (STAT3) Activation*. Journal of Biological Chemistry. 2013;288(5):2986-2993.

183. Yu Z, Zhang W, Kone BC. Signal transducers and activators of transcription 3 (STAT3) inhibits transcription of the inducible nitric oxide synthase gene by interacting with nuclear factor kappaB. The Biochemical journal. 2002;367(Pt 1):97-105.

184. Yoshida Y, Kumar A, Koyama Y, Peng H, Arman A, Boch JA, et al. Interleukin 1 activates STAT3/nuclear factor-kappaB cross-talk via a unique TRAF6- and p65-dependent mechanism. J Biol Chem. 2004;279(3):1768-1776.

185. Muller A, Gasch J, Albring KF, Aberger F, Nivarthi H, Khemeri M, et al. Interplay of transcription factors STAT3, STAT1 and AP-1 mediates activity of the matrix metallo-proteinase-1 promoter in colorectal carcinoma cells. Neoplasma. 2019;66(3):357-366.

186. Schaefer TS, Sanders LK, Nathans D. Cooperative transcriptional activity of Jun and Stat3 beta, a short form of Stat3. Proc Natl Acad Sci U S A. 1995;92(20):9097-9101.

187. Thakur K, Janjua D, Aggarwal N, Chhokar A, Yadav J, Tripathi T, et al. Physical interaction between STAT3 and AP1 in cervical carcinogenesis: Implications in HPV transcription control. Biochimica et biophysica acta Molecular basis of disease. 2023;1869(8):166817.

188. Zhang X, Wrzeszczynska MH, Horvath CM, Darnell JE, Jr. Interacting regions in Stat3 and c-Jun that participate in cooperative transcriptional activation. Molecular and cellular biology. 1999;19(10):7138-7146.

189. Ji Z, He L, Regev A, Struhl K. Inflammatory regulatory network mediated by the joint action of NF-kB, STAT3, and AP-1 factors is involved in many human cancers. Proc Natl Acad Sci U S A. 2019;116(19):9453-9462.

190. Srivastava J, DiGiovanni J. Non-canonical Stat3 signaling in cancer. Mol Carcinog. 2016;55(12):1889-1898.

191. Tammineni P, Anugula C, Mohammed F, Anjaneyulu M, Larner AC, Sepuri NB. The import of the transcription factor STAT3 into mitochondria depends on GRIM-19, a component of the electron transport chain. J Biol Chem. 2013;288(7):4723-4732.

192. Szczepanek K, Chen Q, Derecka M, Salloum FN, Zhang Q, Szelag M, et al. Mitochondrial-targeted Signal transducer and activator of transcription 3 (STAT3) protects against ischemia-induced changes in the electron transport chain and the generation of reactive oxygen species. J Biol Chem. 2011;286(34):29610-29620.

193. Elschami M, Scherr M, Philippens B, Gerardy-Schahn R. Reduction of STAT3 expression induces mitochondrial dysfunction and autophagy in cardiac HL-1 cells. European journal of cell biology. 2013;92(1):21-29.

194. Phillips D, Reilley MJ, Aponte AM, Wang G, Boja E, Gucek M, et al. Stoichiometry of STAT3 and mitochondrial proteins: Implications for the regulation of oxidative phosphorylation by protein-protein interactions. J Biol Chem. 2010;285(31):23532-23536.

195. Yang R, Lirussi D, Thornton TM, Jelley-Gibbs DM, Diehl SA, Case LK, et al. Mitochondrial Ca^{2+} and membrane potential, an alternative pathway for Interleukin 6 to regulate CD4 cell effector function. eLife. 2015;4:e06376.

196. Yang R, Rincon M. Mitochondrial Stat3, the Need for Design Thinking. International journal of biological sciences. 2016;12(5):532-544.

197. Boengler K, Hilfiker-Kleiner D, Heusch G, Schulz R. Inhibition of permeability transition pore opening by mitochondrial STAT3 and its role in myocardial ischemia/reperfusion. Basic research in cardiology. 2010;105(6):771-785.

198. Avalle L, Camporeale A, Morciano G, Caroccia N, Ghetti E, Orecchia V, et al. STAT3 localizes to the ER, acting as a gatekeeper for ER-mitochondrion Ca(2+) fluxes and apoptotic responses. Cell death and differentiation. 2019;26(5):932-942.

199. Shen S, Niso-Santano M, Adjemian S, Takehara T, Malik Shoaib A, Minoux H, et al. Cytoplasmic STAT3 Represses Autophagy by Inhibiting PKR Activity. Molecular Cell. 2012;48(5):667-680.

200. Miao LJ, Huang FX, Sun ZT, Zhang RX, Huang SF, Wang J. Stat3 inhibits Beclin 1 expression through recruitment of HDAC3 in nonsmall cell lung cancer cells. Tumour biology : the journal of the International Society for Oncodevelopmental Biology and Medicine. 2014;35(7):7097-7103.

201. Liu B, Palmfeldt J, Lin L, Colaço A, Clemmensen KKB, Huang J, et al. STAT3 associates with vacuolar H(+)-ATPase and regulates cytosolic and lysosomal pH. Cell research. 2018;28(10):996-1012.

202. Pinno J, Bongartz H, Klepsch O, Wundrack N, Poli V, Schaper F, et al. Interleukin-6 influences stress-signalling by reducing the expression of the mTOR-inhibitor REDD1 in a STAT3-dependent manner. Cell Signal. 2016;28(8):907-916.

203. Nishimoto A, Kugimiya N, Hosoyama T, Enoki T, Li TS, Hamano K. JAB1 regulates unphosphorylated STAT3 DNA-binding activity through protein-protein interaction in human colon cancer cells. Biochemical and biophysical research communications. 2013;438(3):513-518.

204. Braunstein J, Brutsaert S, Olson R, Schindler C. STATs dimerize in the absence of phosphorylation. J Biol Chem. 2003;278(36):34133-34140.

205. Nkansah E, Shah R, Collie GW, Parkinson GN, Palmer J, Rahman KM, et al. Observation of unphosphorylated STAT3 core protein binding to target dsDNA by PEMSA and X-ray crystallography. FEBS letters. 2013;587(7):833-839.

206. Timofeeva OA, Chasovskikh S, Lonskaya I, Tarasova NI, Khavrutskii L, Tarasov SG, et al. Mechanisms of unphosphorylated STAT3 transcription factor binding to DNA. J Biol Chem. 2012;287(17):14192-14200.

207. Timofeeva OA, Tarasova NI, Zhang X, Chasovskikh S, Cheema AK, Wang H, et al. STAT3 suppresses transcription of proapoptotic genes in cancer cells with the involvement of its N-terminal domain. Proc Natl Acad Sci U S A. 2013;110(4):1267-1272.

208. Zhao Y, Zeng C, Tarasova NI, Chasovskikh S, Dritschilo A, Timofeeva OA. A new role for STAT3 as a regulator of chromatin topology. Transcription. 2013;4(5):227-231.

209. Calautti E, Avalle L, Poli V. Psoriasis: A STAT3-Centric View. Int J Mol Sci. 2018;19(1):171.

210. Warshauer JT, Belk JA, Chan AY, Wang J, Gupta AR, Shi Q, et al. A human mutation in STAT3 promotes type 1 diabetes through a defect in CD8+ T cell tolerance. The Journal of experimental medicine. 2021;218(8):e20210759.

211. Fu XY. STAT3 in immune responses and inflammatory bowel diseases. Cell research. 2006;16(2):214-219.

212. Lu HC, Kim S, Steelman AJ, Tracy K, Zhou B, Michaud D, et al. STAT3 signaling in myeloid cells promotes pathogenic myelin-specific T cell differentiation and autoimmune demyelination. Proc Natl Acad Sci U S A. 2020;117(10):5430-5441.

213. Cénit MC, Alcina A, Márquez A, Mendoza JL, Díaz-Rubio M, de las Heras V, et al. STAT3 locus in inflammatory bowel disease and multiple sclerosis susceptibility. Genes & Immunity. 2010;11(3):264-268.

214. Matsuyama T, Kubli SP, Yoshinaga SK, Pfeffer K, Mak TW. An aberrant STAT pathway is central to COVID-19. Cell Death & Differentiation. 2020;27(12):3209-3225.

215. Kleinbongard P. Perspective: mitochondrial STAT3 in cardioprotection. Basic research in cardiology. 2023;118(1):32.

216. Johnson DE, O'Keefe RA, Grandis JR. Targeting the IL-6/JAK/STAT3 signalling axis in cancer. Nature Reviews Clinical Oncology. 2018;15(4):234-248.

217. Hanahan D, Weinberg Robert A. Hallmarks of Cancer: The Next Generation. Cell. 2011;144(5):646-674.

218. Yanagimura N, Takeuchi S, Fukuda K, Arai S, Tanimoto A, Nishiyama A, et al. STAT3 inhibition suppresses adaptive survival of ALK-rearranged lung cancer cells through transcriptional modulation of apoptosis. npj Precision Oncology. 2022;6(1):11.

219. Sun D, Li W, Ding D, Tan K, Ding W, Wang Z, et al. IL-17a promotes hepatocellular carcinoma by increasing FAP expression in hepatic stellate cells via activation of the STAT3 signaling pathway. Cell Death Discovery. 2024;10(1):230.

220. Ma Y, Chen Y, Zhan L, Dong Q, Wang Y, Li X, et al. CEBPB-mediated upregulation of SERPINA1 promotes colorectal cancer progression by enhancing STAT3 signaling. Cell Death Discovery. 2024;10(1):219.

221. Peisl S, Mellenthin C, Vignot L, Gonelle-Gispert C, Bühler L, Egger B. Therapeutic targeting of STAT3 pathways in pancreatic adenocarcinoma: A systematic review of clinical and preclinical literature. PLoS One. 2021;16(6):e0252397.

222. Tan MSY, Sandanaraj E, Chong YK, Lim SW, Koh LWH, Ng WH, et al. A STAT3-based gene signature stratifies glioma patients for targeted therapy. Nature Communications. 2019;10(1):3601.

223. Hüser L, Sachindra S, Granados K, Federico A, Larribère L, Novak D, et al. SOX2-mediated upregulation of CD24 promotes adaptive resistance toward targeted therapy in melanoma. International Journal of Cancer. 2018;143(12):3131-3142.

224. Hüser L, Kokkaleniou MM, Granados K, Dworacek J, Federico A, Vierthaler M, et al. HER3-Receptor-Mediated STAT3 Activation Plays a Central Role in Adaptive Resistance toward Vemurafenib in Melanoma. Cancers (Basel). 2020;12(12):3761.

225. Lui VW, Wong EY, Ho Y, Hong B, Wong SC, Tao Q, et al. STAT3 activation contributes directly to Epstein-Barr virus-mediated invasiveness of nasopharyngeal cancer cells in vitro. Int J Cancer. 2009;125(8):1884-1893.

226. Gordziel C, Bratsch J, Moriggl R, Knösel T, Friedrich K. Both STAT1 and STAT3 are favourable prognostic determinants in colorectal carcinoma. British Journal of Cancer. 2013;109(1):138-146.

227. de Jong PR, Mo JH, Harris AR, Lee J, Raz E. STAT3: An Anti-Invasive Factor in Colorectal Cancer? Cancers (Basel). 2014;6(3):1394-1407.

228. Zhang HF, Chen Y, Wu C, Wu ZY, Tweardy DJ, Alshareef A, et al. The Opposing Function of STAT3 as an Oncoprotein and Tumor Suppressor Is Dictated by the Expression Status of STAT3β in Esophageal Squamous Cell Carcinoma. Clin Cancer Res. 2016;22(3):691-703.

229. He Z, Song B, Zhu M, Liu J. Comprehensive pan-cancer analysis of STAT3 as a prognostic and immunological biomarker. Scientific Reports. 2023;13(1):5069.

230. Röder S, Steimle C, Meinhardt G, Pahl HL. STAT3 is constitutively active in some patients with Polycythemia rubra vera. Experimental hematology. 2001;29(6):694-702.

231. Koskela HL, Eldfors S, Ellonen P, van Adrichem AJ, Kuusanmäki H, Andersson EI, et al. Somatic STAT3 mutations in large granular lymphocytic leukemia. The New England journal of medicine. 2012;366(20):1905-1913.

232. Zerdes I, Wallerius M, Sifakis EG, Wallmann T, Betts S, Bartish M, et al. STAT3 Activity Promotes Programmed-Death Ligand 1 Expression and Suppresses Immune Responses in Breast Cancer. Cancers (Basel). 2019;11(10):1479.

233. Bu LL, Yu GT, Wu L, Mao L, Deng WW, Liu JF, et al. STAT3 Induces Immunosuppression by Upregulating PD-1/PD-L1 in HNSCC. Journal of dental research. 2017;96(9):1027-1034.

234. Zhao C, Li H, Lin H-J, Yang S, Lin J, Liang G. Feedback Activation of STAT3 as a Cancer Drug-Resistance Mechanism. Trends in Pharmacological Sciences. 2016;37(1):47-61.

235. Wang J, Lv X, Guo X, Dong Y, Peng P, Huang F, et al. Feedback activation of STAT3 limits the response to PI3K/AKT/mTOR inhibitors in PTEN-deficient cancer cells. Oncogenesis. 2021;10(1):8.

236. Lee H-J, Zhuang G, Cao Y, Du P, Kim H-J, Settleman J. Drug Resistance via Feedback Activation of Stat3 in Oncogene-Addicted Cancer Cells. Cancer Cell. 2014;26(2):207-221.

237. Van Schaeybroeck S, Kalimutho M, Dunne Philip D, Carson R, Allen W, Jithesh Puthen V, et al. ADAM17-Dependent c-MET-STAT3 Signaling Mediates Resistance to MEK Inhibitors in KRAS Mutant Colorectal Cancer. Cell Reports. 2014;7(6):1940-1955.

238. Zhao D, Chen J, Wang Y, Zhang L, Zhang J, Zhang W, et al. Feed-forward activation of STAT3 signaling limits the efficacy of c-Met inhibitors in esophageal squamous cell carcinoma (ESCC) treatment. Molecular Carcinogenesis. 2021;60(7):481-496.

239. Zheng Z-Y, Chu M-Y, Lin W, Zheng Y-Q, Xu X-E, Chen Y, et al. Blocking STAT3 signaling augments MEK/ERK inhibitor efficacy in esophageal squamous cell carcinoma. Cell Death & Disease. 2022;13(5):496.

240. Vultur A, Villanueva J, Krepler C, Rajan G, Chen Q, Xiao M, et al. MEK inhibition affects STAT3 signaling and invasion in human melanoma cell lines. Oncogene. 2014;33(14):1850-1861.

241. Cheon SK, Kim HP, Park YL, Jang JE, Lim Y, Song SH, et al. Macrophage migration inhibitory factor promotes resistance to MEK blockade in KRAS mutant colorectal cancer cells. Mol Oncol. 2018;12(8):1398-1409.

242. Liu Z, Ma L, Sun Y, Yu W, Wang X. Targeting STAT3 signaling overcomes gefitinib resistance in non-small cell lung cancer. Cell Death & Disease. 2021;12(6):561.

243. Zulkifli AA, Tan FH, Putoczki TL, Stylli SS, Luwor RB. STAT3 signaling mediates tumour resistance to EGFR targeted therapeutics. Molecular and Cellular Endocrinology. 2017;451:15-23.

244. Sen M, Joyce S, Panahandeh M, Li C, Thomas SM, Maxwell J, et al. Targeting Stat3 Abrogates EGFR Inhibitor Resistance in Cancer. Clinical Cancer Research. 2012;18(18):4986-4996.

245. Spitzner M, Ebner R, Wolff HA, Ghadimi BM, Wienands J, Grade M. STAT3: A Novel Molecular Mediator of Resistance to Chemoradiotherapy. Cancers (Basel). 2014;6(4):1986-2011.

246. Sun C-Y, Nie J, Huang J-P, Zheng G-J, Feng B. Targeting STAT3 inhibition to reverse cisplatin resistance. Biomedicine & Pharmacotherapy. 2019;117:109135.

247. Takemoto S, Ushijima K, Kawano K, Yamaguchi T, Terada A, Fujiyoshi N, et al. Expression of activated signal transducer and activator of transcription-3 predicts poor prognosis in cervical squamous-cell carcinoma. Br J Cancer. 2009;101(6):967-972.

248. Gutiérrez-Hoya A, Soto-Cruz I. Role of the JAK/STAT Pathway in Cervical Cancer: Its Relationship with HPV E6/E7 Oncoproteins. Cells. 2020;9(10):2297.

249. Morgan EL, Macdonald A. Manipulation of JAK/STAT Signalling by High-Risk HPVs: Potential Therapeutic Targets for HPV-Associated Malignancies. Viruses. 2020;12(9):977.

250. Janjua D, Thakur K, Aggarwal N, Chaudhary A, Yadav J, Chhokar A, et al. Prognostic and therapeutic potential of STAT3: Opportunities and challenges in targeting HPV-mediated cervical carcinogenesis. Critical reviews in oncology/hematology. 2024;197:104346.

251. Morgan E, Wasson C, Hanson L, Kealy D, Pentland I, McGuire V, et al. STAT3 activation by E6 is essential for the differentiation-dependent HPV18 life cycle. PLoS Pathogens. 2018;14(4):e1006975.

252. Shukla S, Mahata S, Shishodia G, Pandey A, Tyagi A, Vishnoi K, et al. Functional Regulatory Role of STAT3 in HPV16-Mediated Cervical Carcinogenesis. PLoS One. 2013;8(7):e67849.

253. Morgan E, Macdonald A. Autocrine STAT3 activation in HPV positive cervical cancer through a virus-driven Rac1-NFκB-IL-6 signalling axis. PLoS Pathogens. 2019;15(6):e1007835.

254. Arany I, Grattendick K, Tyring S. Interleukin-10 induces transcription of the early promoter of human papillomavirus type 16 (HPV16) through the 5'-segment of the upstream regulatory region (URR). Antiviral Research. 2002;55(2):331-339.

255. Shishodia G, Verma G, Srivastava Y, Mehrotra R, Das BC, Bharti AC. Deregulation of microRNAs Let-7a and miR-21 mediate aberrant STAT3 signaling during human papillomavirus-induced cervical carcinogenesis: role of E6 oncoprotein. BMC cancer. 2014;14:996.

256. Chen CL, Hsieh FC, Lieblein JC, Brown J, Chan C, Wallace JA, et al. Stat3 activation in human endometrial and cervical cancers. Br J Cancer. 2007;96(4):591-599.

257. Yao S, Xu J, Zhao K, Song P, Yan Q, Fan W, et al. Down-regulation of HPGD by miR-146b-3p promotes cervical cancer cell proliferation, migration and anchorage-independent growth through activation of STAT3 and AKT pathways. Cell Death & Disease. 2018;9(11):1055.

258. Tartour E, Gey A, Sastre-Garau X, Pannetier C, Mosseri V, Kourilsky P, et al. Analysis of interleukin 6 gene expression in cervical neoplasia using a quantitative polymerase chain reaction assay: evidence for enhanced interleukin 6 gene expression in invasive carcinoma. Cancer Res. 1994;54(23):6243-6248.

259. Takanol H, Harigaya K, Ishii G, Sugaya Y, Soeta S, Nunoyamal T, et al. Interleukin-6 (IL-6) production in carcinoma of the cervix. Archives of Gynecology and Obstetrics. 1996;258(1):25-33.

260. Tjiong MY, van der Vange N, ten Kate FJ, Tjong AHSP, ter Schegget J, Burger MP, et al. Increased IL-6 and IL-8 levels in cervicovaginal secretions of patients with cervical cancer. Gynecologic oncology. 1999;73(2):285-291.

261. Bauknecht T, Randelzhofer B, Schmitt B, Ban Z, Hernando J-J, Bauknecht T. Response to IL-6 of HPV-18 Cervical Carcinoma Cell Lines. Virology. 1999;258(2):344-354.

262. Hess S, Smola H, Sandaradura De Silva U, Hadaschik D, Kube D, Baldus SE, et al. Loss of IL-6 receptor expression in cervical carcinoma cells inhibits autocrine IL-6 stimulation: abrogation of constitutive monocyte chemoattractant protein-1 production. Journal of immunology (Baltimore, Md : 1950). 2000;165(4):1939-1948.

263. Smola-Hess S, Sandaradura de Silva U, Hadaschik D, Pfister HJ. Soluble interleukin-6 receptor activates the human papillomavirus type 18 long control region in SW756 cervical carcinoma cells in a STAT3-dependent manner. J Gen Virol. 2001;82(Pt 10):2335-2339.

264. Walch-Rückheim B, Pahne-Zeppenfeld J, Fischbach J, Wickenhauser C, Horn LC, Tharun L, et al. STAT3/IRF1 Pathway Activation Sensitizes Cervical Cancer Cells to Chemotherapeutic Drugs. Cancer Research. 2016;76(13):3872-3883.

265. Nakamura H, Taguchi A, Kawana K, Kawata A, Yoshida M, Fujimoto A, et al. STAT3 activity regulates sensitivity to tumor necrosis factor-related apoptosis-inducing ligand-induced apoptosis in cervical cancer cells. Int J Oncol. 2016;49(5):2155-2162.

266. Morgan EL, Macdonald A. JAK2 Inhibition Impairs Proliferation and Sensitises Cervical Cancer Cells to Cisplatin-Induced Cell Death. Cancers (Basel). 2019;11(12):1934.

267. Ramírez de Arellano A, Lopez-Pulido E, Martínez-Neri P, Estrada Chávez C, González Lucano R, Fafutis-Morris M, et al. STAT3 activation is required for the antiapoptotic effects of prolactin in cervical cancer cells. Cancer Cell International. 2015;15(1):83.

268. Wu L, Shen B, Li J, Zhang H, Zhang K, Yang Y, et al. STAT3 exerts pro-tumor and anti-autophagy roles in cervical cancer. Diagnostic pathology. 2022;17(1):13.

269. Wang H, Deng J, Ren H-Y, Jia P, Zhang W, Li MQ, et al. STAT3 influences the characteristics of stem cells in cervical carcinoma. Oncol Lett. 2017;14(2):2131-2136.

270. Wang H, Cai HB, Chen LL, Zhao WJ, Li P, Wang ZQ, et al. STAT3 correlates with stem cell-related transcription factors in cervical cancer. Journal of Huazhong University of Science and Technology [Medical sciences]. 2015;35(6):891-897.

271. Huang LL, Rao W. SiRNA interfering STAT3 enhances DDP sensitivity in cervical cancer cells. European review for medical and pharmacological sciences. 2018;22(13):4098-4106.

272. Li H, Lu Y, Pang Y, Li M, Cheng X, Chen J. Propofol enhances the cisplatin-induced apoptosis on cervical cancer cells via EGFR/JAK2/STAT3 pathway. Biomedicine & Pharmacotherapy. 2017;86:324-333.

273. Stroeder R, Walch-Rückheim B, Fischbach J, Juhasz-Böss I, Rübe C, Solomayer E, et al. Oncostatin M treatment increases the responsiveness toward cisplatin-based chemoradiotherapy in cervical cancer cells in a STAT3-dependent manner. Oncology Letters. 2018;16(3):3351-3358.

274. Schust J, Sperl B, Hollis A, Mayer TU, Berg T. Stattic: a small-molecule inhibitor of STAT3 activation and dimerization. Chemistry & biology. 2006;13(11):1235-1242.

275. Bharadwaj U, Eckols T, Xu X, Kasembeli M, Chen Y, Adachi M, et al. Small-molecule inhibition of STAT3 in radioresistant head and neck squamous cell carcinoma. Oncotarget. 2016;7(18):26307-26330.

276. Xie X, Yu T, Li X, Zhang N, Foster LJ, Peng C, et al. Recent advances in targeting the “undruggable” proteins: from drug discovery to clinical trials. Signal Transduction and Targeted Therapy. 2023;8(1):335.

277. Lu Y, Yang Y, Zhu G, Zeng H, Fan Y, Guo F, et al. Emerging Pharmacotherapeutic Strategies to Overcome Undruggable Proteins in Cancer. International journal of biological sciences. 2023;19(11):3360-3382.

278. Bai L, Zhou H, Xu R, Zhao Y, Chinnaswamy K, McEachern D, et al. A Potent and Selective Small-Molecule Degrader of STAT3 Achieves Complete Tumor Regression In Vivo. Cancer Cell. 2019;36(5):498-511.e417.

279. Liu PC, Dixit V, Mayo M, Dey J, Yuan K, Karnik R, et al. A First-in-Class STAT3 Degrader KT-333 in Development for Treatment of Hematologic Cancers. Blood. 2021;138(Supplement 1):1865-1865.

280. Hall J, Zhang Z, Bhattacharya S, Wang D, Alcantara M, Liang Y, et al. Oligo-PROTAC strategy for cell-selective and targeted degradation of activated STAT3. Molecular therapy Nucleic acids. 2024;35(1):102137.

281. A Phase 1, Multicenter, Open-Label, Dose-Escalation and Expansion Study to Evaluate Safety, Tolerability, Pharmacokinetics, Pharmacodynamics, and Clinical Activity of Intravenously Administered KT-333 in Adult Patients With Relapsed or Refractory Lymphomas, Large Granular Lymphocytic Leukemia, and Solid Tumors [Internet]. 2021. Available from: https://clinicaltrials.gov/study/NCT05225584.

282. Reilley MJ, McCoon P, Cook C, Lyne P, Kurzrock R, Kim Y, et al. STAT3 antisense oligonucleotide AZD9150 in a subset of patients with heavily pretreated lymphoma: results of a phase 1b trial. Journal for ImmunoTherapy of Cancer. 2018;6(1):119.

283. Hong D, Kurzrock R, Kim Y, Woessner R, Younes A, Nemunaitis J, et al. AZD9150, a next-generation antisense oligonucleotide inhibitor of STAT3 with early evidence of clinical activity in lymphoma and lung cancer. Science Translational Medicine. 2015;7(314):314ra185.

284. Leong PL, Andrews GA, Johnson DE, Dyer KF, Xi S, Mai JC, et al. Targeted inhibition of Stat3 with a decoy oligonucleotide abrogates head and neck cancer cell growth. Proc Natl Acad Sci U S A. 2003;100(7):4138-4143.

285. Sen M, Thomas SM, Kim S, Yeh JI, Ferris RL, Johnson JT, et al. First-in-Human Trial of a STAT3 Decoy Oligonucleotide in Head and Neck Tumors: Implications for Cancer Therapy. Cancer Discovery. 2012;2(8):694-705.

286. Ramasamy T, Chen X, Qin B, Johnson DE, Grandis JR, Villanueva FS. STAT3 decoy oligonucleotide-carrying microbubbles with pulsed ultrasound for enhanced therapeutic effect in head and neck tumors. PLoS One. 2020;15(11):e0242264.

287. Sheppard M, Laskou F, Stapleton PP, Hadavi S, Dasgupta B. Tocilizumab (Actemra). Human vaccines & immunotherapeutics. 2017;13(9):1972-1988.

288. Davis CC, Shah KS, Lechowicz MJ. Clinical development of siltuximab. Current oncology reports. 2015;17(7):29.

289. Yang R, Klimentová J, Göckel-Krzikalla E, Ly R, Gmelin N, Hotz-Wagenblatt A, et al. Combined Transcriptome and Proteome Analysis of Immortalized Human Keratinocytes Expressing Human Papillomavirus 16 (HPV16) Oncogenes Reveals Novel Key Factors and Networks in HPV-Induced Carcinogenesis. mSphere. 2019;4(2):e00129-00119.

290. Jiang X, Wang X. Cytochrome C-mediated apoptosis. Annual review of biochemistry. 2004;73:87-106.

291. Laussel C, Léon S. Cellular toxicity of the metabolic inhibitor 2-deoxyglucose and associated resistance mechanisms. Biochemical Pharmacology. 2020;182:114213.

292. Solaini G, Baracca A, Lenaz G, Sgarbi G. Hypoxia and mitochondrial oxidative metabolism. Biochimica et Biophysica Acta (BBA) - Bioenergetics. 2010;1797(6):1171-1177.

293. Bridges HR, Jones AJ, Pollak MN, Hirst J. Effects of metformin and other biguanides on oxidative phosphorylation in mitochondria. The Biochemical journal. 2014;462(3):475-487.

294. Fryknäs M, Zhang X, Bremberg U, Senkowski W, Olofsson MH, Brandt P, et al. Iron chelators target both proliferating and quiescent cancer cells. Scientific Reports. 2016;6(1):38343.

295. Bianchi L, Tacchini L, Cairo G. HIF-1-mediated activation of transferrin receptor gene transcription by iron chelation. Nucleic Acids Res. 1999;27(21):4223-4227.

296. Nowak-Stępniowska A, Osuchowska PN, Fiedorowicz H, Trafny EA. Insight in Hypoxia-Mimetic Agents as Potential Tools for Mesenchymal Stem Cell Priming in Regenerative Medicine. Stem cells international. 2022;2022:8775591.

297. Hsu KF, Wilkins SE, Hopkinson RJ, Sekirnik R, Flashman E, Kawamura A, et al. Hypoxia and hypoxia mimetics differentially modulate histone post-translational modifications. Epigenetics. 2021;16(1):14-27.

298. Davis CK, Jain SA, Bae ON, Majid A, Rajanikant GK. Hypoxia Mimetic Agents for Ischemic Stroke. Frontiers in cell and developmental biology. 2018;6:175.

299. Mole DR. Iron homeostasis and its interaction with prolyl hydroxylases. Antioxidants & redox signaling. 2010;12(4):445-458.

300. Subramanian A, Tamayo P, Mootha V, Mukherjee S, Ebert B, Gillette M, et al. Gene set enrichment analysis: a knowledge-based approach for interpreting genome-wide expression profiles. Proceedings of the National Academy of Sciences of the United States of America. 2005;102(43):15545-15550.

301. Miteva M, Keusekotten K, Hofmann K, Praefcke GJ, Dohmen RJ. Sumoylation as a signal for polyubiquitylation and proteasomal degradation. Sub-cellular biochemistry. 2010;54:195-214.

302. Hickinson DM, Klinowska T, Speake G, Vincent J, Trigwell C, Anderton J, et al. AZD8931, an Equipotent, Reversible Inhibitor of Signaling by Epidermal Growth Factor Receptor, ERBB2 (HER2), and ERBB3: A Unique Agent for Simultaneous ERBB Receptor Blockade in Cancer. Clinical Cancer Research. 2010;16(4):1159-1169.

303. Woodworth CD, Diefendorf LP, Jette DF, Mohammed A, Moses MA, Searleman SA, et al. Inhibition of the epidermal growth factor receptor by erlotinib prevents immortalization of human cervical cells by Human Papillomavirus type 16. Virology. 2011;421(1):19-27.

304. Kim JW, Kim YT, Kim DK, Song CH, Lee JW. Expression of epidermal growth factor receptor in carcinoma of the cervix. Gynecologic oncology. 1996;60(2):283-287.

305. Iida K, Nakayama K, Rahman MT, Rahman M, Ishikawa M, Katagiri A, et al. EGFR gene amplification is related to adverse clinical outcomes in cervical squamous cell carcinoma, making the EGFR pathway a novel therapeutic target. British Journal of Cancer. 2011;105(3):420-427.

306. Scaltriti M, Baselga J. The Epidermal Growth Factor Receptor Pathway: A Model for Targeted Therapy. Clinical Cancer Research. 2006;12(18):5268-5272.

307. Comşa Ş, Cîmpean AM, Raica M. The Story of MCF-7 Breast Cancer Cell Line: 40 years of Experience in Research. Anticancer research. 2015;35(6):3147-3154.

308. Harden ME, Munger K. Human papillomavirus molecular biology. Mutation research Reviews in mutation research. 2017;772:3-12.

309. Basukala O, Banks L. The Not-So-Good, the Bad and the Ugly: HPV E5, E6 and E7 Oncoproteins in the Orchestration of Carcinogenesis. Viruses. 2021;13(10):1892.

310. Igelmann S, Neubauer HA, Ferbeyre G. STAT3 and STAT5 Activation in Solid Cancers. Cancers (Basel). 2019;11(10):1428.

311. Avalle L, Pensa S, Regis G, Novelli F, Poli V. STAT1 and STAT3 in tumorigenesis: A matter of balance. Jak-stat. 2012;1(2):65-72.

312. Demoulin JB, Van Roost E, Stevens M, Groner B, Renauld JC. Distinct roles for STAT1, STAT3, and STAT5 in differentiation gene induction and apoptosis inhibition by interleukin-9. J Biol Chem. 1999;274(36):25855-25861.

313. Przanowski P, Dabrowski M, Ellert-Miklaszewska A, Kloss M, Mieczkowski J, Kaza B, et al. The signal transducers Stat1 and Stat3 and their novel target Jmjd3 drive the expression of inflammatory genes in microglia. Journal of Molecular Medicine. 2014;92(3):239-254.

314. Hosui A, Hennighausen L. Genomic dissection of the cytokine-controlled STAT5 signaling network in liver. Physiological genomics. 2008;34(2):135-143.

315. Costa-Pereira AP, Tininini S, Strobl B, Alonzi T, Schlaak JF, Is'harc H, et al. Mutational switch of an IL-6 response to an interferon-gamma-like response. Proc Natl Acad Sci U S A. 2002;99(12):8043-8047.

316. Kaptein A, Paillard V, Saunders M. Dominant Negative Stat3 Mutant Inhibits Interleukin-6-induced Jak-STAT Signal Transduction (∗). Journal of Biological Chemistry. 1996;271(11):5961-5964.

317. Mohr A, Fahrenkamp D, Rinis N, Müller-Newen G. Dominant-negative activity of the STAT3-Y705F mutant depends on the N-terminal domain. Cell communication and signaling : CCS. 2013;11:83.

318. Wang H, Lei L, Hu J, Li Y. Oncostatin M upregulates Livin to promote keratinocyte proliferation and survival via ERK and STAT3 signalling pathways. Experimental physiology. 2020;105(7):1151-1158.

319. Hoppe-Seyler K, Bossler F, Lohrey C, Bulkescher J, Rösl F, Jansen L, et al. Induction of dormancy in hypoxic human papillomavirus-positive cancer cells. Proceedings of the National Academy of Sciences. 2017:201615758.

320. Heber N, Kuhn BJ, Strobel TD, Lohrey C, Krijgsveld J, Hoppe-Seyler K, et al. The impact of cycling hypoxia on the phenotype of HPV-positive cervical cancer cells. Journal of Medical Virology. 2023;95(12):e29280.

321. Wang B, Han J, Elisseeff JH, Demaria M. The senescence-associated secretory phenotype and its physiological and pathological implications. Nature Reviews Molecular Cell Biology. 2024.

322. Pang X, Gao S, Liu T, Xu FX, Fan C, Zhang JF, et al. Identification of STAT3 as a biomarker for cellular senescence in liver fibrosis: A bioinformatics and experimental validation study. Genomics. 2024;116(2):110800.

323. Yasuda T, Koiwa M, Yonemura A, Miyake K, Kariya R, Kubota S, et al. Inflammation-driven senescence-associated secretory phenotype in cancer-associated fibroblasts enhances peritoneal dissemination. Cell Rep. 2021;34(8):108779.

324. Dimri GP, Lee X, Basile G, Acosta M, Scott G, Roskelley C, et al. A biomarker that identifies senescent human cells in culture and in aging skin in vivo. Proc Natl Acad Sci U S A. 1995;92(20):9363-9367.

325. Lee BY, Han JA, Im JS, Morrone A, Johung K, Goodwin EC, et al. Senescence-associated beta-galactosidase is lysosomal beta-galactosidase. Aging cell. 2006;5(2):187-195.

326. Lin A, Giuliano CJ, Palladino A, John KM, Abramowicz C, Yuan ML, et al. Off-target toxicity is a common mechanism of action of cancer drugs undergoing clinical trials. Sci Transl Med. 2019;11(509):eaaw8412.

327. Peretz L, Besser E, Hajbi R, Casden N, Ziv D, Kronenberg N, et al. Combined shRNA over CRISPR/cas9 as a methodology to detect off-target effects and a potential compensatory mechanism. Scientific Reports. 2018;8(1):93.

328. Bossler F, Hoppe-Seyler K, Hoppe-Seyler F. PI3K/AKT/mTOR Signaling Regulates the Virus/Host Cell Crosstalk in HPV-Positive Cervical Cancer Cells. Int J Mol Sci. 2019;20(9):2188.

329. Zhou T, Georgeon S, Moser R, Moore DJ, Caflisch A, Hantschel O. Specificity and mechanism-of-action of the JAK2 tyrosine kinase inhibitors ruxolitinib and SAR302503 (TG101348). Leukemia. 2014;28(2):404-407.

330. Kuner R, Vogt M, Sultmann H, Buness A, Dymalla S, Bulkescher J, et al. Identification of cellular targets for the human papillomavirus E6 and E7 oncogenes by RNA interference and transcriptome analyses. Journal of Molecular Medicine. 2007;85(11):1253-1262.

331. Rosty C, Sheffer M, Tsafrir D, Stransky N, Tsafrir I, Peter M, et al. Identification of a proliferation gene cluster associated with HPV E6/E7 expression level and viral DNA load in invasive cervical carcinoma. Oncogene. 2005;24(47):7094-7104.

332. Chandarlapaty S, Sawai A, Scaltriti M, Rodrik-Outmezguine V, Grbovic-Huezo O, Serra V, et al. AKT Inhibition Relieves Feedback Suppression of Receptor Tyrosine Kinase Expression and Activity. Cancer Cell. 2011;19(1):58-71.

333. Liu JF, Gray KP, Wright AA, Campos S, Konstantinopoulos PA, Peralta A, et al. Results from a single arm, single stage phase II trial of trametinib and GSK2141795 in persistent or recurrent cervical cancer. Gynecologic oncology. 2019;154(1):95-101.

334. Arjumand W, Merry CD, Wang C, Saba E, McIntyre JB, Fang S, et al. Phosphatidyl inositol-3 kinase (PIK3CA) E545K mutation confers cisplatin resistance and a migratory phenotype in cervical cancer cells. Oncotarget. 2016;7(50):82424-82439.

335. Stich M, Ganss L, Puschhof J, Prigge E-S, Reuschenbach M, Guiterrez A, et al. 5-aza-2'-deoxycytidine (DAC) treatment downregulates the HPV E6 and E7 oncogene expression and blocks neoplastic growth of HPV-associated cancer cells. Oncotarget. 2016;8(32):52104-52117.

336. Duriez PJ, Shah GM. Cleavage of poly(ADP-ribose) polymerase: a sensitive parameter to study cell death. Biochemistry and cell biology = Biochimie et biologie cellulaire. 1997;75(4):337-349.

337. Sallmann FR, Bourassa S, Saint-Cyr J, Poirier GG. Characterization of antibodies specific for the caspase cleavage site on poly(ADP-ribose) polymerase: specific detection of apoptotic fragments and mapping of the necrotic fragments of poly(ADP-ribose) polymerase. Biochemistry and cell biology = Biochimie et biologie cellulaire. 1997;75(4):451-456.

338. Bolognesi B, Lehner B. Reaching the limit. eLife. 2018;7:e39804.

339. Weir SJ, Wood R, Schorno K, Brinker AE, Ramamoorthy P, Heppert K, et al. Preclinical Pharmacokinetics of Fosciclopirox, a Novel Treatment of Urothelial Cancers, in Rats and Dogs. The Journal of pharmacology and experimental therapeutics. 2019;370(2):148-159.

340. Cadassou O, Jordheim LP. OXPHOS inhibitors, metabolism and targeted therapies in cancer. Biochem Pharmacol. 2023;211:115531.

341. Hua H, Kong Q, Zhang H, Wang J, Luo T, Jiang Y. Targeting mTOR for cancer therapy. Journal of Hematology & Oncology. 2019;12(1):71.

342. Rao VA, Klein SR, Agama KK, Toyoda E, Adachi N, Pommier Y, et al. The iron chelator Dp44mT causes DNA damage and selective inhibition of topoisomerase IIalpha in breast cancer cells. Cancer Res. 2009;69(3):948-957.

343. Ciechanover A, Schwartz AL. The ubiquitin-proteasome pathway: the complexity and myriad functions of proteins death. Proc Natl Acad Sci U S A. 1998;95(6):2727-2730.

344. Zheng N, Shabek N. Ubiquitin Ligases: Structure, Function, and Regulation. Annual review of biochemistry. 2017;86(Volume 86, 2017):129-157.

345. Shen T, Shang C, Zhou H, Luo Y, Barzegar M, Odaka Y, et al. Ciclopirox inhibits cancer cell proliferation by suppression of Cdc25A. Genes Cancer. 2017;8(3-4):505-516.

346. Shen T, Zhou H, Shang C, Luo Y, Wu Y, Huang S. Ciclopirox activates ATR-Chk1 signaling pathway leading to Cdc25A protein degradation. Genes Cancer. 2018;9(1-2):39-52.

347. Heppler LN, Frank DA. Inhibit versus Destroy: Are PROTAC Degraders the Solution to Targeting STAT3? Cancer Cell. 2019;36(5):459-461.

348. Poria DK, Sheshadri N, Balamurugan K, Sharan S, Sterneck E. The STAT3 inhibitor Stattic acts independently of STAT3 to decrease histone acetylation and modulate gene expression. Journal of Biological Chemistry. 2021;296:100220.

349. Xia Y, Wang G, Jiang M, Liu X, Zhao Y, Song Y, et al. A Novel Biological Activity of the STAT3 Inhibitor Stattic in Inhibiting Glutathione Reductase and Suppressing the Tumorigenicity of Human Cervical Cancer Cells via a ROS-Dependent Pathway. Onco Targets Ther. 2021;14:4047-4060.

350. Iliev P, Hanke D, Page BDG. STAT Protein Thermal Shift Assays to Monitor Protein-Inhibitor Interactions. Chembiochem : a European journal of chemical biology. 2022;23(20):e202200039.

351. Genini D, Brambilla L, Laurini E, Merulla J, Civenni G, Pandit S, et al. Mitochondrial dysfunction induced by a SH2 domain-targeting STAT3 inhibitor leads to metabolic synthetic lethality in cancer cells. Proc Natl Acad Sci U S A. 2017;114(25):E4924-e4933.

352. Brambilla L, Lahiri T, Cammer M, Levy DE. STAT3 Inhibitor OPB-51602 Is Cytotoxic to Tumor Cells Through Inhibition of Complex I and ROS Induction. iScience. 2020;23(12):101822.

353. McFarland BC, Gray GK, Nozell SE, Hong SW, Benveniste EN. Activation of the NF-κB pathway by the STAT3 inhibitor JSI-124 in human glioblastoma cells. Molecular cancer research : MCR. 2013;11(5):494-505.

354. Smith I, Greenside PG, Natoli T, Lahr DL, Wadden D, Tirosh I, et al. Evaluation of RNAi and CRISPR technologies by large-scale gene expression profiling in the Connectivity Map. PLoS biology. 2017;15(11):e2003213.

355. Hannus M, Beitzinger M, Engelmann JC, Weickert MT, Spang R, Hannus S, et al. siPools: highly complex but accurately defined siRNA pools eliminate off-target effects. Nucleic Acids Res. 2014;42(12):8049-8061.

356. Evers B, Jastrzebski K, Heijmans JP, Grernrum W, Beijersbergen RL, Bernards R. CRISPR knockout screening outperforms shRNA and CRISPRi in identifying essential genes. Nature biotechnology. 2016;34(6):631-633.

357. DepMap 24Q2 Public Release [Internet]. Figshare+. 2024 [cited 09/2024]. Available from: https://plus.figshare.com/articles/dataset/DepMap_24Q2_Public/25880521.

358. Tsherniak A, Vazquez F, Montgomery PG, Weir BA, Kryukov G, Cowley GS, et al. Defining a Cancer Dependency Map. Cell. 2017;170(3):564-576.e516.

359. Groot J, Ott M, Wei J, Kassab C, Fang D, Najem H, et al. A first-in-human Phase I trial of the oral p-STAT3 inhibitor WP1066 in patients with recurrent malignant glioma. CNS oncology. 2022;11(2):Cns87.

360. REVERT- Liver Cancer: A Phase 1b/2 Multicenter, Open-label Study to Evaluate the Safety and Efficacy of TTI-101 as Monotherapy and in Combination in Participants With Locally Advanced or Metastatic, and Unresectable Hepatocellular Carcinoma [Internet]. 2022. Available from: https://clinicaltrials.gov/study/NCT05440708.

361. Kasembeli MM, Singhmar P, Ma J, Edralin J, Tang Y, Adams C, 3rd, et al. TTI-101: A competitive inhibitor of STAT3 that spares oxidative phosphorylation and reverses mechanical allodynia in mouse models of neuropathic pain. Biochem Pharmacol. 2021;192:114688.

362. Watanabe T, Nanamiya H, Kojima M, Nomura S, Furukawa S, Soeda S, et al. Clinical implication of oncogenic somatic mutations in early-stage cervical cancer with radical hysterectomy. Scientific Reports. 2020;10(1):18734.

363. Liu Z, Liu Y, Qian L, Jiang S, Gai X, Ye S, et al. A proteomic and phosphoproteomic landscape of KRAS mutant cancers identifies combination therapies. Molecular Cell. 2021;81(19):4076-4090.e4078.

364. Miekus K, Pawlowska M, Sekuła M, Drabik G, Madeja Z, Adamek D, et al. MET receptor is a potential therapeutic target in high grade cervical cancer. Oncotarget. 2015;6(12):10086-10101.

365. Soto-Cruz I, Rangel-Corona R, Valle-Mendiola A, Moreno-Morales X, Santiago-Pérez R, Weiss-Steider B, et al. The tyrphostin B42 inhibits cell proliferation and HER-2 autophosphorylation in cervical carcinoma cell lines. Cancer investigation. 2008;26(2):136-144.

366. Chew CS, Nakamura K, Petropoulos AC. Multiple actions of epidermal growth factor and TGF-alpha on rabbit gastric parietal cell function. The American journal of physiology. 1994;267(5 Pt 1):G818-826.

367. Gazit A, Osherov N, Posner I, Yaish P, Poradosu E, Gilon C, et al. Tyrphostins. 2. Heterocyclic and alpha-substituted benzylidenemalononitrile tyrphostins as potent inhibitors of EGF receptor and ErbB2/neu tyrosine kinases. Journal of medicinal chemistry. 1991;34(6):1896-1907.

368. Fernández-Sánchez R, Berzal S, Sánchez-Niño MD, Neria F, Gonçalves S, Calabia O, et al. AG490 promotes HIF-1α accumulation by inhibiting its hydroxylation. Current medicinal chemistry. 2012;19(23):4014-4023.

369. Jaleel M, Shenoy AR, Visweswariah SS. Tyrphostins Are Inhibitors of Guanylyl and Adenylyl Cyclases. Biochemistry. 2004;43(25):8247-8255.

370. Sinclair A, Archibeque I, Zhan J, Liu L, Emkey R, Doherty E, et al. Potency and Selectivity Assessment of Small Molecules Against Janus Kinase (JAK) 2: Widely Used AG490 Inhibitor Is Neither Potent Nor Selective for JAK2. Blood. 2011;118(21):4780.

371. Liu Y, Ciotti GE, Eisinger-Mathason TSK. Hypoxia and the Tumor Secretome. Advances in experimental medicine and biology. 2019;1136:57-69.

372. Shi L, Baohua Z, Zehua W. Expression of survivin, cyclinD1, p21WAF1, caspase-3 in cervical cancer and its relation with prognosis. Current Medical Science. 2005;25(1):78-81.

373. Babon JJ, Nicola NA. The biology and mechanism of action of suppressor of cytokine signaling 3. Growth factors (Chur, Switzerland). 2012;30(4):207-219.

374. Caffarel MM, Coleman N. Oncostatin M receptor is a novel therapeutic target in cervical squamous cell carcinoma. The Journal of pathology. 2014;232(4):386-390.

375. Kucia-Tran JA, Tulkki V, Smith S, Scarpini CG, Hughes K, Araujo AM, et al. Overexpression of the oncostatin-M receptor in cervical squamous cell carcinoma is associated with epithelial–mesenchymal transition and poor overall survival. British Journal of Cancer. 2016;115(2):212-222.

376. Chuerduangphui J, Pientong C, Chaiyarit P, Patarapadungkit N, Chotiyano A, Kongyingyoes B, et al. Effect of human papillomavirus 16 oncoproteins on oncostatin M upregulation in oral squamous cell carcinoma. Medical oncology (Northwood, London, England). 2016;33(8):83.

377. Krasilnikov M, Ivanov VN, Dong J, Ronai Z. ERK and PI3K negatively regulate STAT-transcriptional activities in human melanoma cells: implications towards sensitization to apoptosis. Oncogene. 2003;22(26):4092-4101.

378. Wingo SN, Gallardo TD, Akbay EA, Liang M-C, Contreras CM, Boren T, et al. Somatic LKB1 Mutations Promote Cervical Cancer Progression. PLOS ONE. 2009;4(4):e5137.

379. Xie B, Zhang L, Hu W, Fan M, Jiang N, Duan Y, et al. Dual blockage of STAT3 and ERK1/2 eliminates radioresistant GBM cells. Redox Biology. 2019;24:101189.

380. Wang Z, Yin M, Chu P, Lou M. STAT3 inhibitor sensitized KRAS-mutant lung cancers to RAF inhibitor by activating MEK/ERK signaling pathway. Aging. 2019;11(17):7187-7196.

381. Wu S, Wu Y, Lu Y, Yue Y, Cui C, Yu M, et al. STAT1 expression and HPV16 viral load predict cervical lesion progression. Oncol Lett. 2020;20(4):28.

382. Raspaglio G, Buttarelli M, Filippetti F, Battaglia A, Buzzonetti A, Scambia G, et al. Stat1 confers sensitivity to radiation in cervical cancer cells by controlling Parp1 levels: a new perspective for Parp1 inhibition. Cell Death & Disease. 2021;12(10):933.

383. Buttarelli M, Babini G, Raspaglio G, Filippetti F, Battaglia A, Ciucci A, et al. A combined ANXA2-NDRG1-STAT1 gene signature predicts response to chemoradiotherapy in cervical cancer. Journal of Experimental & Clinical Cancer Research. 2019;38(1):279.

384. Nussinov R, Tsai C-J, Jang H. Are Parallel Proliferation Pathways Redundant? Trends in Biochemical Sciences. 2020;45(7):554-563.

385. Lavi O. Redundancy: A Critical Obstacle to Improving Cancer Therapy. Cancer Research. 2015;75(5):808-812.

386. Mesri EA, Feitelson MA, Munger K. Human viral oncogenesis: a cancer hallmarks analysis. Cell host & microbe. 2014;15(3):266-282.

387. Kleine K, König G, Kreuzer J, Komitowski D, Zur Hausen H, Rösl F. The effect of the JE (MCP-1) gene, which encodes monocyte chemoattractant protein-1, on the growth of HeLa cells and derived somatic-cell hybrids in nude mice. Mol Carcinog. 1995;14(3):179-189.

388. Park JS, Kim EJ, Kwon HJ, Hwang ES, Namkoong SE, Um SJ. Inactivation of interferon regulatory factor-1 tumor suppressor protein by HPV E7 oncoprotein. Implication for the E7-mediated immune evasion mechanism in cervical carcinogenesis. J Biol Chem. 2000;275(10):6764-6769.

389. Um SJ, Rhyu JW, Kim EJ, Jeon KC, Hwang ES, Park JS. Abrogation of IRF-1 response by high-risk HPV E7 protein in vivo. Cancer Lett. 2002;179(2):205-212.

390. Zhou F, Chen J, Zhao KN. Human papillomavirus 16-encoded E7 protein inhibits IFN-γ-mediated MHC class I antigen presentation and CTL-induced lysis by blocking IRF-1 expression in mouse keratinocytes. J Gen Virol. 2013;94(Pt 11):2504-2514.

391. Zheng W, Zhao Z, Yi X, Zuo Q, Li H, Guo X, et al. Down-regulation of IFITM1 and its growth inhibitory role in cervical squamous cell carcinoma. Cancer Cell Int. 2017;17:88.

392. Gómez-Herranz M, Nekulova M, Faktor J, Hernychova L, Kote S, Sinclair EH, et al. The effects of IFITM1 and IFITM3 gene deletion on IFNγ stimulated protein synthesis. Cellular Signalling. 2019;60:39-56.

393. Ma W, Tummers B, van Esch EM, Goedemans R, Melief CJ, Meyers C, et al. Human Papillomavirus Downregulates the Expression of IFITM1 and RIPK3 to Escape from IFNγ- and TNFα-Mediated Antiproliferative Effects and Necroptosis. Front Immunol. 2016;7:496.

394. Spurgeon ME, Lambert PF. Mus musculus Papillomavirus 1: a New Frontier in Animal Models of Papillomavirus Pathogenesis. Journal of virology. 2020;94(9):e00002-00020.

395. Kojima H, Kunimoto H, Inoue T, Nakajima K. The STAT3-IGFBP5 axis is critical for IL-6/gp130-induced premature senescence in human fibroblasts. Cell Cycle. 2012;11(4):730-739.

396. Ohtani N, Zebedee Z, Huot TJG, Stinson JA, Sugimoto M, Ohashi Y, et al. Opposing effects of Ets and Id proteins on p16INK4a expression during cellular senescence. Nature. 2001;409(6823):1067-1070.

397. Reznikoff CA, Yeager TR, Belair CD, Savelieva E, Puthenveettil JA, Stadler WM. Elevated p16 at senescence and loss of p16 at immortalization in human papillomavirus 16 E6, but not E7, transformed human uroepithelial cells. Cancer Res. 1996;56(13):2886-2890.

398. Martini H, Passos JF. Cellular senescence: all roads lead to mitochondria. Febs j. 2023;290(5):1186-1202.

399. Aggarwal N, Yadav J, Thakur K, Bibban R, Chhokar A, Tripathi T, et al. Human Papillomavirus Infection in Head and Neck Squamous Cell Carcinomas: Transcriptional Triggers and Changed Disease Patterns. Frontiers in cellular and infection microbiology. 2020;10:537650.

400. Parakh S, Ernst M, Poh AR. Multicellular Effects of STAT3 in Non-small Cell Lung Cancer: Mechanistic Insights and Therapeutic Opportunities. Cancers (Basel). 2021;13(24):6228.

401. Oh DY, Lee SH, Han SW, Kim MJ, Kim TM, Kim TY, et al. Phase I Study of OPB-31121, an Oral STAT3 Inhibitor, in Patients with Advanced Solid Tumors. Cancer research and treatment. 2015;47(4):607-615.

402. Bendell JC, Hong DS, Burris HA, 3rd, Naing A, Jones SF, Falchook G, et al. Phase 1, open-label, dose-escalation, and pharmacokinetic study of STAT3 inhibitor OPB-31121 in subjects with advanced solid tumors. Cancer chemotherapy and pharmacology. 2014;74(1):125-130.

403. Tolcher A, Flaherty K, Shapiro GI, Berlin J, Witzig T, Habermann T, et al. A First-in-Human Phase I Study of OPB-111077, a Small-Molecule STAT3 and Oxidative Phosphorylation Inhibitor, in Patients with Advanced Cancers. The oncologist. 2018;23(6):658-e672.

404. Yoo C, Kang J, Lim HY, Kim JH, Lee MA, Lee KH, et al. Phase I Dose-Finding Study of OPB-111077, a Novel STAT3 Inhibitor, in Patients with Advanced Hepatocellular Carcinoma. Cancer research and treatment. 2019;51(2):510-518.

405. Wong AL, Soo RA, Tan DS, Lee SC, Lim JS, Marban PC, et al. Phase I and biomarker study of OPB-51602, a novel signal transducer and activator of transcription (STAT) 3 inhibitor, in patients with refractory solid malignancies. Annals of Oncology. 2015;26(5):998-1005.

406. Ogura M, Uchida T, Terui Y, Hayakawa F, Kobayashi Y, Taniwaki M, et al. Phase I study of OPB-51602, an oral inhibitor of signal transducer and activator of transcription 3, in patients with relapsed/refractory hematological malignancies. Cancer Sci. 2015;106(7):896-901.

407. Angevin E, Tabernero J, Elez E, Cohen SJ, Bahleda R, van Laethem JL, et al. A phase I/II, multiple-dose, dose-escalation study of siltuximab, an anti-interleukin-6 monoclonal antibody, in patients with advanced solid tumors. Clin Cancer Res. 2014;20(8):2192-2204.

408. Gaykalova DA, Manola JB, Ozawa H, Zizkova V, Morton K, Bishop JA, et al. NF-κB and stat3 transcription factor signatures differentiate HPV-positive and HPV-negative head and neck squamous cell carcinoma. Int J Cancer. 2015;137(8):1879-1889.

409. Verma G, Vishnoi K, Tyagi A, Jadli M, Singh T, Goel A, et al. Characterization of key transcription factors as molecular signatures of HPV-positive and HPV-negative oral cancers. Cancer medicine. 2017;6(3):591-604.

410. Smola S. Immunopathogenesis of HPV-Associated Cancers and Prospects for Immunotherapy. Viruses. 2017;9(9):254.

411. Pahne-Zeppenfeld J, Schröer N, Walch-Rückheim B, Oldak M, Gorter A, Hegde S, et al. Cervical cancer cell-derived interleukin-6 impairs CCR7-dependent migration of MMP-9-expressing dendritic cells. Int J Cancer. 2014;134(9):2061-2073.

412. Heusinkveld M, de Vos van Steenwijk PJ, Goedemans R, Ramwadhdoebe TH, Gorter A, Welters MJ, et al. M2 macrophages induced by prostaglandin E2 and IL-6 from cervical carcinoma are switched to activated M1 macrophages by CD4+ Th1 cells. Journal of immunology (Baltimore, Md : 1950). 2011;187(3):1157-1165.

413. Walch-Rückheim B, Mavrova R, Henning M, Vicinus B, Kim YJ, Bohle RM, et al. Stromal Fibroblasts Induce CCL20 through IL6/C/EBPβ to Support the Recruitment of Th17 Cells during Cervical Cancer Progression. Cancer Res. 2015;75(24):5248-5259.

414. Schröer N, Pahne J, Walch B, Wickenhauser C, Smola S. Molecular pathobiology of human cervical high-grade lesions: paracrine STAT3 activation in tumor-instructed myeloid cells drives local MMP-9 expression. Cancer Res. 2011;71(1):87-97.

415. Noh J, You C, Kang K, Kang K. Activation of OSM-STAT3 Epigenetically Regulates Tumor-Promoting Transcriptional Programs in Cervical Cancer. Cancers (Basel). 2022;14(24):6090.

416. Ran FA, Hsu PD, Wright J, Agarwala V, Scott DA, Zhang F. Genome engineering using the CRISPR-Cas9 system. Nature Protocols. 2013;8(11):2281-2308.

417. O'Leary NA, Wright MW, Brister JR, Ciufo S, Haddad D, McVeigh R, et al. Reference sequence (RefSeq) database at NCBI: current status, taxonomic expansion, and functional annotation. Nucleic Acids Res. 2016;44(D1):D733-745.

418. Frensemeier K, Holzer A, Hoppe-Seyler K, Hoppe-Seyler F. Dickkopf-1 expression is repressed by oncogenic human papillomaviruses (HPVs) and regulates the Cisplatin sensitivity of HPV-positive cancer cells in a JNK-dependent manner. Int J Cancer. 2022;151(12):2215-2228.

419. Chen C, Okayama H. High-efficiency transformation of mammalian cells by plasmid DNA. Molecular and cellular biology. 1987;7(8):2745-2752.

420. Yang D, Strobel TD, Bulkescher J, Tessmer C, Hofmann I, Hoppe-Seyler F, et al. FAM57A (Family with Sequence Similarity 57 Member A) Is a Cell-Density-Regulated Protein and Promotes the Proliferation and Migration of Cervical Cancer Cells. Cells. 2022;11(20):3309.

421. Livak KJ, Schmittgen TD. Analysis of relative gene expression data using real-time quantitative PCR and the 2(-Delta Delta C(T)) Method. Methods (San Diego, Calif). 2001;25(4):402-408.

422. Team RC. R: A Language and Environment for Statistical Computing. R Foundation for Statistical Computing; 2023.

423. Wickham H AM, Bryan J, Chang W, McGowan LD, François R, Grolemund G, Hayes A, Henry L, Hester J, Kuhn M, Pedersen TL, Miller E, Bache SM, Müller K, Ooms J, Robinson D, Seidel DP, Spinu V, Takahashi K, Vaughan D, Wilke C, Woo K, Yutani H. Welcome to the tidyverse. Journal of Open Source Software. 2019;4(43):1686.

424. K S. ggrepel: Automatically Position Non-Overlapping Text Labels with 'ggplot2'. 0.9.5 ed2024.